

NEUTRINOS MEET SUPERSYMMETRY

QUANTUM ASPECTS OF NEUTRINOPHYSICS IN SUPERSYMMETRIC THEORIES

Zur Erlangung des akademischen Grades eines
DOKTORS DER NATURWISSENSCHAFTEN
von der Fakultät für Physik
des Karlsruher Instituts für Technologie (KIT)



genehmigte
DISSERTATION

von

DIPL.-PHYS. WOLFGANG GREGOR HOLLIK

aus Würzburg

Tag der mündlichen Prüfung:	22.05.2015
Referent:	Prof. Dr. Ulrich Nierste
Korreferentin:	Prof. Dr. Milada Margarete Mühlleitner

Wolfgang Gregor Hollik: *Neutrinos Meet Supersymmetry*, Quantum Aspects
of Neutrino Physics in Supersymmetric Theories, © 2015

CONTENTS

1	INTRODUCTION	1
2	PARTICLE PHYSICS IN A NUTSHELL	3
2.1	The Standard Model of Elementary Particles	3
2.1.1	The Gauge Part	3
2.1.2	The Higgs Part	5
2.1.3	The Flavor Part	6
2.2	Supersymmetric Extensions	9
2.2.1	How to Break Supersymmetry	12
2.2.2	The Minimal Supersymmetric Standard Model	13
2.2.3	Radiative Flavor Violation in the MSSM	16
2.3	Extending the Gauge Sector	18
2.3.1	Grand Unification	18
2.3.2	Partial Unification	19
2.4	Neutrinos in the Standard Model and Beyond	20
3	VARIANTS OF NEUTRINO FLAVOR PHYSICS	25
3.1	Neutrinos at tree-level	26
3.2	Radiative Neutrino Mixing	28
3.2.1	The Case of Degenerate Neutrino Masses	29
3.2.2	Renormalizing the Seesaw	37
3.2.3	Renormalizing the Mixing Matrix	42
3.2.4	Remarks on a Resummation of Large Contributions	49
4	THE FATE OF THE SCALAR POTENTIAL	57
4.1	The Effective Potential and its Meaning for the Ground State	58
4.1.1	Path Integral	65
4.1.2	The “Coleman-Weinberg” potential	69
4.1.3	Sea Urchins	72
4.1.4	Improving the potential	78
4.2	The Stability of the Electroweak Vacuum in the MSSM	80
4.2.1	Distinguishing Between different Instabilities	80
4.2.2	Unstable one-loop effective potential with squarks	83
4.2.3	Constraining the Parameter Space by Vacuum Stability	86
5	COMBINING NEUTRINOS AND THE VACUUM	89
5.1	Neutrinos Destabilizing the Effective Potential	91
5.2	Sneutrinos Stabilizing the Effective Potential	93
5.3	Absolute Stability?	97
6	MIXING ANGLES FROM MASS RATIOS	99
6.1	Hierarchical Mass Matrices	100
6.2	Full Hierarchy and the need for corrections	102
6.3	Mixing angles from mass ratios	103
6.3.1	Quark mixing	105

6.3.2	Lepton mixing	105
6.3.3	CP violation	107
7	CONCLUSIONS	109
A	TECHNICALITIES	111
A.1	Spinor Notation and Charge Conjugation	111
A.2	Neutralino and Chargino Mass and Mixing Matrices	111
A.3	Sfermion Mass and Mixing Matrices	113
A.4	Feynman rules for the type I seesaw-extended MSSM	115
A.5	Loop functions	116
B	RELEVANT RENORMALIZATION GROUP EQUATIONS IN THE SM AND BEYOND	119
B.1	SM with heavy singlet neutrinos	119
B.2	MSSM with heavy singlet neutrinos	121
	BIBLIOGRAPHY	123

INTRODUCTION

*In nova fert animus mutatas dicere formas
 corpora; di, coeptis (nam vos mutastis et illas)
 adspirate meis primaque ab origine mundi
 ad mea perpetuum deducite tempora carmen!*

—Publius Ovidius Naso [Metamorphoses]

*My soul is wrought to sing of forms transformed to bodies new and strange!
 Immortal Gods inspire my heart, for ye have changed yourselves and all
 things you have changed! Oh lead my song in smooth and measured strains,
 from olden days when earth began to this completed time!*

—Ovid, *Metamorphoses* [Translation by Brookes More, Boston, 1922.]

Metamorphoses are performed on the way from the visible world as it appears to human eyes down to what we call the “fundamental” level. Fundamental physics follows very simple and very clear rules. The rules of our fundamental laws of nature are symmetry and breaking of symmetries.

Spontaneous symmetry breaking was shown to occur also at the very fundamental level confirmed by the discovery of the Higgs boson at the Large Hadron Collider (LHC) close to Geneva. The Standard Model of elementary particle physics has finished its triumphal procession and shall be completed. However—the Standard Model is not the ultimate truth. Not only that there are observations in nature that cannot be explained within the Standard Model: about 95 % of our universe seems to be unknown and there is no sufficient explanation of why we live in a universe of matter. The missing pieces seem to be triggered by cosmology. There are still conceptual puzzles that lack an explanation: Why are there three families of matter fermions and why do they mix so strangely? And what causes electroweak symmetry to be broken? A further open issue can be solved by a minimal and somewhat symmetric extension of the Standard Models: neutrino masses. The question why they are so small still remains unsettled.

We know since the invention of Quantum Mechanics that we live in a quantum world. Quantum corrections are of importance in any theoretical description of our fundamental processes. Precision calculations are performed and applied to collider phenomena at very high accuracy. Quantum Electrodynamics was tested with an amazing precision. Quantum corrections also guide us through the following pages: we give an explanation of neutrino mixing by virtue of threshold corrections as they may arise in a popular extension of the Standard Model. For that purpose, we start with degenerate neutrino masses at leading order and get the observed deviations from that degenerate pattern by quantum corrections which also generate the mixing. The validity of this description

can be excluded with an upcoming measurement of the neutrino mass: are rather heavy neutrinos excluded by experiment, it gets implausible for such quantum corrections being significant. In a concluding chapter, we give an explanation of large neutrino mixing for a hierarchical mass spectrum in contrast.

Quantum corrections in those extensions are known to have an impact on electroweak symmetry breaking. We investigated their meaning for the parameter range which is favored by quantum models of fermion mixing and found a genuine effect of such corrections which has not yet been described in the literature. The results can then be used to constrain the parameter range from the requirement of the electroweak vacuum being stable and are complementary to existing constraints.

This thesis is structured as follows: We start with an overview of the fundamentals of modern particle physics in Chapter 2 and set up the Standard Model and its popular extensions we deal with throughout this thesis. A special focus lies on supersymmetric extensions and their application on neutrino flavor physics that shall be discussed in Chapter 3. There we propose an explanation for the large observed neutrino mixing based on quantum corrections without referring to tree-level flavor models which is quite orthogonal to what is mostly performed in modern literature. Quantum corrections also possibly destabilize the electroweak vacuum: in Chapter 4 we first review the status of one-loop corrections to the effective Higgs potential and explicitly calculate such corrections for the dominating parts of the Minimal Supersymmetric Standard Model. Transferring this knowledge to the neutrino extension, we show in Chapter 5 that there is no fear of vacuum decay in presence of heavy Majorana neutrinos. Finally, we comment on a further possibility to explain large neutrino (and simultaneously small quark) mixing exploiting the hierarchical mass patterns in Chapter 6.

For the introductory part, we do not intent to give a complete and exhaustive overview of the field. This is simply not possible in a limited amount of space. Nevertheless, we try to give as much information as possible and elaborate some theoretical basement as necessity for the work performed within this thesis. The major achievements as outcome of the following pages is the attempt of a quantum corrected description of neutrino mixing in view of any unknown new physics (where as example of known new physics we take supersymmetry) and the influence of the quantum nature of our basic theory on the stability of the ground state of the theory. Notations are explained where they appear for the first time. Matrices in flavor space are denoted with bold symbols, \mathbf{m} . Upshape labels are put wherever they fit, so e. g. $m_{ij}^X = m_{X,ij} \equiv (\mathbf{M}^X)_{ij}$.

There are marginal notes appearing rather continuously. Their meaning is mostly to be seen as side remarks, where from time to time some commonly known and used notation is introduced for completeness. Generally, this thesis shall be readable and understandable also while ignoring the page margins.

*Thanks to the
ClassicThesis style.*

2.1 THE STANDARD MODEL OF ELEMENTARY PARTICLES

The Standard Model (SM) of elementary particles describes fundamental interactions of the smallest constituents of matter. We call elementary particles elementary, because no substructure has been observed yet and they are sufficient to build up the matter in the universe. Actually, only about five percent of the matter content of our universe is made out of what is described by the SM, see e. g. [1]. The unknown matter species, “Dark Matter”, only interacts gravitationally with our known matter, maybe there are weak gauge interactions [2, 3]. Gravity itself is not included in the SM of elementary particles, all what will be discussed in this thesis is physics without gravity on a flat space time. Cosmology, however, enters through the back door several times.

The interactions of the SM are gauge interactions of the electroweak [4–6] and strong [7, 8] interactions (see Sec. 2.1.1), the self-interaction of the scalar sector leading to spontaneous symmetry breakdown [9, 10] in the electroweak interaction [11–14] (see Sec. 2.1.2) and the interactions of the SM scalar field with the matter fermions which give the flavor of the theory (Sec. 2.1.3).

2.1.1 The Gauge Part

Gallia est omnis divisa in partes tres.
—Gaius Iulius Cæsar, *De bello Gallico*

All Gaul is divided into three parts.

The gauge interactions of the SM are displayed by the group structure

$$SU(3)_c \times SU(2)_L \times U(1)_Y,$$

where the strong and weak interactions are governed by the $SU(3)_c$ and $SU(2)_L$ factors, respectively. The remaining $U(1)$ factor is of the weak hypercharge Y . Matter fields (fermions) are placed in either fundamental or trivial (i. e. singlet) representations of the gauge groups. In this way, we can set up the matter content of the SM: there are twelve quarks where six of them interact with all three gauge interactions and further six are accomplished to fill the Dirac spinor as they are the missing right-handed fields. Furthermore two leptons interact under $SU(2)_L \times U(1)_Y$ and one lepton (right-handed electron) as $SU(2)_L$ singlet carries only hypercharge. There is no right-handed neutrino needed in the SM because it would be a complete singlet under the full gauge group. We have

The strong interaction couples only to colored particles, quarks and gluons, where the $SU(2)_L$ only interacts with left-handed fermions. Right-handed fermions are singlets under $SU(2)_L$.

$$\begin{pmatrix} u_r & u_g & u_b \\ d_r & d_g & d_b \end{pmatrix}_L \quad \begin{matrix} u_{R,r} & u_{R,g} & u_{R,b} \\ d_{R,r} & d_{R,g} & d_{R,b} \end{matrix} \quad \begin{pmatrix} \nu \\ e \end{pmatrix}_L \quad e_R, \quad (2.1)$$

where r, g, b label the three color degrees of freedom (red, green, blue) and the left and right projections of Dirac fermions are given via

$$\psi_{L,R} = P_{L,R}\psi, \text{ with } P_L = \frac{1}{2}(1 - \gamma_5) \quad \text{and} \quad P_R = \frac{1}{2}(1 + \gamma_5)$$

for a generic Dirac spinor ψ .

For some reason, the fermion content of the SM is triplicated and each copy of the particle set (generation) differs by the particle masses. The interaction with the Higgs boson, which sets the masses, also generates transitions among the three generations. With only gauge interactions, we have for one SM generation of matter fields the kinetic Lagrangian

For Dirac spinors,
 $\bar{\Psi} = \Psi^\dagger \gamma^0$.

$$\begin{aligned} \mathcal{L}_{\text{kin}} &= \bar{\Psi} \not{D} \Psi \\ &= \bar{\Psi} \gamma_\mu \left(\partial^\mu - i \frac{g_3}{2} T^a G^{a,\mu} - i \frac{g_2}{2} \vec{\tau} \cdot \vec{W}^\mu - i \frac{g_1}{2} Y B^\mu \right) \Psi, \end{aligned} \quad (2.2)$$

The T^a are the
Gell–Mann matrices
and τ_i the Pauli
matrices.

where the generators of $SU(3)_c$ are denoted by $T^a/2$ and those of $SU(2)_L$ by $\tau_i/2$. The gauge couplings are labeled in an obvious manner and Y is the hypercharge operator. The spinor Ψ shall be used for a generic gauge multiplet; $G^{a,\mu}$, W_i^μ and B^μ are the corresponding $SU(3)_c$, $SU(2)_L$ and $U(1)_Y$ gauge vector bosons.

Further generations can be just added in parallel because gauge interactions do not make inter-generation transitions, so $\bar{\Psi} \not{D} \Psi \rightarrow \bar{\Psi}_i \not{D} \Psi_i$ and $i = 1, \dots, n_G$ counts the number of generations. An interesting observation reveals itself in the “gaugeless limit” with $g_{1,2,3} \rightarrow 0$: neglecting fermion masses but obeying the gauge structure, the SM fermions have an enhanced $[U(3)]^5$ symmetry (see also Chapter 6). The counting is simple: one $U(3)$ factor for each gauge representation because of three generations. There are five gauge representations: left-handed quarks (color triplets and weak doublets), right-handed quarks (color triplets, twice for up and down sector), left-handed leptons (weak doublets) and the right-handed electron. In the gaugeless limit, the global symmetry gets even more enhanced:

We thank Luca Di
Luzio for sharing
this observation
with us.

$$[U(3)]^5 \xrightarrow{g_{1,2,3} \rightarrow 0} U(45).$$

The 45 is 3×15 which is just the triplication of one generation. In the presence of right-handed neutrinos, we have $U(48)$ since the three right-handed neutrinos are complete SM singlets and simply added to the game.

The gauge symmetries of the SM neither allow for gauge boson nor for fermion masses. Masses of gauge bosons violate gauge invariance and also Dirac mass terms of fermions are forbidden in the SM because left- and right-handed fields live in different representations of the gauge groups, so there is no gauge invariant way to construct them. We do not want to slaughter the sacred cow of gauge symmetry in order to introduce particle masses per brute force. A gauge invariant construction of particle masses related to spontaneous symmetry breakdown of the gauge symmetry can be achieved via the Brout–Englert–Guralnik–Hagen–Higgs–Kibble [11–14] mechanism briefly described and introduced in the following section.

We have put the
contributing
authors in
alphabetical order.

2.1.2 The Higgs Part

I think, we have it.

—Rolf Heuer

Eureka!

—Archimedes

The Higgs boson was the missing piece in the SM postulated 1964 and finally discovered in the first run at the LHC [15, 16]. It is a necessary ingredient to perform the spontaneous breakdown of electroweak gauge symmetry in the SM. Spontaneous symmetry breaking happens, once the ground state of the theory does not respect the initial symmetry anymore. In the SM we have an $SU(2) \times U(1)$ gauge symmetry, which is spontaneously broken to the electromagnetic $U(1)$. Unfortunately, the theory does not break itself—up to now, we have the gauge fields and fermions transforming under the fundamental representations. To break the gauge symmetry, we have to introduce additional fields. The most economic extension of the field content is one further fundamental representation of a scalar $H = (h^+, h^0)$, which is an $SU(2)$ doublet. We allow for self-interaction of the scalar field and write down the following potential

$$V(H) = -\mu^2 H^\dagger H + \lambda (H^\dagger H)^2, \quad (2.3)$$

where gauge invariance (no linear and cubic terms) and renormalizability (no monomials higher than four) dictate this structure. The sign of the μ^2 -term now decides whether the symmetry is broken or not, whereas the λ -term has to be chosen positive for V to be bounded from below (for an extended discussion about the stability of scalar potentials see Chapter 4). The minimization with respect to the neutral component ($\mu^2 > 0$) gives a *vacuum expectation value* (*vev*) v to the scalar doublet field

$$\langle H \rangle = \begin{pmatrix} 0 \\ \frac{\mu}{\sqrt{2\lambda}} \end{pmatrix} \equiv \begin{pmatrix} 0 \\ \frac{v}{\sqrt{2}} \end{pmatrix}.$$

We have a freedom of $SU(2)$ -rotation (which is a gauge choice), therefore we can choose the *vev* to be in the neutral component since electric charge is not supposed to be broken. The unbroken generator is given by

$$\frac{1}{2} (\tau_3 + Y) \langle H \rangle = 0$$

and the electric charge as combination of weak hypercharge Y and the third component of weak isospin T_{3W} is given via the Gell-Mann–Nishijima relation

$$Q = T_{3W} + \frac{Y}{2}. \quad (2.4)$$

Expanding around the minimum, we obtain the physical Higgs boson φ^0 and the unphysical charged and pseudoscalar Goldstone bosons χ^+ and χ^0 , respectively:

$$H = \begin{pmatrix} \chi^+ \\ \frac{1}{\sqrt{2}} (v + \varphi^0 + i\chi^0) \end{pmatrix}.$$

Gauge fields transform in the adjoint representation.

The upper component carries electric charge +1 where the lower one is electrically neutral, for this purpose the $U(1)_Y$ -charge of that scalar has to be +1 according to Eq. (2.4). $\frac{dV}{dh^0} = 0$

This way, we recover the unpleasant factor $1/\sqrt{2}$ from above which we keep to coincide with half of the literature.

Doing this procedure, the Goldstone bosons are “eaten” by the gauge bosons.

The main point is, that the gauge boson masses can be calculated as combination of gauge couplings and vevs, which is true in any spontaneously broken gauge symmetry.

The Goldstone bosons remain massless and can be absorbed by gauge choice into the gauge bosons which acquire masses and a longitudinal degree of freedom. Through the kinetic couplings to the gauge bosons, $(D_\mu H)^\dagger(D^\mu H)$, and the existence of v , they acquire partially a mass and mix to the physical W bosons (electrically charged) and the Z which is neutral and a mixture of W_3^μ and B^μ . The photon A^μ (the orthogonal state to the Z) remains massless. Details are omitted because this is common textbook knowledge, see e. g. [17, 18]. The masses are

$$M_W^2 = v^2 \frac{g_2^2}{4} \quad \text{and} \quad M_Z^2 = v^2 \frac{g_1^2 + g_2^2}{4}.$$

The ratio of the two gauge couplings determines the weak mixing angle θ_w , which is the angle of the $SO(2)$ rotation transforming (W_3^μ, B^μ) into (Z^μ, A^μ) , $\tan \theta_w = g_1/g_2$. Inverting the mass relations, we obtain with the measured masses and gauge couplings $v = 246 \text{ GeV}$ which sets the electroweak scale.

2.1.3 The Flavor Part

The bodies of which the world is composed are solids, and therefore have three dimensions. Now, three is the most perfect number,—it is the first of numbers, for of one we do not speak as a number, of two we say both, but three is the first number of which we say all. Moreover, it has a beginning, a middle, and an end.

—Aristotle

Yukawa introduced a fermion–scalar interaction to describe pion–nucleon interaction in the same way. This coupling is still called Yukawa coupling though used in a different sense.

The Higgs scalar is there, spontaneous symmetry breaking has happened, especially we have $h^0 = (v + \varphi^0)/\sqrt{2}$. We exploit this fact to generate fermion masses via the same mechanism, coupling the Higgs doublet to the fermions via Yukawa interactions. To construct gauge invariant Dirac mass terms, we have to contract the $SU(2)$ doublets with the Higgs doublet and append the singlet right-handed fermions:

$$-\mathcal{L}_{\text{Yuk}}^{\text{SM}} = Y_{ij}^d \bar{Q}_{L,i} \cdot H d_{R,j} - Y_{ij}^u \bar{Q}_{L,i} \cdot \tilde{H} u_{R,j} + Y_{ij}^e \bar{L}_{L,i} \cdot H e_{R,j} + \text{h. c.}, \quad (2.5)$$

where the dot product denotes $SU(2)$ invariant multiplication (which gives the minus sign for up-type Yukawa) and the charge conjugated Higgs doublet

$$\tilde{H} = i \tau_2 H^* = \begin{pmatrix} (h^0)^* \\ -h^- \end{pmatrix}.$$

The couplings Y_{ij}^f of Eq. (2.5) with $f = u, d, e$ are arbitrary matrices in flavor (i. e. generation) space where the indices $i, j = 1, \dots, n_G$ count the number of generations. Up to now, we know $n_G = 3$ copies of SM fermions, where a fourth sequential fermion generation is excluded after the Higgs discovery [19].

Eqs. (2.2) and (2.5) define two different bases which can be transformed into each other and produce fermion mixing phenomena. After the Higgs doublet acquires its v_{ev} , Eq. (2.5) gives masses to the fermions, where

$$\mathbf{m}^f = \frac{v}{\sqrt{2}} \mathbf{Y}^f \quad (2.6)$$

defines the mass matrices. The basis, in which \mathbf{m}^f is diagonal is therefore called *mass basis*. In contrast, the gauge interactions of Eq. (2.2) define the *interaction basis*. The interplay of gauge multiplets combining two *a priori* independent mass matrices (for the up and the down sector) results in the generation (flavor) mixing of the weak charged interaction. To elaborate on this feature, which prepares especially for Chapters 3 and 6, we rotate into the mass eigenbasis using bi-unitary transformations

$$\mathbf{Y}^f \rightarrow \mathbf{S}_L^f \mathbf{Y}^f \left(\mathbf{S}_R^f \right)^\dagger = \hat{\mathbf{Y}}^f = \text{diagonal}. \quad (2.7)$$

In view of the gauge representation of the fermions as indicated in Eq. (2.5), we cannot rotate left-handed up and down fermions independently since both form a doublet. Obeying the gauge structure, we have three independent rotations in the quark sector:

$$Q_{L,i} \rightarrow Q'_{L,i} = S_{L,ij}^Q Q_{L,j}, \quad (2.8a)$$

$$u_{R,i} \rightarrow u'_{R,i} = S_{R,ij}^u u_{R,j}, \quad (2.8b)$$

$$d_{R,i} \rightarrow d'_{R,i} = S_{R,ij}^d d_{R,j}. \quad (2.8c)$$

This set of transformations is not sufficient to simultaneously diagonalize the mass matrices \mathbf{m}^u and \mathbf{m}^d . We can determine \mathbf{S}^Q and \mathbf{S}^u from the up-type Yukawa coupling via $\hat{\mathbf{Y}}^u = \mathbf{S}^Q \mathbf{Y}^u (\mathbf{S}^u)^\dagger$; then we need a further unitary matrix \mathbf{V} from the left to diagonalize

$$\tilde{\mathbf{Y}}^d = \mathbf{S}^Q \mathbf{Y}^d (\mathbf{S}^d)^\dagger \quad \text{as} \quad \hat{\mathbf{Y}}^d = \mathbf{V} \tilde{\mathbf{Y}}^d = \mathbf{V} \mathbf{S}^Q \mathbf{Y}^d (\mathbf{S}^d)^\dagger.$$

The matrix \mathbf{V} measures the misalignment of Yukawa couplings; if $\mathbf{V} = \mathbf{1}$ the alignment of up and down Yukawa would be exact and both up and down mass matrices are simultaneously diagonal. Now, we see the outcome of the transformation into the mass eigenbasis: the neutral current interactions (or $SU(2)_L$ singlet-like) are unaffected and still flavor conserving thanks to the unitarity of mixing matrices. In contrast, the charged current interaction $\mathcal{L}_{CC} = -\frac{ig_2}{\sqrt{2}} W_\mu^+ J_L^\mu + \text{h. c.}$ reveals the mixing matrix \mathbf{V} as leftover in the left-handed charged fermion current J_L^μ . Performing the transformations into the mass basis from above, we have

$$J_L^\mu = \bar{u}_L \gamma^\mu d_L \xrightarrow{(2.8)} \bar{u}'_L \mathbf{S}_L^Q \gamma^\mu (\mathbf{S}_L^Q)^\dagger \mathbf{V}^\dagger d'_L. \quad (2.9)$$

We identify in Eq. (2.9) the Cabibbo–Kobayashi–Maskawa [20, 21] (CKM) matrix as $\mathbf{V}_{CKM} = \mathbf{V}^\dagger$. The CKM matrix describes the threefold mixing of

It can be easily shown that the left and right unitary matrices $\mathbf{S}_{L,R}$ diagonalize the left and right Hermitian products, $\mathbf{S}_L \mathbf{Y} \mathbf{Y}^\dagger (\mathbf{S}_L)^\dagger$ and $\mathbf{S}_R \mathbf{Y}^\dagger \mathbf{Y} (\mathbf{S}_R)^\dagger$ with $(\mathbf{S}_{L,R}^f)^\dagger \mathbf{S}_{L,R}^f = \mathbf{1}$.

CP is the combined charge-parity transformation. Parity transformations describe discrete transitions from left- to right-handed coordinate systems (and vice versa) via $\vec{x} \rightarrow -\vec{x}$. Charge transformations flip all charges similar to complex conjugation which flips the sign in front of the imaginary unit.

the SM generations and gives a possibility for CP violation, which was the reason why Kobayashi and Maskawa extended the two-generation description to a third generation. A mixing matrix of two flavors cannot violate CP because all complex phases can be absorbed in redefinitions of the fermion fields whereas a 3×3 unitary matrix has three angles and six phases from which only five phases can be removed because one global phase can stay arbitrary. The most convenient way of parametrizing the three rotations with one complex phase was introduced by [22] and is commonly used as “standard parametrization” [23]. This parametrization decomposes the CKM matrix into three successive rotation with one mixing angle for each rotation in the 2-3, 1-3 and 1-2 plane, respectively:


$$\begin{aligned} V_{\text{CKM}} &= V_{23}(\theta_{23})V_{13}(\theta_{13}, \delta_{\text{CKM}})V_{12}(\theta_{12}) \quad (2.10) \\ &= \begin{pmatrix} 1 & 0 & 0 \\ 0 & c_{23} & s_{23} \\ 0 & -s_{23} & c_{23} \end{pmatrix} \begin{pmatrix} c_{13} & 0 & s_{13}e^{-i\delta_{\text{CKM}}} \\ 0 & 1 & 0 \\ -s_{13}e^{i\delta_{\text{CKM}}} & 0 & c_{13} \end{pmatrix} \begin{pmatrix} c_{12} & s_{12} & 0 \\ -s_{12} & c_{12} & 0 \\ 0 & 0 & 1 \end{pmatrix} \\ &= \begin{pmatrix} c_{12}c_{13} & s_{12}c_{13} & s_{13}e^{-i\delta_{\text{CKM}}} \\ -s_{12}c_{23} - c_{12}s_{23}s_{13}e^{i\delta_{\text{CKM}}} & c_{12}c_{23} - s_{12}s_{23}s_{13}e^{i\delta_{\text{CKM}}} & s_{23}c_{13} \\ s_{12}s_{23} - c_{12}c_{23}s_{13}e^{i\delta_{\text{CKM}}} & -c_{12}s_{23} - s_{12}c_{23}s_{13}e^{i\delta_{\text{CKM}}} & c_{23}c_{13} \end{pmatrix}, \end{aligned}$$

with $c_{ij} = \cos \theta_{ij}$, $s_{ij} = \sin \theta_{ij}$ and δ_{CKM} is the CKM CP-phase. We single out two important features of this parametrization which will be convenient in the further course of this thesis: (a) the separation into three rotations in three different flavor planes allows to keep track of the individual contributions in the final result (this can be seen from the upper left matrix elements, where $V_{ij}^{\text{CKM}} \sim s_{ij}$) and (b) the CP phase sits in the 1-3 rotation which for both quark and lepton mixing has the smallest angle.

The SM as described so far has no room for lepton mixing. The Yukawa Lagrangian (2.5) can be exactly diagonalized for the charged leptons, because we have two free rotations that can be absorbed into redefinitions of the lepton fields. Mass terms for neutrinos are not scheduled in the SM. As it is a minimal theory, there are no right-handed neutrinos since they are pure gauge singlets and do not interact. The only interaction they would have are Yukawa interactions with left-handed neutrinos. Flavor mixing, however, needs fermion masses. So the observation of neutrino oscillations (see as reviews [23, 24, and references therein]) already hints towards new physics beyond the minimal SM. More about neutrino flavor follows in Sec. 2.4.

The CKM matrix has been measured with amazing precision [23]

The magnitudes of CKM elements can be displayed as follows $|V_{\text{CKM}}| =$



$$|V_{\text{CKM}}| = \begin{pmatrix} 0.97427 \pm 0.00014 & 0.22536 \pm 0.00061 & 0.00355 \pm 0.00015 \\ 0.22522 \pm 0.00061 & 0.97343 \pm 0.00015 & 0.0414 \pm 0.0012 \\ 0.00886^{+0.00033}_{-0.00032} & 0.0405^{+0.0011}_{-0.0012} & 0.99914 \pm 0.00005 \end{pmatrix}. \quad (2.11)$$

2.2 SUPERSYMMETRIC EXTENSIONS

De gustibus non est disputandum.

—Jean Anthelme Brillat–Savarin

Supersymmetry (SUSY) is the only symmetry extension of the S -matrix which is *not* a direct product of any internal symmetry group and the Poincaré group of space-time as stated in the Coleman–Mandula (CM) theorem [26]. As loophole in the CM theorem, the Haag–Łopuszański–Sohnius theorem [27] proposes supersymmetries as extension of the space-time symmetry (Poincaré symmetry) in a way that fermionic generators (in the spinor representation of the Lorentz group) transform bosons into fermions and vice versa.

The fermionic generators Q_α^N of SUSY obey a so-called pseudo Lie algebra [27], which is the anti-commutator relation

$$\{Q_\alpha^N, \bar{Q}_\beta^M\} = 2\gamma_{\alpha\beta}^\mu P_\mu \delta^{NM}, \quad (2.12)$$

with the Dirac γ -matrices as structure constants (together with a Kronecker δ). The indices N, M count the number of SUSY generators. $N = 1$ corresponds to one generator as in the MSSM. The operators Q_α^N are Majorana spinors, where α is a spinor index; the Hermitian conjugate is $\bar{Q}_\alpha^N = (Q_\alpha^N)^\dagger$, and P_μ the generator of space-time translations also known as 4-momentum vector. Conserved currents related to SUSY (“supercurrents”) are spin 3/2 currents, where the conserved quantity of the energy-momentum P_μ is the energy-momentum tensor, a spin 2 quantity, see e. g. [28]. In this way, SUSY is a candidate to combine gravity and gauge theories—the field connected to the supercurrent is the spin 3/2 gravitino whereas the one related to the conserved energy-momentum is the graviton. However, SUSY extends the Poincaré algebra of space-time and therefore also the structure of space-time itself has to be extended, which leads to the “superspace”. The Poincaré group includes the four-dimensional rotations of the Lorentz group $SO(1, 3)$ and translations in Minkowski space

$$x^\mu \rightarrow x'^\mu = \Lambda^\mu_\nu x^\nu + a^\nu,$$

with the Lorentz transformation Λ^μ_ν and a constant vector a^μ . Generator of spatial translations is the 4-momentum P^μ , for which

$$[P_\mu, P_\nu] = 0, \quad (2.13a)$$

$$[L_{\mu\nu}, P_\rho] = i(g_{\mu\nu}P_\rho - g_{\mu\rho}P_\nu) \quad (2.13b)$$

hold with $L^{\mu\nu} = i(x^\mu \partial^\nu - x^\nu \partial^\mu) = x^\mu P^\nu - x^\nu P^\mu$ and

$$[L^{\mu\nu}, L^{\rho\sigma}] = i(g^{\nu\rho}L^{\mu\sigma} - g^{\mu\rho}L^{\nu\sigma} - g^{\nu\sigma}L^{\mu\rho} + g^{\mu\sigma}L^{\nu\rho}). \quad (2.13c)$$

Eqs. (2.13) are called the *Poincaré algebra*.

The fundamental fields of the SM fit into irreducible representations of

A direct product means that any internal symmetry generator shall commute with the generators of Poincaré symmetry. Fermionic generators, however, obey anti-commutation relations which lead to so-called graded Lie algebras (details in any good textbook about supersymmetry, e. g. [25]).

The superspace is a conceptually different concept than the object introduced in [29].

We consider Minkowski space with the metric $g_{\mu\nu} = \text{diag}(1, -1, -1, -1)$.

Scalars (trivial representation), left and right chiral spinors, vectors, ...

the Poincaré group whose invariants are related to mass and spin. Extending the Poincaré algebra with the fermionic generators from Eq. (2.12), one gets in addition

$$[P^\mu, Q_\alpha] = 0, \quad (2.14a)$$

$$[L^{\mu\nu}, Q_\alpha] = -\Sigma_{\alpha\beta}^{\mu\nu} Q_\beta. \quad (2.14b)$$

$\Sigma_{\mu\nu}$ can be defined via the γ -matrices, $\Sigma_{\mu\nu} = \frac{i}{4} [\gamma_\mu, \gamma_\nu]$.

Left and right chiral superfields, Vector superfields, ...

The spinorial coordinates are Grassmann numbers, $\theta_\alpha^2 = 0$.

Eqs. (2.12), (2.13) and (2.14) form the *super-Poincaré algebra*. Particles of supersymmetric field theories fit into irreducible representations of the super-Poincaré algebra. A *supermultiplet* contains bosonic and fermionic degrees of freedom; in a similar manner fermionic coordinates θ are needed. Superspace coordinates are complex,

$$\begin{aligned} y^\mu &= x^\mu - i\theta\sigma^\mu\bar{\theta}, \\ \bar{y}^\mu &= x^\mu + i\theta\sigma^\mu\bar{\theta}. \end{aligned} \quad (2.15)$$

We have $\sigma^\mu = (\mathbb{1}_2, \sigma^i)$ ($i = 1, 2, 3$), the vector of Pauli matrices. All superfields \mathcal{F} are functions of the superspace coordinates, $\mathcal{F}(x, \theta, \bar{\theta})$.

CHIRAL SUPERFIELDS The lowest representation of the Super Poincaré algebra are *chiral superfields*, that contain a scalar field ϕ and a fermionic component ξ . Additionally, there is an *auxiliary field* F that can be eliminated with the equations of motion (eom) because there are no kinetic terms for F in the SUSY Lagrangian. These eom result in scalar mass terms (F -terms). For completeness, we give the full superspace expansion of the left chiral superfield $\Phi = \{\phi, \xi, F\}$ and its complex conjugate

The fermion field ξ is a Weyl spinor.

The complex conjugated field Φ^\dagger is called right-chiral.

$$\begin{aligned} \Phi(y, \theta) &= \phi(y) + \sqrt{2}\theta\xi(y) + \theta\theta F(y), \\ \Phi^\dagger(\bar{y}, \bar{\theta}) &= \phi^*(\bar{y}) + \sqrt{2}\bar{\theta}\bar{\xi}(\bar{y}) + \bar{\theta}\bar{\theta}F^*(\bar{y}). \end{aligned} \quad (2.16)$$

It is convenient (and also convention) to work only with left-chiral superfields, so right-handed fermions of the SM are squeezed into the left-chiral representation via charge and complex conjugation. If we have a SM fermion f_L and its scalar superpartner \tilde{f}_L , they fit into the left-chiral $F_L = \{\tilde{f}_L, f_L\}$. Their right-handed colleagues are put into a left-chiral superfield as $\bar{F}_R = \{\tilde{f}_R^*, f_R^c\}$. It is necessary to treat right-handed fermions separately, because they transform differently under the SM gauge group. The gauge representation and the Poincaré representation, however, must not be mixed up. Poincaré left-handed fields can be obtained via charge conjugation. Note that charge conjugation does not change the gauge representation from the singlet to a doublet representation.

The bar over F_R is not to be confused with the Dirac-bar. It shall keep in mind that the component fields are conjugated.

VECTOR SUPERFIELDS Chiral superfields are spin 0 and spin 1/2 fields. The spin 1 gauge bosons of the SM have to have a different super-Poincaré representation. Vector superfields V are real fields, so $V^\dagger = V$, and can be constructed out of chiral superfields, see e. g. [30]. There is a gauge freedom (“supergauge”) in the space of vector superfields which allows to choose a particular gauge to reduce the most general representation of a

vector superfield to one vector field $A_\mu(x)$, one complex two-component spinor $\lambda(x)$ and one auxiliary field $D(x)$ which again can be eliminated using the eom. This special supergauge choice is known as *Wess–Zumino gauge* [31] and we have

$$V_{W-Z}(x, \theta, \bar{\theta}) = \theta \sigma^\mu \bar{\theta} A_\mu(x) + \theta \theta \bar{\theta} \bar{\lambda}(x) + \theta \lambda(x) \bar{\theta} \bar{\theta} + \frac{1}{2} \theta \theta \bar{\theta} \bar{\theta} D(x). \quad (2.17)$$

INTERACTING SUPERFIELDS The non-gauge interactions of chiral superfields can be written in the following *superpotential*:

$$\mathcal{W}(\Phi) = h_i \Phi_i + \frac{1}{2} \mu_{ij} \Phi_i \Phi_j + \frac{1}{3!} f_{ijk} \Phi_i \Phi_j \Phi_k. \quad (2.18)$$

The superpotential is a holomorphic function of chiral superfields, contains therefore only left-chiral (or only right-chiral) superfields and has mass dimension three. The supersymmetric Lagrangian can be obtained from the superpotential as the “highest component”, i. e. the coefficient in front of $\theta\theta$. This can be seen from the definition of the action [32]

$$S = \int d^4x \int d^2\theta d^2\bar{\theta} \left[\Phi_i^\dagger \Phi_i + \mathcal{W}(\Phi) \delta^{(2)}(\bar{\theta}) + \mathcal{W}^\dagger(\Phi^\dagger) \delta^{(2)}(\theta) \right].$$

The kinetic term $\Phi_i^\dagger \Phi_i$ can be put into (super)gauge invariant shape by inserting the gauge supermultiplet

$$\Phi_i^\dagger \Phi_i \rightarrow \Phi_i^\dagger \left(e^{gV} \right)_{ij} \Phi_j$$

with some gauge coupling g , such that

$$\mathcal{L} = \Phi_j^\dagger \left(e^{gV} \right)_{ij} \Phi_j \Big|_{\theta\theta\bar{\theta}\bar{\theta}} + \left[\mathcal{W}(\Phi) \Big|_{\theta\theta} + \text{h. c.} \right]. \quad (2.19)$$

SUPERSYMMETRIC MASS TERMS AND SCALAR POTENTIALS There are still auxiliary fields around. Eliminating the F -fields with $\partial\mathcal{L}/\partial F_i^* = 0$ and $\partial\mathcal{L}/\partial F_i = 0$ leads to

$$\begin{aligned} F_i &= - \frac{\partial \mathcal{W}^\dagger}{\partial \Phi_i^\dagger} \Big| = -h_i^* - m_{ij}^* \phi_j^* - \frac{1}{2} f_{ijk}^* \phi_j^* \phi_k^*, \\ F_i^* &= - \frac{\partial \mathcal{W}}{\partial \Phi_i} \Big| = -h_i - m_{ij} \phi_j - \frac{1}{2} f_{ijk} \phi_j \phi_k, \end{aligned} \quad (2.20)$$

which results in the scalar F -term potential

$$V_F(\phi, \phi^*) = F_i^* F_i = \frac{\partial \mathcal{W}^\dagger}{\partial \Phi_i^\dagger} \Big| \frac{\partial \mathcal{W}}{\partial \Phi_i} \Big|. \quad (2.21)$$

The D -terms are eliminated analogously via $\partial\mathcal{L}/\partial D = 0$ with

$$D^a = -g \phi_i^\dagger T_{ij}^a \phi_j, \quad (2.22)$$

for each gauge symmetry with coupling g and generators T_{ij}^a . Analogously, we get the D -term potential

$$V_D(\phi, \phi^*) = \frac{1}{2} D^a D^a = g^2 \left(\phi_j^\dagger T_{ij}^a \phi_j \right) \left(\phi_k^\dagger T_{kl}^a \phi_l \right), \quad (2.23)$$

The trilinear couplings f_{ijk} of the superpotential are dimensionless and symmetric in $\{i, j, k\}$, the bilinear couplings m_{ij} have mass dimension one and the tadpole coupling h_i dimension two.

Integration over Grassmann numbers behaves like differentiation, “ $\int d^2\theta = \partial^2/\partial\theta^2$ ”.

The notation $\Big|_X$ means that the coefficient in front of X is taken.

The notation $\Big|_{\theta=0=\bar{\theta}}$ means that the derivative is evaluated at $\theta=0=\bar{\theta}$.

Superpartners are abbreviated with a tilde over the symbol, \tilde{f} for a sfermion or squark \tilde{q} ; similarly \tilde{W} , \tilde{B} ; admixtures like neutralinos $\tilde{\chi}^0$ or charginos $\tilde{\chi}^\pm$.

The term soft breaking shall reflect the fact that all SUSY breaking couplings are related to the couplings of the superpotential and the full theory still is supersymmetric, only the ground state breaks the symmetry. Soft breaking terms are hence related to a vev and are dimensionful quantities that do not introduce quadratic divergences.

In a SUSY theory, bosonic and fermionic zero-point energies exactly cancel to zero in contrast to a non-supersymmetric theory.

SETTING THE LANGUAGE Fermions of the SM get scalar superpartners in a supersymmetric theory. Those are called *scalar fermions* or *sfermions*. Vector fields of the SM get fermionic (Majorana) spinor partners that are denoted with the suffix *-ino* like *gaugino*, *gluino*, *electroweakino*. The superpartners of the Higgs scalars are fermions as well and therefore also called *higgsinos* (though Higgs fields are chiral superfields).

2.2.1 How to Break Supersymmetry

Unfortunately, SUSY has not yet been observed in fundamental interactions. If so, e. g. charged scalar particles with the mass of the electron must have been seen. Since no selectrons appear in atomic physics, no squarks have been detected in high energy collisions, gluinos and electroweakinos hide maybe somewhere, SUSY has to be badly broken. Actually, SUSY breaking is constructed in a way to happen “softly”. However, mass terms for superpartners are needed to shift their masses into the TeV regime to cope with their hide-and-seek play. We do not go into the details of collider phenomenology, maybe there are some stripes left in the SUSY landscape to find at least some superpartners at the electroweak scale (100 GeV rather than 10 TeV). The SUSY corrections we calculate and exploit in Chapter 3 anyway are *non-decoupling* contributions. So, if all SUSY parameters are shifted uniformly to higher scales, the results do not alter. In this way, we may use flavor physics as an indirect probe of SUSY breaking. Soft breaking is expected to be the result of a spontaneous symmetry breakdown and all mass terms and mass dimensional couplings are related to some vev. In this case, if SUSY is broken via a process as the Higgs mechanism, all masses generated by this breaking are of the same scale. However, breaking of SUSY is different from spontaneous breaking of any internal symmetry: broken SUSY leads to a non-zero vacuum energy density since a supersymmetric ground state always has exactly zero energy. We are only interested in the phenomenological output of SUSY breaking that can be described very elegantly as shown below. There is a vast amount of concepts on the market which cannot be reviewed as it is to be seen complementary to most SUSY phenomenology. We also can only refer to a small subset of literature which comprises interesting ideas like dynamical SUSY breaking [33–37]. SUSY breaking occurs in a “hidden” sector where the highest component of a superfield acquires a vev—in case of chiral superfields one has *F*-type breaking [38]; in case of vector supermultiplets *D*-type breaking [39]. Neither in the description of O’Raifeartaigh nor Fayet–Iliopoulos a deeper reason for the vev is given as it is in the dynamical models. SUSY breaking has then to be transmitted from the hidden to the visible sector via some mediator fields—popular attempts are gauge mediation, see e. g. as review [40] (also in combination with dynamical breaking [41, 42], “supercolor” in contrast to technicolor [43–45]), and anomaly mediation [46, 47]. Minimal supergravity [48] allows to combine and break local $N = 1$ SUSY and grand

unified theories. Finally, the determination of the Higgs boson mass allows to slightly discriminate between the different types of models [49].

For the phenomenological processing of soft SUSY breaking, we may be ignorant of the dynamics behind SUSY breaking and mediation of SUSY breaking. Instead, the soft breaking terms are added to the supersymmetric Lagrangian without deeper knowledge of their origin,

$$\mathcal{L} = \mathcal{L}_{\text{SUSY}} + \mathcal{L}_{\text{soft}}. \quad (2.24)$$

The soft breaking Lagrangian $\mathcal{L}_{\text{soft}}$ comprises mass terms \tilde{m}_ϕ^2 for the scalar components of chiral superfields and gaugino Majorana mass terms M_λ for the fermionic parts of vector supermultiplets. Moreover, mimicking the polynomial structure of the superpotential there are trilinear, bilinear and linear terms in the scalar components of chiral superfields allowed

$$\begin{aligned} \mathcal{L}_{\text{soft}} = & -\phi_i^* \left(\tilde{m}_\phi^2 \right)_{ij} \phi_j - \frac{1}{2} (M_\lambda \lambda^a \lambda^a + \text{h. c.}) \\ & + \left(\frac{1}{3!} \mathcal{A}_{ijk} \phi_i \phi_j \phi_k - \frac{1}{2} \mathcal{B}_{ij} \phi_i \phi_j + \mathcal{C}_i \phi_i + \text{h. c.} \right). \end{aligned} \quad (2.25)$$

Certainly, the terms of (2.25) are not allowed to break internal symmetries. The \mathcal{A} - and \mathcal{B} -terms are symmetric in their indices and obviously carry mass dimension one and two, respectively. \mathcal{C} -terms are only present if there are tadpole terms in the superpotential which only may occur for gauge singlets. We see no connection to superpotential parameters in the SUSY breaking terms and stick to the notation of Eq. (2.25) instead of factorizing artificially the superpotential parameters as partially done in the literature [32] writing e. g. $\mathcal{A}_{ijk} = \mathcal{A}_{ijk} / f_{ijk}$.

2.2.2 The Minimal Supersymmetric Standard Model

We now have the ingredients to set up the Minimal Supersymmetric Standard Model (MSSM)—which indeed comprises broken SUSY. The matter content of the MSSM is given by the chiral superfields of 3×15 SM fermions (2.1), the vector supermultiplets of the $\text{SU}(3)_c \times \text{SU}(2)_L \times \text{U}(1)_Y$ gauge interactions and the Higgs—which is part of a chiral superfield and has to be doubled [52]. The today's language of the MSSM was basically set by [53]; a comprehensive overview of supersymmetry, supergravity and particle physics was given in [54].

The superpotential of the MSSM is given by

$$\mathcal{W}_{\text{MSSM}} = \mu H_d \cdot H_u - Y_{ij}^e H_d \cdot L_{L,i} \bar{E}_{R,j} + Y_{ij}^u H_u \cdot Q_{L,i} \bar{U}_{R,j} - Y_{ij}^d H_d \cdot Q_{L,i} \bar{D}_{R,j}, \quad (2.26)$$

where the bilinear μ -term is the only dimensionful parameter of the superpotential and itself no SUSY parameter which causes conceptual problems and solutions to that problem [55, 56]. In order to have Yukawa couplings to both up and down type fermions, there are two Higgs doublets H_u and

Soft breaking does not induce quadratic divergences at one-loop [50].

The signs of \mathcal{A} -, \mathcal{B} - and \mathcal{C} -terms are of no meaning and depend on the convention. To interpret soft breaking masses as masses, their signs are fixed.

We do not consider the “non-holomorphic” \mathcal{A} -terms like $\mathcal{A}'_{ijk} \phi_i \phi_j \phi_k^$ [51].*

Looking at the dates of the most important SUSY publications, we find the golden age of SUSY about more than thirty years ago.

Fermion masses are with $\langle h_u^0 \rangle = v_u$ and $\langle h_d^0 \rangle = v_d$ given by $m^u = v_u Y^u / \sqrt{2}$, $m^d = v_d Y^d / \sqrt{2}$ and $m^e = v_d Y^e / \sqrt{2}$.

H_u has hypercharge $+1/2$, $H_d -1/2$.

H_u couples to up type fields, H_d to down type fields in Eq. (2.26).

The doublet superfields are correspondingly $Q_L = \{\tilde{q}_L, q_L\}$ and $L_L = \{\tilde{\ell}_L, \ell_L\}$.

Despite of the subscript R , f_R^c are left-handed Weyl fermions.

$\mathcal{L}_{\text{soft}}$ together with F - and D -terms gives the mass squared matrices of sfermions and the gaugino/higgsino mass matrices. Diagonalization of these matrices result in flavor changing vertices. Mass and diagonalization matrices are specified in App. A.

Clarifications about the spinor notation in App. A.

The F -terms give additional interactions of sfermions and Higgses and are of importance for sfermion mass terms and the analysis of the minimum structure of the scalar potential. The D -terms are determined by gauge couplings squared and give the quadrilinear terms in the Higgs (and sfermion) potential.

H_d with different $U(1)_Y$ -charges (capitals denote chiral superfields),

$$H_u = \begin{pmatrix} H_u^+ \\ H_u^0 \end{pmatrix}, \quad H_d = \begin{pmatrix} H_d^0 \\ -H_d^- \end{pmatrix}. \quad (2.27)$$

The left-handed quarks and leptons form the $SU(2)_L$ -doublet chiral superfields $Q_L = (U_L, D_L)$ and $L_L = (N_L, E_L)$ with $U_L = \{\tilde{u}_L, u_L\}$, $D_L = \{\tilde{d}_L, d_L\}$ up and down (s)quarks and $N_L = \{\tilde{\nu}_L, \nu_L\}$, $E_L = \{\tilde{e}_L, e_L\}$ (s)neutrino and (s)electron, respectively. The $SU(2)_L$ singlets are in the left-chiral representations $\bar{U}_R = \{u_R^*, u_R^c\}$, $\bar{D}_R = \{d_R^*, d_R^c\}$ and $\bar{E}_R = \{e_R^*, e_R^c\}$. Generation indices are suppressed, where in Eq. (2.26) $i, j = 1, 2, 3$.

SOFT BREAKING IN THE MSSM SUSY has to be softly broken in the MSSM, so we set the soft breaking Lagrangian according to Eq. (2.25) with the fields of the MSSM and have

$$\begin{aligned} -\mathcal{L}_{\text{soft}}^{\text{MSSM}} = & \tilde{q}_{L,i}^* (\tilde{m}_Q^2)_{ij} \tilde{q}_{L,j} + \tilde{u}_{R,i}^* (\tilde{m}_u^2)_{ij} \tilde{u}_{R,j} + \tilde{d}_{R,i}^* (\tilde{m}_d^2)_{ij} \tilde{d}_{R,j} \\ & + \tilde{\ell}_{L,i}^* (\tilde{m}_\ell^2)_{ij} \tilde{\ell}_{L,j} + \tilde{e}_{R,i}^* (\tilde{m}_e^2)_{ij} \tilde{e}_{R,j} \\ & + \left[h_d \cdot \tilde{\ell}_{L,i} A_{ij}^e \tilde{e}_{R,j}^* + h_d \cdot \tilde{q}_{L,i} A_{ij}^d \tilde{d}_{R,j}^* + \tilde{q}_{L,i} \cdot h_u A_{ij}^u \tilde{u}_{R,j}^* + \text{h. c.} \right] \\ & + m_{h_d}^2 |h_d|^2 + m_{h_u}^2 |h_u|^2 + (B_\mu h_d \cdot h_u + \text{h. c.}) \\ & + \frac{1}{2} (M_1 \tilde{\lambda}_0 \tilde{\lambda}_0 + \text{h. c.}) + \frac{1}{2} (M_2 \vec{\lambda} \vec{\lambda} + \text{h. c.}) \\ & + \frac{1}{2} (M_3 \tilde{\lambda}^a \tilde{\lambda}^a + \text{h. c.}). \end{aligned} \quad (2.28)$$

The scalar mass and trilinear terms are self-explanatory; B_μ is the Higgs B -term and gaugino masses are $M_{1,2,3}$ with labels according to the gauge couplings $g_{1,2,3}$. The gauginos are written as Weyl spinors.

THE 2HDM OF THE MSSM SUSY dictates the Lagrangian: the supersymmetric part is related to the superpotential which sets the interactions among chiral superfields; the SUSY breaking part is given by $\mathcal{L}_{\text{soft}}^{\text{MSSM}}$. The scalar potential, however, does not only include $V_{\text{soft}} = -\mathcal{L}_{\text{soft}}$, but also F -terms and D -terms. We have two Higgs doublets, so the most general Higgs potential resembles the potential of a two-Higgs-doublet model (2HDM) [57, 58]:

$$\begin{aligned} V = & m_{11}^2 h_d^\dagger h_d + m_{22}^2 h_u^\dagger h_u + (m_{12}^2 h_u \cdot h_d + \text{h. c.}) \\ & + \frac{\lambda_1}{2} (h_d^\dagger h_d)^2 + \frac{\lambda_2}{2} (h_u^\dagger h_u)^2 + \lambda_3 (h_u^\dagger h_u) (h_d^\dagger h_d) \\ & + \lambda_4 (h_u^\dagger h_d) (H_d^\dagger H_u) + \left(\frac{\lambda_5}{2} (H_u \cdot H_d)^2 \right. \\ & \left. - \lambda_6 (H_d^\dagger H_d) (H_u \cdot H_d) - \lambda_7 (H_u^\dagger H_u) (H_u \cdot H_d) + \text{h. c.} \right). \end{aligned} \quad (2.29)$$

In the MSSM, the parameters of Eq. (2.29) are calculated by the methods described in this chapter above. Working this out, one finds that no contributions at the tree-level for the self-couplings $\lambda_{5,6,7}$ exist. Moreover, the potential is constructed in such a way, that λ_4 does not show up in neutral Higgs interactions. The mass terms are a combination of the μ -parameter and soft breaking masses:

$$m_{11}^2 = |\mu|^2 + m_{h_d}^2, \quad m_{22}^2 = |\mu|^2 + m_{h_u}^2, \quad m_{12}^2 = B_\mu, \quad (2.30a)$$

$$\lambda_{1,2} = -\lambda_3 = \frac{g_1^2 + g_2^2}{4}, \quad \lambda_4 = \frac{g_2^2}{2}. \quad (2.30b)$$

For a reasonable theory, the scalar potential has to be bounded from below, i. e. there are no directions with $V \rightarrow -\infty$. There are three simple conditions to be fulfilled in order to avoid unboundedness from below [58],

$$\lambda_1 > 0, \quad \lambda_2 > 0 \quad \text{and} \quad \lambda_3 > -\sqrt{\lambda_1 \lambda_2}, \quad (2.31)$$

which are always fulfilled in the MSSM at tree-level with (2.30b). No more conditions are needed for the tree-level MSSM, because $\lambda_{5,6,7} = 0$.

If the mass matrix formed out of m_{ij}^2 has one negative eigenvalue, the scalar components of the Higgs doublets acquire vevs

$$\langle h_u \rangle = \frac{1}{\sqrt{2}} \begin{pmatrix} 0 \\ v_u \end{pmatrix}, \quad \langle h_d \rangle = \frac{1}{\sqrt{2}} \begin{pmatrix} v_d \\ 0 \end{pmatrix},$$

assuming that electromagnetic U(1) stays intact. The individual vevs are fixed via the W mass, $v_u^2 + v_d^2 = v^2 = 4M_W^2 / g_2^2$, and the ratio is to be seen as free parameter

$$\tan \beta = \frac{v_u}{v_d}. \quad (2.32)$$

The requirement of spontaneous symmetry breaking gives relations between the tree-level parameters of the 2HDM potential (2.29)

$$m_{11}^2 = m_{12}^2 \tan \beta - \frac{v^2}{2} \cos 2\beta \lambda_1, \quad (2.33a)$$

$$m_{22}^2 = m_{12}^2 \cot \beta + \frac{v^2}{2} \cos 2\beta \lambda_2. \quad (2.33b)$$

We get the mass matrices for CP-even and CP-odd as well as charged components as second derivative of the potential with respect to the corresponding fields. Expanding the Higgs doublets around their vevs,

$$h_u = \begin{pmatrix} \chi_u^+ \\ \frac{1}{\sqrt{2}} (v_u + \varphi_u^0 + i\chi_u^0) \end{pmatrix}, \quad h_d = \begin{pmatrix} \frac{1}{\sqrt{2}} (v_d + \varphi_d^0 + i\chi_d^0) \\ -\chi_d^- \end{pmatrix},$$

we have eight dynamical fields (charged fields are complex) out of which three Goldstone bosons have to be eaten by the gauge fields; five physical

This can be seen writing $h_u^\dagger h_d = h_u^- h_d^0 - h_u^{0} h_d^-$.*

We then have $v_u = v \sin \beta$ and $v_d = v \cos \beta$.

Conditions (2.33) ensure that the global minimum of (2.29) is determined by v_u and v_d .

fields remain: two CP-even (h^0 and H^0), one CP-odd (A^0) and the charged Higgses (H^\pm). If CP is conserved and not spontaneously broken; otherwise h^0 , H^0 and A^0 mix. The mass of the pseudoscalar A^0 can be related to the yet unconstrained tree-level mass parameter, $2m_{12}^2 = m_{A^0}^2 \sin 2\beta$, and is then also a free parameter of the theory.

All we have at hand are g_1^2 , g_2^2 and vev relations, v^2 and $\tan \beta$.

More about effective potentials in Chapter 4. The idea is to calculate the Higgs potential at one- or two-loop order and obtain the masses as for the tree-level potential.

We use FeynHiggs at some later point to determine the lightest MSSM Higgs mass.

The MSSM predicts a rather light Higgs boson $m_{h^0} \leq M_Z$ if no radiative corrections are taken into account. Already one-loop corrections lift the lightest Higgs mass well above M_Z [59–62] and are quite needed, if we want to explain the discovered Higgs boson mass at 125 GeV [15, 16]. The dominant radiative corrections at one-loop are related to the large top Yukawa coupling Y_t and originate in diagrams with stops or tops. If already one-loop corrections are large, two loops are of equal importance and have been calculated diagrammatically [63–66] as well as in the effective potential approach including two-loop effects [67–72]. The independent approaches of diagrammatic and effective potential calculations were shown to coincide up to known differences [73]. Current up-to-date tools for numerical evaluation of MSSM calculations obtain those corrections (and some more) as FeynHiggs [66, 74–77] or popular MSSM spectrum generators as SoftSUSY [78], SuSpect [79] and SPheno [80]. The three-loop SUSY-QCD effects are also available [81, 82] and ready to use in the computer code H3m [82]. Three-loop corrections are not only important to reduce the theoretical uncertainty in the precise prediction of the light MSSM Higgs mass but also give important contributions for multi-TeV stops [83]. Spectrum generators may be combined and compared using the Mathematica package SLAM [84].

If superpartners are generically heavy and the Higgs scalars of the 2HDM, however, remain light, the MSSM can be matched at the full one-loop level to an effective 2HDM where the couplings are determined via SUSY parameters at the decoupling scale [85].

2.2.3 Radiative Flavor Violation in the MSSM

The masses and mixings of the fermions in the SM (and MSSM) enter via the Yukawa couplings which are *ad hoc* parameters, though dimensionless. A problem or rather a puzzle in that respect is the question why the masses (Yukawa couplings) of the first two generations are so small compared to the third generation. Two–Higgs–Doublet models give a handle on the comparability of top and bottom mass via $\tan \beta$, since in the MSSM $m_t/m_b = \tan \beta Y_t/Y_b$ and $m_t(1 \text{ TeV})/m_b(1 \text{ TeV}) \approx 60$: assuming $\tan \beta = 60$, the top and bottom Yukawa coupling are of equal size, $Y_t \approx Y_b$.

It is intriguing to keep only the large third generation Yukawa couplings and postulate

$$Y_{u,d,e} = \begin{pmatrix} 0 & 0 & 0 \\ 0 & 0 & 0 \\ 0 & 0 & Y_{t,b,\tau} \end{pmatrix},$$

Evaluating running \overline{MS} masses at the SUSY scale.

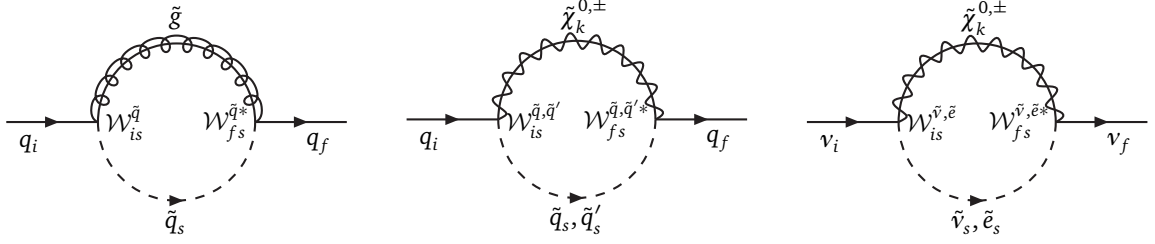


FIGURE 1: Flavor changing self-energies in the MSSM: gluino–squark, neutralino/chargino–squark and neutralino–sneutrino/chargino–slepton loops (from left to right). Similar diagrams exist for the charged lepton propagator.

via imposing flavor symmetries as \mathbb{Z}_2 or $U(2)$ for the first two generations, see e. g. [87–92]. The idea of vanishing zeroth order fermion masses with a mass generation at the loop-level was already pointed out by Weinberg [93] and applied in the context of grand unified models [94, 95]; an exhaustive analysis of radiative fermion masses in grand unified theories can be found in [96]. Radiative SUSY mass models allow to produce certain hierarchies in the mass matrices [97], induce chiral symmetry breaking via soft SUSY breaking [98] and generate Yukawa couplings radiatively [99]. Moreover, SUSY threshold corrections are important to obtain Yukawa unification [100]. Imposing non-minimal flavor violation (NMFV) in the MSSM, radiative flavor violation (RFV) can be used to suppress the SUSY flavor changing contributions and generate the quark mixing of the CKM matrix radiatively [87–90]. On the other hand, some contributions can be enhanced [102]. RFV in the MSSM has been extensively studied and constrains the parameter space giving additional relations between flavor observables [103–106].

We do not follow the very ambitious goal at the moment to simultaneously generate the fermion masses radiatively and accomplish for the mixing. The motivation behind RFV is to see the flavor changing off-diagonals in the CKM matrix (2.11) as small perturbations arising from higher-order effects. Flavor mixing in this description enters via loops of supersymmetric particles. The general soft SUSY breaking Lagrangian of Eq. (2.28) has arbitrary flavor structure that can be confined using either minimal flavor violation (MFV) techniques [107–109] or RFV. Key ingredient are flavor changing self-energies shown in Fig. 1 which can be decomposed in chirality-flipping and chirality conserving pieces

$$\begin{aligned} \Sigma_{fi}(p) &= \Sigma_{fi}^{RL}(p^2)P_L + \Sigma_{fi}^{LR}(p^2)P_R \\ &+ \not{p} \left[\Sigma_{fi}^{LL}(p^2)P_L + \Sigma_{fi}^{RR}(p^2)P_R \right], \end{aligned} \quad (2.34)$$

with $\Sigma_{fi}^{LL,RR}(p^2) = \left(\Sigma_{if}^{LL,RR}(p^2) \right)^*$ and $\Sigma_{fi}^{RL}(p^2) = \left(\Sigma_{if}^{LR}(p^2) \right)^*$.

The application of RFV to the lepton mixing matrix is given in Chapter 3, where we calculate SUSY threshold corrections to degenerate neutrino masses and generate both mass splittings and mixing angles. In the further course of Chapter 3, we apply the mixing matrix renormalization of [110]

An amusing application of the radiative mass mechanism was found in the observation that $m_e/m_\mu \approx \mathcal{O}(\alpha)$ [86].

A very brief overview about Grand Unification is given in Sec. 2.3.

With the term NMFV we denote potentially arbitrary flavor structures in the soft breaking terms, especially the A-terms. The consequences of NMFV in Supra theories were discussed in [101].

MFV means that all FV stems from the standard Yukawa couplings—in softly broken SUSY this means that e. g. trilinear A-terms are chosen aligned with Yukawa couplings.

See e. g. [110, 111].

to the lepton mixing matrix via SUSY self-energies. This approach has already been used in the CKM renormalization of the MSSM [89, 90] and for the leptonic case [112], where the neutrino self-energies were omitted. They, however, may give sizable contributions if neutrinos are not hierarchical in their masses.

2.3 EXTENDING THE GAUGE SECTOR

Supersymmetry is a symmetry extension of the fundamental description of particle interactions. The symmetry group which is afflicted is the Poincaré group of space-time. According to the Haag–Łopuszański–Sohnius theorem, SUSY is the only non-trivial extension of the symmetries of the S-matrix. However, a *trivial* symmetry extension in terms of the Coleman–Mandula theorem is an enlargement of the internal symmetry group. This can be either accomplished by adding additional gauge group factors to the SM group or by embedding the SM gauge group into *one* symmetry group. The latter is known as *Grand Unification* (GU). Towards a higher symmetry description of nature, the most natural would be to combine SUSY and GU. We comment briefly on Grand and Partial Unification in the following to get a perspective on the unified picture.

Grand Unified theories also give natural explanations of puzzles like neutrino mass and charge quantization.

Grand Unification is basically driven by the fact that the three gauge couplings tend to unify—in the MSSM nearly perfectly at a scale $Q_{\text{GUT}} = 2 \times 10^{16}$ GeV.

We cannot even discuss the most generic aspects of Grand Unified Theories in any detail because we neither really need it in the course of this thesis nor do we perform any calculations in GUT.

The D-factor is a kind of parity symmetry [116].

The labels s and a denote symmetric and antisymmetric representations.

2.3.1 Grand Unification

When shall we three meet again?

—First Witch [William Shakespeare, *Macbeth*]

The gauge groups and the gauge representations of the SM are chosen on purely phenomenological grounds. When the SM was proposed, there were also no hints for neutrino masses. In this respect, the particle content of the SM is minimal on the one hand and full of assumptions on the other hand. It is even more surprising that it perfectly fits into Grand Unification.

For the purpose followed in this short section, we give the most intriguing example of a Grand Unified Theory (GUT) which is astonishingly simple, combines all different representations of fermions in the SM into *one* representation and gives an explanation for small neutrino masses. The smallest simple Lie group which includes the SM gauge group and provides a single representation for the $15 + 1$ SM fermions of one generation is $\text{SO}(10)$, proposed by Georgi [113] and Fritzsch and Minkowski [114]. Moreover, $\text{SO}(10)$ can be decomposed either to $\text{SU}(5) \times \text{U}(1)$, which contains the Georgi–Glashow model [115], or

$$\text{SO}(10) \rightarrow \text{SO}(6) \times \text{SO}(4) \simeq \text{SU}(4) \times \text{SU}(2)_{\text{L}} \times \text{SU}(2)_{\text{R}} \times D,$$

which hints towards *partial unification* and shall be explained in Sec. 2.3.2.

With the SM fermions in the spinor representation of $\text{SO}(10)$, there are three candidates for mass terms as $\mathbf{16} \otimes \mathbf{16} = \mathbf{10}_s \oplus \mathbf{120}_a \oplus \mathbf{126}_s$ to construct $\text{SO}(10)$ invariant Yukawa couplings [117, 118]. Constraining

ourselves to symmetric representations (and therewith symmetric Yukawa couplings), the Yukawa Lagrangian is given by

$$-\mathcal{L}_Y^{\text{SO}(10)} = \left(\mathbf{16}_i Y_{ij}^{10} \mathbf{16}_j \right) \mathbf{10}_H + \left(\mathbf{16}_i Y_{ij}^{126} \mathbf{16}_j \right) \overline{\mathbf{126}}_H, \quad (2.35)$$

where $i, j = 1, 2, 3$ count generations and H labels Higgs representations of scalars obtaining a v_{ev} . The coupling to the $\overline{\mathbf{126}}_H$ generates neutrino Majorana masses—for the right-handed neutrinos at a high scale and for the left-handed neutrinos via a seesaw type I+II combination at the electroweak scale [120].

There are a lot of issues to be addressed in SO(10) GUT (also in SU(5) similar tasks arise). First of all, the large symmetry group has to be broken to the SM group. To do so, there are in general several Higgs representations at work to perform the symmetry breaking steps. We want to live in a SUSY environment and therefore have to address one special issue of SUSY GUTs: compared to the SM group, SO(10) has rank = 5 (the rank gives the number of simultaneously diagonal generators; SU(N) has rank = $N - 1$ and SO($2N$) has rank = N). Breaking SO(10) down reduces the group rank, which induces non-vanishing D -terms breaking SUSY at the same scale. To avoid broken SUSY at a high scale, one introduces another Higgs multiplet in the conjugated representation of the rank-reducing multiplet ($\mathbf{126}_H$) that cancels the other v_{ev} and keep SUSY intact [121]; additionally the extra field is needed to cancel chiral anomalies [122]. The *minimal* SUSY SO(10) Higgs content responsible for GUT breaking, neutrino masses and electroweak breaking would then consist of $\mathbf{210}_H$ breaking SO(10) to a partially unified group; $\overline{\mathbf{126}}_H$ and $\mathbf{126}_H$ responsible for neutrino Majorana masses; and $\mathbf{10}_H$ which contains the two MSSM Higgs doublets [121, 123, 124]. The minimal SUSY SO(10) model still is in quite a good shape if RG corrections are included into a fit of flavor data (quark and lepton) [125] where it was disfavored by the fit without RGE [126]. Despite the large representations, the gauge coupling stays perturbative even beyond the Planck scale if threshold and gravitational corrections are taken into account [127].

2.3.2 Partial Unification

When the hurlyburly's done.

—Second Witch [William Shakespeare, *Macbeth*]

SO(10) as a framework gives an excellent playground to study partial unification: an enlarged gauge group as it appears by deconstruction of the GUT group via symmetry breaking in the top-down approach. The partially unified picture allows to restore parity, e. g. gives an explanation why the weak interaction only couples to left-handed fermions, and simultaneously generates Majorana masses for neutrinos [129]. This intermediate symmetry is known as left-right symmetry, $SU(3)_c \times SU(2)_L \times SU(2)_R \times U(1)_{B-L}$ and additionally gauges the $B - L$ number. A slightly

The coupling to the $\mathbf{120}_H$ gives no relation between down type fermions [119].

An introduction to seesaw mechanisms is given in Sec. 3.1.

We cannot discuss SO(10) in detail but rather want to point out a viable framework, which gives seesaw neutrinos “for free”.

In view of no SUSY particles at the LHC, one may wonder whether it is not too bad to break SUSY at a high scale.

Interestingly, the fits of [125] prefer the non-minimal model with an additional $\mathbf{120}_H$.

The SUSY version and its connection to the more general picture of radiative corrections to neutrino mixing has been studied in [128].

more unified group is $SU(4)_c \times SU(2)_L \times SU(2)_R$ which also can be broken out of $SO(10)$ [130] and unifies quarks and leptons below the GUT scale where lepton number advances to the “fourth color” [131].

2.4 NEUTRINOS IN THE STANDARD MODEL AND BEYOND

„Liebe Radioaktive Damen und Herren“

—Wolfgang Pauli, Dec 4 1930

As pointed out in the introduction to the SM, Sec. 2.1, neutrinos are exactly massless in the model. However, extensions of the gauge sector as briefly mentioned in Sec. 2.3 naturally incorporate neutrino masses. On the one hand, it would be a puzzle if neutrinos were exactly massless. On the other hand, observations clearly contradict the SM in that point—we shortly refer to the Review of the Particle Data group and the appropriate references therein [23]. Experimentally, the physical mass squared differences can be obtained

$$\begin{aligned}\Delta m_{21}^2 &= 7.50_{-0.17}^{+0.19} \times 10^{-5} \text{ eV}^2, \\ \Delta m_{31}^2 &= 2.457 \pm 0.047 \times 10^{-3} \text{ eV}^2,\end{aligned}\tag{2.36}$$

In case of an inverted mass spectrum (where neutrino number 3 is the lightest) a slightly different Δm_{31}^2 is found. Actually, the sign of Δm_{31}^2 is still unknown which gives the ambiguity.

where $\Delta m_{ji}^2 = m_j^2 - m_i^2$ and we restricted ourselves to the result of a normal hierarchy ($\Delta m_{31}^2 > 0$) as follows from a global fit of neutrino oscillation data [132].

The choice of three right-handed neutrinos is done on symmetric grounds, moreover motivated by $SO(10)$.

Actually, masses for neutrinos can be very simply added to the SM Yukawa Lagrangian that was given in Eq. (2.5), adding three right-handed neutrinos to the SM what we then call νSM ,¹

$$\mathcal{L}^{\nu\text{SM}} = \frac{1}{2} \mathcal{L}_{\text{Yuk}}^{\text{SM}} + Y_{ij}^{\nu} \bar{L}_{L,i} \cdot H \nu_{R,j} - \frac{1}{2} \overline{\nu_{R,i}^c} M_{ij}^{\text{R}} \nu_{R,j} + \text{h. c.}\tag{2.37}$$

The Majorana mass M_{R} for right-handed neutrinos can be added without harm, because they are gauge singlets anyway. Because of the same reason, its value is not restricted to the electroweak scale. In view of a partially unified scenario, we assume the scale M_{R} somewhat below the GUT scale, $M_{\text{R}} \approx 10^{12\dots 14} \text{ GeV}$.

Deriving the neutrino mass matrix out of (2.37), one gets

$$-\mathcal{L}_{\text{mass}}^{\nu} = \begin{pmatrix} \nu_L & \nu_L^c \end{pmatrix} \begin{pmatrix} 0 & \mathbf{m}_{\nu}^{\text{D}} \\ \mathbf{m}_{\nu}^{\text{DT}} & \mathbf{M}_{\text{R}} \end{pmatrix} \begin{pmatrix} \nu_L \\ \nu_L^c \end{pmatrix} + \text{h. c.},\tag{2.38}$$

Remarks about spinor notation in App. A.

where $\mathbf{m}_{\nu}^{\text{D}} = \frac{\nu}{\sqrt{2}} \mathbf{Y}^{\nu}$ is the Dirac mass matrix and ν_L^c the charge conjugated right-handed neutrino. We have switched to the less heavy Weyl spinor notation (and only deal with left-handed Weyl spinors); the $\nu_L^{(c)}$ are 3-vectors in flavor space.

The mass matrix of Eq. (2.38) can be *perturbatively* diagonalized with an approximate unitary matrix

Approximate unitary means $\mathbf{U}^{\dagger} \mathbf{U} = \mathbf{1} + \mathcal{O}(\rho^2)$.

¹ The factor $\frac{1}{2}$ in front of $\mathcal{L}_{\text{Yuk}}^{\text{SM}}$ has to be included because $\mathcal{L}_{\text{Yuk}}^{\text{SM}} + \text{h. c.} = 2\mathcal{L}_{\text{Yuk}}^{\text{SM}}$.

$$U = \begin{pmatrix} \mathbf{1} & \boldsymbol{\rho} \\ -\boldsymbol{\rho}^\dagger & \mathbf{1} \end{pmatrix},$$

with $\boldsymbol{\rho} = \mathbf{m}_\nu^D M_R^{-1}$, see e. g. [133], such that

$$U^T \begin{pmatrix} M_L & \mathbf{m}_\nu^D \\ \mathbf{m}_\nu^{DT} & M_R \end{pmatrix} U = \begin{pmatrix} \mathbf{m}_L^\nu + \mathcal{O}(m_\nu^{D^4} M_R^{-3}) & \mathcal{O}(m_\nu^{D^3} M_R^{-2}) \\ \mathcal{O}(m_\nu^{D^3} M_R^{-2}) & \mathbf{m}_R^\nu + \mathcal{O}(m_\nu^{D^4} M_R^{-3}) \end{pmatrix}, \quad (2.39)$$

where

$$\begin{aligned} \mathbf{m}_L^\nu &= M_L - \mathbf{m}_\nu^D M_R^{-1} \mathbf{m}_\nu^{DT}, \\ \mathbf{m}_R^\nu &= M_R. \end{aligned} \quad (2.40)$$

Mass matrices like the one of Eq. (2.39) follow directly from SO(10) GU with an intermediate left-right symmetric breaking scale [134]. The left-handed Majorana mass can be achieved via couplings to an $SU(2)_L$ triplet Higgs which acquires a small v_{ev} via a v_{ev} seesaw (see Sec. 3.1).

The diagonalization of the light neutrino mass matrix \mathbf{m}_L^ν determines a mixing matrix which shall play the same role as the CKM matrix in the quark sector. Neutrino mixing was first proposed by Pontecorvo [135] and further developed by Maki, Nakagawa and Sakata [136]; we refer to the leptonic mixing matrix thus as Pontecorvo–Maki–Nakagawa–Sakata (PMNS) matrix. However, differently to the quark case, the PMNS matrix is not the additional transformation needed to diagonalize the second Yukawa coupling. Without right-handed neutrinos, there is no lepton mixing and we can always diagonalize Y^e (which defines the *charged lepton basis*). Doing so, we redefine the lepton fields

$$L_{L,i} \rightarrow L'_{L,i} = S_{L,ij}^L L_{L,j}, \quad (2.41a)$$

$$e_{R,i} \rightarrow e'_{R,i} = S_{R,ij}^e e_{R,j}, \quad (2.41b)$$

analogously to Eq. (2.8). Without loss of generality, we can always choose M_R diagonal, $(S_R^\nu)^* M_R (S_R^\nu)^\dagger$, redefining

$$\nu_{R,i} \rightarrow \nu'_{R,i} = S_{R,ij}^\nu \nu_{R,j}. \quad (2.41c)$$

All transformations are now fixed and Y^ν stays an arbitrary matrix in flavor space—which can be smartly parametrized in terms of knowns and unknowns, see Eq. (3.7). The object we have to deal with is anyway not Y^ν but \mathbf{m}_L^ν , which is also a complex symmetric matrix. We then have

$$\hat{\mathbf{m}}_L^\nu = U_{\text{PMNS}}^* \mathbf{m}_L^\nu U_{\text{PMNS}}^\dagger = \text{diagonal}. \quad (2.42)$$

The mixing matrix of the charged current is found to be indeed U_{PMNS} with $\nu'_{L,i} \rightarrow \nu''_{L,i} = U_{ij}^{\text{PMNS}} \nu'_{L,i}$:

$$\begin{aligned} \mathcal{L}_{\text{CC}}^\ell &= -\frac{ig_2}{\sqrt{2}} W_\mu^+ \bar{e}_L \gamma^\mu \nu_L + \text{h. c.} \\ &\rightarrow -\frac{ig_2}{\sqrt{2}} W_\mu^+ \bar{e}'_L S_L^L \gamma^\mu (S_L^L)^\dagger U_{\text{PMNS}}^\dagger \nu''_L \gamma^\mu \nu_{L,i} + \text{h. c.} \end{aligned} \quad (2.43)$$

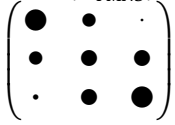
The diagonalization procedure is the same including a left-handed Majorana mass already at the Lagrangian level, so we put it there.

M_R is a complex symmetric matrix that is diagonalized via Takagi diagonalization [137] with a unitary matrix S_R^ν .

The primed and double-primed fields are in the mass basis. With $S_L^L (S_L^L)^\dagger = \mathbf{1}$, U_{PMNS}^\dagger remains in the W -vertex. Note that the PMNS matrix is defined “upside-down” compared to the CKM matrix of Eq. (2.9).

The PMNS matrix is parametrized conveniently in the same way as the CKM matrix in Eq. (2.10). Majorana neutrinos (since they are real) do not allow to absorb as many phases as Dirac fermions, so two more complex phases survive, $U_{\text{PMNS}} = V_{\text{CKM}}\mathbf{P}$ with a phase matrix $\mathbf{P} = \text{diag}(e^{i\alpha_1}, e^{i\alpha_2}, 1)$. The absolute values are going to be determined with better and better precision; within the 3σ intervals we have [132]

The magnitudes of PMNS elements can be displayed with the central values as $|U_{\text{PMNS}}| =$



$$|U_{\text{PMNS}}| = \begin{pmatrix} 0.801\dots 0.845 & 0.514\dots 0.580 & 0.137\dots 0.158 \\ 0.225\dots 0.517 & 0.441\dots 0.699 & 0.614\dots 0.793 \\ 0.246\dots 0.529 & 0.464\dots 0.713 & 0.590\dots 0.776 \end{pmatrix}. \quad (2.44)$$

NEUTRINOS MEET SUPERSYMMETRY: EXTENSION OF THE MSSM The most economic extension of the Minimal Supersymmetric Standard Model to incorporate massive neutrinos is the extension by right-handed neutrino superfields. We supersymmetrize the νSM and call this νMSSM with the following superpotential

$$\mathcal{W}_{\nu\text{MSSM}} = \mathcal{W}_{\text{MSSM}} + Y_{ij}^\nu H_u \cdot L_{L,i} \bar{N}_{R,j} + \frac{1}{2} M_{ij}^R \bar{N}_{R,i} \bar{N}_{R,j}. \quad (2.45)$$

In $\text{SO}(10)$ the fields assigned to right-handed neutrinos are in the same representation as all the other matter fields. So it is necessary to have the same number.

For aesthetic reasons, we introduce three right-handed neutrino superfields $\bar{N}_{R,i} = \{\tilde{\nu}_{R,i}^*, \nu_{R,i}^c\}$, the same number as left-handed fields as motivated from $\text{SO}(10)$ GU.

Compared to the MSSM, the extension with right-handed neutrinos also comes along with additional soft SUSY breaking terms: one more soft mass matrix, a Higgs–sneutrino trilinear coupling and the sneutrino B -term. We add the following soft breaking Lagrangian:

$$-\mathcal{L}_{\text{soft}}^{\tilde{\nu}} = \left(\tilde{m}_\nu^2 \right)_{ij} \tilde{\nu}_{R,i} \tilde{\nu}_{R,j}^* + \left(\tilde{\ell}_{L,i} \cdot h_u A_{ij}^\nu \tilde{\nu}_{R,j}^* + \left(\mathbf{B}_\nu^2 \right)_{ij} \tilde{\nu}_{R,i}^* \tilde{\nu}_{R,j}^* + \text{h.c.} \right). \quad (2.46)$$

We write the neutrino B -term in a way that suggests no connection to \mathbf{M}_R although it can be seen as “Majorana-like” soft breaking mass (and therefore denoted here as \mathbf{B}_ν^2 to make clear that it carries mass dimension two). The usual way in the literature [138–141] is to write it down as $\mathbf{B}_\nu^2 = b_\nu \mathbf{M}_R$ where b_ν is a parameter of the SUSY scale.

In general, flavor off-diagonal entries in the soft breaking contributions do influence observation of flavor changing neutral currents (FCNC) in charged lepton physics. Especially leptonic flavor violation in decays as $\mu \rightarrow e\gamma$ has never been observed, so the tightest bounds on new SUSY contributions may kill most parameter configurations of the model. Nevertheless, these constraints only affect the charged lepton sector: The flavor mixing parts of soft squared masses for the lepton doublet as well as the trilinear selectron coupling A^e have to be negligible, at least for the first two generations. Bounds on 2-3 mixing are less stringent. If we impose minimal flavor violation in the charged sector and allow for large flavor-mixing contributions in the neutrino A -terms, lepton flavor violating FCNC

In general, $\ell_j \rightarrow \ell_i \gamma$ with $j > i$.

are safe. An aesthetic aspect of this description might be the underlying SUSY breaking mechanism, leading to MFV in the well-known part of the theory and somehow complete anarchy in the part, which is not accessible yet. At this point, we imply that such a mechanism is viable and leads to the observed amount of flavor mixing.

THE SNEUTRINO SQUARED MASS MATRIX Due to the Majorana structure, the sneutrino mass matrix gets blown up—similar to the neutrino mass matrix in the non-supersymmetric ν SM—and there are twelve physical sneutrino mass eigenstates instead of only three in the MSSM, whereupon half of them are heavy—similar to the heavy (mostly right-handed) neutrinos:

$$(\mathcal{M}_{\tilde{\nu}})^2 = \frac{1}{2} \begin{pmatrix} \mathcal{M}_{L^*L}^2 & \mathcal{M}_{L^*L^*}^2 & \mathcal{M}_{L^*R^*}^2 & \mathcal{M}_{L^*R}^2 \\ \mathcal{M}_{LL}^2 & \mathcal{M}_{LL^*}^2 & \mathcal{M}_{LR^*}^2 & \mathcal{M}_{LR}^2 \\ \mathcal{M}_{RL}^2 & \mathcal{M}_{RL^*}^2 & \mathcal{M}_{RR^*}^2 & \mathcal{M}_{RR}^2 \\ \mathcal{M}_{R^*L}^2 & \mathcal{M}_{R^*L^*}^2 & \mathcal{M}_{R^*R^*}^2 & \mathcal{M}_{R^*R}^2 \end{pmatrix} \quad (2.47)$$

$$\equiv \frac{1}{2} \begin{pmatrix} \mathcal{M}_{LL}^2 & \mathcal{M}_{LR}^2 \\ (\mathcal{M}_{LR}^2)^\dagger & \mathcal{M}_{RR}^2 \end{pmatrix},$$

in a basis $\tilde{\nu} = (\tilde{\nu}_L, \tilde{\nu}_L^*, \tilde{\nu}_R, \tilde{\nu}_R)^T$, such that $\mathcal{L}_{\tilde{\nu}}^{\text{mass}} = \tilde{\nu}^\dagger \mathcal{M}_{\tilde{\nu}}^2 \tilde{\nu}$, where the individual 6×6 blocks have the following hierarchies in the orders of magnitude [140]:

$$(\mathcal{M}_{\tilde{\nu}})^2 = \frac{1}{2} \begin{pmatrix} \mathcal{M}_{LL}^2 & \mathcal{M}_{LR}^2 \\ (\mathcal{M}_{LR}^2)^\dagger & \mathcal{M}_{RR}^2 \end{pmatrix} \approx \begin{pmatrix} \mathcal{O}(M_{\text{SUSY}}^2) & \mathcal{O}(M_{\text{SUSY}} m_R) \\ \mathcal{O}(M_{\text{SUSY}} M_R) & \mathcal{O}(M_R^2) \end{pmatrix}, \quad (2.48)$$

which has a similar hierarchy as the full neutrino mass matrix

$$\mathcal{M}_\nu \approx \begin{pmatrix} 0 & \mathcal{O}(v) \\ \mathcal{O}(v) & \mathcal{O}(M_R) \end{pmatrix}.$$

In an analogous treatment to the neutrino sector, we can approximately diagonalize Eq. (2.48) and get an effective light sneutrino squared mass matrix—the RR block does not change significantly. Especially, there is no distinct left-right mixing in the active sneutrino sector (because right-handed neutrinos and their scalar partners are heavy and integrated out well above the SUSY scale). However, a mixing of the left-handed partner fields with their complex conjugate is left, which contributes to Majorana mass corrections at one loop (see Sec. 3.2).

The light sneutrino mass matrix has the following structure [140]:

$$\mathcal{M}_{\tilde{\nu}_i}^2 = \mathcal{M}_{LL}^2 - \mathcal{M}_{LR}^2 (\mathcal{M}_{RR}^2)^{-1} (\mathcal{M}_{LR}^2)^\dagger + \mathcal{O}(M_{\text{SUSY}}^4 M_R^{-2}), \quad (2.49)$$

which provides a correction term to the MSSM sneutrino mass $\sim M_{\text{SUSY}}^4 / M_R^2$. This term is absent, if there is no LR mixing in the sneutrino sector or the

We impose RFV in the lepton sector as described in Sec. 3.2.

Note that in the MSSM there are no right-handed neutrinos. So the number of states is doubled twice.

Each $\tilde{\nu}_X^{()}$ ($X = L, R$) is a 3-vector in flavor space.*

right-handed mass is sent to infinity. Especially it provides a seesaw-like connection between left-right mixing (i. e. trilinear couplings A_ν) and the heavy neutrino mass scale. Though this contribution ought to be small, it induces a mass splitting of order of the light neutrino masses.

Performing the perturbative diagonalization, we find lepton number violating terms in the 6×6 light sneutrino squared mass matrix:

$$\mathcal{M}_{\tilde{\nu}_\ell}^2 = \begin{pmatrix} \mathbf{m}_{\Delta L=0}^2 & (\mathbf{m}_{\Delta L=2}^2)^* \\ \mathbf{m}_{\Delta L=2}^2 & (\mathbf{m}_{\Delta L=0}^2)^* \end{pmatrix}, \quad (2.50)$$

where the $\Delta L = 0$ block preserves total lepton number, while generation mixing is allowed, and the $\Delta L = 2$ block violates lepton number by two units.

Explicitly, the entries of the 3×3 sub-matrices are given by [140]:

$$\mathbf{m}_{\Delta L=0}^2 = \tilde{\mathbf{m}}_\ell^2 + \frac{1}{2} M_Z^2 \cos 2\beta + \mathbf{m}_\nu^D \mathbf{m}_\nu^{D\dagger} - \mathbf{m}_\nu^D \mathbf{M}_R (\mathbf{M}_R^2 + \tilde{\mathbf{m}}_\nu^2)^{-1} \mathbf{M}_R \mathbf{m}_\nu^D + \mathcal{O}(M_{\text{SUSY}}^2 M_R^{-2}), \quad (2.51a)$$

$$\begin{aligned} \mathbf{m}_{\Delta L=2}^2 = & \mathbf{m}_\nu^{D*} \mathbf{M}_R [\mathbf{M}_R^2 + (\tilde{\mathbf{m}}_\nu^2)^T]^{-1} \mathbf{m}_\nu^{D\dagger} X_\nu^\dagger \\ & + X_\nu^* \mathbf{m}_\nu^{D*} (\mathbf{M}_R^2 + \tilde{\mathbf{m}}_\nu^2)^{-1} \mathbf{M}_R \mathbf{m}_\nu^D \\ & - 2 \mathbf{m}_\nu^{D*} \mathbf{M}_R [\mathbf{M}_R^2 + (\tilde{\mathbf{m}}_\nu^2)^T]^{-1} (\mathbf{B}_\nu^2) (\mathbf{M}_R^2 + \tilde{\mathbf{m}}_\nu^2)^{-1} \mathbf{M}_R \mathbf{m}_\nu^{D\dagger} \\ & + \mathcal{O}(M_{\text{SUSY}}^2 M_R^{-2}), \end{aligned} \quad (2.51b)$$

where $X_\nu \mathbf{m}_\nu^D = -\mu \cot \beta \mathbf{m}_\nu^{D*} + \nu_u \mathbf{A}^\nu$.

Diagonalizing $\mathcal{M}_{\tilde{\nu}_\ell}^2$ of Eq. (2.50) yields the six physical light sneutrino mass eigenvalues, which are pairwise degenerate. In the literature for the one generation case [142] as well as for the general case [140] it is proposed to transform into the CP eigenbasis and to deal with real, self-conjugate mass eigenstates. To perform this transformation, we use

$$\mathcal{P} = \frac{1}{\sqrt{2}} \begin{pmatrix} \mathbf{1} & i \mathbf{1} \\ \mathbf{1} & -i \mathbf{1} \end{pmatrix},$$

such that $\tilde{\mathcal{M}}_{\tilde{\nu}_\ell}^2 = \mathcal{P}^\dagger \mathcal{M}_{\tilde{\nu}_\ell}^2 \mathcal{P}$ now is in the CP basis. If $\mathcal{W}^{\tilde{\nu}}$ diagonalizes the matrix $\tilde{\mathcal{M}}_{\tilde{\nu}_\ell}^2$, so does $\mathcal{Z}^{\tilde{\nu}} = \mathcal{P} \mathcal{W}^{\tilde{\nu}}$ with respect to $\mathcal{M}_{\tilde{\nu}_\ell}^2$.

In this basis, the Feynman rules take a particularly convenient form, where one only has to evaluate ‘‘half’’ of the mixing matrix, since $\mathcal{Z}_{i+3,s}^{\tilde{\nu}} = \mathcal{Z}_{is}^{\tilde{\nu}*}$ for $i = 1, \dots, 3$ and $s = 1, \dots, 6$. The Feynman rules and details concerning the mixing matrices are given in App. A.

Anyhow, for our analysis, we only perform a numerical diagonalization for which the perturbative approach is an overkill and may be used to understand the structures behind. In principle, we can directly diagonalize the full 12×12 sneutrino mass matrix. Numerical cancellations and instabilities can be avoided using higher working precision. Still, it is more convenient to work in the effective theory with only light sneutrinos and Eq. (2.50). Discussing the anatomy of flavor changing contributions, we shall later switch to the full theory.

The $\Delta L = 2$ terms are the one $\sim \tilde{\nu}_L^{(*)} \tilde{\nu}_L^{(*)}$ which violate the global $U(1)_L$ charge.

The full sneutrino mass matrix is derived in App. A.

Physics of neutrino masses is physics beyond the SM. The SM *per se* has no room for massive neutrinos. Weinberg’s “Model of Leptons” [5] is a minimal model describing lepton physics back in the sixties. However, since the observation of neutrino oscillations, we know that this simplest model cannot be true. In the SM there are no right-handed neutrinos, Majorana mass terms among left-handed fields are forbidden by gauge symmetry. We discuss several possibilities how to generate effectively a left-handed Majorana mass term at tree-level in Sec. 3.1 respecting the gauge structure of the SM. In any case, the following effective operator is the only possible dimension-five operator [149]

$$\mathcal{L}_{\text{dim } 5} = \frac{\lambda_{ij}}{\Lambda} (L_i \cdot H) C (H \cdot L_j), \quad (3.1)$$

where the dot product denotes SU(2)-invariant multiplication and C the charge conjugation matrix. The interaction is suppressed by a heavy scale Λ that is not restricted by the physics of the SM. In this construction, the neutrino mass matrix is given by the combination $v^2 \lambda / (2\Lambda)$, where the λ_{ij} are dimensionless couplings that in general mix flavor. Eq. (3.1) violates explicitly lepton number ($\Delta L = 2$) and can be tested by the observation of neutrinoless double beta decay [150–152]. The presence of the non-renormalizable term (3.1) is sufficient to explain neutrino masses *within* the field content of the SM [153], however, to build a UV complete theory so-called seesaw mechanisms were elaborated [129, 154–157].

The existence of such an operator with an *a priori* arbitrary flavor structure sets the stage for lepton flavor physics. Without loss of generality, we work in the basis where the charged lepton Yukawa couplings are diagonal and get the PMNS matrix from the diagonalization of the neutrino mass matrix only:

$$\hat{\lambda} = U_{\text{PMNS}}^* \lambda U_{\text{PMNS}}^\dagger = \text{diagonal}. \quad (3.2)$$

Note that λ in general is a complex symmetric matrix, so U_{PMNS} is a *unitary* matrix. The eigenvalues (proportional to the masses) can be defined complex, depending on the proper definition of U_{PMNS} (see Secs. 2.1.3 and 2.4). There are additional phases that cannot be absorbed into redefinitions of the fields, which would be possible for Dirac neutrinos [158–160]. In the presence of the Weinberg Operator (3.1), Neutrinos are Majorana fermions. It is a matter of taste whether to choose complex masses (as done e. g. in Sec. 3.2.1) or to assign Majorana phases to the mixing matrix (as discussed in Sec. 2.4). The latter choice makes it obvious that Majorana phases can never be observed in neutrino oscillations [160].

At that time, there was no solar neutrino problem [143–148] but the MNS matrix was already proposed [136].

Eq. (3.1) is usually called “Weinberg Operator” since Weinberg introduced it.

In Dirac space $C = i\gamma_2\gamma_0$ and C has the properties $C^\dagger = C^T = C^{-1} = -C$.

We refer to this choice as charged lepton basis or interaction basis, because for charged leptons mass and interaction states then are the same.

This diagonalization procedure is known as Takagi diagonalization [137].

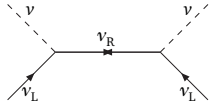
A rough estimate gives a glance at the order of magnitude of the high scale Λ : let us assume the couplings $\hat{\lambda}_i \sim \mathcal{O}(1)$ and the resulting neutrino masses $m_i^\nu \sim \mathcal{O}(0.1 \text{ eV})$, then with $\nu \sim \mathcal{O}(100 \text{ GeV})$ we get $\Lambda \sim \mathcal{O}(10^{13} \text{ GeV})$:

$$0.1 \text{ eV} = 0.1 \frac{(100 \text{ GeV})^2}{10^{13} \text{ GeV}} = 0.1 \frac{10^4 \cdot 10^9 \text{ eV}}{10^{13}}.$$

3.1 NEUTRINOS AT TREE-LEVEL

There are also possibilities to generate neutrino Majorana masses at the loop level, see e. g. [161, and references therein].

$$\varepsilon = \begin{pmatrix} 0 & 1 \\ -1 & 0 \end{pmatrix}$$



Because of the presence of the Dirac Yukawa coupling to left-handed leptons, we call ν_R right-handed neutrinos.

There are three possible ways to construct a UV complete theory leading to the operator (3.1), which can be seen by rewriting it in SU(2)-invariant ways and inserting the missing multiplets into the effective operator [162].

TYPE I We introduce the SU(2) metric ε to express the invariant multiplication by matrix products (Lorentz-invariant multiplication in Dirac space is understood without further notation)

$$\mathcal{L}_{\text{dim } 5} \sim (L^T \varepsilon H) C (H^T \varepsilon L),$$

and find as candidate for the full Lagrangian

$$\mathcal{L}_I = Y_\nu (L^T \varepsilon H) C \nu_R + \frac{1}{2} M_R (\nu_R^c)^T C \nu_R. \quad (3.3)$$

The additional fields ν_R have to be singlets under the SM gauge group in order to give (3.1) after having integrated them out and couple to left-handed leptons via a Dirac-like Yukawa coupling Y_ν [163]. Singlets are not protected by any gauge symmetry and can acquire a Majorana mass term as shown in Eq. (3.3). The mechanism behind this Majorana mass is unknown or not specified, especially it is not related to electroweak symmetry breaking, therefore unrestricted by scale considerations. In the case of only one right-handed neutrino, M_R is identical to the scale Λ . If there is a stronger hierarchy in right-handed masses, the ν_{Ri} have to be integrated out successively [164, 165]. For symmetry reasons, we shall use the type I seesaw mechanism with three right-handed neutrinos, motivated e. g. by SO(10) GUTs.

TYPE II A similar deconstruction can be done using a scalar triplet motivated by an embedding into left-right symmetric models [129, 154, 157, 166]:

$$\mathcal{L}_{\text{dim } 5} \sim \frac{1}{2} (L^T \varepsilon \sigma_i C L) (H^T \varepsilon \sigma_i H),$$

where the σ_i are the generators of SU(2). The UV complete theory can be built with a scalar triplet

$$\Delta = \delta_i \frac{\sigma_i}{2} = \begin{pmatrix} \delta^+ / \sqrt{2} & \delta^{++} \\ \delta^0 & -\delta^+ / \sqrt{2} \end{pmatrix}$$

$$\sigma_1 = \begin{pmatrix} 0 & 1 \\ 1 & 0 \end{pmatrix},$$

$$\sigma_2 = \begin{pmatrix} 0 & -i \\ i & 0 \end{pmatrix},$$

$$\sigma_3 = \begin{pmatrix} 1 & 0 \\ 0 & -1 \end{pmatrix}.$$

coupling both to the lepton and Higgs doublets such that

$$\mathcal{L}_{\text{II}} = Y_{\Delta} \left(L^T \varepsilon \sigma_i C L \right) + \mu_{\Delta} \delta_i^* \left(H^T \varepsilon \sigma_i H \right) + M_{\Delta} \delta_i^* \delta_i. \quad (3.4)$$

The inclusion of scalar triplets acquiring a vev has to be treated with care since triplet $vevs$ spoil one famous and important relation of the SM, the ρ -parameter [167]

$$\rho = \frac{M_W^2}{M_Z^2 \cos^2 \theta_W}.$$

At tree-level in the SM, $\rho = 1$, but radiative corrections show deviations from that prediction even at one-loop [168]. Since the ρ -parameter is precisely measured ($\rho = 1.00040 \pm 0.00024$) [23] and calculated with high precision in the SM [169], any deviation induced by triplet $vevs$ has to be small in a sense that the triplet vev itself has to be small. On the other hand, if a Higgs triplet of $SU(2)_L$ generates a Majorana mass for left-handed neutrinos at tree-level, its vev is restricted to be rather small compared to the electroweak scale anyway. The Higgs triplet ($\langle \delta^0 \rangle = v_{\Delta}$) e. g. alters the relation to

$$\rho = \frac{M_W^2}{M_Z^2 \cos^2 \theta_W} = 1 + \frac{4v_{\Delta}^2}{v^2},$$

for general scalar representations acquiring $vevs$ v_i the ρ -parameter is given by

$$\rho = 1 + \frac{\sum_i \left(4T_i(T_i + 1) - 3Y_i^2 \right) |v_i|^2 c_i}{\sum_i 2Y_i^2 |v_i|^2},$$

where Y_i and T_i are hypercharge and weak isospin of the i -th Higgs multiplet and $c_i = 1$ for complex and $c_i = \frac{1}{2}$ for real representations, see [170] and [171].

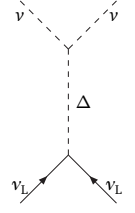
TYPE III The third variant needs to introduce exotic fermions (calling singlets not exotic), namely triplets under $SU(2)$ [172].

$$\mathcal{L}_{\text{dim } 5} \sim -\frac{1}{2} \left(L^T \varepsilon \sigma_i H \right) C \left(L^T \varepsilon \sigma_i H \right).$$

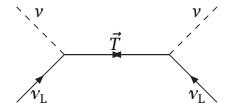
The triplet fermions $\vec{T} = T_i \sigma_i$ again are Majorana fermions coupling to the standard leptons via an appropriate Yukawa coupling:

$$\mathcal{L}_{\text{III}} = Y_T \left(L^T \varepsilon \sigma_i H \right) C T_i + M_T T_i^T C T_i. \quad (3.5)$$

While seesaws of type I and II can be naturally incorporated in popular extensions of the SM and follow immediately from common grand unified scenarios as $SO(10)$ [114, 119, 120, 173, 174], the triplet fermion extension follows a different philosophy and shall not be considered any further in this thesis.



Which is the case for triplets making Majorana neutrino masses [158].



3.2 RADIATIVE NEUTRINO MIXING

The tree-level formulation of neutrino masses and mixing is in general sufficient to explain a non-trivial mixing pattern. Take e. g. the type I seesaw mechanism: working with a diagonal right-handed mass matrix \mathbf{M}_R , the neutrino Yukawa coupling cannot be constrained and stays a rather arbitrary matrix. Inverting the decomposition of the effective mass operator

$$\mathbf{m}_\nu = -v^2 \mathbf{Y}_\nu \mathbf{M}_R^{-1} \mathbf{Y}_\nu^T \quad (3.6)$$

yields the famous Casas-Ibarra relation [175]

$$\mathbf{Y}_\nu = \sqrt{\mathbf{M}_R} \mathcal{R} \sqrt{\boldsymbol{\kappa}} \mathbf{U}_{\text{PMNS}}^\dagger, \quad (3.7)$$

with an (arbitrary) complex orthogonal matrix \mathcal{R} . The diagonal Matrix $\boldsymbol{\kappa}$ contains the light neutrino masses, $\mathbf{m}_\nu = v^2 \boldsymbol{\kappa}$, and \mathcal{R} in general has three complex mixing angles. Together with three right-handed masses, there are nine free parameters that do not change the low-energy phenomenology. Moreover, Eq. (3.7) is only a reparameterization of the unknown—there is no hint to the origin of the mixing angles in \mathbf{U}_{PMNS} .

Generalizations with an arbitrary number of singlet neutrinos are straightforward, see [158], though they do not permit any relation like Eq. (3.7).

Radiative corrections to neutrino masses and mixing are generically less intensively studied than tree-level realizations. On the one hand, quantum effects from the renormalization group (RG) evolution play an important role comparing low-energy observables with flavor models at the high scale. On the other hand, threshold corrections at an intermediate scale bring completely different aspects of neutrino flavor into the game.

Threshold corrections and RG corrections interplay in the determination of the corrected neutrino mass matrix

$$m_{AB}^\nu = m_{AB}^{(0)} + m_{AC}^{(0)} I_{CB} + I_{AC} m_{CB}^{(0)}, \quad (3.8)$$

where I_{AB} denote the corrections and $\mathbf{m}^{(0)}$ is the tree-level mass matrix [176–179]. Capital indices are in the interaction or flavor basis ($A, B = e, \mu, \tau$) and $\mathbf{I} = \mathbf{I}^{\text{RG}} + \mathbf{I}^{\text{th}}$ is the sum of RG and threshold corrections. The threshold corrections can be calculated diagrammatically via self-energy diagrams as discussed in Sec. 3.2.1, the RG corrections are to be obtained from the integration of the renormalization group equation for the neutrino mass operator [179–183].

BRIEF DISCUSSION OF RG EFFECTS The contributions from the renormalization group are known to give a sizable effect for quasi-degenerate neutrino masses [180, 184–189]. Especially the choice of the same CP parity for two mass eigenstates may lead to large mixing at low scale irrespective of the original mixing at the high scale [190, 191], known as infrared fixed points [189]. The effect from the renormalization group severely depends on the Majorana phases: for a vanishing Majorana phase, maximal mixing patterns get diluted on the way to the high scale [192]

for quasi-degenerate ($m_0 \sim \mathcal{O}(1 \text{ eV})$) neutrino masses. If, on the contrary, the phase is large or the overall mass scale is much smaller than 1 eV, maximal mixing is preserved. Likewise, zero mixing (as follows from the assignment $m_1 = m_2 = m_3$) is conserved [193] irrespective of the Majorana phase difference $|\alpha_1 - \alpha_2|$. We therefore neglect contributions that preserve specific mixing patterns for the low-energy threshold corrections.

In the following sections, we shall discuss different aspects of threshold corrections to neutrino masses and mixing. First, we start with an exactly degenerate mass pattern at the tree-level and figure out, whether threshold corrections have the power to generate the observed differences in mass squares *and* the non-trivial mixing. Exact degeneracy comes along with trivial mixing. Threshold corrections both lift the degenerate masses and therewith mix different interaction states. Second, we discuss a scenario implementing a non-trivial mixing pattern already at tree-level with threshold corrections modifying the seesaw mass of Eq. (3.6) at the loop level. Third, we renormalize the mixing matrix directly and resum the enhanced contributions $\sim m_{\nu_i} \Sigma_{ij}^{\nu} / \Delta m_{ij}^2$ in case of quasi-degenerate spectra.

3.2.1 The Case of Degenerate Neutrino Masses

Degenerate neutrino masses are probably an amusing gimmick of nature. Where in the early times of the SM no masses for the electrically neutral fermions were foreseen, the observed flavor oscillations provide sizable but small mass differences of the individual neutrino species. Any direct measurement of neutrino mass still lacks the discovery [23, 195–198]. If the overall mass scale $m_{\nu}^{(0)}$ is much larger than the mass differences, the neutrino spectrum is *quasi-degenerate*. The masses are easily calculated and expanded in $\Delta m_{ij}^2 / (m_{\nu}^{(0)})^2$:

$$|m_{\nu_1}| = m_{\nu}^{(0)}, \quad (3.9a)$$

$$|m_{\nu_2}| = \sqrt{(m_{\nu}^{(0)})^2 + \Delta m_{21}^2} \approx m_{\nu}^{(0)} + \frac{1}{2} \Delta m_{21}^2, \quad (3.9b)$$

$$|m_{\nu_3}| = \sqrt{(m_{\nu}^{(0)})^2 + \Delta m_{31}^2} \approx m_{\nu}^{(0)} + \frac{1}{2} \Delta m_{31}^2. \quad (3.9c)$$

The measurement of the “effective electron neutrino mass” which is done via the endpoint of the β spectrum gives a robust determination of $m_{\nu}^{(0)}$,

$$\left(m_{\nu}^{(0)}\right)^2 = \langle m_{\beta}^2 \rangle - \sum_i |\mathcal{U}_{ei}|^2 \Delta m_{i1}^2 \quad (\text{normal hierarchy}),$$

where the indirect measurement using neutrinoless double- β -decay may suffer from destructive interference due to Majorana phases (or other new physics). Complementary to measurements in the laboratory, estimates or bounds on the neutrino mass can be achieved by cosmological observations. Cosmology constrains the sum of relativistic neutrino masses $\sum m_{\nu}$ (and by the same time counts the number of active neutrino states) but the bounds are not quite robust. Let us take a look into

In the last two scenarios, the masses may not be degenerate.

The content and the results of this section was published in [194].

We define the mass square differences $\Delta m_{ij}^2 = m_{\nu_i}^2 - m_{\nu_j}^2$ and only discuss the normal hierarchy. For inverted hierarchy, the lightest neutrino mass is $m_{\nu_3} = m_{\nu}^{(0)}$.

$\langle m_{\beta}^2 \rangle = \sum_i |\mathcal{U}_{ei}|^2 m_i^2$, with \mathcal{U} the neutrino mixing matrix.

$$\langle m_{\beta\beta}^2 \rangle = \left| \sum_i \mathcal{U}_{ei} m_{\nu_i} \right|^2$$

the PLANCK report [199]: depending on the fit model, several bounds are proposed; the strongest is $\sum m_\nu < 0.23 \text{ eV}$, relaxing spatial flatness one finds $\sum m_\nu < 0.32 \text{ eV}$. In any case, all analyses are based on the standard cosmological ΛCDM model.

While a positive direct neutrino mass measurement in the near future will immediately put us into the quasi-degenerate regime, cosmology disfavors this possibility with increasing significance. In any case, quasi-degenerate neutrino masses need a cautious treatment from the flavor symmetry point of view, see e. g. [200–203]. Exact degeneracy, however, is a direct consequence of $\text{SO}(3)$ or $\text{SU}(3)$ invariance. We now want to keep the fundamental flavor symmetry for neutrinos intact and figure out whether radiative breaking has the power to produce the observed deviations from degeneracy and simultaneously the mixing matrix.

Majorana neutrinos require $\text{SO}(3)$.

Note that exactly degenerate neutrinos have no mixing at tree-level.

Corrections to degenerate masses can be treated very easily performing a re-diagonalization of the corrected mass matrix (3.8). In general, the tree-level mass matrix $\mathbf{m}^{(0)}$ is not diagonal in the flavor basis. Transforming into the mass eigenbasis (at tree-level) using the tree-level mixing matrix $U^{(0)}$ results in a non-diagonal corrected mass matrix whose off-diagonal elements stem from the off-diagonal threshold corrections:

$$m_{ab}^\nu = m_a^{(0)} \delta_{ab} + \left(m_a^{(0)} + m_b^{(0)} \right) I_{ab}, \quad (3.10)$$

where small indices a, b now are meant to be in the mass basis and

$$I_{ab} = \sum_{A,B} I_{AB} U_{Aa}^{(0)} U_{Bb}^{(0)}.$$

Eq. (3.10) reveals two interesting observations: first, if any $m_b^{(0)} = -m_a^{(0)} = m$, \mathbf{m}^ν simplifies tremendously to (e. g. $m_1^{(0)} = -m_2^{(0)} = m_3^{(0)}$)

$$\mathbf{m}^\nu = m \begin{pmatrix} 1 + 2U_{A1}U_{B1}I_{AB} & 0 & 2U_{A1}U_{B3}I_{AB} \\ 0 & -1 - 2U_{A2}U_{B2}I_{AB} & 0 \\ 2U_{A1}U_{B3}I_{AB} & 0 & 1 + 2U_{A3}U_{B3}I_{AB} \end{pmatrix}, \quad (3.11)$$

and there is only one off-diagonal entry left (remember that Majorana mass matrices are symmetric)—which can be eliminated using one free rotation [176, 177, 179]. Second, in the case $\mathbf{m}^{(0)} = m_\nu^{(0)} \mathbf{1}$, the observed flavor mixing is directly a result of non-universal (and flavor non-diagonal) threshold corrections. For exact degeneracy, there are three free rotations which can be used to diagonalize \mathbf{I} [194].

CP PHASES AND MAJORANA NEUTRINOS The case of Majorana neutrinos does not allow us to rotate away as many CP phases as for Dirac fermions. In general, there are two more phases left, such that the complete diagonalization matrix can be written as a product of a unitary matrix with three angles and one phase and a phase matrix: $U_\nu = \mathbf{P}U^{(0)}$ with

$\mathbf{P} = \text{diag}(e^{i\alpha_1}, e^{i\alpha_2}, 1)$. The Majorana phases $\alpha_{1,2}$ can then be absorbed in a redefinition of the masses instead of a redefinition of the fields:

$$\mathbf{m}^{(0)} \rightarrow \mathbf{P}^* \mathbf{U}^{(0)*} \mathbf{m}^{(0)} \mathbf{U}^{(0)\dagger} \mathbf{P}^\dagger = m_0 \text{diag}(e^{-2i\alpha_1}, e^{-2i\alpha_2}, 1).$$

We have chosen the phases in a particular way to have a real and positive m_3 .

Under the assumption of CP conservation in the Majorana phases, we take $\alpha_{1,2} \in \{0, \pm\frac{\pi}{2}\}$ and assign the relative CP parity of the respective mass eigenstate to the mass eigenvalue, so e. g. $m_1^{(0)} = -m_2^{(0)} = m_3^{(0)}$ as discussed in the following.

THE CASE $m_1^{(0)} = -m_2^{(0)} = m_3^{(0)}$ The two-fold degeneracy leaves a freedom of rotation which is in the 1-3 plane ($\mathbf{U} \rightarrow \mathbf{U}\mathbf{R}_{13}$ with a real rotation matrix \mathbf{R}_{13} and two fixed angles in \mathbf{U}) and the full diagonalization of \mathbf{m}^ν in Eq. (3.11) can be done solving the equation

$$\sum_{A,B} U_{A1} U_{B3} I_{AB} = 0, \quad (3.12)$$

which, for fixed mixing angles in \mathbf{U} can be done by choosing appropriate I_{AB} . An interesting exercise now is to find out, how many nonzero contributions in \mathbf{I} are needed to fully reproduce the masses. The squared mass differences can be easily calculated from Eq. (3.11)

$$\Delta m_{ab}^2 \approx \tilde{m}^2 \left[(1 + 2U_{Aa} U_{Ba} \tilde{I}_{AB})^2 - (1 + 2U_{Ab} U_{Bb} \tilde{I}_{AB})^2 \right]. \quad (3.13)$$

Shifting all corrections by an overall flavor universal constant, $I_{AB} \rightarrow \tilde{I}_{AB} = I_{AB} - I_0 \delta_{AB}$, does neither change the mixing angles nor does it affect the ratio $\Delta m_{31}^2 / \Delta m_{21}^2$ [179]. The effect on the mass parameter m factors out and manifests itself also as a shift and can be absorbed by a redefinition: $\tilde{m} = (1 + 2I_0)m$.

With only flavor diagonal threshold corrections $I_{AA} = I_A = I_e, I_\mu, I_\tau$ we can try to fix the third, free mixing angle θ_{13} in terms of the other two and the I_A :

$$s_{13} = c_{23} s_{23} \frac{s_{12}}{c_{12}} \frac{I_\mu - I_\tau}{I_e - s_{23}^2 I_\mu - c_{23}^2 I_\tau}, \quad (3.14)$$

which is a generalization of the result from [179] which was given for $I_\mu = 0$. Let us now take the mixing angles as input values and determine one of the flavor diagonal corrections in terms of the others

$$I_e = s_{23}^2 I_\mu + c_{23}^2 I_\tau + \frac{c_{12} s_{23} c_{23}}{c_{12} s_{13}} (I_\mu - I_\tau). \quad (3.15)$$

It is, however, not possible to fit the large ratio $\Delta m_{31}^2 / \Delta m_{21}^2 \approx 33$ together with the rather large value $s_{13} \approx 0.15$ instead of $\theta_{13} \approx 0^\circ$ without introducing non-perturbative values of I_A even for a highly degenerate neutrino mass spectrum. The situation changes in the presence of the

Examination of other configurations as $m_1^{(0)} = m_2^{(0)} = -m_3^{(0)}$ or $-m_1^{(0)} = m_2^{(0)} = m_3^{(0)}$ are qualitatively the same and can be treated analogously, which is not done here because there are basically no new insights from other sign assignments.

As defined in Sec. 2.1.3 we again use the shortcuts $s_{ij} = \sin \theta_{ij}$ and $c_{ij} = \cos \theta_{ij}$.

Solutions exist for some $I_A > 1$.

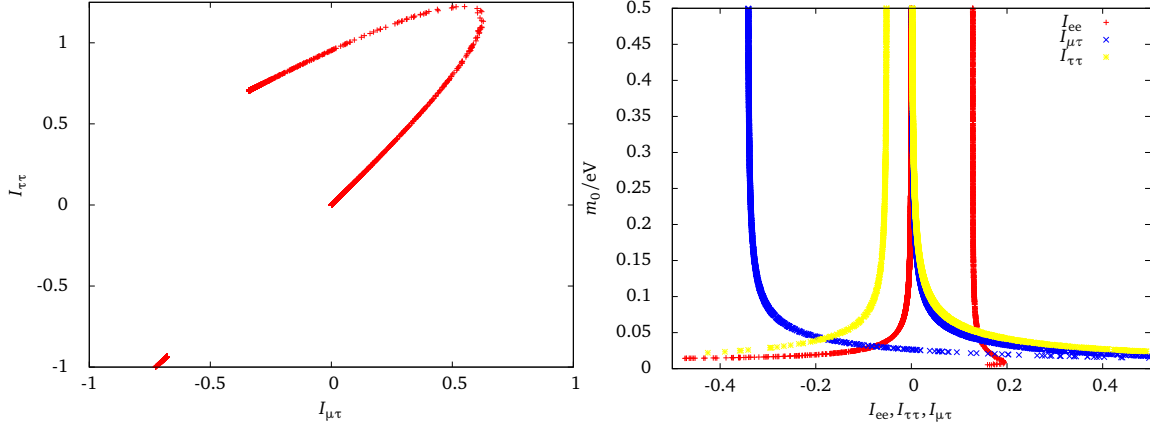


FIGURE 2: The allowed ranges for $I_{\tau\tau}$ and $I_{\mu\tau}$ for Δm_{31}^2 and Δm_{21}^2 within their 1σ ranges (the mixing angles are taken at the central values). The left plot shows the dependence on the lightest neutrino mass m_0 in the vertical direction. There is one class of solutions where all three non-vanishing elements of I are close to zero. (Taken from [194].)

Dirac CP phase $\delta_{\text{CP}} \neq 0$, of course. Then the situation also gets much more complicated. An easier and not uninteresting option is to study the influence of flavor changing threshold corrections. With a dominant $I_{\mu\tau}$ we can indeed find viable solutions with a reasonable θ_{13} ,

We obtain the corresponding result from [176, 179],
 $s_{13} = -\tan\theta_{12}\cot 2\theta_{23}$ in the limit $I_A \rightarrow 0$.

$$s_{13} = \frac{(I_{\mu}c_{23}s_{23} - I_{\mu\tau}\cos 2\theta_{23})\tan\theta_{12}}{I_{\tau}c_{23}^2 + I_{\mu\tau}\sin 2\theta_{23} - I_e}, \quad (3.16)$$

and the correct masses even for not too heavy (i. e. not too degenerate) neutrinos ($m \approx 0.1$ eV). The interesting results are shown in Fig. 2. There is one class of solutions where all non-zero I_{AB} are close to zero and give the correct Δm_{ij}^2 and θ_{13} .

THE EXACT DEGENERATE SITUATION: $m_1^{(0)} = m_2^{(0)} = m_3^{(0)}$ Let us assign the same CP parities to all three neutrino mass eigenstates—Eq. (3.10) does not show any zero entry, but obviously can be diagonalized by diagonalizing the perturbation I only:

We are working with Majorana neutrinos, therefore the mass matrix \mathbf{m}^ν as well as the threshold correction matrix I is symmetric.

$$\mathbf{m}^\nu = m \mathbb{1} + m \begin{pmatrix} I_{11} & I_{12} & I_{13} \\ I_{12} & I_{22} & I_{23} \\ I_{13} & I_{23} & I_{33} \end{pmatrix}, \quad (3.17)$$

and m is the common neutrino mass.

We can now play an amusing game: Experimentally, θ_{23} , the atmospheric mixing angle, is measured to be roughly maximal $|\theta_{23}| \approx \frac{\pi}{4}$ with a small deviation of a few degrees. A maximal mixing in the 2-3 plane can be achieved via the rotation matrix

$$U_{23} = \begin{pmatrix} 1 & 0 & 0 \\ 0 & \frac{1}{\sqrt{2}} & \frac{1}{\sqrt{2}} \\ 0 & -\frac{1}{\sqrt{2}} & \frac{1}{\sqrt{2}} \end{pmatrix}.$$

And up to recently, all measurements of the third mixing angle θ_{13} were consistent with zero. Taking these two phenomenological observations as starting point, we arrive at a determination of θ_{12} in terms of I_{11} , I_{22} and I_{12} only

$$\theta_{12} \approx \frac{1}{2} \arctan \left(\frac{2\sqrt{2}I_{12}}{2I_{22} - I_{11}} \right), \quad (3.18)$$

where we have exploited $\theta_{13} \approx 0$ in order to approximate $I_{13} \approx I_{12}$. After performing the 2-3 rotation with U_{23} , we are left with

$$I' = U_{23}^* I U_{23}^\dagger = \begin{pmatrix} I_{11} & \frac{I_{12}+I_{13}}{\sqrt{2}} & -\frac{I_{12}-I_{13}}{\sqrt{2}} \\ \frac{I_{12}+I_{13}}{\sqrt{2}} & 2I_{22} & 0 \\ -\frac{I_{12}-I_{13}}{\sqrt{2}} & 0 & 0 \end{pmatrix}. \quad (3.19)$$

The eigenvalues of m^ν can also be calculated in terms of the same three I_{ij} with $m_3 = m$. Altogether, there are four free parameters left (m , I_{11} , I_{22} and I_{12}) required for fitting three masses and one mixing angle (θ_{12}). The other two mixing angles were set to phenomenologically motivated distinct values ($\theta_{13} = 0$ and $\theta_{23} = \pi/4$) and shall receive small corrections in the following.

We relax the restrictions required for $\theta_{23} = \pi/4$ ($I_{33} = I_{22}$) and $\theta_{13} = 0$ ($I_{13} = I_{12}$) in a way that we first parametrize deviations:

$$\begin{aligned} I_{33} &= I_{22} + \varepsilon, \\ I_{13} &= I_{12} + \delta. \end{aligned} \quad (3.20)$$

The matrix of threshold corrections is then written as

$$I = \begin{pmatrix} I_{11} & I_{12} & I_{12} + \delta \\ I_{12} & I_{22} & I_{23} \\ I_{12} + \delta & I_{23} & I_{22} + \varepsilon \end{pmatrix}, \quad (3.21)$$

where we have also lifted the artificial requirement $I_{23} = I_{22}$ which had no influence on θ_{23} before anyway. We also need the full freedom of all flavor non-diagonal corrections to fit three mixing angles and three masses (namely I_{11} , I_{22} , I_{12} , I_{23} , δ and ε) and assign the ‘‘unperturbed’’ mass parameter m to be the lightest neutrino mass $m = m_\nu^{(0)}$. Any flavor-universal contribution in the threshold corrections can be again simply added as a shift in the diagonals: $\tilde{I}_A = I_A - I_0$ for $A = e, \mu, \tau$.

As a proof of principle, we perform a brief numerical analysis for two benchmark scenarios, where one corresponds to a possible discovery of neutrino mass at the KATRIN experiment ($m_\nu^{(0)} = 0.35$ eV) and the other one lies at the lower edge of quasi-degenerate neutrino masses (but still allowed by the tightest Λ CDM cosmology bounds, $m_\nu^{(0)} = 0.1$ eV). The results are shown in Tab. 1. It is gratifying to see that the entries of I are in both cases of the size of a typical radiative correction $\lesssim \mathcal{O}(1/100)$ (note

Where recently means ≤ 3 years: the first (high sigma) non-zero measurements date from late 2012 [204].

We implicitly set the whole 2-3 block to the same values: $I_{23} = I_{33} = I_{22}$.

The KATRIN collaboration states the possibility of a discovery with $m_\nu^{(0)} \geq 0.35$ eV and a 95% exclusion with $m_\nu^{(0)} < 0.2$ eV [197].

TABLE 1: Values of the threshold corrections needed to obtain the observed mixing angles and mass splittings for a common neutrino mass of 0.1 eV and 0.35 eV.

	$m_0 = 0.1 \text{ eV}$	$m_0 = 0.35 \text{ eV}$
I_{11}	3.54×10^{-3}	3.00×10^{-4}
I_{12}	1.19×10^{-2}	1.02×10^{-3}
I_{22}	4.67×10^{-2}	4.01×10^{-3}
I_{23}	5.43×10^{-2}	4.67×10^{-3}
ε	2.28×10^{-2}	1.96×10^{-2}
δ	6.73×10^{-5}	1.56×10^{-5}
I	$\begin{pmatrix} 0.354 & 1.19 & 1.20 \\ 1.19 & 4.67 & 5.43 \\ 1.20 & 5.43 & 6.96 \end{pmatrix} \times 10^{-2}$	$\begin{pmatrix} 0.300 & 1.02 & 1.03 \\ 1.02 & 4.01 & 4.67 \\ 1.03 & 4.67 & 5.97 \end{pmatrix} \times 10^{-3}$

that we only want to generate tiny deviations from the degenerate pattern in a regime where the physical masses are only slightly non-degenerate) and show a hierarchy as $1 < 2 < 3$ for labeling the generations. This observation can be used in any new physics model with flavor changing low-energy threshold corrections.

A crucial point in the discussion is the behavior of the generic threshold corrections with the lightest neutrino mass. In case the overall mass scale $m_\nu^{(0)}$ drops below 0.1 eV, the spectrum loses the degeneracy property which is reflected in values $I_{AB} \simeq 0.1$ as can be seen in Fig. 3. Corrections are needed that are not of the size of typical perturbative corrections. The hierarchical regime ($m_\nu^{(0)} \ll 0.1 \text{ eV}$) needs a special kind of flavor symmetry breaking where the degenerate patterns only needs a symmetry that guarantees equal masses. For a given symmetry breaking chain, the hierarchy can be exploited to construct the mixing matrix out of the mass ratios (see Chapter 6 and Ref. [205]).

For radiative neutrino mixing, on one hand one has to ensure that there is no mixing at the tree-level. On the other hand, working with degenerate neutrinos imposing SO(3) or SU(3) flavor symmetries fulfills this requirement automatically.

THRESHOLD CORRECTIONS IN THE ν MSSM: NMFV Non-minimal Flavor Violation (NMFV) in the soft SUSY breaking terms allow to play an amusing game: is it possible to generate the observed neutrino flavor mixing via soft SUSY breaking? The philosophy behind this reasoning was explained in [206]. In this way, flavor violation enters by means of supersymmetric loop corrections. Since the origin of SUSY breaking stays unknown, we connect the flavor puzzle in the SM to the “hidden sector”.

The superpotential of the ν MSSM was introduced in Sec 2.4, Eq. (2.45). With the term “ ν MSSM” we denote the Minimal Supersymmetric Standard Model (MSSM) extended with right-handed neutrinos and no further specification of a UV theory, especially the right-handed Majorana masses

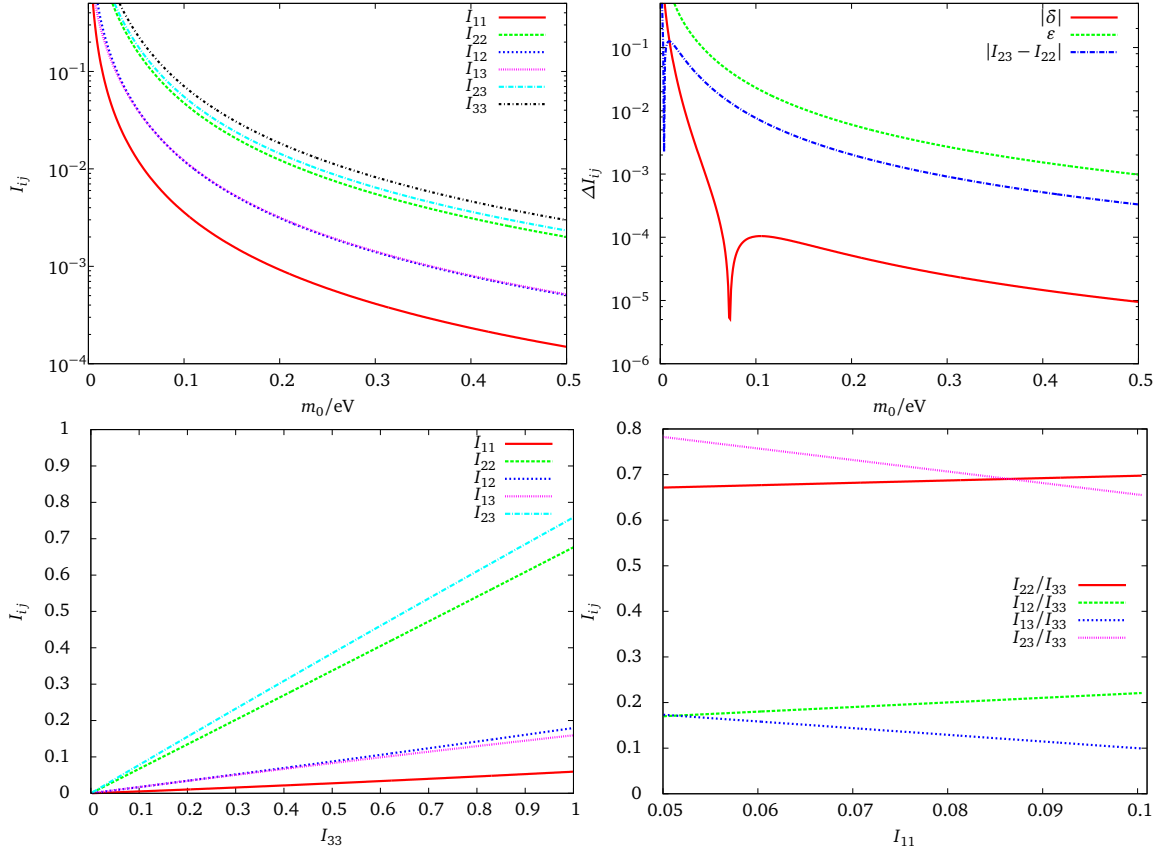


FIGURE 3: Graphical representation of the individual threshold corrections to the neutrino mass. The first row shows the dependence on the absolute neutrino mass scale: the larger $m_\nu^{(0)}$ the smaller the corrections can be. The upper right plot shows the deviations from equal values: $\delta = I_{13} - I_{12}$ and $\varepsilon = I_{33} - I_{22}$ as defined in Eq. (3.20). The lower line shows the interplay of the individual I_{jk} compared to I_{33} , similar plots can be done for other combinations. The lower right plot shows the I_{jk} normalized to the largest contribution I_{33} . (Taken from [194].)

are just present irrespective of any symmetry breaking mechanism which generates them. We assume degenerate soft breaking masses,

$$\tilde{m}_\ell^2 = \tilde{m}_\nu^2 = M_{\text{SUSY}}^2 \mathbf{1},$$

in order to avoid large leptonic FCNC observables as $\ell_j \rightarrow \ell_i \gamma$ or $\ell_j \rightarrow \ell_i \ell_i \ell_i$ (with $(i, j = 1, 2, 3$ and $i < j)$). The flavor violating contribution then lies in the trilinear sneutrino-Higgs couplings A^V only, if we ignore the flavor structure of the neutrino B -term.

The SUSY threshold corrections to the neutrino mass matrix can be calculated in terms of neutrino self-energies [140]

$$\begin{aligned} \left(\mathbf{m}_\nu^{1\text{-loop}} \right)_{ij} &= \left(\mathbf{m}_\nu^{(0)} \right)_{ij} + \\ &\text{Re} \left[\Sigma_{ij}^{(\nu),S} + \frac{m_{\nu_i}^{(0)}}{2} \Sigma_{ij}^{(\nu),V} + \frac{m_{\nu_j}^{(0)}}{2} \Sigma_{ji}^{(\nu),V} \right], \end{aligned} \quad (3.22)$$

The assignment $\tilde{m}_\nu^2 = \tilde{m}_\ell^2$ is only for convenience and not a necessary choice.

with the decomposition of the neutrino self-energy

$$\begin{aligned} \Sigma_{ij}^{(\nu)}(p) = & \Sigma_{ij}^{(\nu),S}(p^2)P_L + \Sigma_{ij}^{(\nu),S^*}(p^2)P_R + \\ & \not{p} \left[\Sigma_{ij}^{(\nu),V}(p^2)P_L + \Sigma_{ij}^{(\nu),V^*}(p^2)P_R \right]. \end{aligned} \quad (3.23)$$

Eq. (3.23) is the application of decomposition (2.34) for Majorana fermions.

For Majorana neutrinos, the self-energy is flavor symmetric ($\Sigma_{ij} = \Sigma_{ji}$ and the coefficients in front of the left and right projectors (P_L and P_R respectively) are related via complex conjugation. The neutrino self-energies are evaluated at $p^2 = 0$ because we can neglect the neutrino masses compared to the superheavy particles in the loop (the same is true for all supersymmetric corrections to SM fermion self-energies).

The generic flavor changing self-energies have already been calculated in [128] and are in agreement with [140]. We are interested in the influence of the soft breaking sneutrino parameters, so we give the sneutrino-chargino and -neutralino self-energy (mixing matrices defined in App. A):

B_0 and B_1 are the standard Passarino-Veltman two-point loop functions, see App. A.

$$\left(\Sigma^{(\nu),S} \right)_{ij} = \frac{1}{4(2\pi)^2} B_0(m_{\tilde{\chi}_k^0}, m_{\tilde{\nu}_s}) m_{\tilde{\chi}_k^0} \left(\frac{-i}{\sqrt{2}} \right)^2 \times \quad (3.24a)$$

$$\left(g_2 Z_{2k}^N - g_1 Z_{1k}^N \right)^2 \mathcal{Z}_{i's}^{\tilde{\nu}*} \mathcal{Z}_{j's}^{\tilde{\nu}*} (\mathbf{U}_{\text{PMNS}})_{i'i} (\mathbf{U}_{\text{PMNS}})_{j'j},$$

$$\left(\Sigma^{(\nu),V} \right)_{ij} = \frac{1}{4(2\pi)^2} B_1(m_{\tilde{\chi}_k^0}, m_{\tilde{\nu}_s}) \left(\frac{-i}{\sqrt{2}} \right)^2 \times \quad (3.24b)$$

$$\left| g_2 Z_{2k}^N - g_1 Z_{1k}^N \right|^2 \mathcal{Z}_{i's}^{\tilde{\nu}} \mathcal{Z}_{j's}^{\tilde{\nu}*} (\mathbf{U}_{\text{PMNS}}^*)_{i'i} (\mathbf{U}_{\text{PMNS}})_{j'j},$$

where summation over repeated indices is understood.

We now look for suitable values of A^ν in order to produce the structure of the generic threshold correction as elaborated above, i. e. solve the equation $m I_{ij} = (\mathbf{m}_\nu^{1\text{-loop}})_{ij} - m \delta_{ij}$ in terms of A_{ij}^ν . Because the dependence on the neutrino mass parameter $m_\nu^{(0)}$ is quite interesting, we vary the neutrino mass in a wider range, shown in Fig. 4.

The same is true for the application in Sec. 3.2.3.

The results are qualitatively very stable under variation of the free SUSY parameters. In any case, we need large neutrino A -terms to get the structure of the threshold corrections as for the generic discussion. Effectively, the combination A^ν / M_{SUSY} drives the corrections. For the analysis presented here we vary the values of the following variables randomly in the given intervals:

$$\begin{aligned} M_{\text{SUSY}} & \in [500, 5000] \text{ GeV}, \\ M_1 & \in [0.3, 3] M_{\text{SUSY}}, \\ M_2 & \in [1, 5] M_{\text{SUSY}}, \\ \mu & \in [-15, 15] \text{ TeV}, \\ \tan \beta & \in [10, 60]. \end{aligned} \quad (3.25)$$

As expected, for low values of the absolute neutrino mass m_0 where the deviation from the degenerate pattern is large, the SUSY threshold

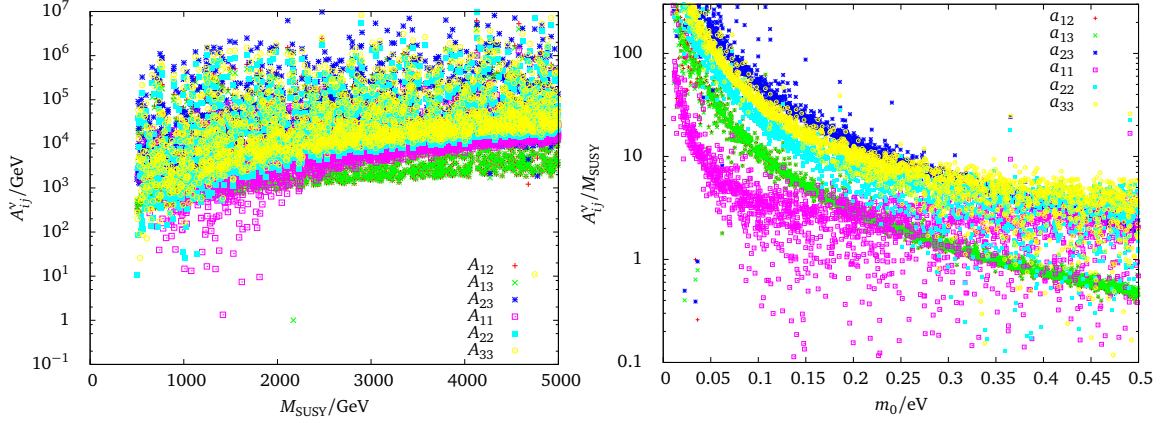


FIGURE 4: The left plot shows values of A^V for the variation of parameters specified in (3.25). The lightest neutrino mass $m_\nu^{(0)}$ was chosen in the regime plotted on the right side, where we rescaled all trilinear soft breaking couplings with the SUSY scale, $a_{ij} = A_{ij}^V / M_{\text{SUSY}}$. The values of a_{12} and a_{13} are roughly the same since they differ only by a small parameter as described in the generic discussion. (Taken from [194].)

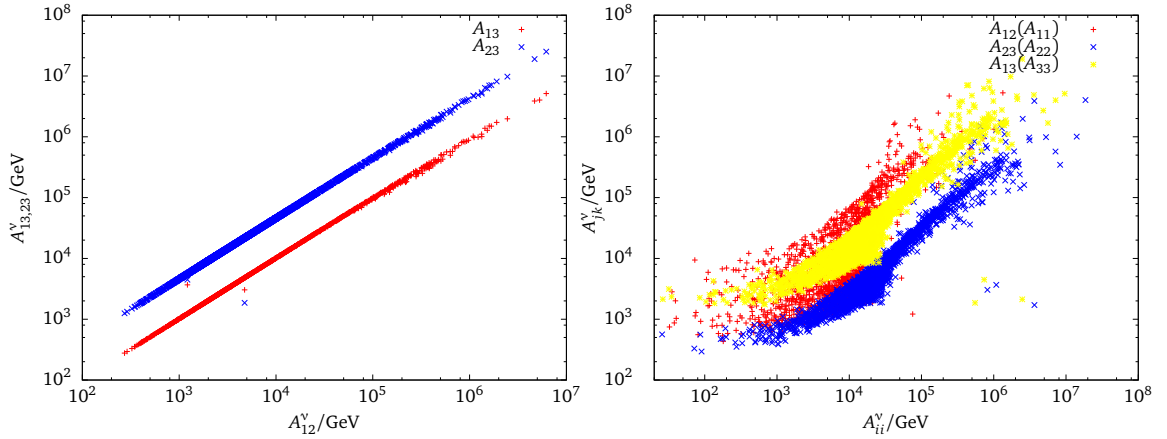


FIGURE 5: Correlations between the different elements of A^V found to reproduce neutrino masses and mixings. The left plot shows the off-diagonals with respect to A_{12}^V where the right shows the correlation with the diagonal entries. (Taken from [194].)

corrections measured in the values of A^V have to be large as shown in Fig. 4 where we plotted the ratio $a_{ij} = A_{ij}^V / M_{\text{SUSY}}$. The left-hand side of Fig. 4 compared to the right-hand side shows that basically this ratio is the parameter which drives the corrections and has the same shape as the I_{ij} dependent on m_0 where the size of the A_{ij}^V depending on the SUSY scale also is sensitive to the parameters of the theory.

3.2.2 Renormalizing the Seesaw

In the previous Section and in the following we discuss supersymmetric threshold corrections to neutrino mixing with NMFV soft breaking trilinear couplings. There is, however, a part of the corrections which is independent of soft breaking terms (a genuine F -term contribution to the

The expression $\text{diag}(x_i)$ means a diagonal matrix with entry x_i in the i -th diagonal element.

As will turn out, g is something like $g_1 \nu_\nu^2 / (16\pi^2)$.

sneutrino mass matrix) and nevertheless alters the flavor structure of the renormalized light neutrino mass, if the heavy neutrinos are not degenerate. This type of corrections gives a logarithmically enhanced contribution to the one-loop seesaw mass formula with a logarithm of the heavy neutrino mass:

$$\Delta \mathbf{m}_\nu \sim \mathbf{Y}_\nu \mathbf{M}_R^{-1} \left\{ \mathbf{1} + g \text{diag} \left[\log \left(\frac{M_{\text{SUSY}}^2}{M_{R,i}^2} \right) \right] \right\} \mathbf{Y}_\nu^T, \quad (3.26)$$

where g is some loop suppressed coupling factor. This case becomes important if the right-handed neutrinos are hierarchical. The influence on the flavor pattern of Eq. (3.26) disappears completely for degenerate right-handed neutrinos; in that case $\log(M_{\text{SUSY}}^2/M_R^2)/M_R$ is proportional to the identity matrix, and the full flavor structure of the seesaw mass term sits in the product of neutrino Yukawa couplings $\mathbf{Y}_\nu \mathbf{Y}_\nu^T$.

For the description of the effect, it is sufficient to discuss a reduced parameter set of the ν MSSM with a left-right mixing in the sneutrino sector only from the F -term contribution to the mass matrix $\sim M_R m_\nu^D$:

$$\mathcal{W} \supset \mu H_d \cdot H_u + Y_{ij}^\nu H_d \cdot L_{L,i} \bar{N}_{R,j} + \frac{1}{2} M_{ij}^R \bar{N}_{R,i} \bar{N}_{R,j}, \quad (3.27a)$$

$$\mathcal{L}_m^{\tilde{\nu}} \supset |\nu_u|^2 \tilde{\nu}_L^* \mathbf{Y}_\nu \mathbf{Y}_\nu^\dagger \tilde{\nu}_L + |\nu_u|^2 \tilde{\nu}_R^* \mathbf{Y}_\nu^* \mathbf{Y}_\nu^T \tilde{\nu}_R - \nu_d \mu^* \tilde{\nu}_L \mathbf{Y}_\nu \tilde{\nu}_R^* + \frac{\nu_u}{2} \tilde{\nu}_L \mathbf{Y}_\nu \mathbf{M}_R^* \tilde{\nu}_R + \text{h. c.}$$

$$+ \frac{1}{4} \tilde{\nu}_R^* \mathbf{M}_R \mathbf{M}_R^* \tilde{\nu}_R + \mathcal{L}_{\text{soft}},$$

$$\mathcal{L}_{\text{soft}} = \tilde{\nu}_L^* \tilde{\mathbf{m}}_\ell^2 \tilde{\nu}_L + \tilde{\nu}_R^* \tilde{\mathbf{m}}_\nu^2 \tilde{\nu}_R, \quad (3.27c)$$

and without soft breaking trilinear and bilinear couplings $h_u^0 \tilde{\nu}_L^* \mathbf{A}_\nu \tilde{\nu}_R$ and $\tilde{\nu}_R^* \mathbf{B}_\nu^2 \tilde{\nu}_R^*$, respectively. In the following, we also neglect the μ -term contribution in the sneutrino mass matrix (which is multiplied with the smaller ν_d anyway).

The sneutrino squared mass matrix can then be expressed in terms of the right-handed Majorana mass \mathbf{M}_R , the Dirac mass $\mathbf{m}_\nu^D = \frac{\nu_u}{\sqrt{2}} \mathbf{Y}_\nu$ and the generic soft SUSY breaking mass $m_S = M_{\text{SUSY}}$ (let us simplify the discussion with $\tilde{\mathbf{m}}_\ell^2 = \tilde{\mathbf{m}}_\nu^2 = m_S^2 \mathbf{1}$):

$$\mathcal{M}_\nu^2 = \frac{1}{2} \begin{pmatrix} \mathcal{M}_{LL}^2 & \mathcal{M}_{LR}^2 \\ (\mathcal{M}_{LR}^2)^\dagger & \mathcal{M}_{RR}^2 \end{pmatrix} \quad (3.28)$$

$$\mathcal{M}_{LL}^2 = \begin{pmatrix} \mathbf{m}_\nu^{D\dagger} \mathbf{m}_\nu^D + m_S^2 & 0 \\ 0 & \mathbf{m}_\nu^{D\dagger} \mathbf{m}_\nu^D + m_S^2 \end{pmatrix}, \quad (3.29)$$

$$\mathcal{M}_{LR}^2 = \begin{pmatrix} \frac{1}{2} \mathbf{m}_\nu^{D*} \mathbf{M}_R & 0 \\ 0 & \frac{1}{2} \mathbf{m}_\nu^D \mathbf{M}_R^* \end{pmatrix},$$

$$\mathcal{M}_{RR}^2 = \begin{pmatrix} \frac{1}{2} \mathbf{M}_R \mathbf{M}_R^* + \mathbf{m}_\nu^D \mathbf{m}_\nu^{D\dagger} + m_S^2 & 0 \\ 0 & \frac{1}{2} \mathbf{M}_R^* \mathbf{M}_R + \mathbf{m}_\nu^{D*} \mathbf{m}_\nu^D + m_S^2 \end{pmatrix},$$

note that $\mathbf{M}_R^T = \mathbf{M}_R$. We have chosen a basis $\vec{N} = (\tilde{\nu}_L, \tilde{\nu}_L^*, \tilde{\nu}_R^*, \tilde{\nu}_R)^T$ with 3-vectors in flavor space $\tilde{\nu}_{L,R}^{(*)}$, suppressing generation indices.

Due to the large hierarchy between m_S and M_R , the “right-handed” superpartners of the neutrinos have basically the mass M_R , where the “left-handed” ones live at m_S .

CORRECTIONS TO TYPE I SEESAW The tree-level seesaw mass formula carries a structure where the inverse right-handed Majorana mass is sandwiched between Dirac Yukawa couplings, $\sim \mathbf{Y}_\nu \mathbf{M}_R^{-1} \mathbf{Y}_\nu$. The SUSY one-loop corrections to the seesaw mass operator carry the same sandwich-like structure, $\sim v_u^2 \mathbf{Y}_\nu$ (something) \mathbf{Y}_ν^T , but between the two Yukawa couplings something more happens. Two Dirac Yukawas are essential to include two chirality flips in order to intermediately have right-handed (s)neutrinos and therefore the suppression with $1/M_R$ in the loop. Moreover, we need one lepton flow flip that has to be induced by one Majorana mass insertion as shown in Fig. 6, such that both diagrams show a $\Delta L = 2$ transition. We estimate the diagram to the right of Fig. 6 to be

$$\sim \frac{g_1^2}{16\pi^2} \mathbf{Y}_\nu \mathbf{M}_R \frac{1}{m_R^2} \mathbf{Y}_\nu^T.$$

We calculate the loop diagram in the mass insertion approximation, where the fields running in the loop are interaction eigenstates and do not refer to mass eigenstates. The mixing occurs via the couplings. In a world without μ -term, there is no Higgsino mixing (and $m_{\tilde{H}} = 0$) and the diagram simplifies accordingly:

$$\begin{aligned} -i \Sigma_{if}^\nu &= \frac{v_u^2 g_1^2}{4} \int \frac{d^D q}{(2\pi)^D} \times \\ &\sum_{k=1}^{n_R} \frac{M_{R,k} Y_{ik}^\nu Y_{fk}^\nu}{(q - m_{\tilde{B}})(q - m_{\tilde{H}}) \left((p - q)^2 - m_{\tilde{\nu}_{\ell,i}}^2 \right) \left((p - q)^2 - m_{\tilde{\nu}_{R,k}}^2 \right)} \\ &\stackrel{\mu \rightarrow 0}{=} \frac{v_u^2 g_1^2}{4} \int \frac{d^D q}{(2\pi)^D} \times \\ &\sum_{k=1}^{n_R} \frac{(q^2 + q m_{\tilde{B}}) M_{R,k} Y_{ik}^\nu Y_{fk}^\nu}{(q^2 - m_{\tilde{B}}^2) q^2 \left((p - q)^2 - m_{\tilde{\nu}_{\ell,i}}^2 \right) \left((p - q)^2 - m_{\tilde{\nu}_{R,k}}^2 \right)} \\ &\stackrel{p \rightarrow 0}{=} \frac{v_u^2 g_1^2}{4} \frac{i}{16\pi^2} \sum_{k=1}^{n_R} M_{R,k} Y_{ik}^\nu Y_{fk}^\nu C_0(m_{\tilde{B}}, m_{\tilde{\nu}_{\ell,i}}, m_{\tilde{\nu}_{R,k}}) \left(\frac{4\pi}{Q^2} e^{-\gamma_E} \right)^\epsilon. \end{aligned} \quad (3.30)$$

For vanishing external momenta, the loop integral reduces to C_0 and the one-loop self-energy yields

$$\begin{aligned} \Sigma_{if}^\nu &= \frac{v_u^2 g_1^2}{64\pi^2} \sum_{k=1}^{n_R} \frac{Y_{ik}^\nu Y_{fk}^\nu}{m_{\tilde{\nu}_{\ell,i}}^2 - m_{\tilde{B}}^2} \times \\ &\left[\frac{m_{\tilde{B}}^2}{m_{\tilde{\nu}_{R,k}}^2} \log \left(\frac{m_{\tilde{B}}^2}{m_{\tilde{\nu}_{R,k}}^2} \right) - \frac{m_{\tilde{\nu}_{\ell,i}}^2}{m_{\tilde{\nu}_{R,k}}^2} \log \left(\frac{m_{\tilde{\nu}_{\ell,i}}^2}{m_{\tilde{\nu}_{R,k}}^2} \right) \right], \end{aligned} \quad (3.31)$$

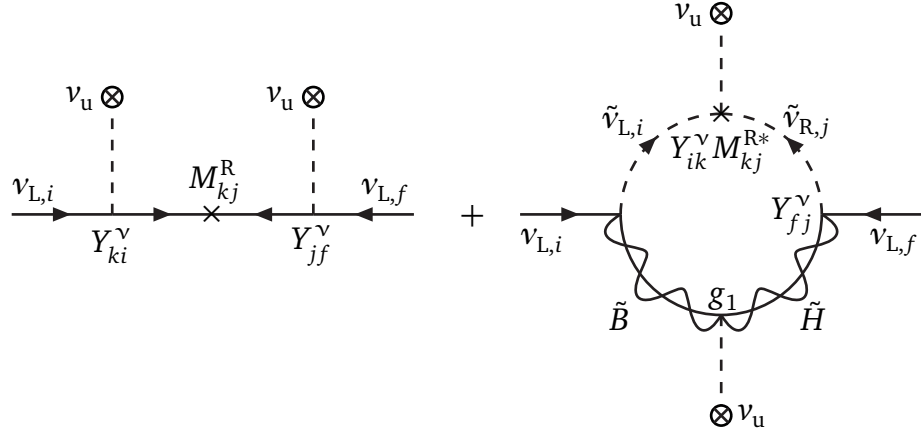


FIGURE 6: Tree-level plus one-loop contribution to the type I seesaw mass formula for the light neutrinos.

where we have used standard conventions for the loop functions (our definition of C_0 is given in App. A), approximated $M_{R,k} \approx m_{\tilde{\nu}_{R,k}}$ and expanded in small mass ratios like $m_S^2/m_{\tilde{\nu}_R}^2$, where m_S is either $m_{\tilde{B}}$ or $m_{\tilde{\nu}_\ell}$.

The mass splitting of the light sneutrinos is of the order of the mass splitting of light neutrinos—and therefore completely negligible compared to the SUSY scale m_S .

The light sneutrinos can easily be taken degenerate, since their masses are dominated by the soft SUSY breaking mass parameters and deviations are of the order of the light neutrino mass squared. The heavier sneutrinos get their mass basically from the Majorana mass term.

However, by assuming a similar hierarchy in the neutrino Yukawa coupling as for charged particles' Yukawa couplings (quarks and leptons), to end up with a quasi-degenerate light neutrino mass spectrum, the heavy eigenvalues can differ over several orders of magnitude.

In the case of degenerate SUSY masses, i. e. the limit $m_{\tilde{\nu}_\ell} \rightarrow m_{\tilde{B}} \rightarrow m_S$, Eq. (3.31) reduces to a logarithmically enhanced contribution to the tree-level neutrino mass operator $\kappa = Y_\nu M_R^{-1} Y_\nu^T$:

$$\Delta\kappa_\nu = \frac{g_1^2}{64\pi^2} Y_\nu \mathfrak{M}_R^{-1} Y_\nu^T, \quad (3.32)$$

where \mathfrak{M}_R^{-1} is a diagonal matrix with the entries $\log(m_S^2/m_{\tilde{\nu}_{R,k}}^2)/m_{\tilde{\nu}_{R,k}}$. Up to small corrections $\mathcal{O}(m_S)$, $m_{\tilde{\nu}_R} = M_R$. Therefore, one has to re-diagonalize the neutrino mass matrix

$$\begin{aligned} \mathbf{m}_\nu &= v_u^2 (\kappa_\nu + \Delta\kappa_\nu) \\ &= v_u^2 Y_\nu \text{diag} \left(\frac{1}{m_{\tilde{\nu}_{R,k}}} + \frac{g_1^2}{64\pi^2} \frac{\log(m_S^2/m_{\tilde{\nu}_{R,k}}^2)}{m_{\tilde{\nu}_{R,k}}} \right) Y_\nu^T, \end{aligned} \quad (3.33)$$

which for exactly degenerate right-handed masses $m_{\tilde{\nu}_{R,k}} = M_{R,k} = M_R$ has the same flavor structure as the tree-level version: $\sim Y_\nu Y_\nu^T$. In general, the tree-level PMNS matrix $U_{\text{PMNS}}^{(0)}$ diagonalizes the combination $Y_\nu M_R^{-1} Y_\nu^T$ which gets altered by the logarithm in the diagonal matrix in between the Yukawas. The physical PMNS matrix therefore can be significantly changed by the logarithmic structure and deviate from any pre-specified pattern.

The tree-level mixing matrix may be governed by flavor symmetries.

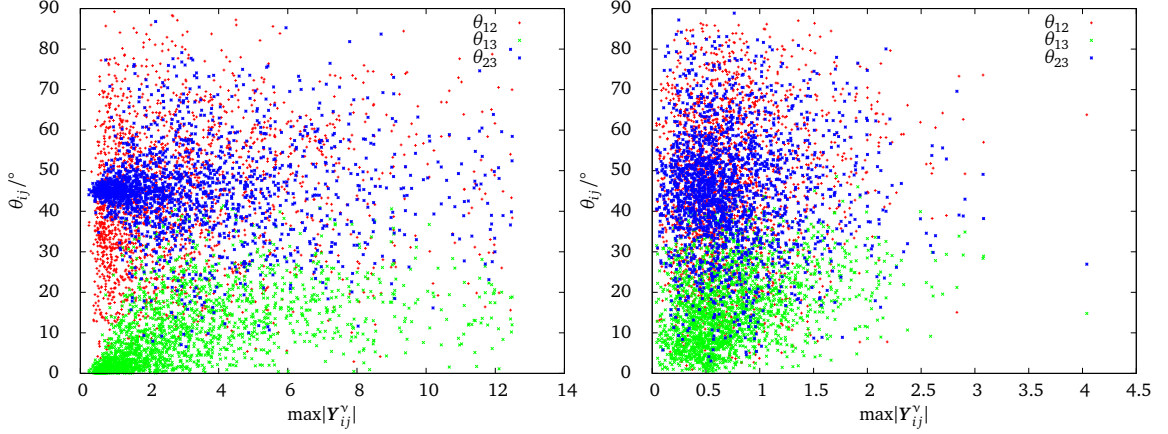


FIGURE 7: Scatter plots for the corrected neutrino mixing angles $\theta_{ij} = \theta_{12}, \theta_{13}, \theta_{23}$ for quasi-degenerate right-handed masses (left panel) and a strong hierarchy in the heavy spectrum (right panel). An interesting observation is that θ_{12} nearly scatters over the complete range, especially for Yukawa couplings and irrespectively of the heavy spectrum. Also from an initially zero θ_{13} , this mixing angle could be as large as 30° . We have constrained the larger value of the Dirac neutrino Yukawa coupling to be perturbative (generally defined as $< 4\pi$).

Eq. (3.33) now defines the new mixing matrix as

$$\mathbf{U}_{\text{PMNS}}^* \mathbf{m}_\nu \mathbf{U}_{\text{PMNS}}^\dagger \sim \mathbf{U}_{\text{PMNS}}^* (\boldsymbol{\kappa}_\nu + \Delta \boldsymbol{\kappa}_\nu) \mathbf{U}_{\text{PMNS}}^\dagger.$$

Moreover, since the combination $\mathbf{Y}_\nu \mathbf{M}_R^{-1} \mathbf{Y}_\nu^T$ is destroyed, the tree-level inversion given by the Casas-Ibarra formula makes the one-loop corrections sensitive to the arbitrary flavor structure of \mathbf{Y}_ν , parametrized in three complex angles of \mathcal{R} in Eq. (3.7).

A similar relation was found for the non-supersymmetric contribution from the Higgs and Z boson [207, 208].

We look for deviations from a tribimaximal mixing pattern at the tree-level, especially $\theta_{13} \neq 0$, and figure out how much deviation from this very specific pattern is possible. The annoying part is the treatment of the *a priori* arbitrary structure of \mathbf{Y}_ν . To be as generic as possible, we randomly scatter values for the three complex mixing angles in the complex orthogonal matrix \mathcal{R} and consider for comparison two scenarios: one with roughly degenerate right-handed masses $m_{\nu_{R,k}} \approx m_{\bar{\nu}_{R,k}}$ that vary within two orders of magnitudes (exact degenerate masses do not alter the mixing as discussed above) and second a large splitting with the three right-handed masses in the range $10^5 \dots 10^{14}$ GeV. Results are shown in Fig. 7. Since the Casas-Ibarra parametrization also needs the light masses as input (and always gives correct results), we fix $m_\nu^{(0)} = 0.3$ eV.

The presence of hierarchical right-handed masses therefore alters any preset mixing pattern. Without the need of flavor changing soft breaking terms, we, however, can still only achieve rather mild deviations from the initial $\theta_{13} = 0$. The other angles are allowed to scatter over the full range. The biggest deviation from $\theta_{13} = 0$ is also only possible for drastically large values of $|\mathcal{R}_{ij}|$. Since the angles of \mathcal{R} are complex, its magnitudes of matrix elements are allowed to be larger than 1. This behavior gets

The Casas-Ibarra parametrization relies on the tree-level formulation.

Actually, we can assign any tree-level mixing in principle. However, (tri)bimaximal mixing is very close to the observed structures and can be motivated by a vast set of flavor symmetry models.

Nevertheless, θ_{13} can be as large as 30° .

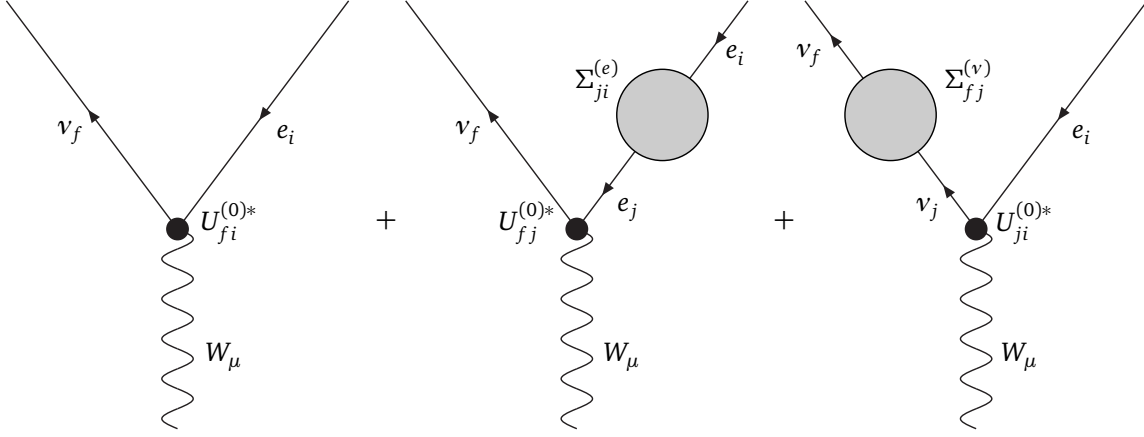


FIGURE 8: Renormalization of the lepton mixing matrix by flavor changing self-energies at external legs according to the method by Denner and Sack [110].

also reflected into the definition of Y_ν which anyhow challenges flavor model building (if one seeks an explanation of the strange values). To be conservative, we also constrain the resulting Y_ν to be perturbative and only allow solutions with $\max |Y_{ij}^\nu| < 4\pi$.

3.2.3 Renormalizing the Mixing Matrix

The mixing matrix of the charged current has a contribution from both up-type and down-type fermions as elaborated in Sec. 2.1.3 and 2.4. In a general basis (charged leptons not necessarily diagonal), the PMNS matrix is given by the combination

$$U_{\text{PMNS}} = \mathbf{S}_L^e (\mathbf{S}_L^\nu)^\dagger.$$

The flavor diagonal terms in this procedure are infinite anyway as can be seen from below.

In contrast to the quark mixing matrix, up and down sector are interchanged by convention.

Corrections to the mass matrices alter both \mathbf{S}_L^e and \mathbf{S}_L^ν . The off-diagonal contributions can be absorbed by the following procedure into the mixing matrix, the diagonal contributions on the other hand can be absorbed into the wave function renormalization.

We proceed with the diagrams of Fig. 8 and multiply the renormalization factors from the left (neutrino leg) and right (electron leg) being aware of the Hermitian conjugate mixing matrix in the vertex.

$$\begin{aligned} U_{\text{PMNS}} &= (\mathbf{1} + \Delta U_L^e)^\dagger U^{(0)} (\mathbf{1} + \Delta U_L^\nu)^\dagger \\ &\approx U^{(0)} + (\Delta U_L^e)^\dagger U^{(0)} + U^{(0)} (\Delta U_L^\nu)^\dagger, \end{aligned} \quad (3.34)$$

where $U^{(0)}$ denotes the unrenormalized, “bare” mixing matrix that is determined from tree-level flavor physics as in Sec. 3.2.1. Altogether, the renormalized interaction vertex with the W -Boson can then be written as

$$\frac{g}{\sqrt{2}} \gamma^\mu P_L U^{(0)\dagger} \rightarrow \frac{g}{\sqrt{2}} \gamma^\mu P_L (U^{(0)\dagger} + \mathbf{D}_L + \mathbf{D}_R), \quad (3.35)$$

where $\mathbf{D}_L, \mathbf{D}_R$ are the correction matrices concerned with the left and right leg respectively. We have simply transferred the description from [89].

The full contributions can be easily calculated attaching the generic self-energies Eq. (3.23) to the vertex and exploiting the equations of motion

$\not{p}u(p_i) = m_i u(p_i)$
for Dirac spinors u .

$$D_{L,fi} = \sum_{j=1}^n [\Delta U_L^{\nu}]_{fj} U_{ji}^{(0)\dagger} \quad (3.36a)$$

$$= \sum_{j \neq f} \frac{m_{\nu_f} \left(\Sigma_{fj}^{(\nu),S} + m_{\nu_f} \Sigma_{fj}^{(\nu),V} \right) + m_{\nu_j} \left(\Sigma_{fj}^{(\nu),S^*} + m_{\nu_f} \Sigma_{fj}^{(\nu),V^*} \right)}{m_{\nu_j}^2 - m_{\nu_f}^2} U_{ji}^{(0)\dagger},$$

$$D_{R,fi} = \sum_{j=1}^n U_{fj}^{(0)\dagger} [\Delta U_L^e]_{ji} \quad (3.36b)$$

$$= \sum_{j \neq i} U_{fj}^{(0)\dagger} \frac{m_{e_i} \left(\Sigma_{ji}^{(e),LR} + m_{e_i} \Sigma_{ji}^{(e),LL} \right) + m_{e_j} \left(\Sigma_{ji}^{(e),RL} + m_{e_i} \Sigma_{ji}^{(e),RR} \right)}{m_{e_i}^2 - m_{e_j}^2}.$$

The charged lepton contribution can be simplified and expanded in small mass ratios like m_μ/m_τ :

$$\Delta U_L^e = \begin{pmatrix} 0 & \frac{1}{m_\mu} \Sigma_{12}^{(e),LR} & \frac{1}{m_\tau} \Sigma_{13}^{(e),LR} \\ \frac{-1}{m_\mu} \Sigma_{21}^{(e),RL} & 0 & \frac{1}{m_\tau} \Sigma_{23}^{(e),LR} \\ \frac{-1}{m_\tau} \Sigma_{31}^{(e),RL} & \frac{-1}{m_\tau} \Sigma_{32}^{(e),RL} & 0 \end{pmatrix}, \quad (3.37)$$

where we have neglected the chirality conserving self-energy contributions which are suppressed by $1/M_{\text{SUSY}}$ compared to the chirality flipping ones, see Refs. [89, 112].

In fact, this expansion does not work for neutrinos, especially not for the case in which all neutrinos are nearly of equal mass. There, we have to deal with the complete expression of $\Delta U_L^{(\nu)}$. Once again, we can safely neglect the Σ^V part in Eq. (3.36a). For trivial tree-level mixing, $U_{ij}^{(0)} = \delta_{ij}$, we are left with

$$D_{L,fi} = [\Delta U_L^{(\nu)}]_{fi} = \frac{m_{\nu_f} \Sigma_{fi}^{(\nu),S} + m_{\nu_i} \Sigma_{fi}^{(\nu),S^*}}{m_{\nu_i}^2 - m_{\nu_f}^2}. \quad (3.38)$$

For the numerical analysis later on we shall keep all the contributions for convenience. Nevertheless, the simplifications of Eqs. (3.37) and (3.38) are enlightening to see where the dominant contributions come from.

In principle, Eq. (3.34) shows two independent contributions, that are numerically quite different as well. The correction from the charged lepton leg suffers from a similar hierarchy in masses (with a result shown in Eq. (3.37)) as the renormalization of the quark mixing matrix does in Ref. [89] and lies numerically in the same ballpark. So ΔU_L^e may only account for minor corrections in the sub-percent regime. Nevertheless, the corrections from the neutrino leg are significantly enhanced due to the quasi-degenerate property of the neutrino mass spectrum. Only for a

This means that corrections from the charged lepton leg only give CKM-like corrections and cannot account for the large leptonic mixing as also discussed in [112].

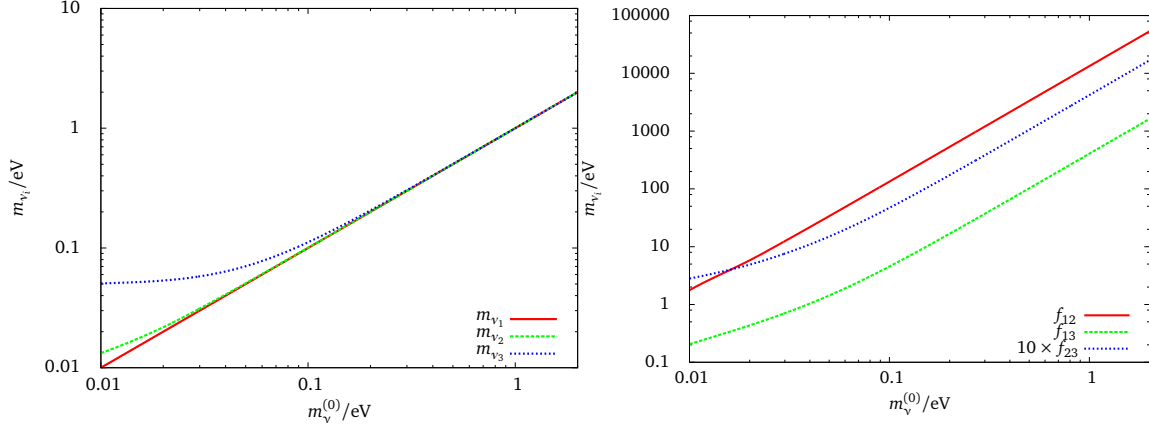


FIGURE 9: The neutrino mass spectrum gets more and more degenerate for increasing $m_{\nu}^{(0)}$ as can be seen from the left side. The right side shows the increase of the enhancement factors f_{ij} , for better visibility f_{23} was multiplied by a factor of ten to separate it from f_{13} .

strongly hierarchical spectrum, the enhancement is gone similar to the hierarchical charged leptons. In this case, the large leptonic mixing follows from the method given in Chap. 6 and [205]. We see from eq. (3.38) an enhancement factor [209]

$$f_{fi} = \frac{m_{\nu_f} m_{\nu_i}}{\Delta m_{fi}^2}, \quad (3.39)$$

σ^ν is a dimensionless quantity parametrizing the loop correction and therefore suppressed at least by one loop-factor $1/16\pi^2$ and the couplings inside the loop.

writing the self-energy $\Sigma_{fi}^{(\nu),S} = m_{\nu_i} \sigma_{fi}^\nu$. The increase of f_{fi} with the neutrino mass (and therefore the degree of degeneracy in the spectrum) is shown in Fig. 9. In this way, we can express the corrections in a model-independent way to figure out how large they have to be in order to give the right mixing and have

$$D_{L,fi} = \sum_{j \neq f} f_{fj} \sigma_{fj}^\nu U_{ij}^{(0)*}, \quad (3.40)$$

with an arbitrary tree-level mixing matrix $U^{(0)}$. Estimates for σ_{fi}^ν for no mixing in $U^{(0)}$ and tribimaximal mixing are shown in Fig. 10.

Eq. (3.39) can be large in the case of a “large” neutrino mass as it might be measured by the KATRIN experiment in the near future. For an absolute neutrino mass around the discovery limit 0.35 eV and the measured mass squared differences $\Delta m_{21}^2 \approx 7.50 \times 10^{-5} \text{ GeV}^2$ and $\Delta m_{31}^2 \approx 2.46 \times 10^{-3} \text{ GeV}^2$ we have e. g. $f_{21} \approx 1634$ and $f_{31} \approx 50$. This property may account for a larger 1-2 mixing compared to the 1-3 mixing, when starting from the no-mixing hypothesis at tree-level.

The determination of the three mixing angles obviously only needs to take into account the upper triangle: namely the absolute value of the U_{13} entry (sometimes called U_{e3}) fixes $\sin \theta_{13}$ which can then be used to get $\sin \theta_{12}$ from U_{12} and $\sin \theta_{23}$ from U_{23} . This procedure is well-known and was basically used during the years to precisely measure the mixing angles in absence of 1-3 mixing.

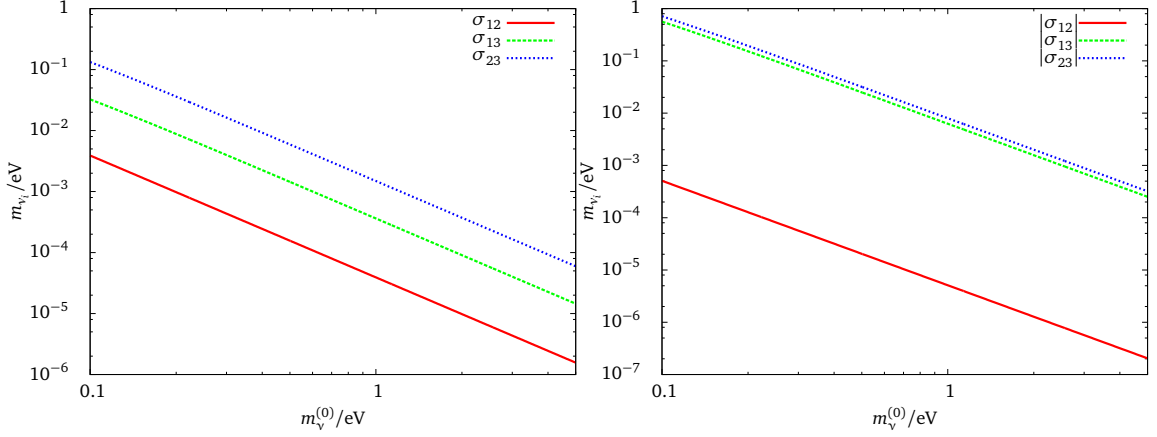


FIGURE 10: The model-independent analysis of the generic corrections σ_{ij} as expected shows a decreasing behavior with increasing neutrino mass: the more degenerate the spectrum, the smaller corrections are needed. We show the result for $U^{(0)} = \mathbb{1}$ left and for tribimaximal mixing at the tree-level right.

To figure out what is possible by means of those corrections, we take a look at the case without tree-level flavor mixing and get the following (and pretty obvious) dependence on the corrections from the electron and neutrino leg:

$$U_{12} = [\Delta U_L^e]_{21}^* + [\Delta U_L^\nu]_{21}^*, \quad (3.41a)$$

$$U_{13} = [\Delta U_L^e]_{31}^* + [\Delta U_L^\nu]_{31}^*, \quad (3.41b)$$

$$U_{23} = [\Delta U_L^e]_{32}^* + [\Delta U_L^\nu]_{32}^*. \quad (3.41c)$$

If, by contrast, we consider a model with only no tree-level θ_{13} (as in a tribimaximal mixing scenario), radiative corrections will lead to a non-vanishing U_{13}^{PMNS}

$$U_{13} = [\Delta U_L^e]_{12}^* U_{23}^{(0)} + [\Delta U_L^e]_{13}^* U_{33}^{(0)} + U_{11}^{(0)} [\Delta U_L^\nu]_{13}^* + U_{12}^{(0)} [\Delta U_L^\nu]_{23}^*, \quad (3.42)$$

even if the tree-level structure of no 1-3 mixing is preserved in the loop and there is no loop-induced mixing from the charged leptons. Take for this all $[\Delta U_L^e]_{ij} = 0$ in Eq. (3.42) and also $[\Delta U_L^\nu]_{13} = 0$, then U_{13} is uniquely determined by the tree-level $U_{12}^{(0)}$ and the loop correction to the 2-3 mixing

$$U_{13} = U_{12}^{(0)} [\Delta U_L^\nu]_{23}^*. \quad (3.43)$$

Therefore the size of $[\Delta U_L^\nu]_{23}$ is fixed to $U_{13}^{\text{exp}} / U_{12}^{\text{TBM}} \approx 0.15 \times \sqrt{3} \approx 0.26$ in order to give the right U_{13} , which already is quite large for a typical loop correction due to the enhancement factor f_{32} . The correction $[\Delta U_L^\nu]_{23}$ is calculated in the underlying full theory which gives the self-energies. However, if the flavor structure is preserved in the loop, the size may

The tribimaximal mixing is given by [210] $U^{\text{TBM}} =$

$$\begin{pmatrix} \sqrt{\frac{2}{3}} & \frac{1}{\sqrt{3}} & 0 \\ -\frac{1}{\sqrt{6}} & \frac{1}{\sqrt{3}} & -\frac{1}{\sqrt{2}} \\ -\frac{1}{\sqrt{6}} & \frac{1}{\sqrt{3}} & \frac{1}{\sqrt{2}} \end{pmatrix}.$$

be estimated the following: $[\Delta U_L^{\nu}]_{23} \sim U_{23}^{\text{TBM}} / (16\pi^2) \times f_{32} \approx \frac{1}{\sqrt{2}} \frac{50}{16\pi^2} \approx 0.22$, where the factor $\frac{1}{16\pi^2}$ estimates the loop suppression and $f_{32} \approx f_{31} \approx 50$ was chosen for $m_{\nu}^{(0)} = 0.35$ eV as described above. This estimate even indicates that the new physics in the loop needed to generate U_{13} also may follow tribimaximal mixing.

Corrections of this type have the power to completely mix up all imaginable tree-level mixing patterns resulting in the observed PMNS structure. Especially, it is feasible to get the PMNS matrix out of a theory with no flavor mixing in the standard model fermions, where the flavor enters in the loops as one has the power of sufficiently large loop corrections.

NEUTRINO MIXING MATRIX RENORMALIZATION IN THE MSSM Let us again discuss the effect of radiative neutrino mixing in extensions of the MSSM. The flavor changing self-energies are the same as previously discussed and given in Eq. (3.24). Differently from the situation in Sec. 3.2.1, we now do not insist on degenerate neutrinos but in principle allow for an arbitrary mass spectrum before imposing the SUSY loop corrections. However, the spectrum is assumed to be sufficiently degenerate and the mass squared differences are the measured ones given in Eq. (2.36).

Again, we want to figure out how much the flavor off-diagonal sneutrino soft breaking terms can account for lepton mixing. We do not want to induce large flavor violation in the charged lepton sector, therefore we take the soft masses flavor-universal

$$\tilde{m}_{\ell}^2 = \tilde{m}_e^2 = \tilde{m}_{\nu}^2 = M_{\text{SUSY}}^2 \mathbf{1}.$$

Besides soft masses there are two more flavor matrices in the soft breaking Lagrangian (talking about the ν MSSM): the trilinear sneutrino–Higgs coupling A^{ν} and the bilinear B_{ν}^2 for the superpartners of right-handed neutrinos. Literally, B_{ν}^2 is the soft breaking counterpart of the right-handed Majorana mass in the superpotential—and therefore suspected to carry information from the high scale. As an order-of-magnitude estimate, we therefore follow the suggestions of [139, 140] and assign $B_{\nu}^2 = b_{\nu} M_{\text{R}}$, where b_{ν} is supposed to be a parameter of the SUSY scale.

We now allow for non-minimal flavor violating A - and B -terms and find values for the off-diagonal contributions in such a way that the flavor changing self-energies reproduce the weak current mixing matrix according to Eqs. (3.35) and (3.36), see also [206]. The charged lepton contribution Eq. (3.37) is not only negligible compared to the enhanced neutrino one, we also suppress flavor changing soft breaking terms in order to avoid large charged leptonic FCNC.

There are a few more parameters which we cannot and do not want to constrain: besides the gaugino masses M_1 and M_2 , the μ -parameter of the superpotential as well as $\tan\beta$ and M_{SUSY} are arbitrarily and randomly chosen. We additionally scan over the lightest neutrino mass, $m_{\nu}^{(0)}$ and go as low as 10 meV. The renormalized masses, however, are not constrained to fit the corresponding physical masses for the purpose of Fig. 11. We

We assume the “right-handed” sneutrino mass also a parameter of the SUSY scale, because SUSY breaking a priori has nothing to do with heavy neutrinos. In any case, \tilde{m}_{ν}^2 is negligible in the mass matrix if the right-handed Majorana mass is much heavier than a typical SUSY mass, $M_{\text{R}} \gg M_{\text{SUSY}}$.

We artificially set $A^e \equiv \mathbf{0}$.

We take the following parameter ranges: $M_{\text{SUSY}} \in [0.5, 5]$ TeV, $M_1 \in [0.3, 3] M_{\text{SUSY}}$, $M_2 \in [0.5, 5] M_{\text{SUSY}}$, $\mu \in [-5, 5]$ TeV and $\tan\beta \in [5, 60]$.

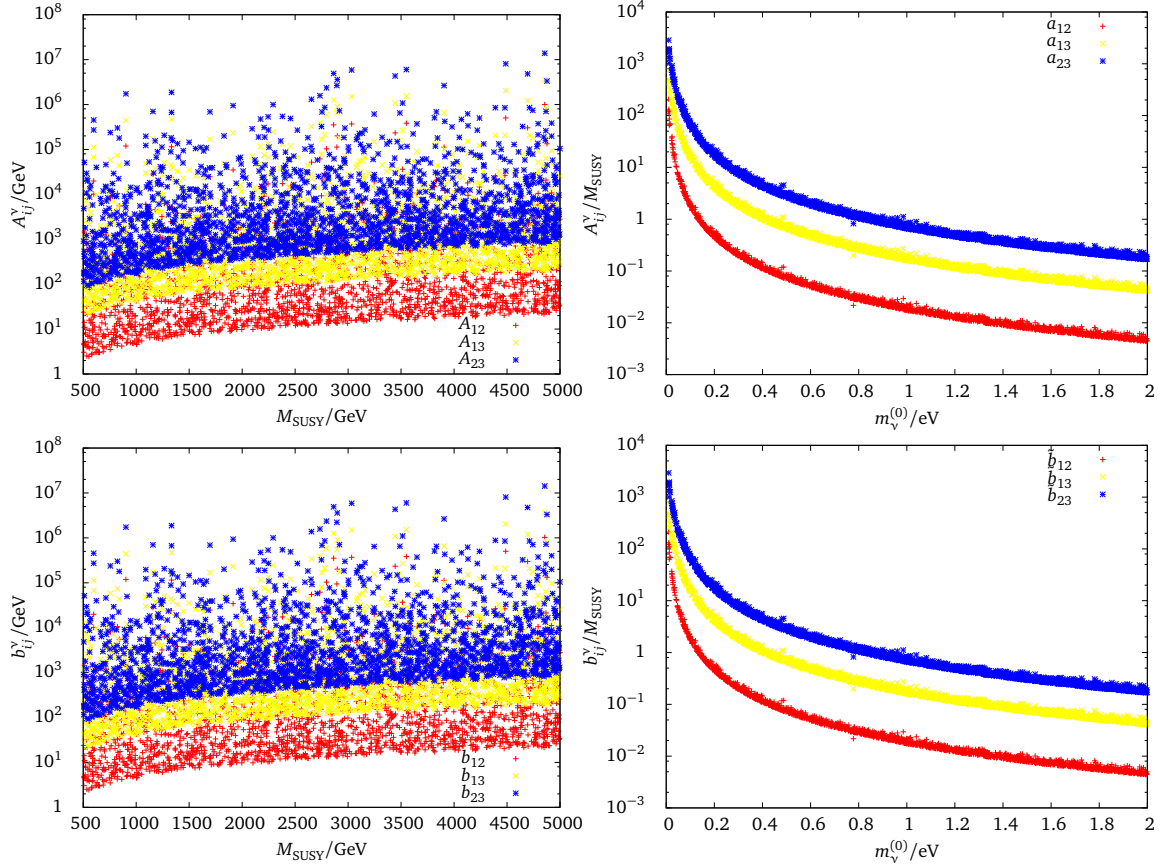


FIGURE 11: The determination of soft SUSY breaking sneutrino parameters, A_{ij}^Y and $(B_{\nu}^2)_{ij}$, shows an interesting behavior: the two *a priori* independent parameter sets are very much the same! For the production of those plots, we varied several input parameters as the SUSY scale M_{SUSY} and the lightest neutrino mass $m_{\nu}^{(0)}$ (which is also shown in the plots on the left and right respectively). The additional parameters which have been varied basically play no role in the ratio $a_{ij} = A_{ij}^Y/M_{\text{SUSY}}$ and $\tilde{b}_{ij} = b_{ij}^Y/M_{\text{SUSY}}$ that reproduce the neutrino mixing matrix.

want to study the flavor mixing contribution of the self-energies. Interestingly, the results for A^{ν} and B_{ν}^2 are identical! Why that?

The reason behind this unsettling observation lies on one hand in the choice of the neutrino parameters, on the other hand it is a physical result of the flavor structure of the self-energies. To understand Fig. (11), we confess our input choice: the neutrino Yukawa coupling was chosen to unity ($Y^{\nu} = \mathbf{1}$) and the scale of right-handed masses appropriately to have the right order of magnitude for the effective light neutrino mass. This choice has degenerate neutrino masses with mass $m_{\nu}^{(0)}$. Because individual contributions for different flavors do not mix (i. e. $\Sigma_{ij} \sim A_{ij}^Y, b_{ij}^Y$), the flavor-diagonal self-energies do not alter the result for the flavor-changing ones and can therefore be adjusted in such a way that the renormalized masses equal the physical ones.

We can see from the structure of the dominant diagrams shown in

The heavy propagator of $\tilde{\nu}_R$ counts as $\frac{1}{M_R^2}$.

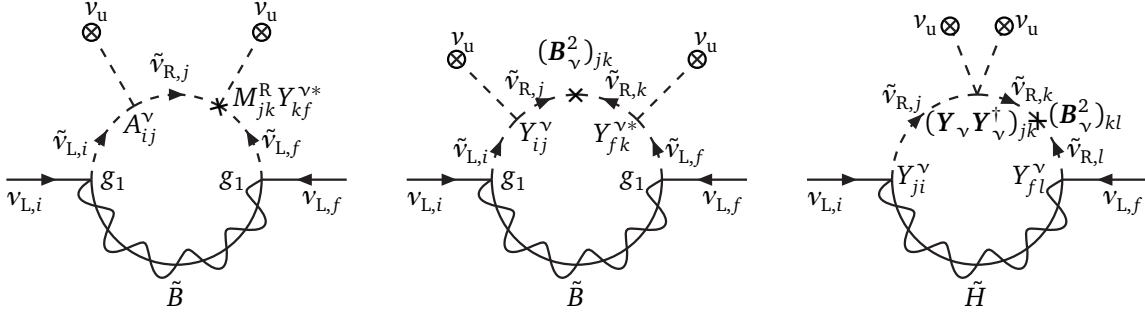


FIGURE 12: Self-energies renormalizing the neutrino Majorana mass with contributing A^ν (Σ^A , left) and B^2 (Σ^B , middle). The diagram on the outer right (Σ^C) shows a suppressed contribution of B^2 . The cross shows the $\Delta L = 2$ insertion.

Fig. 12 that the scaling of both A - and B -term contribution is the same: The A -term diagram scales as

$$\Sigma^A \sim A^\nu \frac{1}{M_R^2} M_R Y^\nu = y_\nu A^\nu / M_R,$$

and the B -term contribution

$$\Sigma^B \sim (Y^\nu)^\top M_R \frac{1}{M_R^2} B_\nu^2 \frac{1}{M_R^2} M_R Y^\nu = y_\nu^2 B_\nu^2 / M_R^2 = y_\nu^2 \mathbf{b}_\nu / M_R,$$

We also made use
of the replacement
 $B_\nu^2 = M_R \mathbf{b}_\nu$.

with $Y^\nu = y_\nu \mathbf{1}$ and $M_R = M_R \mathbf{1}$. As can be seen from the third diagram of Fig. 12, there are also contributions that are suppressed with more inverse powers of M_R , e. g.

$$\Sigma^C \sim (Y^\nu)^\top \frac{1}{M_R^2} Y^\nu (Y^\nu)^\dagger \frac{1}{M_R^2} B_\nu^2 \frac{1}{M_R^2} Y^\nu \sim \frac{y_\nu^4 B_\nu^2}{M_R^6} \sim \frac{y_\nu^4 \mathbf{b}_\nu}{M_R^5}.$$

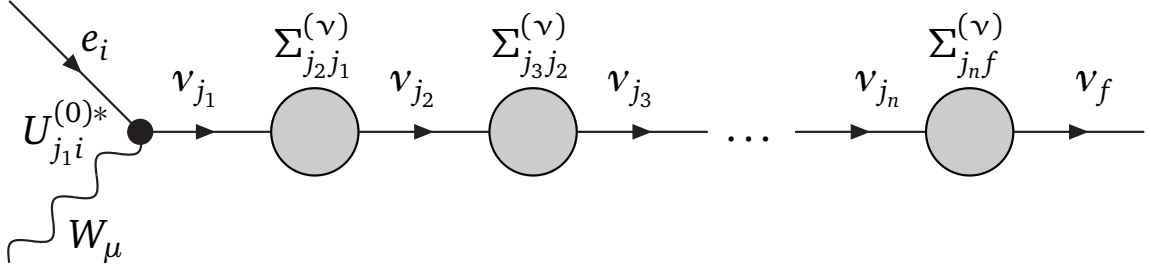
The dominant behavior already showed up in the effective mass matrices of light sneutrino states, Eq. (2.51a), the $\Delta L = 2$ contribution exactly has one (symmetrized) term from the LR transition,

$$\sim m_\nu^{D*} M_R \left[M_R^2 + (\tilde{m}_\nu^2)^\top \right]^{-1} m_\nu^{D\dagger} X_\nu^\dagger \sim \frac{v_u^2 A_\nu^\dagger}{M_R},$$

and one with the “soft SUSY breaking Majorana mass” B_ν^2 ,

$$\sim m_\nu^{D*} M_R \left[M_R^2 + (\tilde{m}_\nu^2)^\top \right]^{-1} B_\nu^2 (M_R^2 + \mathcal{M}_\nu^2)^{-1} M_R m_\nu^{D\dagger} \sim \frac{v_u^2 y_\nu^2 B_\nu^2}{M_R^2}.$$

In a way, we are free to choose either A^ν or B_ν^2 to generate neutrino mixing radiatively. In scenarios where there is a connection between A^ν and A^e , such as GUT-inspired models and LR-symmetry, large sneutrino A -terms lead to large FCNC contributions for charged leptons. In those cases, the sneutrino B -term may be the appropriate choice for radiative lepton flavor violation.


 FIGURE 13: Dyson resummation of the neutrino propagator at the W vertex.

3.2.4 Remarks on a Resummation of Large Contributions

The realization of quasi-degenerate neutrino mass eigenstates—as would be the case for the mass squared differences Δm_ν^2 being much smaller than the light neutrino mass: $\Delta m_\nu^2 \ll m_\nu^{(0)}$ —may lead to arbitrarily large corrections due to Eq. (3.39) shown in Fig. 9. Those large contributions in general have to be resummed. To clarify the meaning of those radiative corrections we perform a Dyson resummation of self-energies on the neutrino propagator, shown in Fig. 13. However, unlike the usual case, we have to deal with flavor non-diagonal self-energy matrices that carry chirality structures as well.

The general formalism of propagator dressing for inter-generation mixing, Majorana and unstable fermions was already explored by Refs. [211–215], in the following we review those results of Dyson resummed propagators and apply them to our formulation of mixing matrix renormalization by the means of SUSY corrections as described in Sec. 3.2.3.

As in Eq. (3.23), we decompose the self-energy matrix into its Lorentz-covariants:

$$\Sigma = \not{p} \left(\Sigma_L^V P_L + \Sigma_R^V P_R \right) + \Sigma_L^S P_L + \Sigma_R^S P_R,$$

where we have omitted flavor indices. To keep track of the proper counting, we remind us that the “scalar” components carry mass dimension one whereas the “vectorial” part has dimension zero.

Performing a Dyson resummation for the most generic propagators, we have to pay attention for both Dirac and flavor matrices. As usual, we write the resummed propagator as

$$\begin{aligned} iS(p) &= \frac{i}{\not{p} - m - \Sigma} \\ &= \frac{i}{\not{p} \left(1 - \Sigma_L^V P_L - \Sigma_R^V P_R \right) - \left(m + \Sigma_L^S P_L + \Sigma_R^S P_R \right)}, \end{aligned} \quad (3.44)$$

which can be decomposed in the following way:

$$\begin{aligned} iS(p) &= \frac{1}{D(p^2)} \left\{ \left[\not{p} \left(1 - \Sigma_L^V \right) + \left(m + \Sigma_L^S \right) \right] P_L \right. \\ &\quad \left. + \left[\not{p} \left(1 - \Sigma_R^V \right) + \left(m + \Sigma_R^S \right) \right] P_R \right\}, \end{aligned} \quad (3.45)$$

“Usual” means a situation like in QED: the resummed propagator is just given by the geometrical series $\frac{i}{\not{p} - m - \Sigma}$.

The notation is intuitive: $\frac{1}{\not{p} - m - \Sigma}$ means $[\not{p} - m - \Sigma]^{-1}$. We have to keep in mind, that Σ is not only a matrix in Dirac space, but also in flavor space.

where the denominator $D(p^2)$ can be obtained as

$$\begin{aligned} D(p^2) &= \left[\not{p} - m - \not{p} \left(\Sigma_L^V P_L + \Sigma_R^V P_R \right) - \left(\Sigma_L^S P_L + \Sigma_R^S P_R \right) \right] \times \\ &\quad \left[\not{p} + m - \left(\Sigma_L^V P_L + \Sigma_R^V P_R \right) + \left(\Sigma_L^S P_R + \Sigma_R^S P_R \right) \right] \quad (3.46) \\ &= p^2 \left(1 - \Sigma_L^V \right) \left(1 - \Sigma_R^V \right) - \left(m + \Sigma_L^S \right) \left(m + \Sigma_R^S \right). \end{aligned}$$

In the case of Majorana fermions, we have (using $\Sigma_L^V = \Sigma_R^{V*} = \Sigma^V$ and $\Sigma_L^S = \Sigma_R^{S*} = \Sigma^S$)

$$D(p) = p^2 \left| 1 - \Sigma^V \right|^2 - \left| m + \Sigma^S \right|^2. \quad (3.47)$$

However, for general self-energy *matrices* the situation gets worse, since we have to deal with matrix algebra. The result for the dressed propagator is given by [211, 214]:

$$S_{ij}(p) = \not{p} \left(\hat{\Sigma}_R^V \right)_{ij} P_R + \not{p} \left(\hat{\Sigma}_L^V \right)_{ij} P_L + \left(\hat{\Sigma}_R^S \right)_{ij} P_R + \left(\hat{\Sigma}_L^S \right)_{ij} P_L, \quad (3.48)$$

and the coefficients are obtained by the expressions

$$\hat{\Sigma}_R^V = (A_L)^{-1} (p^2 - C_R C_L)^{-1}, \quad (3.49a)$$

$$\hat{\Sigma}_L^V = (A_R)^{-1} (p^2 - C_L C_R)^{-1}, \quad (3.49b)$$

$$\hat{\Sigma}_R^S = (A_R)^{-1} B_L (A_L)^{-1} (p^2 - C_R C_L)^{-1}, \quad (3.49c)$$

$$\hat{\Sigma}_L^S = (A_L)^{-1} B_R (A_R)^{-1} (p^2 - C_L C_R)^{-1}, \quad (3.49d)$$

where

$$C_R = B_R (A_R)^{-1}, \quad C_L = B_L (A_L)^{-1}, \quad (3.50)$$

and

$$(A_{L,R})_{ij} = \delta_{ij} - \left(\Sigma_{L,R}^V \right)_{ij}, \quad (B_{L,R})_{ij} = m_i^0 \delta_{ij} + \left(\Sigma_{L,R}^S \right)_{ij}. \quad (3.51)$$

The inverse of a matrix can be computed using the adjoint $\text{adj}(M)$:

$$M^{-1} = \frac{1}{\det(M)} \text{adj}(M),$$

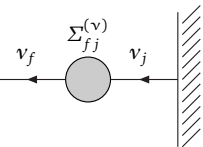
such that

$$(p^2 - M)^{-1} = \frac{\text{adj}(p^2 - M)}{\det(p^2 - M)},$$

with $M = C_R C_L, C_L C_R$.

Eqs. (3.48), (3.49), (3.50) and (3.51) define the full propagator, including all flavor mixing effects from the self-energies. In order to redo the calculation which resulted in Eq. (3.36a), we have to recall and clarify the meaning of the mixing matrix renormalization with external legs. The external-leg contribution to the full matrix element of the flavor transition is given by

$$\mathcal{M}_{\text{leg}}^V = \bar{u}(p_f) \Sigma_{fj}^{(v)} \frac{1}{\not{p} - m_j}, \quad (3.52)$$



The notation might be a bit confusing: while Σ are self-energy components, $\hat{\Sigma}$ are the components of the dressed propagator.

where we only include *flavor changing contributions* with $j \neq f$ to the mixing matrix counterterms ΔU_L^ν of Eq. (3.34). The flavor diagonal parts vanish in the field renormalization of the external particle (and also renormalize the mass). In this description, the external leg is only partially amputated. Let us remind the procedure to arrive from the n -point Green's function at the S -matrix elements via truncation of external field lines. The *truncated* Green's function are given through multiplication with inverse propagators, see e. g. [216, and original references]:

$$\tilde{G}_n(p_1, \dots, p_n) = G_2^{-1}(p_1, -p_1) \cdots G_2^{-1}(p_n, -p_n) G_n(p_1, \dots, p_n). \quad (3.53)$$

We then have the truncated 2-point function including the self-energy correction

$$\left[\frac{i}{\not{p} - m_f} \frac{1}{i} \Sigma_{ff}^{(\nu)} \frac{i}{\not{p} - m_j} \right]_{\text{trunc}} = (\not{p} - m_f) \frac{1}{\not{p} - m_f} \frac{1}{i} \Sigma_{ff}^{(\nu)} \frac{1}{\not{p} - m_j} (\not{p} - m_j),$$

which is $\tilde{G}_2 = \frac{1}{i} \Sigma_{ff}^{(\nu)}$. In Eq. (3.52), we can only truncate “half” of the external lines, since one is internally connected to the vertex. Multiplication from the right with the inverse propagator, $(\not{p} - m_f)$, and appending the wave function $\bar{u}(p_f)$ yields the expression (3.52), modulo the LSZ factor.

The same can be done using instead the dressed propagator of Eq. (3.44) decomposed in (3.48). We have infinitely many self-energy insertions as in Fig. 13 with $n \rightarrow \infty$ and Eq. (3.52) turns to

$$\mathcal{M}_{\text{leg}}^\nu = \bar{u}(p_f) (\not{p} - \mathbf{m} - \Sigma^{(\nu)}) \frac{1}{\not{p} - \mathbf{m} - \Sigma^{(\nu)}}, \quad (3.54)$$

with \mathbf{m} and $\Sigma^{(\nu)}$ matrices in flavor space. The flavor diagonal part goes into the field renormalization and redefines the masses as

$$\bar{u}_f(p_f) (\not{p} - m_f - \Sigma_{ff}^{(\nu)}) \frac{1}{\not{p} - m_f - \Sigma_{ff}^{(\nu)}} = \bar{u}_f(p_f),$$

which is a generalization of the wave function renormalization conditions of [212] or rather [217]. This is only correct as approximation, if the off-diagonal self-energy terms are small; in general, the inverse matrix depends on those. We also keep the diagonal flavor dependence in the full propagator, so this condition is not to be seen strict. For the flavor changing part, a $\Sigma_{ff}^{(\nu)}$ factor remains (with $\bar{u}(p_f) \not{p} = \bar{u}(p_f) m_f$) and we have

$$\left(\mathcal{M}_{\text{leg}}^\nu \right)_{fj} = -\bar{u}(p_f) \Sigma_{ff}^{(\nu)} \frac{1}{\not{p} - \mathbf{m} - \Sigma^{(\nu)}}, \quad (3.55)$$

which, inserted into the full matrix element for the flavor changing transition in the W -vertex, gives

$$\begin{aligned} \bar{u}_\nu(p_f) \left[\Delta \hat{U}_L^{(\nu)} \right]_{fj} \left(i \frac{g_2}{\sqrt{2}} \gamma^\mu P_L U_{ji}^{(0)\dagger} \right) u_e(p_i) = \\ \bar{u}_\nu(p_f) \left(i \Sigma_{ff}^\mu \right) i S_{j'j}(p_f) i \left(\Gamma_W^\mu \right)_{ji} u_e(p_i), \end{aligned}$$

We do not explicitly write the field renormalization constants because the flavor changing corrections are finite.

We identify the mass eigenstates as those corresponding to the renormalized pole mass.

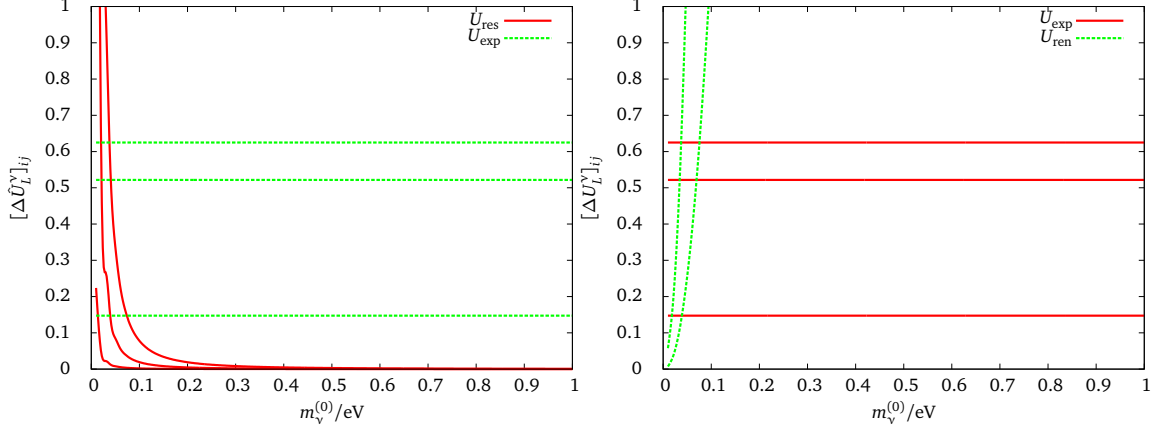


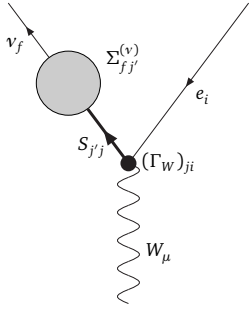
FIGURE 14: We have inverted the formulae for the mixing matrix renormalization to find the proper values of off-diagonal A^V -terms. The same values of A_{ij}^V leading to the right amount of mixing in the formulation of Eq. (3.38) starting from trivial mixing give negligible contributions once the flavor-changing self-energies are resummed (labeled as U_{res}). The enhancement factor is not present anymore, once diagrams are resummed. On the other hand, if one takes the resummed expression to determine the off-diagonal A^V -terms, the same values in Eq. (3.38) give—as expected—diverging results (U_{ren}).

with the (unrenormalized) vertex $(\Gamma_W^\mu)_{ij} = \frac{g_2}{\sqrt{2}} \gamma^\mu P_L U_{ij}^{(0)\dagger}$, and the “dressed” counterterm matrix $\Delta \hat{U}_L^{(\nu)}$ turns out to be

$$\begin{aligned}
 -[\Delta \hat{U}_L^{(\nu)}]_{fi} &= m_{\nu_f}^2 \Sigma_{ff}^{(\nu),V} (\hat{\Sigma}_{ji}^{(\nu),V})^* + m_{\nu_f} (\Sigma_{ff}^{(\nu),V})^* (\hat{\Sigma}_{ji}^{(\nu),S})^* \\
 &\quad + m_{\nu_f} \Sigma_{ff}^{(\nu),S} (\hat{\Sigma}_{ji}^{(\nu),V})^* + (\Sigma_{ff}^{(\nu),S})^* (\hat{\Sigma}_{ji}^{(\nu),S})^*,
 \end{aligned} \tag{3.56}$$

where we made use of the Majorana-specific relations $\Sigma_R^V = \Sigma_L^{V*}$ and $\Sigma_R^S = \Sigma_L^{S*}$ and readopted the obvious notation of Eqs. (3.36a) and (3.38). The dressed propagator components $\hat{\Sigma}^{V,S}$ are given in Eqs. (3.49) and summation over j is implied of course in Eq. (3.56). A similar relation holds for the charged lepton contribution—which one may resum as well, though it is not parametrically enhanced as the neutrino leg.

The interesting results including the Dyson resummation of the neutrino propagator compared to the unresummed formulation are displayed in Fig. 14. We adjust the diagonal A -terms according to the mass renormalization of Eq. (3.22) in order to fix the diagonal neutrino masses. The off-diagonals are then chosen to generate the PMNS off-diagonals and therewith the leptonic mixing angles. As can be seen from Fig. 14, the resummed counterterms $[\Delta \hat{U}_L^\nu]_{ij}$ immediately drop down where the unresummed corrections get enhanced by $m_{\nu_i} m_{\nu_j} / \Delta m_{ji}^2$. For the purpose of Fig. 14, we fed the A -terms responsible for the appropriate PMNS mixing into the either resummed or unresummed formulae. The plot on the left side shows proper mixing if the unresummed counterterms are used, the plot on the right side has proper mixing for the resummed version. On the other hand, using the resummation, the unresummed counterterms



explode when the enhancement gets sizable (note that they are parametrically enhanced by large A -terms anyway).

Note, that the $\hat{\Sigma}^{V,L}$ depend on the momentum squared, which is for the neutrino contribution the mass squared of the outgoing neutrino (in this case, we cannot set $p^2 = 0$, see Eqs.(3.49) and (3.50), (3.51)). Moreover, it is worth noting that the dressed propagator components carry negative mass dimension, $[\hat{\Sigma}^V] = -2$ and $[\hat{\Sigma}^S] = -1$, which is crucial for the counterterm (3.56) being dimensionless and the full dressed propagator of dimension minus one.

Let us perform a simple and rough order of magnitude estimate: The only mass scale that appears outside the self-energy loops is the scale of light neutrinos. Especially the dimensionful self-energies should not exceed the tree-level masses. Moreover, all quantities related to loops are suppressed by a factor of $\sim 10^{-2}$. Estimating the values of Eq. (3.56), we find that the mass scale drops out and an overall loop-factor is left, so the suppression might be $\sim 10^{-2}$! The leading terms of the $\hat{\Sigma}$ are not loop-suppressed. However, the situation for the dressed self-energies is not so clear as for the undressed ones. Looking at Eqs. (3.49) and the definitions of the matrices A , B , and C shows that the loop-suppression factor is subdominant, since the self-energies only enter as corrections to order-one parameters in A and B and the overall suppression factor is again the general loop-factor.

Although the possible *enhancement* of Eq. (3.38) is absent in Eq. (3.56), we add up more contributions including the diagonal ones by summing over $j = 1, \dots, n_G$ numbers of neutrinos. Therefore, we also collect flavor non-diagonal contributions from sources, that were not available with the method described in the previous section. Especially, there can be resulting effects to mixing angles that are not there at tree-level—take for example a theory with extended flavor structures as the ν MSSM. In such theories, one can in principle introduce additional flavor violating terms like the trilinear A -terms—however, by dressing the propagators and therefore the mixing matrix, it is not anymore a one-to-one correspondence that each A_{ij} generates a corresponding mixing matrix element U_{ij} (with i and j the same) and we get contributions to one element from the others. Since the counterterm elements in Eq. (3.56) are of the form $\hat{\Sigma}\Sigma$, where $\hat{\Sigma}$ denotes the dressed self-energies, one easily sees that for example the 1-3 element gets a contribution

$$\left[\Delta\hat{U}_L^{(\nu)}\right]_{13} \sim \hat{\Sigma}_{1j}\Sigma_{j3} = \hat{\Sigma}_{11}\Sigma_{13} + \hat{\Sigma}_{12}\Sigma_{23} + \hat{\Sigma}_{13}\Sigma_{33}.$$

Even if Σ_{13} as well as $\hat{\Sigma}_{13}$ vanishes — there is the term from $(1, 2) \times (2, 3)$ left: $\hat{\Sigma}_{12}\Sigma_{23}$ and the third mixing angle gets a finite renormalization by the other two mixing contributions.

The interesting behavior of the Dyson resummed corrections to the neutrino mixing matrix is displayed in Fig. 15. Here, we notice two things: first, in the case without resummation the strength of the corrections ($\sim A_{ij}^V/M_{\text{SUSY}}$ and $\sim b_{ij}^V/M_{\text{SUSY}}$) decreases with a more and more de-

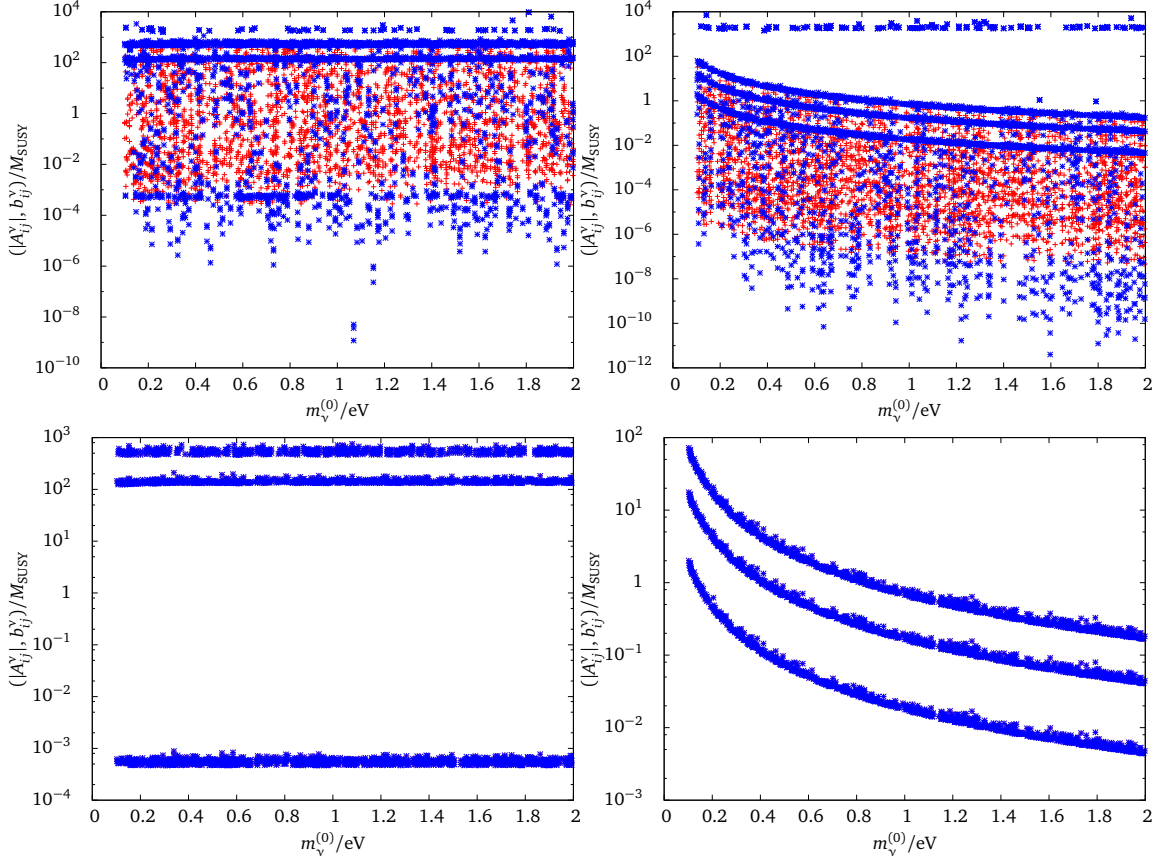


FIGURE 15: We compare the Dyson resummed (left panel) and not resummed (right panel) solutions for A^V -terms (red crosses) and b^V -terms (blue stars). In the first row, we also varied the scale of the neutrino Yukawa coupling from $\sim 10^{-6} \dots 1$. Where only blue stars are seen are the points similar to Fig. 11 where A^V - and b^V -terms are the same. This only holds for the $y_{\nu} = 1$ case because of the different scaling with the Yukawa coupling of the contributions as discussed in 3.2.2.

generate neutrino mass spectrum. This observation is not striking but rather what we expected, because of the increasing enhancement factor $f_{ij} = m_{\nu_i} m_{\nu_j} / \Delta m_{ji}^2$. For the resummed contributions there is no dependence on the neutrino mass—also as expected, because the mass dependent factor was absorbed in the resummation. Second, if we do not restrict the overall neutrino Yukawa coupling to $y_{\nu} = 1$, but let it flow in some regime (for this display, we have chosen $y_{\nu} \in [10^{-6}, 1]$), the needed correction strength can be significantly reduced into the percent regime or even lower.

Still, we assume for
simplicity
 $Y^{\nu} = y_{\nu} \mathbf{1}$.

One can argue whether it is reasonable to follow the previously described procedure in order to cope with the enhancement which results from the quasi-degenerate property of the neutrino mass spectrum. On one hand, we are dealing with the flavor off-diagonal effects of the self-energies as small effects, renormalizing the masses only via the diagonal contributions. On the other hand, the self-energies themselves may still be perfectly perturbative and the large contributions are rather due to the en-

hancement factor of Eq. (3.39) leading to large entries of D_L in Eq. (3.40). Ignoring the charged lepton contribution, we have

$$\mathbf{U}_{\text{ren}} = \mathbf{U}^{(0)} \left(\mathbf{1} + \Delta \mathbf{U}_L^{\nu\dagger} \right). \quad (3.57)$$

Summing up similar contributions, it is probably better to include the full $\Delta \mathbf{U}_L^\nu$ and not only the propagator part, so

$$\mathbf{U}_{\text{res}} = \mathbf{U}^{(0)} \left(\mathbf{1} + \Delta \mathbf{U}_L^{\nu\dagger} + \left(\Delta \mathbf{U}_L^{\nu\dagger} \right)^2 + \dots \right) = \mathbf{U}^{(0)} \left(\mathbf{1} - \Delta \mathbf{U}_L^{\nu\dagger} \right)^{-1}. \quad (3.58)$$

The matrix $\Delta \mathbf{U}_L^\nu$ has only off-diagonal elements in the description according to Sec. 3.2.3 and the inverse is easily calculated with $[\Delta \mathbf{U}_L^{\nu\dagger}]_{ij} = f_{ij} \sigma_{ij} \equiv u_{ij}$ (we take the self-energies as real and remind the reader of the symmetric property of Majorana self-energies)

$$\begin{pmatrix} 1 & u_{12} & u_{13} \\ -u_{12} & 1 & u_{23} \\ -u_{13} & -u_{23} & 1 \end{pmatrix}^{-1} = \frac{1}{\det \mathbf{u}} \begin{pmatrix} 1 + u_{23}^2 & u_{12} - u_{13}u_{23} & u_{13} + u_{12}u_{23} \\ & 1 + u_{13}^2 & u_{23} - u_{12}u_{13} \\ & & 1 + u_{12}^2 \end{pmatrix}, \quad (3.59)$$

with $\det \mathbf{u} = 1 + u_{12}^2 + u_{13}^2 + u_{23}^2$. It is interesting to note, that with $U_{ij}^{\text{res}} = u_{ij}/(1 + u_{ij}^2)$ at most mixing matrix elements of 0.5 can be generated from trivial tree-level mixing only! Additional contributions that interplay in Eq. (3.59) tend to diminish the results further. We conclude, that for large $u_{ij} \sim A_{ij}^\nu$ the proper mixing matrix elements get severely reduced and due to the fact that there now exists an upper bound on U_{ij}^{res} , we can never generate the observed neutrino mixing in this procedure. In the resummed propagator approach, we still have been able to find values of A_{ij}^ν which reproduce the PMNS mixing.

To conclude this digression on our attempts to resum the previously discussed large contributions to neutrino mixing, we state that neither of the described ways shall be applied at all. Furthermore, the perturbative approach to the mixing matrix renormalization which is valid for quark mixing (and has been successfully applied in the MSSM [89]) is actually wrong if large mixings or quasi-degenerate masses are considered. The approach relies on the neglect of $(\Delta U_L^f)^2$ terms which formally can be included as in Eq. (3.58). However, the mass and mixing renormalization cannot be disentangled anymore once there are substantial mixing effects. Instead, the inverse propagator of Eq. (3.44) defines actually a new mass matrix. Diagonalization of this matrix leads to a proper renormalization of mass eigenvalues and mixing matrix elements. This procedure has already been addressed in Sec. 3.2.1 and now has been shown to also be the proper procedure for non-degenerate masses. However, a not exactly degenerate mass spectrum at tree-level already intrinsically obeys a mixing pattern. We have argued in Sec. 3.2.1 that degenerate masses are somehow more likely to produce such a quasi-degenerate physical mass spectrum radiatively. In case the masses are rather hierarchical, radiative corrections are small anyway.

SUMMARY OF CHAPTER 3 In this chapter, we investigated the influence of radiative corrections to the origin of neutrino mixing. The large mixing angles in the lepton sector compared to the quark CKM matrix suggest a tree-level mechanism at work that generates this large mixing. However, we showed that especially in the case of degenerate neutrinos at tree-level where there is no mixing at all, one-loop threshold corrections have the power not only to lift the degeneracy but also to reproduce the large mixing angles. A supersymmetric theory has generic flavor violation in soft SUSY breaking. If we impose an MSSM extended by right-handed Majorana neutrinos, we can generate neutrino mixing stemming from soft breaking trilinear couplings. Without degenerate masses, there has to be a tree-level mixing at work, which again can be trumped by radiative corrections. The SUSY threshold corrections to the leptonic mixing matrix are enhanced by the quasi-degenerate pattern of neutrino mass eigenstates—as long as their masses are not strongly hierarchical. Additionally, it was shown that hierarchical right-handed Majorana masses also enter the radiative corrections and alter the tree-level mixing pattern even without soft SUSY breaking. In any case, taking (SUSY) one-loop corrections into account, the proposed tree-level flavor structure whatever it may be gets significantly changed. The most powerful corrections to do so are, of course, flavor changing threshold corrections. Those allow to connect the observed flavor with SUSY breaking in a supersymmetric context. This way, we may solve the flavor puzzle by solving the SUSY breaking puzzle.

The following introduction follows basically standard textbook descriptions—see e. g. [17, 18, 218]. To get a comprehensive overview, it is nevertheless necessary to carefully take a look into those (or other) standard references. It is not the purpose of this thesis to review textbook knowledge—however, it is somehow compulsory and convenient to have a short survey over the field before getting started into the phenomenology of effective potentials.

The main purpose of the following introduction is to set the language and notation.

We observe in nature the spontaneous breakdown of a fundamental symmetry. The breaking of electroweak symmetry directly reflects the fact, that W and Z bosons are massive. In the SM, this property is added by hand by virtue of a scalar field having a potential whose minimum does not respect the original symmetry anymore. That way, we have spontaneous symmetry breaking (SSB) at the cost of introducing a new field *and* adjusting the model parameters (i. e. the μ -term of the Higgs potential) manually. The theory does not give SSB itself. Does it?

In a seminal paper, Coleman and Weinberg (CW) showed that SSB can (and does) occur, once quantum corrections to the classical potential are switched on [219]. They started with a symmetric theory, calculated the *effective potential* explicitly and pointed out, that the one-loop effective potential itself leads to spontaneous symmetry breaking.

At roughly the same time, Jackiw derived the effective potential directly from the path integral and generalized the formulation to multiple scalar fields [220]. Lee and Sciacaluga came from a different direction and showed, that the one-loop effective potential can be obtained from integrating one-loop tadpole diagrams [221]. This method does not only provide an efficient and straightforward way to calculate effective potentials diagrammatically doing the resummation of all diagrams via the integral, but also glimpses towards something called the *renormalization group improved* (RGI) effective potential. Improving the effective potential means stabilizing it with respect to the choice of the renormalization scale. It turns out, that not only the RGI potential is scale invariant, but also any of its derivatives—and thereby the derived n -point functions.

We briefly recapitulate the ground-breaking achievements of Coleman and Weinberg, Jackiw, as well as Lee and Sciacaluga, and discuss the meaning of the RGI effective potential. Later on, we apply the machinery to the MSSM, reproduce the CW result and discuss its implications on the stability of the electroweak vacuum in the presence of light stops and sbottoms (where light means TeV-ish).

4.1 THE EFFECTIVE POTENTIAL AND ITS MEANING FOR THE GROUND STATE

Note that in field theory, the Lagrangian \mathcal{L} is the Lagrangian density—to end up with “ $L = T - V$ ” we have to integrate over space: $L = \int d^3x \mathcal{L}$.

$\bar{\phi}$ is commonly called “classical field” because it behaves like a classical field value rather than an operator.

In general, not every possible value of $\bar{\phi}$ can be achieved with translationally invariant J . There are some “forbidden” regions following from non-perturbative effects [223].

For simplicity, we suppress here consistently the label $_{1\text{PI}}$ in the notation of the 1PI potential.

In classical field theory, the meaning of the field theoretical potential $V(\phi)$ of a field ϕ is analogous to the potential energy of a particle in classical mechanics: $V(\phi)$ denotes the potential energy *density* of that field ϕ . Things have to be defined properly in a quantum field theory where the classical field ϕ turns into a quantum field.

In a quantum world, the “potential” turns to be the *generating functional* for one-particle irreducible (1PI) Green’s functions and can be derived in the path integral formalism as was shown by Jackiw [220]. For clarity, we distinguish between the 1PI-potential $V_{1\text{PI}}(\phi)$ and the *effective potential* $V_{\text{eff}}(\bar{\phi})$ of a field ϕ according to Dannenberg [222]. In that view, $V_{\text{eff}}(\bar{\phi})$ has the same meaning as the classical field theoretical potential—where the field $\phi = \phi(x)$ has to be replaced by a constant value $\bar{\phi}(x) = \bar{\phi}$ which can be seen as the vacuum expectation value

$$\bar{\phi} = \left. \frac{\langle 0|\phi|0\rangle}{\langle 0|0\rangle} \right|_J \tag{4.1}$$

in presence of external sources J . In this way, the ground state of the theory is determined by the value of $\bar{\phi}$ in the limit of vanishing sources, $v = \bar{\phi}|_{J \rightarrow 0}$. For this field value, the potential V of a real scalar field in

$$\mathcal{L} = \frac{1}{2} (\partial_\mu \phi)^2 - V(\phi)$$

is minimized:

$$\left. \frac{dV}{d\phi} \right|_{\phi=\bar{\phi}=v} = 0. \tag{4.2}$$

The *classical potential* V_{cl} is identical to the potential written in the Lagrangian density—in quantum field theory language it is the “*tree-level*” potential. For a real scalar field this could be (including only renormalizable terms obeying a global \mathbb{Z}_2 reflection symmetry $\phi \rightarrow -\phi$)

$$V_{\text{cl}} = V(\phi) = m^2 \phi^2 + \lambda \phi^4.$$

In the case $m^2 < 0$, the minimum of the potential does not respect the original symmetry anymore, so it is spontaneously broken. The 1PI potential now is the sum of all 1PI diagrams that contribute to V as a function of ϕ . On the classical level, “*tree-level*”, “*effective*” and “*1PI*” potential are equivalent and given by the same expression. Sticking to renormalizable operators, this potential can at most be a quartic polynomial. The loop expansion also adds 1PI diagrams with more external legs to the potential. In general, those diagrams include an arbitrary number of external legs:

$$V(\phi) = - \sum_{n=2}^{\infty} \frac{1}{n!} \tilde{G}^{(n)}(p=0) \phi^n, \tag{4.3}$$

where $\tilde{G}^{(n)}$ is the 1PI n -point Green's function (evaluated at vanishing external momenta, $p = 0$). Looking at Eq. (4.3), it is obvious that this potential is the *generating function* for all 1PI n -point diagrams which can be obtained by differentiating with respect to ϕ .

The 1PI (effective)¹ potential as given in Eq. (4.3) interpreted as the non-derivative part of the Lagrangian density going beyond tree-level is a powerful tool to survey the structure of SSB. Treating the one-loop potential as a function of $\bar{\phi}$, its minimal value determined via Eq. (4.2) describes the ground state of the quantum theory—and is therefore a better approximation to the proper ground state.

THE LOOP EXPANSION Summing up all one-loop diagrams with an arbitrary number of external legs also goes beyond fixed-order perturbation theory: each vertex which adds one (in a ϕ^3) or two (ϕ^4 theory) external legs comes along with one power of the coupling. The n -point contribution is actually $\mathcal{O}(\lambda^n)$. Nevertheless, it is a feasible way to use an on first sight artificial expansion in an $\mathcal{O}(1)$ parameter a which is defined via the condition

$$\mathcal{L}(\phi, \partial_\mu \phi, a) = a^{-1} \mathcal{L}(\phi, \partial_\mu \phi).$$

The important point here is that a multiplies the complete Lagrangian as it is, irrespective of shifts and scaling in the fields. A power-series expansion in a is equivalent to an expansion in the number of loops: each vertex obviously brings one factor a^{-1} whereas every internal line or propagator of a diagram contributes a —the propagator is the inverse of the quadratic terms, that also come along with a^{-1} . The power P of a which multiplies each diagram can be easily calculated as the difference of internal lines I and vertices V ($P = I - V$) and the number of loops is given by

$$L = P + 1 = I - V + 1,$$

because tree-level diagrams shall take a^{-1} as the total Lagrangian.

The loop expansion still lacks knowledge of higher order terms (namely two-loop contributions) if we stop the expansion at first power. Moreover, non-perturbative effects like bound state formation that also lead to spontaneous symmetry breaking [225, 226] cannot be included in that formalism.

DISTINCTION BETWEEN EFFECTIVE AND 1PI POTENTIAL For completeness, we also briefly review the discussion about the so-called “convexity problem” which was clarified by Dannenberg [222] and comprehensively reviewed in the appendix of Sher's Physics Report [227]. The problem, in fact, does not exist. However, connected to the question of convexity is the existence and interpretation of an imaginary part of the effective potential addressed by Weinberg and Wu [228].

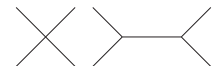
¹ The language used for this potential is not unique throughout the literature. Since more commonly *effective* instead of *1PI* is used, we will adiabatically change notation.

The subtle difference between generating function and functional will be pointed out in Sec. 4.1.1 about the path integral.

The easy thing with the effective potential is, that it is an ordinary function of the classical value $\bar{\phi}$ and minimization can be done without pain.

The argumentation basically follows [219] whereas the original idea behind the loop expansion is hidden in [224].

Actually, a can be identified with the Planckian constant \hbar which also multiplies the full Lagrangian and exactly equals one, $\hbar = 1$, in natural units.



Tree diagrams have a^{-1} because they only include one vertex or two vertices and one internal line.

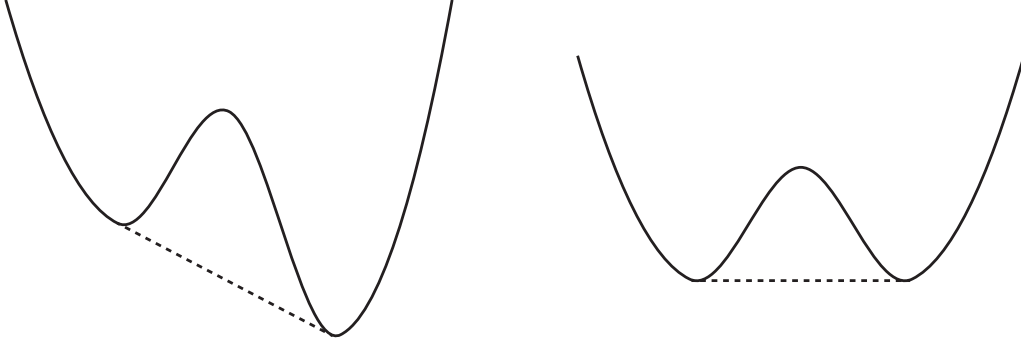


FIGURE 16: The convex envelope for the non-convex potential with non-degenerate minima is given by the dashed interpolation left. In case both minima are degenerate, the convex effective potential is flat in between the extrema (right).

The state $|\Omega\rangle$ is the vacuum state in presence of external sources J :
 $|\Omega\rangle \xrightarrow{J \rightarrow 0} |0\rangle$.

The decay rate which is supposed to be calculable from the imaginary part has to be seen for the decay from a spatially averaged (i. e. constant) field value which is localized in field space (like the minimum of some non-convex potential) into a spatially localized configuration like a bubble. This is only valid during the phase transition. This decay rate is not to be confused with the decay of the false vacuum itself [231, 232].

The rigorous distinction between 1PI and effective potential follows from the path integral and shall be elucidated in Sec. 4.1.1, whereas the pictorial interpretation shown in Fig. 16 can be understood quantum-mechanically: we define the effective potential $V_{\text{eff}}(\bar{\phi})$ as the expectation value of the energy density $\langle \Omega | \mathcal{H} | \Omega \rangle$ where $\bar{\phi} = \langle \Omega | \phi(x) | \Omega \rangle$. This is the real and convex potential for the spatially constant field value $\bar{\phi}$, see [228] and [229, 230]. The potential which is field theoretically calculable, however, is a different though related object. For the sake of clarity, we call this explicitly $V_{1\text{PI}}(\phi)$. If we now consider a potential as drawn in Fig. 16 on the right-hand side, where there are two minima at two distinct values in field space (say $\bar{\phi} = \pm\sigma$), the energy density for field values $|\bar{\phi}| < \sigma$ in between the two minima is minimized by a superposition of the two vacuum configurations $\bar{\phi} = \sigma$ and $\bar{\phi} = -\sigma$ and the average energy density is given by $V(\sigma) = V(-\sigma)$, which is the dashed line in Fig. 16, right. For most purposes in quantum field theory, however, we are interested in configurations where the state is *localized* in field space (a homogeneous state) but may be averaged (constant) in space-time, $\phi(x) = \bar{\phi}$. Such localized configurations are unstable because the operation of field localization does not commute with the Hamiltonian and therefore they decay, where the decay rate can be estimated from the imaginary part of the (1PI) potential [228]. Configurations like this are the case if we are interested in perturbative excitations around a local minimum—as done in electroweak theory where we expand around the minimum. A similar configuration may happen where we have to expand around the local minimum of Fig. 16 on the left: it may have happened that the universe while cooling down ended up in the higher minimum. The transition to the deeper minimum is then a phase transition and the relevant potential is given by $V_{1\text{PI}}$ rather than V_{eff} , which corresponds to the dashed curve and only has the global minimum. Using V_{eff} , no phase transition could happen. Instead, $V_{1\text{PI}}$ can be taken as the analytic continuation of V_{eff} , see [227] and [233, 234].

The occurrence of an imaginary part in the effective potential is related to the non-convexity of the classical potential, which can be easily seen

rewriting the CW potential that will be introduced in Eq. (4.29) as done in [228]

$$V_{1\text{-loop}}(\phi) = V(\phi) + \frac{1}{64\pi^2} [V''(\phi)^2 \ln V''(\phi)] + P(\phi), \quad (4.4)$$

where $V''(\phi)$ is the second derivative (i. e. the mass term) of the classical (tree-level) potential. Now, $V_{1\text{-loop}}$ develops an imaginary part when the argument of the logarithm drops negative, thus $V''(\phi) < 0$ which means V is non-convex where $V_{1\text{-loop}}$ is complex.

An illustrative example of a decaying configuration was given in [236]: let us distribute electric charges in a way that in a given (and arbitrarily large) space-time region there is a constant electric field. In QED, the constant electric field will pair-produce electrons and positrons from the vacuum with a non-vanishing probability which shield the external charges and destroy the constant field. Such a configuration obviously is unstable which follows from the imaginary part of the analytic continuation.

VACUUM DECAY The semiclassical description of a false vacuum decaying into the true vacuum configuration was first given by Coleman himself [237] from which this brief review heavily draws. Quantum corrections to the semiclassical theory were then considered in a follow-up paper [238] which is essential to calculate transition rates.

In many field theories as extensions of the SM with more scalars, Grand Unified Theories, supersymmetric theories, but even the SM itself false vacua as shown in Fig. 16 may appear. The question whether we live in a false or the true vacuum is of cosmological importance: an infinitely old universe inevitably ends up in the true vacuum (global minimum). However, we know that our universe is not infinitely old and we know the history of hot big bang: as the universe cooled down, we may have ended up in the false vacuum.

A situation like this is drawn in Fig. 17, where we assume to have ended up for some reason in the classically stable equilibrium state $\phi = \phi_+$. The state of lowest energy, however, is given by $\phi = \phi_-$. This state can classically only be reached by thermodynamic fluctuations—or via barrier penetration in a quantum world. For simplicity, we only consider a single real scalar field with a given potential energy density U

$$\mathcal{L} = \frac{1}{2} \partial_\mu \phi \partial^\mu \phi - U(\phi). \quad (4.5)$$

The decay probability Γ of the false vacuum per unit volume V follows the exponentially suppressed solution for barrier penetration

$$\Gamma/V = Ae^{-B/\hbar} [1 + \mathcal{O}(\hbar)], \quad (4.6)$$

where the quantum theory will give corrections $\mathcal{O}(\hbar)$ and the factor V follows from the fact that the emerging solutions (named “bounce solution”) are not translation invariant and all spatial translations have to be integrated over. As pictorial view, Coleman states that for a decaying vacuum,

The problem only occurs, if a wrong (unstable) vacuum state was used to build up the effective potential as was pointed out in [235]. Nevertheless, the resolution of the problem still lies in the use of vocabulary.

The term “false vacuum” describes exactly what it is: the true vacuum is expected to be the global minimum of the potential energy (density) whereas a local minimum mimics the vacuum. By knowledge of quantum mechanics, classically stable expansions around that minimum will decay with certain probability to the deeper ground state.

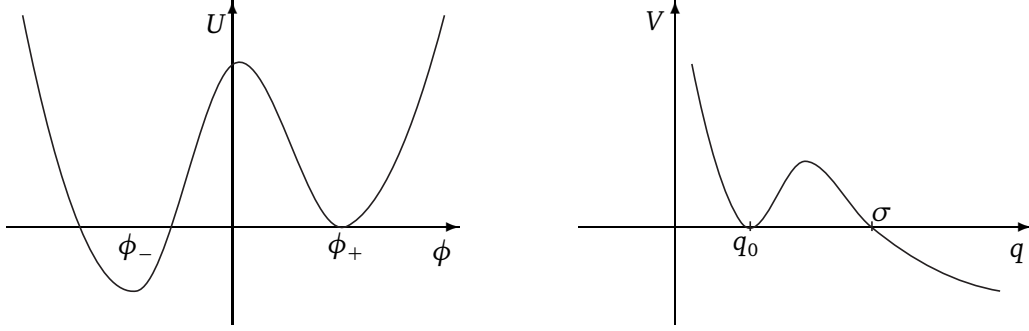


FIGURE 17: Unstable potentials: on the left side, we have a false vacuum configuration at ϕ_+ where the true vacuum lies at ϕ_- . The potential on the right side shows a quantum mechanical analogue, where the local minimum at q_0 is classically stable.

the product of Γ/V with the four-volume of the past light cone has to be of order one to observe this decay. The coefficients A and B have to be calculated in the underlying theory which, in general, is not even possible.

The presence of a bounce solution can be seen from the quantum mechanical tunneling process as an allegory for the barrier penetration of the vacuum state. Consider the quantum mechanics of a single particle in one space dimension with a potential drawn in Fig. 17 on the right side. Classically, the equilibrium at q_0 is stable forever, whereas the quantum particle can penetrate the wall until it escapes at $q = \sigma$ and propagates freely for $q > \sigma$. The analogue of Eq. (4.6) is given by

$$\Gamma = Ae^{-B/\hbar} [1 + \mathcal{O}(\hbar)], \quad (4.7)$$

where the division by unit volume is a division by one and B can be calculated using the WKB method

$$B = 2 \int_{q_0}^{\sigma} dq \sqrt{2V}. \quad (4.8)$$

A generalization in more than one dimensions was given by [239] but makes no difference for the qualitative discussion (details in [237]). The interesting observation Coleman made, is that, using the Euler-Lagrange equation for the one-particle Lagrangian $L = \frac{1}{2}\dot{q}^2 - V(q)$,

$$\frac{d}{dt} \frac{\partial L}{\partial \dot{q}} = \frac{\partial L}{\partial q}$$

$$\ddot{q} = -\frac{dV}{dq},$$

The potential energy in Fig. 17 was adjusted in such a way that the total energy $E = 0$.

Traditionally, $\delta \int dq \sqrt{2(E-V)} = 0$ is considered, which is Eq. (4.9) with fixed integration limits, $E = 0$ and $V \rightarrow -V$.

This actually causes the transition to imaginary time.

and energy conservation $\frac{1}{2}\dot{q}^2 + V = E$, $\dot{q} = \text{const}$. In order to minimize B , we have to consider the variation

$$\delta \int_{q_0}^{\sigma} dq \sqrt{2V} = 0, \quad (4.9)$$

whose solutions are determined by the differential equation

$$\frac{d^2 q}{d\tau^2} = \frac{dV}{dq}, \quad (4.10)$$

where we have substituted the time by imaginary time $\tau = it$. The energy conservation now turns to

$$\frac{1}{2} \left(\frac{dq}{d\tau} \right)^2 - V = 0$$

and Hamilton's principle

$$\delta \int d\tau L_E = 0,$$

with the "Euclidean" version of the Lagrangian, $L_E = \frac{1}{2} \left(\frac{dq}{d\tau} \right)^2 + V$. Choosing the time where the particle "reaches" σ to be $\tau = 0$, the classical equilibrium $q = q_0$ is only reached in the limit $\tau \rightarrow -\infty$ and the "velocity" vanishes at $\tau = 0$: $dq/d\tau = 0$. The solution for B from Eq. (4.8) turns then to be

$$\int_{q_0}^q dq \sqrt{2V} = \int_{-\infty}^0 d\tau L_E.$$

The equation of motion is invariant under $\tau \rightarrow -\tau$, so the particle bounces at $\tau = 0$ and goes back to q_0 as $\tau \rightarrow +\infty$. The coefficient B of the "bounce solution" is just given by the Euclidean action

$$B = \int_{-\infty}^{+\infty} d\tau L_E = S_E. \quad (4.11)$$

The difficulty in the generalization to a quantum field theory lies in the calculation of the Euclidean action for the bounce solution. To find the bounce, take the equations of motion for the scalar Lagrangian (4.5) in imaginary time description

$$\left(\frac{\partial^2}{\partial \tau^2} + \vec{\nabla}^2 \right) \phi = U'(\phi) \quad (4.12)$$

and impose the bounce boundary conditions

$$\lim_{\tau \rightarrow \pm\infty} \phi(\tau, \vec{x}) = \phi_+ \quad (4.13a)$$

and

$$\frac{\partial \phi}{\partial \tau}(0, \vec{x}) = 0. \quad (4.13b)$$

Because of $SO(4)$ invariance under Euclidean rotations, condition (4.13a) can be identified with

$$\lim_{|\vec{x}| \rightarrow \infty} \phi(\tau, \vec{x}) = \phi_+,$$

which gives the pictorial description of a spatially growing bubble of the decaying vacuum, where the false vacuum stays unchanged in regions far

These requirements can be identified with boundary conditions for the equation of motion (4.10), $\left. \frac{dq}{d\tau} \right|_{\tau=0} = 0$ and $\lim_{\tau \rightarrow \pm\infty} q(\tau) = q_0$.

away from a bubble induced by quantum fluctuations. The final result can be simplified using SO(4) invariance and writing $\tau^2 + |\vec{x}|^2 = \rho^2$, then Eq. (4.11) turns to

$$B = 2\pi^2 \int_0^\infty \rho^3 d\rho \left[\frac{1}{2} \frac{d\phi}{d\rho} + U(\phi) \right] \tag{4.14}$$

with boundary conditions

$$\left. \frac{d\phi}{d\rho} \right|_{\rho=0} = 0, \quad \text{and} \quad \phi(\infty) = \phi_+.$$

Practically, one would obtain $\phi(\rho)$ as numerical solution for this differential equation and integrates Eq. (4.14) numerically to get B.

The equation of motion (4.12) determines $\phi(\rho)$:

$$\frac{d^2\phi}{d\rho^2} + \frac{3}{\rho} \frac{d\phi}{d\rho} = \frac{dU}{d\phi}.$$

What is left is the determination of the coefficient A in front of the exponent. However, the precise value of A does not play a significant role for the estimate of the decay rate. Therefore, only rough numerical estimates exist, where the exact analytical calculation [238] yields

$$A = \frac{B^2}{4\pi^2} \sqrt{\frac{\det' [-\partial^2 + U''(\phi)]}{\det [-\partial^2 + U''(\phi_+)]}}. \tag{4.15}$$

A has to have mass dimension four and is a dimensionful parameter related to the scale of the problem, so the expectation is a rough estimate of feelings.

The bounce solution is given by ϕ , and ϕ_+ is the position of the false vacuum. The determinant is generically difficult to evaluate (where \det' means the determinant without zero eigenvalues). Therefore, the value of A is usually estimated by the height and width of the barrier, because one expects A to be of the fourth power of the scale related to the barrier. The uncertainty of A can then be estimated to be $\sim e^{15\dots 20}$ which can be related to an effective uncertainty of B [227]. Sher takes as estimate on A the barrier height⁴. For all practical purposes, a standardized height is used related to the electroweak scale and $A \approx (100 \text{ GeV})^4$ [240–242]. Stable configurations are then determined by $S_E[\phi]/\hbar \gtrsim 400$ for a universe lifetime of 10^{10} years.

We may at least refer to the comfortable situation of observers observing the universe today as necessary condition for a stable vacuum.

OTHER IMPLICATIONS OF FALSE VACUA The question about stability, instability or metastability of any ground state, especially the electroweak vacuum we are believing to live in, is of major importance for the existence of observers in a current situation. Call this *anthropic principle*, in any case the fact that observers observe a certain broken phase which seems to be somehow stable makes us believe that it has to be like this. Previously, we discussed estimates on the vacuum life time and completely masked out its meaning. If we find configurations for the effective potential of a theory which predicts extremely short lifetimes of false vacua, we may argue that in view of a 13.8 billion year old universe any state with a lifetime much less than this number for sure has been decayed. Configurations of charge and color breaking false or true vacua as may occur in various

SUSY models, where the drastically enhanced scalar sector also contains colored scalars, will be postponed to the MSSM section 4.2.

One interesting question to deal with is the influence of gravitational effects: imagine the transition of a false into a true vacuum releasing a vast amount of energy. This energy portion is expected to grow with the volume of the newly formed bubble. The bubble grows as the gain in volume energy supersedes the surface energy. Without gravity, a growing bubble can always be generated as long as it appears to be large enough. Including gravity into the game, we have to deal with the Schwarzschild radius of the energy density inside the bubble which also grows with the energy. Coleman and De Luccia [243] have shown (and proven) with very clear arguments that gravitation plays no significant role—as far as it was understood at that time (with no new insights in the modern literature). The obvious thing is that conservation of energy is not violated by the tunneling process and in the end the total energy of the bubble (inner negative volume energy and positive surface energy) has to be exactly zero. Therefore the gravitational field cannot do anything. In general, gravity has the tendency to prevent false vacua from decay and reduces the decay probability. Finally, Coleman and De Luccia discuss the possibility of living in the leftovers from an early decay of a false vacuum where the world *outside* the bubble corresponds to the true vacuum. In this special scenario (decay into zero cosmological constant) the probability for decay gets enhanced by gravitational effects.

The existence of several vacua (even in the pure SM there is a second minimum in the effective potential popping up around the Planck scale) allows also for *degenerate* vacua and thus coexisting phases. From the demand of such coexisting phases, Froggatt and Nielsen [244] predicted about 16 years prior to the discovery the SM Higgs mass to be 135 ± 9 GeV which just at the edge of the errors covers the recently discovered Higgs boson [15, 16] and they significantly reduced the uncertainty of the (at that time recently measured) top mass and shifted the central value down to 173 GeV (from 180 ± 12 GeV) with 5 GeV uncertainty. The foundation of this prediction is the “multiple point principle” (MPP), first applied to coexistence of gauge couplings at the Planck scale [247, 248].² Similar to coexisting phases in condensed matter physics (the presence of ice, water and vapor at the triple point of water), specific quantities take only very specific values after the surroundings are fixed. The vacuum stability issue was used to give lower bounds on the SM Higgs mass [249–263].

4.1.1 Path Integral

The most stringent derivation of the effective potential without explicitly calculating Feynman diagrams follow from the path integral definition.

² H. B. Nielsen answered the question about the reason behind the MPP that there are no deeper reasons behind most principles therefore they are principles [private communication, PASCOS 2014].

Correlated to the total energy density is the question of the cosmological constant. In a pure quantum field theory on fixed Minkowski space time, arbitrary constants can be added and subtracted to any potential energy density such that there is no absolute zero energy. Two non-degenerate vacua make a cosmological constant either appear or disappear after vacuum decay, adjusting the parameter in the either true or false vacuum we choose to live in.

There are many papers predicting many values of the Higgs mass, so Ref. [244] is for sure not the only one being right within the errors. The MPP also allows to form a dark matter candidate from top bound states with a reduced top mass [245, 246].

Jackiw calls the Feynman diagrammatic calculation “an onerous task” which it indeed is, as described in the section about sea urchin diagrams, Sec. 4.1.3.

Jackiw calculated the effective potential for n self-interacting scalar fields up to two-loop precision [220]. The expansion of the path integral allows to keep track of the loop-expansion, as each term comes along with a factor \hbar counting the number of loops.

Already the two loop case gets much more involved.

The effective potential is defined via the *effective action* which follows from the generating functional $\mathcal{W}[J(x)]$ of connected Green's functions

$$i\mathcal{W}[J] = \sum_{n=0}^{\infty} \frac{(-i)^n}{n!} \int d^4x_1 \cdots d^4x_n G^{(n)}(x_1, \dots, x_n) J(x_1) \cdots J(x_n). \quad (4.16)$$

$\mathcal{Z}[J]$ gives all Green's functions. The relevant ones for scattering amplitudes, however, are only the connected ones. Also for the definition of the potential, which gives the (self-)interaction, only connected Green's functions are important. (Disconnected Green's functions do not describe interactions.)

The “partition functional” $\mathcal{Z}[J]$ gives the unconnected Green's functions

$$\mathcal{Z}[J] \equiv e^{-i\mathcal{W}[J]} = \int \mathcal{D}\Phi e^{iS[\Phi] - i \int d^4x J[x]\Phi(x)} \quad (4.17)$$

and the vacuum transition amplitude from $t = -\infty$ to $t \rightarrow +\infty$ in presence of sources $J(x)$

$$\mathcal{Z}[J] = \langle 0_{-\infty} | 0_{+\infty} \rangle_J.$$

The classical action is defined via the Lagrangian of the theory $S[\Phi] = \int d^4x \mathcal{L}(\Phi)$ and the generic field Φ may represent all fields in that theory.

The effective action is the generating functional of 1PI Green's functions and follows from a Legendre transform

$$\Gamma_{\text{eff}}[\Phi(x)] = \mathcal{W}[J] - \int d^4x J(x)\Phi(x). \quad (4.18)$$

The *classical* field value $\bar{\phi}$ minimizes Γ_{eff} with respect to J ,

$$\bar{\phi} = \frac{\delta \mathcal{W}[J]}{\delta J(x)} \quad \text{such that} \quad \left. \frac{\delta \Gamma_{\text{eff}}[\Phi]}{\delta \Phi(x)} \right|_{\Phi=\bar{\phi}} = -J(x).$$

Spontaneous symmetry breaking occurs, if $\bar{\phi} \neq 0$ even for vanishing source $J(x)$: $\delta \Gamma_{\text{eff}} / \delta \bar{\phi} \big|_{J=0} = 0$, and Γ_{eff} is still minimized. The *effective potential* is a space-time independent quantity following from Γ_{eff} after division by the 4-volume

In general, $\Gamma_{\text{eff}}[\bar{\phi}] = \int d^4x \left[-V_{\text{eff}}(\bar{\phi}) + \frac{1}{2} (\partial_\mu \bar{\phi})^2 Z(\bar{\phi}) + \dots \right]$, which for $\bar{\phi} = \text{const.}$ reduces to Eq. (4.19).

$$\Gamma_{\text{eff}}[\bar{\phi}] = -V_{\text{eff}}(\bar{\phi}) \int d^4x. \quad (4.19)$$

$V_{\text{eff}}(\bar{\phi})$ is now an ordinary function of $\bar{\phi}$.

The effective potential V_{eff} is the generating function (not functional) of connected 1PI diagrams where the n -point vertex functions $\tilde{G}^{(n)}$ (for zero external momenta) follow from the n -th derivative and $\bar{\phi} \rightarrow 0$:

$$V_{\text{eff}}(\bar{\phi}) = - \sum_{n=1}^{\infty} \frac{1}{n!} \bar{\phi}^n \tilde{G}^{(n)}(p_i = 0). \quad (4.20)$$

In this way, V_{eff} is defined via the generating functional of 1PI Green's function and therefore, using this language, V_{eff} and $V_{1\text{PI}}$ are identical. To

resolve the convexity problem which was an issue in the early literature of effective potentials, we refer to Dannenberg [222] and his dictionary. The crucial point is, that Γ_{eff} is the *double* Legendre transform of Γ_{1PI} which can be seen from Eq. (4.18) using $\mathcal{W}[J]$ as generating functional of connected Green's functions, where

$$\mathcal{W}[J] = \Gamma_{\text{1PI}}[\Phi(x)] - \int d^4x J(x)\Phi(x) \quad (4.21)$$

itself is the Legendre transform of Γ_{1PI} being the generating functional of 1PI diagrams. Since Legendre transforms are convex functions, the double Legendre transform of Γ_{1PI} is the convex envelope of this function(al).

There is one further issue related to the imaginary part of the effective potential, which is connected to a non-convex tree-level potential and shall be picked up later where appropriate.

PATH INTEGRAL DERIVATION OF THE EFFECTIVE POTENTIAL In the following, we briefly state the result of Jackiw's path integral calculation of the effective potential [220] without going into details. In Ref. [220] not only the formal proof of the path integral derivation is given, also the first two-loop result for the effective potential of self-interacting scalars and a recalculation of the CW model (radiative breaking of massless, scalar QED) in arbitrary gauge was performed. The latter calculation already raises the discussion about gauge dependence of the effective potential and its physical interpretation, see for a modern discussion and resolution of that problem [264–266].

The main argument uses the existence of the “classical” (x -independent) field value $\bar{\phi}$ which has the meaning of a *vev*. From the classical action $S[\phi] = \int d^4x \mathcal{L}[\phi(x)]$, we obtain the shifted action $S[\phi + \bar{\phi}]$ which formally can be expanded as Taylor series around $\phi = 0$

$$S[\phi + \bar{\phi}] = S[\bar{\phi}] + S'[\bar{\phi}]\phi + \frac{1}{2}S''[\bar{\phi}]\phi^2 + \frac{1}{3!}S'''[\bar{\phi}]\phi^3 + \dots,$$

where the prime denotes derivative (variation) with respect to ϕ , $S'[\bar{\phi}] = \left. \frac{\delta}{\delta\phi} S[\phi + \bar{\phi}] \right|_{\phi=0}$. Then

$$e^{i\Gamma_{\text{eff}}[\bar{\phi}]} = \int_{\text{1PI}} \mathcal{D}\phi e^{iS[\phi + \bar{\phi}]} \stackrel{\text{1-loop}}{=} e^{iS[\bar{\phi}]} \int_{\text{1PI}} \mathcal{D}\phi e^{i\frac{1}{2}S''[\bar{\phi}]\phi^2} = e^{iS[\bar{\phi}]} \frac{1}{\sqrt{\det \mathcal{L}''(\bar{\phi})}}, \quad (4.22)$$

where the integral is performed over all 1PI configurations and $\mathcal{L}''(\bar{\phi}) = \partial^2 - V''(\bar{\phi})$ with the tree-level potential $V(\phi)$.

The shift defines a new Lagrangian [220] via

$$S[\phi + \bar{\phi}] - S[\bar{\phi}] - \int d^4x \phi(x) \left. \frac{\delta S[\phi]}{\delta\phi(x)} \right|_{\phi=\bar{\phi}} = \int d^4x \tilde{\mathcal{L}}(\bar{\phi}, \phi(x)). \quad (4.23)$$

According to Dannenberg, “the resolution of the convexity problem lies not in physics but in vocabulary”. Having this in mind, we use the terms “effective” and “1PI” synonymously throughout this thesis and never refer to the “true” effective potential (which is convex).

The gauge dependence issue is not relevant for the purpose followed in the following, because we do not calculate the gauge part anyway.

We thank Luminita Mihaila for pointing this and Eq. (4.22) out in her institute's seminar talk in November 2014.

This allows to nicely find Eq. (4.26) from $\Gamma_{\text{eff}}[\bar{\phi}] = -i \ln \left[\frac{\exp(iS[\bar{\phi}])}{\sqrt{\det \mathcal{L}''(\bar{\phi})}} \right] = S[\bar{\phi}] + \frac{i}{2} \ln \det \mathcal{L}''(\bar{\phi})$. The effective potential has an additional minus sign.

\mathcal{L}'' in general is a matrix in the space of multiple scalar fields $\phi = \phi_a$ with $a = 1, \dots, n$.

The new Lagrangian $\tilde{\mathcal{L}}$ comprises interaction terms with $\bar{\phi}$ -dependent couplings. In this way, we decompose $\tilde{\mathcal{L}}$ into a propagator and an interaction part according to [220]:

$$\int d^4x \tilde{\mathcal{L}}(\bar{\phi}, \phi(x)) = \int d^4x d^4y \frac{1}{2} \phi_a(x) iD_{ab}^{-1}(\bar{\phi}; x, y) \phi_b(y) + \int d^4x \tilde{\mathcal{L}}_1(\bar{\phi}, \phi(x)), \quad (4.24)$$

where we generalized the notation to an arbitrary number of scalars, $a, b = 1, \dots, n$, and suppressed indices where possible. The propagator is to be calculated in an obvious manner

$$iD_{ab}^{-1}(\bar{\phi}; x, y) = \left. \frac{\delta^2 S[\phi]}{\delta \phi_a(x) \delta \phi_b(y)} \right|_{\phi=\bar{\phi}}. \quad (4.25)$$

Transformation into momentum space follows straightforwardly

$$iD_{ab}^{-1}(\bar{\phi}; x, y) = \int d^4x e^{ikx} iD_{ab}^{-1}(\bar{\phi}; x, 0),$$

such that the effective potential can be obtained as

$$V_{\text{eff}}(\bar{\phi}) = V_0(\bar{\phi}) - \frac{1}{2} i\hbar \int \frac{d^4k}{(2\pi)^4} \ln \det [iD_{ab}^{-1}(\bar{\phi}; k)] + i\hbar \left\langle \exp \left(\frac{i}{\hbar} \int d^4x \tilde{\mathcal{L}}_1(\bar{\phi}; \phi(x)) \right) \right\rangle, \quad (4.26)$$

where $V_0(\bar{\phi})$ denotes the tree contribution and the determinant operates on all indices a, b counting for internal and spin degrees of freedom. The last terms means calculation of the vev in between the angular brackets and averaging over space-time and is $\mathcal{O}(\hbar^2)$ contributing to the two-loop potential. The one-loop contribution to the effective potential can then be evaluated (as an example for a single-scalar theory)

$$V_1(\bar{\phi}) = -\frac{i\hbar}{2} \int \frac{d^4k}{(2\pi)^4} \ln [k^2 - m^2(\bar{\phi})]$$

with the field-dependent mass $m(\bar{\phi}) = V_0''(\bar{\phi})$. Introducing a cut-off Λ , the integration results in [220]

$$V_1(\bar{\phi}) = \frac{\hbar}{64\pi^2} \left[\Lambda^4 \ln \left(1 + \frac{m^2(\bar{\phi})}{\Lambda^2} \right) - m^4(\bar{\phi}) \ln \left(1 + \frac{\Lambda^2}{m^2(\bar{\phi})} \right) + \Lambda^2 m^2(\bar{\phi}) \right] \quad (4.27)$$

up to an omitted overall constant Λ^4 . In dimensional regularization, the D -dimensional integral can be performed after Wick rotation to Euclidean space [264] (where $D = 4 - 2\epsilon$)

$$-\frac{i}{2} Q^{2\epsilon} \int \frac{d^Dk}{(2\pi)^D} \ln (-k^2 + m^2) = \frac{1}{4} \frac{m^4}{(4\pi)^2} \left(\ln \frac{m^2}{Q^2} - \frac{3}{2} - \Delta_\epsilon \right), \quad (4.28)$$

with the renormalization scale Q and $\Delta_\epsilon = \frac{1}{\epsilon} - \gamma_E + \ln 4\pi$.

In the spirit of Jackiw [220], we explicitly write factors of \hbar to make obvious that the loop expansion is an expansion in \hbar .

In the \hbar -expansion, $\frac{i}{\hbar} \mathcal{L}_1$ is $\mathcal{O}(\hbar)$ and the first term in the expansion of the exponential vanishes in between the angular brackets.

Note that this causes the cosmological constant problem!

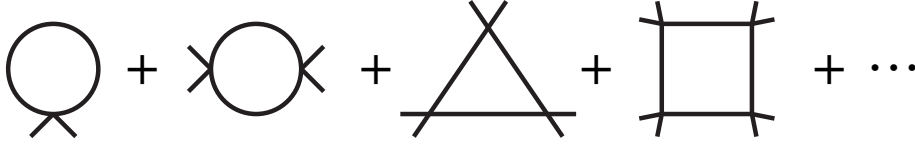


FIGURE 18: The one-loop effective potential for scalar ϕ^4 theory.

4.1.2 The “Coleman-Weinberg” potential

What today is known as CW potential is the result of a Feynman diagrammatic calculation of the one-loop effective potential. The result is identical to Jackiw’s path integral derivation and the integrated tadpole of Lee and Sziacaluga. Moreover, CW showed that the calculation is applicable not only to scalar ϕ^4 theory (sample diagrams shown in Fig. 18), but also to scalar QED, non-abelian gauge theories and theories with fermions. And the basic formula is very simple and easy to use:

$$V_{1\text{-loop}} = \frac{1}{64\pi^2} \sum_i c_i \text{Tr} \left[\mathcal{M}_i^4(\bar{\phi}) \ln[\mathcal{M}_i^2(\bar{\phi})/Q^2] + P_i(\bar{\phi}) \right], \quad (4.29)$$

where the sum runs over all fields in the loop and the trace over the mass matrices \mathcal{M}_i . The coefficients c_i count the number of spin degrees of freedom (and are negative for fermionic states). In the mass matrices, the v is replaced by the classical field $\bar{\phi}$ and Q is the renormalization scale. In the definition of the effective potential, there is one arbitrariness left due to the choice of the renormalization scheme which expresses itself in certain polynomials $P_i(\bar{\phi})$.

Similar to the diagrammatic method described in the following section (which was used to explicitly derive the one-loop potential with third generation squarks), CW sum over all 1PI n -point Green’s functions and perform the loop-integration after the summation. In Sec. 4.1.3, we do it the other way round and sum after integration.

There are two issues to treat with care as CW point out in their paper [219]: one is the correct interplay of combinatorial factors (symmetry factors of the diagrams and statistical factors like a Bose $\frac{1}{2}$ factor). Second, in the derivation there appear superficially infrared divergent diagrams that result in singularities at $\bar{\phi} = 0$ for an initially massless theory. There is one confusing paragraph in [219] stating this infrared singularity becomes obvious if one calculates radiative corrections to the propagator at $p^2 = 0$ which would behave like $p^2 \ln p^2$ (which goes to zero as $p^2 \rightarrow 0$). Actually, the effective potential itself is calculated at vanishing external momenta to give the vacuum configuration of the theory. According to CW, this infrared singularity can be avoided staying away from $\bar{\phi} = 0$. Is the effective potential invalid at the origin?

The infrared behavior can be directly seen in the one-loop potential

$$V = \frac{\lambda}{4!} \bar{\phi}^4 - \frac{1}{2} B \bar{\phi}^2 - \frac{1}{4!} C \bar{\phi}^4 + i \int \frac{d^4 k}{(2\pi)^4} \sum_{n=1}^{\infty} \frac{1}{2n} \left(\frac{\frac{1}{2} \lambda \bar{\phi}^2}{k^2 + i\epsilon} \right)^n, \quad (4.30a)$$

The trace can be taken as the sum over the mass eigenvalues.

In the \overline{MS} scheme for a scalar field in the loop, e. g. $P(\bar{\phi}) = -\frac{3}{2}$, whereas for gauge fields $P(\bar{\phi}) = -\frac{5}{6}$.

The tree-level Lagrangian without counterterms for massless ϕ^2 theory is given by $\mathcal{L} = \frac{1}{2}(\partial_\mu \phi)^2 - \frac{\lambda}{4!}$.

with renormalization constants B and C . After summation and Wick rotation to Euclidean space

$$V = \frac{\lambda}{4!} \bar{\phi}^4 - \frac{1}{2} B \bar{\phi}^2 - \frac{1}{4!} C \bar{\phi}^4 + \frac{1}{2} \int \frac{d^4 k}{(2\pi)^4} \ln \left(1 + \frac{\lambda \bar{\phi}^2}{2k^2} \right). \quad (4.30b)$$

Now, performing the integral and introducing a momentum cut off Λ , CW obtain

$$V = \frac{\lambda}{4!} \bar{\phi}^4 - \frac{1}{2} B \bar{\phi}^2 - \frac{1}{4!} C \bar{\phi}^4 + \frac{\lambda \Lambda^2}{64\pi^2} \bar{\phi}^2 + \frac{\lambda^2 \bar{\phi}^4}{256\pi^2} \left(\ln \frac{\lambda \bar{\phi}^2}{2\Lambda^2} - \frac{1}{2} \right), \quad (4.31)$$

and after applying renormalization conditions to remove the constants B and C , the final result for the tree plus one-loop effective potential in scalar ϕ^4 theory is given by

$$V = \frac{\lambda}{4!} \bar{\phi}^4 + \frac{\lambda^2 \bar{\phi}^4}{256\pi^2} \left(\ln \frac{\bar{\phi}^2}{Q^2} - \frac{25}{6} \right), \quad (4.32)$$

with the renormalization scale Q entering via the renormalization conditions,

$$\left. \frac{d^2 V}{d \bar{\phi}^2} \right|_{\bar{\phi}=0} = 0 \quad \text{and} \quad \left. \frac{d^4 V}{d \bar{\phi}^4} \right|_{\bar{\phi}=Q} = \lambda(Q).$$

The renormalization scale Q is *a priori* an arbitrary number with mass dimension one—and has to be chosen in a proper way. This choice may be a simplification of the calculation (e. g. $Q = \bar{\phi}$ to make the logarithm vanish [267]) or a specific fixed scale choice in order not to make all the corrections vanish but intrinsically make them small in a neighborhood where the corrections shall vanish, short: $Q = v$ such that for classical field values $\bar{\phi} = v$ at the minimum the logarithm vanishes.

Similar considerations can be done and have been done for calculating effective scalar potentials in e. g. massless scalar QED and the electroweak SM [219] as well as the effective potential for a Yang–Mills field [268]. In any case, once gauge fields are added to the theory and the derivation of the effective potential, this object becomes explicitly gauge dependent, whereas physical observables that can be derived from it (e. g. tunneling rates, not the instability scale [264]) stay gauge invariant, especially the value of the potential at its minima [265, 266]. The issue of gauge invariance is not relevant if one only considers scalar theories or, as done in Sec. 4.2, a scalar subset which gives the dominant contribution to the loop-corrected effective potential.

The effective potential in the given description is a good approximation where $\bar{\phi}$ is close to the minimum determined by Eq. (4.2). However, for field values $\bar{\phi} \gg v$, where the logarithm $\ln(\bar{\phi}/v)$ becomes large, the expansion becomes unreliable (the same holds for very small field values $\bar{\phi} \approx 0$). In order to avoid this, the effective potential has to be improved via the RG as already briefly stated in the introduction to this chapter

Details about the proper scale choice follow in the description of the RGI potential.

Ref. [268] is interesting in such a way that the authors derive the analogous expression to the scalar effective potential with Yang–Mills fields as external (and internal) particles.

The small $\bar{\phi}$ divergence corresponds to CW's IR singularity and is absent with masses.

and discussed in greater detail in Sec. 4.1.4. What stays a bit unclear is the question what defines a large logarithm. This becomes clear, if largely separated scales are discussed as one compares the electroweak with the Planck scale [253, 256, 258, 259, 261, 262, 269–283] or the scale of heavy neutrinos as done in Chap. 5 and [274, 284–286]. To get a feeling: field values $\bar{\phi} \approx 3\nu$ as discussed in Sec. 4.2 produce $\ln 3 \approx 1$, which is not a large number (therefore we do not include the RGI potential in Sec. 4.2). On the other hand, $\ln(\bar{\phi}/\nu) \approx 4\pi$ for $\bar{\phi} \approx 3 \times 10^5 \nu$ indeed is a large number. This comparison is to justify the use of the RGI potential for the description of instabilities caused by heavy neutrino fields and not for SUSY scale instabilities.

INTEGRATING THE TADPOLE The diagrammatic result of CW can be very elegantly obtained by the method of Lee and Sciaccaluga [221]. Especially the evaluation of the combinatorial factors in the diagrammatic calculation can be very exhausting as shown in the following section. The tadpole method exploits the utilization of the effective potential as generating function of n -point functions. The loop-expansion gives the corresponding loop counting for the n -point function. In this way, the first derivative of the one-loop potential gives the one-loop tadpole T_1

$$\frac{\partial V_{\text{eff}}(\bar{\phi})}{\partial \bar{\phi}} = G^{(1)} \equiv T_1(\bar{\phi}). \quad (4.33)$$

Inverting Eq. (4.33) gives V_{eff} after integration of the tadpole with respect to $\bar{\phi}$. For a single scalar field with self-coupling potential $P(\phi)$, the tadpole can be easily calculated in dimensional regularization yielding

$$T_1(\bar{\phi}) = \frac{f(\bar{\phi})}{32\pi^2} \left[M^2(\bar{\phi}) \ln \frac{M^2(\bar{\phi})}{Q^2} - M^2(\bar{\phi}) \right], \quad (4.34)$$

where the functions f and M are defined via derivatives of the potential

$$M^2(\bar{\phi}) = \left. \frac{\partial^2 P(\phi)}{\partial \phi^2} \right|_{\phi=\bar{\phi}} \quad \text{and} \quad f(\bar{\phi}) = \left. \frac{\partial^3 P(\phi)}{\partial \phi^3} \right|_{\phi=\bar{\phi}} \equiv \frac{\partial M^2(\bar{\phi})}{\partial \bar{\phi}}.$$

Therefore, the integration gives including a generic prefactor N

$$\begin{aligned} V_1(\bar{\phi}) &= \frac{N}{32\pi^2} \int d\bar{\phi}' \frac{\partial M^2(\bar{\phi}')}{\partial \bar{\phi}'} M^2(\bar{\phi}') \ln \frac{M^2(\bar{\phi}')}{Q^2} \\ &= \frac{N}{32\pi^2} \int dM^2 M^2 \ln \frac{M^2}{Q^2} \\ &= \frac{N}{64\pi^2} M^4(\bar{\phi}) \left(\ln \frac{M^2(\bar{\phi})}{Q^2} - \frac{3}{2} \right). \end{aligned} \quad (4.35)$$

N already has to be present in the equation for T.

The prefactor N collects all spin, color and charge degrees of freedom. A squark e. g. gets $N = 3$, where the corresponding quark has $N = -3 \cdot 2$. Eq. (4.35) once again reproduces the generic CW formula.

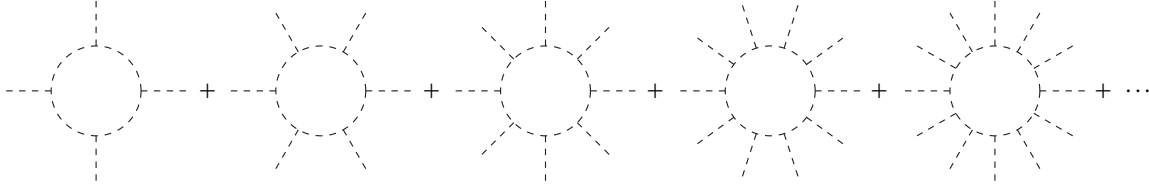


FIGURE 19: Summing up the one-loop potential for a triple scalar coupling up to infinitely many external legs. We refer to diagrams with an arbitrary number of external legs as *sea urchin diagrams*.

4.1.3 Sea Urchins

Coleman and Weinberg [219] performed their calculation of the effective potential by directly resumming all one-loop 1PI diagrams, and calculated the loop integral after summation. The tadpole integration method by Lee and Sciaccaluga [221] includes the sum over all diagrams implicitly by the integral over the one-loop tadpole and Jackiw's path integral derivation [220] also implicitly includes all n -point diagrams in the determinant and the integration over the loop momentum follows after the implicit sum. Formally, summation and integration can only be exchanged with care. We shall, however, show that it makes no difference for the calculation of the effective potential and explicitly resum the series of analytical n -point Green's functions. The interesting point is, that we can trace back the loop-integral to derivatives of the tadpole functions. For the sake of generality (and because of later applicability to SUSY models), we consider triple and quadruple scalar couplings and restrict ourselves to the contribution from one class of heavy fields in the loop. This is the case when we calculate the Higgs effective potential by means of heavy squark fields in the loop and *do not* consider the effective quark potential, which is impossible to calculate (and analyze) analytically.

The effective potential is the generating function of n -point diagrams. Sample diagrams are shown in Fig. 19, where we only show triple scalar couplings (we also shall start our discussion with those). Corrections to renormalizable operators would stop immediately after the first diagram, which gives a correction to a certain self-coupling λ_i if the external lines are related to Higgs fields, say H_u and/or H_d . The loop expansion allows to attach more external lines, even an infinite number of such spikes. We refer to the spiky diagrams as *sea urchin diagrams* for obvious reasons.

Each term in the expansion by the number of external legs defines an effective self-coupling, which can be obtained backwards from the derivative of the effective potential. This allows to cross-check the methods. As we will see, the direct summation of sea urchins results in exactly the same structure as what follows immediately from the compact result given many times, cf. Eqs. (4.4), (4.29), (4.28), (4.35). Therefore, we define

$$\begin{aligned} \mathcal{V}(\Phi^\dagger\Phi) &= m^2\Phi^\dagger\Phi + \frac{\lambda^{(4)}}{2}(\Phi^\dagger\Phi)^2 + \frac{\lambda^{(6)}}{3}(\Phi^\dagger\Phi)^3 + \dots \\ &= m^2\Phi^\dagger\Phi + \sum_{n=2}^{\infty} \frac{\lambda^{(2n)}}{n}(\Phi^\dagger\Phi)^n, \end{aligned} \quad (4.36)$$

All functions and series are well-behaved, so we can interchange sum and integral.

Up to now, no sparticles have been found at the LHC, so squarks have to be heavy if they exist. Nevertheless, heavy stops are desired to get a reasonably heavy Higgs. Therefore, it is not unlikely to have multi-TeV squarks, one Higgs below 130 GeV and heavier Higgses in between. Such scenarios also allow to consider an effective 2HDM where SUSY corrections generate some of the generic Higgs couplings. Details on that were already given in Sec. 2.2.2 and follow even more in Sec. 4.2.

explicitly for a complex scalar field Φ . The bilinear term $\sim m^2$ is to be seen as a tree-level mass which gets renormalized by a UV counterterm. The self-couplings only receive finite corrections and in the following, we are only interested in the one-loop self-couplings. In principle, there is a $\lambda_{\text{tree}}^{(4)}$ which, however, is only an additive constant to the loop-induced quartic coupling. All others ($\lambda^{(>4)}$) are exclusively loop-generated. We get the coupling of the $2n$ -point function by differentiating with respect to Φ, Φ^\dagger :

$$\lambda^{(2n)} = \frac{n}{(n!)^2} \left(\frac{\partial}{\partial \Phi^\dagger} \right)^n \left(\frac{\partial}{\partial \Phi} \right)^n \mathcal{V} \Big|_{\Phi^\dagger, \Phi=0}. \quad (4.37)$$

To be clear on factors $n!$ and n and some more appearing in the following: the $1/(n!)^2$ in Eq. (4.37) eats up factors $n!$ coming from the derivative and the n in the numerator is just the factor $1/n$ from the definition of self-couplings of the potential in Eq. (4.36). Likewise, we can calculate $\lambda^{(2n)}$ as one-loop diagrams and match the Green's functions to the effective potential. Exploiting this fact, the loop calculation yields an expression like

$$-i\lambda_{\text{loop}}^{(2n)} = i \frac{(n!)^2}{n} \frac{\gamma_{2n}}{16\pi^2} N L_n(m_1, m_2), \quad (4.38)$$

where γ_{2n} denotes the $2n$ -point vertex, L_n some loop- $2n$ -point-function and m_1, m_2 are the masses of two different fields running in the loop. N counts for example the numbers of color.

Marrying (4.37) with (4.38): to perform the matching, we have to identify the loop potential contribution with the result from the effective potential. Given in Eq. (4.38) is the *truncated* Green's function missing external fields. The effective potential follows by appending those fields Φ and Φ^\dagger as

$$\mathcal{V}_{\text{loop}}(\Phi^\dagger \Phi) = \sum_{n=0}^{\infty} \frac{1}{(n!)^2} \lambda_{\text{loop}}^{(2n)} (\Phi^\dagger \Phi)^n. \quad (4.39)$$

Now, Eqs. (4.39) and (4.36) describe the same object in the full or the effective theory, respectively. The mass term was omitted.

The potential can be expressed in terms of the loop-derived quantity:

$$\mathcal{V}_{\text{loop}}^{\geq 4}(\Phi^\dagger \Phi) = -\frac{N}{16\pi^2} \sum_{n=2}^{\infty} \gamma^{2n} L_n(m_1, m_2), \quad (4.40)$$

which will be breathed with life in the following.

We perform a sample calculation in a scalar theory which can be motivated from the MSSM. Consider a superpotential of two Higgs doublets and two chiral quark superfields

$$\mathcal{W} = \mu H_d \cdot H_u - Y_t Q \cdot H_u \bar{T}. \quad (4.41)$$

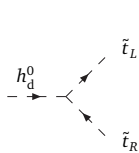
The triple coupling induces the top Yukawa coupling, which is important for the fermionic contribution to the effective potential, and a quadrilinear

The field Φ takes the role of the “classical field” as it appears externally.

Φ has to be replaced by the Higgs field h^0 later on.

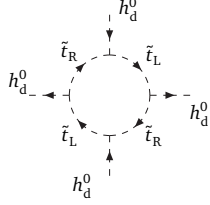
The occurrence of the factor $(n!)^2/n$ in Eq. (4.38) can be seen from the symmetries of the diagram: the internal lines of the diagrams are different at each vertex. Contracting all vertices to a connected diagram then gives a symmetry factor $n!(n-1)!$. By drawing only one diagram, we forget about the others—so this factor ends up in the numerator. There are no further symmetry factors, so we receive a prefactor of $n!(n-1)!$.

The superfield formalism was introduced in Sec. 2.2.2. Higgs fields and Q are $SU(2)$ doublet fields. For the moment, we ignore the bottom Yukawa coupling.



$$= -i\mu Y_t^*$$

stop-Higgs coupling $\sim \tilde{t}_{L,R}^* \tilde{t}_{L,R} h_u^{0*} h_u^0$, which will be discussed later. Leaving out soft SUSY breaking terms (the full case will also be discussed later and in Sec. 4.2), the only trilinear stop-Higgs coupling is due to the F -term contribution and couples to the “wrong” Higgs doublet, $\sim \mu Y_t^* \tilde{t}_R^* \tilde{t}_L h_d^0$. This vertex is quite unique since it is oriented (by the direction of complex fields) and couples three distinct fields. We calculate the one loop four point function (i.e. the one loop correction to the tree-level λ_1) for equal left and right stop masses. We work in the flavor basis, where the internal lines are no mass eigenstates and are propagators with the soft breaking left and right stop masses \tilde{m}_L and \tilde{m}_R ($N_c = 3$ is the number of colors)



$$-i\lambda^{(4)} = iN_c \frac{|\mu Y_t|^4}{16\pi^2} D_0(\tilde{m}_L, \tilde{m}_R, \tilde{m}_L, \tilde{m}_R) \quad (4.42)$$

$$\stackrel{\tilde{m}_{L,R}=\tilde{m}}{=} iN_c \frac{|\mu Y_t|^4}{16\pi^2} \frac{1}{3!} \left(\frac{d}{d\tilde{m}^2} \right)^3 A_0(\tilde{m}),$$

which can be easily generalized to the $2n$ point function resulting in $\lambda_{\text{loop}}^{(2n)}$:

$$-i\lambda_{\text{loop}}^{(2n)} = iN_c \frac{|\mu Y_t|^{2n}}{16\pi^2} \frac{(n!)^2}{n} \frac{1}{(2n-1)!} \left(\frac{d}{d\tilde{m}^2} \right)^{2n-1} A_0(\tilde{m}), \quad (4.43)$$

where

$$\left(\frac{d}{d\tilde{m}^2} \right)^{2n-1} A_0(\tilde{m}) = (-1)^{n-1} \frac{(2n-3)!}{(\tilde{m}^2)^{2n-2}}.$$

Therefore, we can write the effective self-couplings in the following form:

$$\lambda^{(2n)} = -\frac{N_c}{16\pi^2} \frac{|\mu Y_t|^{2n}}{\tilde{m}^2} (\tilde{m}^2)^2 \frac{(n!)^2}{n} \frac{(2n-3)!}{(2n-1)!} \underbrace{\phantom{\frac{(2n-3)!}{(2n-1)!}}}_{(2-6n+4n^2)^{-1}}. \quad (4.44)$$

Now, we can combine Eq. (4.44) and the loop potential of Eq. (4.39) resulting in an infinite series that can be resummed to

$$\mathcal{V}_{\text{loop}}^{\geq 4} = -\frac{N_c \tilde{m}^4}{16\pi^2} \sum_{n=2}^{\infty} \frac{x^{2n}/n}{2-6n+4n^2}, \quad (4.45)$$

where we defined the dimensionless quantities

$$x^2 = \left(\frac{\mu Y_t}{\tilde{m}^2} \right)^2 h_d^\dagger h_d.$$

The sum of Eq. (4.45) can be evaluated yielding

$$\begin{aligned} \mathcal{V}_{\geq 4} &= -\frac{N_c \tilde{m}^4}{16\pi^2} \frac{1}{2} \left(3x^2 - 4x \text{Artanh}(x) - (1+x^2) \ln(1-x^2) \right) \\ &= -\frac{N_c \tilde{m}^4}{32\pi^2} \left(3x^2 - (1+x)^2 \ln(1+x) - (1-x)^2 \ln(1-x) \right), \end{aligned} \quad (4.46)$$

Definitions of the loop functions A_0 and D_0 are given in App. A. There are also some (obvious) technicalities how to arrive at the derivative for equal masses.

At the end, we are interested in the neutral component's direction $\sim h_d^0$. Because of $SU(2)$ invariance, we also get the full potential from the calculation of the h_d^0 part.

where the last replacement $\text{Artanh} = \frac{1}{2}(\ln(1+x) - \ln(1-x))$ can be done for $|x| < 1$ which is also the radius of convergence of the infinite sum (4.45). Likewise, for $|x| > 1$, $\log(1-x)$ develops an imaginary part which corresponds to the values of $\langle h_d^0 \rangle$ for which one stop mass-squared eigenvalue drops negative—an obvious relation to a non-convex potential at tree-level, in this case it is the stop potential. The imaginary part, however, is puzzling since it rises with $x^2 \sim |h_d^0|^2$. On the other hand, the lightest stop is tachyonic as $x > 1$ and its mass² drops with x . Given the superpotential of Eq. (4.41) and only including the $\mu^* Y_t$ -term and the soft breaking masses, the field dependent stop squared mass matrix is

$$\mathcal{M}_{\tilde{t}}^2(h_d^0) = \begin{pmatrix} \tilde{m}_L^2 & -\mu^* Y_t h_d^{0*} \\ -\mu Y_t^* h_d^0 & \tilde{m}_R^2 \end{pmatrix},$$

and the two eigenvalues setting $\tilde{m}_L = \tilde{m}_R = \tilde{m}$,

$$\tilde{m}_{1,2}^2 = \tilde{m}^2(1 \pm x).$$

Such a situation would be excluded anyway (loop corrections to the stop masses may rescue the tachyonic mass in some regime) and is either a sign of a wrong theory or some missing ingredient. There is indeed something missing which is actually an important contribution to the stability of the potential, the $|Y_t h_u^0|^2$ -term. Now, we could argue that this does not matter because it gives a contribution to a different direction in field space ($\sim h_u^0$ not h_d^0). To be prepared for full stop contribution to the Higgs effective potential $V_{\text{eff}}^{\tilde{t}}(h_u^0, h_d^0)$, we want to be complete and also add the missing soft SUSY breaking trilinear coupling $\sim A_t h_u^0 \tilde{t}_L^* \tilde{t}_R$. The full (ignoring potential stop vevs, $\langle \tilde{t}_L \rangle = \langle \tilde{t}_R \rangle = 0$) stop mass matrix is then given by

$$\mathcal{M}_{\tilde{t}}^2(h_u^0, h_d^0) = \begin{pmatrix} \tilde{m}_L^2 + |Y_t h_u^0|^2 & -\mu^* Y_t h_d^{0*} + A_t h_u^0 \\ -\mu Y_t^* h_d^0 + A_t^* h_u^{0*} & \tilde{m}_R + |Y_t h_u^0|^2 \end{pmatrix} \quad (4.47)$$

and the eigenvalues by ($\tilde{m}_L = \tilde{m}_R = \tilde{m}$)

$$\tilde{m}_{1,2} = \tilde{m}^2(1 \pm x + y), \quad (4.48)$$

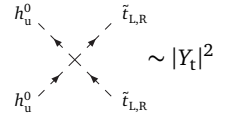
with

$$x^2 = \frac{|A_t h_u^0 - \mu^* Y_t h_d^{0*}|^2}{\tilde{m}^4} \quad \text{and} \quad y = \frac{|Y_t h_u^0|^2}{\tilde{m}^2}. \quad (4.49)$$

Using the generic formula (4.29), it is very easy to obtain the one-loop potential induced by stop fields in the loop:

$$V_{1\text{-loop}}^{\tilde{t}} = \frac{N_c \tilde{m}^4}{32\pi^2} \left[(1+x+y)^2 \ln(1+x+y) + (1-x+y)^2 \ln(1-x+y) - (x^2 + y^2 + 2y)(3 - 2 \ln(\tilde{m}^2/Q^2)) \right], \quad (4.50)$$

The main question is, whether one can trust the expansion beyond the radius of convergence. For the discussion of vacuum stability, we take the analytic continuation where the potential becomes complex and ignore both issues related to the imaginary part and radius of convergence.



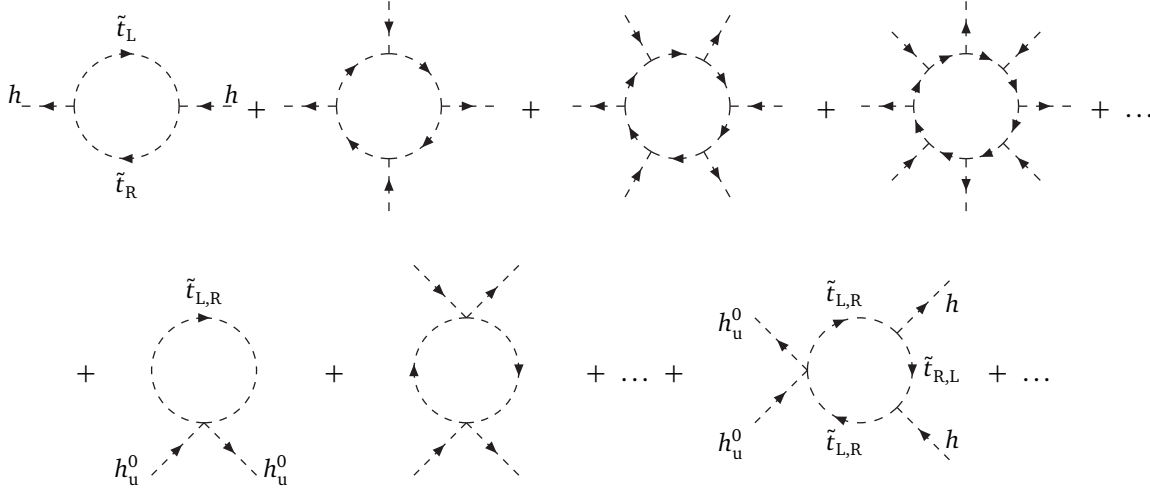


FIGURE 20: The series of n -point Green's functions contributing to the Higgs effective potential with top squarks running in the loop.

where we kept the renormalization scale dependence (because we can). Eq. (4.50) follows directly from Eq. (4.46) with $\pm x \rightarrow \pm x + y$ modulo the polynomial in y . The direct resummation of the series of 1PI n -point Green's functions, however, seems to be impossible for the generic setup, where the stop fields do not only couple to one Higgs field but also to a linear combination of h_u and h_d , $h = h_d^{0*} - h_u^0 A_t / (\mu^* Y_t)$ which appear mixed in the series shown in Fig. 20. Note that the $|h_u^0|^2$ coupling preserves “chirality”, where the trilinear coupling $\sim h$ flips $L \rightarrow R$ and vice versa.

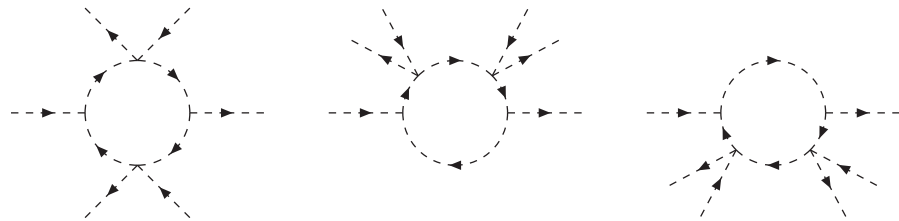
The summation includes mixed powers of $|h_u^0|^2$ and $|h|^2$ and has the form

$$V_{1\text{-loop}} = - \sum_{k=0}^{\infty} \sum_{n=0}^{\infty} a_{kn} (h^* h)^k (h_u^{0*} h_u^0)^n. \quad (4.51)$$

The coefficients a_{kn} can be calculated from the loop diagrams with $2k + 2n$ legs, where k counts the number of $\tilde{t}_R^* - \tilde{t}_L - h$ vertices (and the conjugated ones) and n counts the quadrilinear $\tilde{t}_{R,L}^* - \tilde{t}_{R,L} - h_u^{0*} - h_u^0$ vertices.

The calculation of the coefficient a_{k0} has already been performed above, the symmetry factor is found to be effectively $1/k$. A similar result can be obtained for a_{0n} from the pure quadrilinear coupling diagrams. The dependence on the masses in the loop is in both cases a certain derivative of the tadpole function $A_0(m^2)$. For the mixed diagrams like

The three diagrams give the contribution to the same order in the expansion Eq. (4.51), $k = 1$ and $n = 2$.



the combinatorics is more involved. We start with the trilinear coupling diagrams from above (Fig. 19) which have $k!(k-1)!$ internal symmetries.

Divided by $(k!)^2$ from the $2k$ -th derivative of the effective potential, we get $1/k$. Now, we attach quadrilinear vertices to the k -point trilinear coupling diagram. Remember that the quadrilinear coupling preserves chirality, the trilinear one flips it. Therefore, the n -th quadrilinear coupling just “sits” on top of any propagator and we only have to count how many possibilities are there to distribute one such coupling on an existing diagram. The same problem arises if one has a box of colored gummy bears having k colors (the existing k propagators) and one takes n bears out of the box. How many combinations are possible? The answer is

$$\frac{(n+k-1)!}{(n-1)!k!} = \binom{n+k-1}{k}.$$

We can now give the explicit and generic coefficients a_{kn}

$$a_{k0} = |\mu Y_t|^{2k} \frac{1}{k} I_{k,k}(\tilde{m}_L^2, \tilde{m}_R^2) \quad \text{for } k \geq 1, \quad (4.52a)$$

$$a_{0n} = |Y_t|^{2n} \frac{1}{n} [I_{n,0}(\tilde{m}_L^2) + I_{0,n}(\tilde{m}_R^2)] \quad \text{for } n \geq 1, \quad (4.52b)$$

$$a_{kn} = |\mu|^{2k} |Y_t|^{2k+2n} \frac{1}{k} \sum_{j=0}^n \frac{(j+k-1)! (n-j+k-1)!}{j!(k-1)! (n-j)!(k-1)!} \times \quad (4.52c)$$

$$I_{k+j,k+n-j}(\tilde{m}_L^2, \tilde{m}_R^2) \quad \text{for } n, k \geq 1.$$

The loop-functions $I_{p,q}(\tilde{m}_L^2, \tilde{m}_R^2)$ are result of the one-loop integrals with p propagators with mass \tilde{m}_L^2 and q propagators with \tilde{m}_R^2 :

$$I_{p,q}(\tilde{m}_L^2, \tilde{m}_R^2) = \frac{N_c}{16\pi^2} \frac{1}{(p-1)!(q-1)!} \frac{\partial^{p-1}}{\partial (\tilde{m}^2)^{p-1}} \frac{\partial^{q-1}}{\partial (\tilde{m}_R^2)^{q-1}} \times \quad (4.53a)$$

$$\frac{A_0(\tilde{m}_L^2) - A_0(\tilde{m}_R^2)}{\tilde{m}_L^2 - \tilde{m}_R^2} \quad \text{for } p, q \geq 1,$$

$$I_{n,0}(\tilde{m}^2) = \frac{N_c}{16\pi^2} \frac{1}{(n-1)!} \frac{\partial^{n-1} A_0(\tilde{m}^2)}{\partial (\tilde{m}^2)^{n-1}} \quad \text{for } n \geq 1, \quad (4.53b)$$

$$I_{0,n}(\tilde{m}^2) = I_{n,0}(\tilde{m}^2). \quad (4.53c)$$

This series can be resummed and compared term by term with the derivatives following from the potential (4.50). The complete supersymmetric contribution to the one-loop Higgs potential contains also the fermionic part (which is easy) and, to be SU(2) invariant, the same diagrams from the (s)bottom sector. Once, the potential is fixed (SM minimum at the right positions, $v_u = v \sin \beta$ and $v_d = v \cos \beta$ and the lightest Higgs mass $m_{h^0} = 125 \text{ GeV}$, via e. g. fixing A_t), the influence of the bottom squark drives an instability below the SUSY scale (see [287] and Sec. 4.2). A similar result may hold for the top squark contribution, if A_t is not fixed.

The results obtained in the section above are part of [287].

4.1.4 Improving the potential

In the n -loop expansion, the effective potential depends on the renormalization scale Q as well as the dimensionless and dimensionful couplings λ_i , see e. g. [219, 230]:

$$V_{\text{eff}} = V(\lambda_i, \phi, Q).$$

The full potential to all orders in perturbation theory shall not depend on the renormalization scale. To finite order in some expansion (like the loop expansion) one has to wangle for the desired behavior with the procedure described in this section. Eq. (4.55) is the Callan-Symanzik equation for an arbitrary n -point function generated by V .

The renormalization scale Q , however, is arbitrary, though usually chosen in a way to keep the corrections (i. e. the logarithms) small. In general, the potential should not depend on the choice of this parameter, which can be expressed in the differential equation

$$Q \frac{d}{dQ} V(\lambda_i, \phi, Q) = 0. \quad (4.54)$$

The couplings and fields of the theory are renormalized and therefore also depending on the scale Q . Exploiting this fact, we get the renormalization group equation (RGE) for the effective potential by applying the chain rule to Eq. (4.54)

$$\left[Q \frac{\partial}{\partial Q} + \beta_i(\lambda_i) \frac{\partial}{\partial \lambda_i} - \gamma_\phi \frac{\partial}{\partial \phi} \right] V(\lambda_i, \phi, Q), \quad (4.55)$$

where we defined the β functions for the couplings as

$$\beta_i(\lambda_i) = Q \frac{d\lambda_i(Q)}{dQ} \quad (4.56)$$

and the anomalous dimension of the field ϕ

$$\gamma_\phi(\phi/Q) = -\frac{d\phi}{dQ}. \quad (4.57)$$

If we are now interested in the effective potential at some arbitrary scale Q knowing the potential at the value of the classical field $\bar{\phi}$, we easily obtain this by solving the RGE for the couplings (i. e. integrating the β functions) and replacing all couplings in V_{eff} by the RG improved ones evaluated at the scale Q . For convenience, let us define the logarithmic derivative

$$Q \frac{d}{dQ} = \frac{d}{d \ln Q / Q_0} = \frac{d}{dt}, \quad t = \ln \frac{Q}{Q_0},$$

for some arbitrary but fixed scale Q_0 . This scale conveniently is chosen to be the electroweak scale. Then the parameters of the effective potential can be written as

$$\phi(t) = \xi(t) \bar{\phi}, \quad (4.58)$$

with the field renormalization ξ expressed as

$$\xi(t) = \exp \left(- \int_0^t dt' \gamma(t') \right). \quad (4.59)$$

Any coupling $\lambda_i(t)$ can be determined from the coupling $\lambda_i(t=0)$:

$$\lambda_i(t) = \lambda_i(0) + \int_0^t dt' \beta_i(t'). \quad (4.60)$$

The t -dependence of the renormalization scale $Q(t)$ follows directly from the definition of t : $d \ln(Q/Q_0) / dt = 1$,

$$Q(t) = Q_0 e^t.$$

Note that not only the effective potential itself, but also its n -th derivatives in ϕ are scale-independent [267]:

$$\frac{dV_{\text{eff}}^{(n)}}{dt} = 0,$$

with

$$V_{\text{eff}}^{(n)} = \xi^n(t) \frac{\partial^n}{\partial \phi(t)^n} V_{\text{eff}}(\lambda_i(t), \phi(t), Q(t)). \quad (4.61)$$

In that way, all the couplings derived from the potential according to Eq. (4.61) are scale-independent.

The efficiency in the use of the RG improvement lies in the very simple fact (pointed out clearly by Kastening [288]) that solving the one-loop β -functions and including them in the *tree-level* formula indeed gives a better approximation in the sense that the dependence on the renormalization scale vanishes. In a ϕ^4 theory without m^2 -term, as elaborated by CW, the RGI effective potential can be written as

$$V_{\text{eff}}(\phi) = \frac{\lambda(Q)}{4!} \phi^4, \quad (4.62)$$

where $V(\phi=Q) = \lambda Q^4/4!$ and

$$\lambda(Q) = \frac{\lambda}{4!} \left[1 - \frac{3\lambda}{2(4\pi)^2} \ln \frac{\phi^2}{Q^2} \right]^{-1}.$$

Eq. (4.62) is identical to the CW result

$$V_1^{\text{CW}} = \frac{\lambda^2 \phi^4}{16(4\pi)^2} \left(\ln \frac{\lambda \phi^2}{2Q} - \frac{3}{2} \right)$$

after expanding in the logarithmic term ($\ln(\phi^2/Q^2) \approx 0$ around $Q \approx \phi$) and rescaling

$$Q^2 \rightarrow \frac{2Q^2}{\lambda} \exp \frac{3}{2}.$$

The task to do for obtaining the RGI potential is the following: determine the effective potential and solve the RGE for the couplings and evaluate the potential at the scale $Q(t) = \phi(t)$. This procedure, however, gets complicated in case of more fields and more scales related to those fields as briefly discussed in the beginning of Chapter 5.

There is actually a typo in [288] in the line after Eq. (5).

4.2 THE STABILITY OF THE ELECTROWEAK VACUUM IN THE MSSM

The Higgs effective potential is needed to a high accuracy to give precise determinations of the minimization conditions, because we know that there are nontrivial minima.

For the discussion about truncated series, see Sec. 4.2.2

Also in [291] radiative breaking was suggested to cure the problem, but it persists.

The MSSM is a multi-scalar theory. Not only the two Higgs doublets (with also electrically charged directions in field space) but scalar superpartners of SM fermions influence the stability of the electroweak vacuum as well. The calculation of the *full* scalar potential at one (or even more) loop(s) is a formidable if not impossible task, where the pure Higgs effective potential is already known up to two-loop accuracy [289].

4.2.1 Distinguishing Between different Instabilities

The scalar potential of the MSSM possesses any possible dangers, where a complete analysis should always include *all* directions in field space and if loop corrections are taken into account, a truncation of the potential after renormalizable terms may give a wrong estimate.

An exhaustive overview of tree-level instabilities in the MSSM scalar potential was given by the authors of [290] with a useful classification of constraints. The existence of charge and color breaking (CCB) global minima in SUSY theories was already detected in the early 1980s in the context of electroweak breaking in supergravity models at tree-level [291] and via radiative breaking [292–294]. Estimates on metastable vacua comparing the tunneling time with the lifetime of the universe were also already proposed at that time [295]. However, it is generically difficult to survey all possibly dangerous directions, so specific “rays” in field space are chosen (which limit the validity) like $\langle h_u^0 \rangle = \langle \tilde{t}_L \rangle = \langle \tilde{t}_R \rangle$, which was generalized to more realistic configurations where the Higgs *vevs* do not coincide with the CCB minima in [296]. Constraints on soft SUSY breaking trilinear couplings *A*-terms were given by [297] and $\tan\beta$ bounds in [298]. The most general MSSM is even more involved when the full flavor structure is taken into account and allows to set even stronger bounds on the flavor violating soft breaking terms than FCNC constraints [299].

There are in principle three constraints from instable electroweak vacua: limits from potentials being unbounded from below (UFB) (also known as triviality bounds), such from CCB minima and charge and color *conserving* deeper minima. The latter limit has not yet been discussed in the literature and is a genuine one-loop effect, see Sec.4.2.2. It might be that the global minimum in such configurations indeed is CCB, the detailed analysis is beyond the scope of this chapter.

4.2.1.1 Unboundedness From Below

Considering the scalar potential of the MSSM at tree-level

$$V_0 = V_F + V_D + V_{\text{soft}},$$

where the individual components were introduced in Sec. 2.2.2, one finds certain directions in field space (details omitted) where the potential drops

down to minus infinity if certain parameters have some specific values. The field theoretical potential is related to the total energy density. If it is unbounded from below, conservation of energy is violated, thus such configurations are forbidden. Fixing those specific rays in field space, one obtains constraints on the parameters of the potential, e. g. [300, 301]

$$\begin{aligned} m_1^2 + m_2^2 - 2|m_3|^2 &\geq 0, \\ m_2^2 - \mu^2 + \tilde{m}_{L_i}^2 &\geq 0. \end{aligned}$$

UFB directions can only occur if the mass parameters are chosen inappropriately, because quadrilinear and positive F -terms will take over and turn UFB to CCB directions [290]. In order to organize the various UFB directions, the authors of [290] propose three classifications: including only $\langle h_u^0 \rangle$ and $\langle h_d^0 \rangle$, taking *one* more field into account (where they choose to take the lepton doublet) and the $\langle h_d^0 \rangle = 0$ limit corresponding to $\tan \beta \rightarrow \infty$.

4.2.1.2 Charge and Color Breaking Minima

The “traditional” CCB constraints follow from a minimization of the scalar potential in certain directions of field space, say $\langle \tilde{t}_R \rangle = \langle \tilde{t}_L \rangle = \langle h_u^0 \rangle \neq 0$ and can be expressed in inequalities constraining A -terms [297]

$$A_t^2 \leq 3 \left(\tilde{m}_Q^2 + \tilde{m}_t^2 + m_2^2 \right), \quad (4.63)$$

with similar relations for A_b and A_τ . Generalizations (which are more involved) for $\langle \tilde{t}_L \rangle \neq \langle \tilde{t}_R \rangle$ were found in [302]. An optimized version of this class of bounds was given by [290], where the one-loop effective potential was included to set the renormalization scale at which the tree-level potential has to be evaluated.³ The logic here follows [300], where the appropriate scale choice has to be such that the logarithms in V_1 are small and the one-loop potential vanishes at that scale. The importance of all V_1 contributions, even small ones, however was emphasized in a different context [303]. Eq. (4.63) gives very strong constraints that can be relaxed taking the vacuum tunneling rates into account compared to the lifetime of the universe [241]; this bound gets modified in view of the Higgs discovery [242]. CCB constraints are a powerful and often investigated tool to find limitations on MSSM parameters, see e. g. [304, 305]. Thus, it is also quite worthwhile working on an improvement of such conditions.

Even more important are generalizations of Eq. (4.63) with general, flavor-violating trilinear soft terms [299]. The bounds read very similarly

$$|A_{ij}^u|^2 \leq Y_{u_k}^2 \left(\tilde{m}_{Q_i}^2 + \tilde{m}_{u_j}^2 + m_2^2 \right), \quad k = \max(i, j). \quad (4.64)$$

Note the absence of the prefactor 3; the presence of the Yukawa coupling in front of the combination of soft masses appears or disappears with the

The parameters m_i correspond to the mass parameters of the 2HDM. In SUSY theories, m_3 is given by the soft breaking Higgs B_μ term.

Charged Higgs vevs play no role in the MSSM. It can be shown that the minimum in the MSSM always has $\langle h_u^+ \rangle = \langle h_d^- \rangle = 0$, this is not true for other scalars [290].

This inequality is generally ascribed to [291] in the literature, but never stated there. What is given instead, “ $A \leq 3$ ”, follows from equal soft masses ($\tilde{m}_Q = \tilde{m}_t = m_2 = \tilde{m}$) and a scaling of the trilinear soft breaking term with the same mass, $A_t \sim \tilde{m}$.

³ We have some doubts on that method, because V_1 as evaluated in Sec. 4.1.3 has a Q -independent part leading to a deeper minimum which was missed in earlier times.

convention for the A -terms. Casas and Dimopoulos [299] use the more convenient one for flavor physics which is also used throughout this thesis and given in Sec. 2.2.2, where the A -terms are independent of Yukawa couplings. Eq. (4.64) and its siblings for the down and charged lepton sector give very strong constraints on the flavor-violating soft breaking terms, more stringent than most FCNC observables and rule out large values of A_{ij} by the demand for a stable electroweak vacuum. Metastability considerations weaken the bounds a bit, however, they are still one of the strongest constraints for flavor violation in the soft breaking sector [306].

To be complete, a full one-loop analysis for CCB minima has to be performed which makes it impossible to give analytic results [307, 308]. In general, one-loop minimization conditions tend to stabilize the potential and its v evs with respect to the renormalization scale as long as the v evs are “small” ($\lesssim 1$ TeV) and hint to a breakdown of perturbation theory for larger field values. Therefore CCB minima of such large values are not trustworthy [308]. Moreover, CCB extrema are found to be rather saddle points since one class of scalar mass squares is negative and the convex hull [309] shall be taken as approximation for the effective potential where it is non-convex [307]. Similar to our findings described in Sec. 4.2.2, no UFB directions occur using one-loop minimization. However, it was stated that no “alternative MSSM minima” were found and no absolute CCB minima [310] using only nonzero stop v evs. We give arguments why this in general (including also sbottom v evs) is not the case.

We found the same conclusions for our charge and color conserving minima. CCB saddle points with tachyonic squarks, however rather hint to another more global CCB minimum. Maybe this one can be found more efficiently using the convex hull.

4.2.1.3 Charge and Color Conserving Minima

Another possible class of instabilities in the MSSM scalar potential that have not yet been discussed in such a great detail as CCB minima are charge and color *conserving* deeper minima. Such minima preserve the gauge symmetries of the MSSM as they appear in the same direction of field space as the “standard” v evs, v_u or v_d . The principle occurrence of such minima was noted in [310]. We show a viable example of such a situation in Sec. 4.2.2 based on the one-loop potential given in Eq. (4.50). Adding to $V_{1\text{-loop}}^{\tilde{t}+\tilde{b}}$ the tree-level potential with its standard minima, the loop-generated minimum may lie deeper. However, this point is related to a tachyonic squark mass eigenvalue and thus rather a saddle point in field space. The global minimum is supposed to lie in that direction.

As we will see, the global minimum of the full scalar potential is again charge and color breaking.

In Fig. 21, we show an example for a charge and color conserving deeper minimum which is loop-induced. The tree-level as well as the renormalizable one-loop potential up to $\sim x^4$ show only one minimum, of course. The position of that minimum is basically fixed by the quadratic term, $v^2 = m^2/\lambda$, considering an ordinary ϕ^4 potential. On the other hand, the pure one-loop potential of Eq. (4.50) itself has a minimum which always occurs at a position $x > 1$. If only the scalar trilinear vertices are taken into account, $V_{1\text{-loop}}^{\tilde{t}}$ develops a quadratically rising imaginary part, shown by the dashed curve in Fig. 21. This imaginary part does not show up, when also the quadrilinear terms are included, which is a

$$V_0(x) = -m^2x^2 + \lambda x^4$$

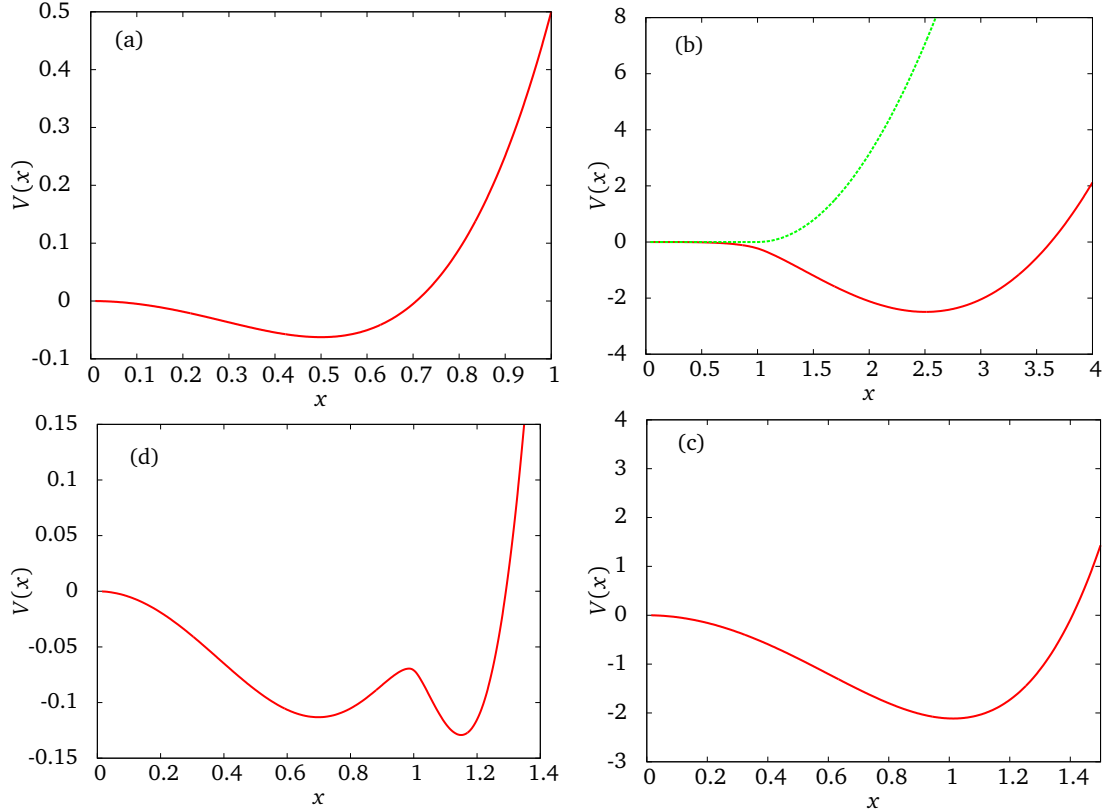


FIGURE 21: Illustrations of the tree and one-loop potential according to Eq. (4.50). Clockwise from the upper left: (a) A generic tree-level potential $V(x) = -m^2 x^2 + \lambda x^4$. The position of the vev can be adjusted with m^2 if λ is fixed, $v^2 = m^2/\lambda$. (b) $\text{Re } V_{1\text{-loop}}^{\tilde{t}}$ for $y = 0$. Shown in dashed red is the imaginary part which rises for $x > 1$. The green curve is the real part (analytic continuation) of the complex effective potential. (c) $V_{1\text{-loop}}^{\tilde{t}}$ with $y = x^2$, for the definitions of x and y cf. Eq. (4.49). No imaginary part shows up. (d) Tree + one-loop potential with some appropriately chosen weighting factors to make both minima appear. The smaller one ($x \approx 0.7$) corresponds to the minimum of the tree-level potential above, where the deeper minimum at $x > 1$ results from the one-loop potential.

hint that the full scalar potential in use (Higgs and stop) is well-behaved. The complex nature would indicate a non-convex tree-level direction, in this case corresponding to a tachyonic stop direction. We show no imaginary part related to the non-convex Higgs potential at tree-level, because it is not included in the one-loop part. A tachyonic eigenvalue at position of the second minimum is undesirable and rather hints towards a CCB global minimum.

We only consider $V_{1\text{-loop}}^{\tilde{t}}$, not $V_{1\text{-loop}}^{h_u^0}$ with h_u^0 fields in the loop.

4.2.2 Instable one-loop effective potential with squarks

For the analysis of the tree plus one-loop effective potential in the MSSM, we only include the (s)top/(s)bottom contribution which is dominated by the large top (and for large $\tan\beta$ also bottom) Yukawa coupling. Contributions from gauge fields are neglected. The only place where we keep the gauge couplings is the self-coupling of Higgs fields stemming from D -terms. We also neglect D -term contributions in the squark masses. The Higgs quartics are needed to have a tree-level Higgs potential which is bounded from below and where electroweak symmetry breaking happens.

Charged Higgs directions are irrelevant for the discussion of stability [290] and by SU(2) invariance, it is sufficient to calculate the potential for the neutral components and only discuss instabilities in neutral directions. Not to violate supersymmetry, we have to include the fermionic contributions, as well. Effective potentials for chiral superfields do not break SUSY radiatively [311]. The final result in the $\overline{\text{MS}}/\overline{\text{DR}}$ scheme reads

$$V_{\text{eff}} = V_0 + V_1^{\tilde{t}} + V_1^t + V_1^{\tilde{b}} + V_1^b \quad (4.65)$$

$$= m_{11}^{2\text{tree}} |h_d^0|^2 + m_{22}^{2\text{tree}} |h_u^0|^2 - 2 \text{Re} \left(m_{12}^{2\text{tree}} h_u^0 h_d^0 \right) + \frac{g_1^2 + g_2^2}{8} \left(|h_d^0|^2 - |h_u^0|^2 \right)^2$$

$$+ \frac{N_c \tilde{M}_t^4}{32\pi^2} \left[(1 + x_t + y_t)^2 \ln(1 + x_t + y_t) + (1 - x_t + y_t)^2 \ln(1 - x_t + y_t) \right.$$

$$\left. - (x_t^2 + 2y_t) \left(3 - 2 \ln(\tilde{M}_t^2/Q^2) \right) - 2y_t^2 \ln(y_t) + \{t \leftrightarrow b\} \right],$$

with $\tilde{M}_{t,b}^2 = (\tilde{m}_Q^2 + \tilde{m}_{t,b}^2)/2$ the average soft breaking mass and the generalizations of (4.49) for stop/sbottom with $\tilde{m}_Q \neq \tilde{m}_t, \tilde{m}_b$:

$$x_t^2 = \frac{|A_t h_u^0 - \mu^* Y_t h_d^{0*}|^2}{\tilde{M}_t^4} + \frac{(\tilde{m}_Q^2 - \tilde{m}_t^2)^2}{4\tilde{M}_t^4}, \quad y_t = \frac{|Y_t h_u^0|^2}{\tilde{M}_t^2}, \quad (4.66a)$$

$$x_b^2 = \frac{|A_b h_d^0 - \mu^* Y_b h_u^{0*}|^2}{\tilde{M}_b^4} + \frac{(\tilde{m}_Q^2 - \tilde{m}_b^2)^2}{4\tilde{M}_b^4}, \quad y_b = \frac{|Y_b h_d^0|^2}{\tilde{M}_b^2}. \quad (4.66b)$$

The tree-level potential V_0 is the neutral Higgs part of Eq. (2.29), which was written in a way that only $\lambda_{1\dots 3}$ contribute to neutral Higgs phenomenology. We want to fix the tree-level mass parameters $m_{11}^{2\text{tree}}$ and $m_{22}^{2\text{tree}}$ in a way that the standard vacuum arises at $v = 246 \text{ GeV}$ and expand the Higgs fields around that minimum:

$$h_u^0 = \frac{1}{\sqrt{2}} (v_u + \varphi_u + i\chi_u), \quad h_d^0 = \frac{1}{\sqrt{2}} (v_d + \varphi_d + i\chi_d). \quad (4.67)$$

The minimization conditions have to include the derivative of the one-loop potential as one-loop extension of Eq. (2.33)

$$m_{11}^{2\text{tree}} = m_{12}^{2\text{tree}} \tan \beta - \frac{v^2}{2} \cos 2\beta \lambda_1^{\text{tree}} - \frac{1}{v \cos \beta} \frac{\delta}{\delta \varphi_d} V_1 \Big|_{\substack{\varphi_{u,d} \rightarrow 0 \\ \chi_{u,d} \rightarrow 0}}, \quad (4.68a)$$

$$m_{22}^{2\text{tree}} = m_{12}^{2\text{tree}} \cot \beta + \frac{v^2}{2} \cos 2\beta \lambda_2^{\text{tree}} - \frac{1}{v \sin \beta} \frac{\delta}{\delta \varphi_u} V_1 \Big|_{\substack{\varphi_{u,d} \rightarrow 0 \\ \chi_{u,d} \rightarrow 0}}. \quad (4.68b)$$

Out of the potential, we obtain the mass matrices for the real (scalar) and imaginary (pseudoscalar) components of the Higgs field

$$\mathcal{M}_{\text{re},ij}^2 = \frac{\delta^2 V}{\delta \varphi_i \delta \varphi_j} \Big|_{\substack{\varphi_{u,d} \rightarrow 0 \\ \chi_{u,d} \rightarrow 0}}, \quad \mathcal{M}_{\text{im},ij}^2 = \frac{\delta^2 V}{\delta \chi_i \delta \chi_j} \Big|_{\substack{\varphi_{u,d} \rightarrow 0 \\ \chi_{u,d} \rightarrow 0}}. \quad (4.69)$$

One eigenvalue of pseudoscalar masses has to be zero which corresponds to the Goldstone mode. The one-loop effective potential determination of the light Higgs mass m_{h^0} , however, is not sufficient to deal with the present precision. We therefore decided better to calculate the mass of the lightest Higgs boson with FeynHiggs 2.10.0 [66, 74–76] in order to include the dominant two- and three-loop contributions. The connection to the effective potential is then made via the pseudoscalar mass m_{A^0} which is not so sensitive to radiative corrections but rather governed by $m_{12}^{2\text{tree}}$ that is adjusted to fit m_{A^0} from FeynHiggs. We work in the decoupling limit $m_{A^0}, m_{H^\pm}, m_{H^0} \gg m_{h^0}$. The trilinear soft breaking coupling in the stop sector A_t is used to produce the right Higgs mass $m_{h^0} \approx 125$ GeV, where A_b is of less importance and can be set to zero. It also has practically no influence on the formation of a deeper minimum, neither in h_u^0 nor in h_d^0 direction.

We evaluate the one-loop potential at the renormalization scale $Q = \tilde{M}_t$ and set again $\tilde{m}_Q = \tilde{m}_t = \tilde{m}_b = \tilde{M}_t = \tilde{M}_b \equiv \tilde{m}$ to simplify the discussion and reduce the amount of arbitrary parameters. A_t is fixed by the Higgs mass, $A_b = 0$ and μ as well as $\tan\beta$ are kept as free parameters. In Sec. 4.2.3, we use the vacuum stability criterion to constrain the parameter space in the μ - $\tan\beta$ plane. Because the scale of interest (M_{SUSY}) is close by to the electroweak scale, we also do not include the RG running and use the “unimproved” potential in our discussion. Large values of $\tan\beta$ are known to give a sizable effect on the bottom mass, where we actually have to resum the $\tan\beta$ enhanced contributions to the bottom Yukawa coupling as

$$Y_b = \frac{m_b}{v_d(1 + \Delta_b)}, \quad (4.70)$$

with $\Delta_b = \pm\alpha_s(Q = M_{\text{SUSY}}) \tan\beta / 3\pi$ in the limit of degenerate SUSY masses for the QCD contributions [312]. We are dominantly interested in the stop/sbottom contribution to the one-loop Higgs potential, so we take those particles to be rather light (~ 1 TeV) where especially the gluino is expected to be rather heavy—so Δ_b is small and does not alter the bottom Yukawa coupling much. On the other hand, Y_b still gets significantly altered taking the SUSY threshold corrections into account. While the gluino contribution decouples with large gluino mass $M_{\tilde{G}}$, the same from the higgsino does not for increasing higgsino mass. Though the higgsino part is numerically smaller, it is not negligible. Both contributions sum up together, $\Delta_b = \Delta_b^{\text{gluino}} + \Delta_b^{\text{higgsino}}$, where [312–315]

$$\Delta_b^{\text{gluino}} = \frac{2\alpha_s}{3\pi} \mu M_{\tilde{G}} \tan\beta C_0(\tilde{m}_{\tilde{b}_1}, \tilde{m}_{\tilde{b}_2}, M_{\tilde{G}}), \quad (4.71a)$$

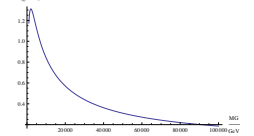
$$\Delta_b^{\text{higgsino}} = \frac{Y_t^2}{16\pi^2} \mu A_t \tan\beta C_0(\tilde{m}_{\tilde{t}_1}, \tilde{m}_{\tilde{t}_2}, \mu). \quad (4.71b)$$

There are also bino and wino contributions which we ignore due to our policy of ignoring gauge couplings in all loop contributions. As can be seen from Eq. (4.71), the bottom Yukawa coupling (4.70) gets enhanced

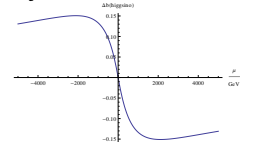
Likewise, the one-loop diagrammatic calculation gives too poor results.

The electroweak contributions from charged Higgsino-stop and Wino are important for large μA_t and μM_2 .

For illustration, we show the behavior of Δ_b^{gluino} with the gluino mass:



And the same for $\Delta_b^{\text{higgsino}}$ with μ varying from -5 TeV to $+5$ TeV (we take $\tilde{m}_{\text{soft}} = 1$ TeV and $A_t = -1.5$ TeV)



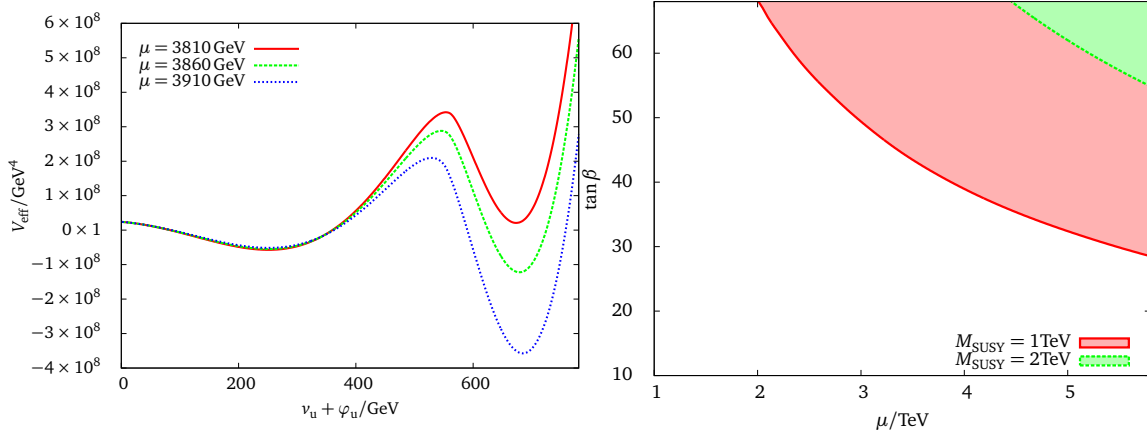


FIGURE 22: The effective potential $V_0 + V_1$ in the v_u direction develops a second minimum for suitable configurations. Especially the μ parameter of the superpotential drives the steepness of this instability. From the requirement of both vacua being degenerate, we can derive a bound in the μ - $\tan\beta$ plane for which the standard electroweak vacuum is unstable. The parameters for the plot on the left side are fixed to $\tan\beta = 40$, $M_{\text{SUSY}} = 1 \text{ TeV}$ and $m_{A^0} = 800 \text{ GeV}$ to coincide with [287]. We have taken the negative A_t -solution for the light Higgs mass (from -1416 GeV to -1468 GeV in the displayed curves) where $A_b = 0$.

for a negative sign of μ . This effect can be reverted with a negative A_t for the higgsino case.

The bottom resummation including the higgsino contribution was mistakenly ignored in [287], which is obviously wrong because it has an important effect. Moreover, in [287] the tree-level bottom Yukawa coupling was not evaluated at the SUSY scale but at the scale of the bottom mass. Compared to the bottom Yukawa coupling at the SUSY scale, it was about a factor 1.6 too large. On the other hand, including $\Delta_b^{\text{higgsino}}$, we can significantly enhance Y_b again and find the same observation of multiple vacua in roughly the same regime of μ - $\tan\beta$ —however, this only works if μ and A_t have a different sign! In such a way, we can give quite complementary constraints to what is usually obtained.

The bottom mass and therewith the Yukawa coupling is a running (\overline{MS}) parameter which is very sensitive to the scale choice.

The assignment $\text{sign}A_t = -\text{sign}\mu$ can be seen from Eqs. (4.70) and (4.71b) which enhances Y_b .

4.2.3 Constraining the Parameter Space by Vacuum Stability

The one-loop effective potential shows a strong dependence on the μ -parameter which is displayed in Fig. 22 on the left hand side. Small changes in this parameter obviously lead from a stable configuration to an unstable one. It is intriguing to figure out the “multiple point”, so the value of μ for which the two vacua are degenerate. This corresponding curve in the μ - $\tan\beta$ plane gives an exclusion contour: everything to the upper right corner is excluded by the formation of a second, deeper charge and color conserving minimum.

VACUUM DECAY Let us briefly address the question whether this at first sight unstable configuration is really instable or rather metastable in a

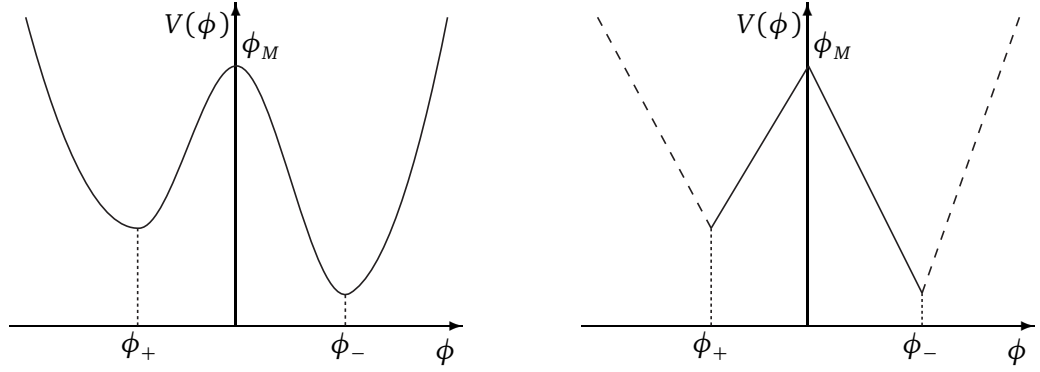


FIGURE 23: We approximate the potential barrier with a triangle according to [316]. We denote the position of the local maximum with ϕ_M and of the higher (unstable) minimum with ϕ_+ . The global minimum is at ϕ_- . Correspondingly, the values of the potential are denoted with V_M , V_+ and V_- .

cosmological sense. How large (or small) is the decay time of our vacuum at $246/\sqrt{2}$ GeV? Finding the bounce reduces to finding solutions of the bounce differential equation which can be complicated. Numerical techniques already suffer from the boundary condition “ $\phi'(0) = 0$ ” together with $\phi'(\rho)/\rho$ in the differential equation and may be cured using non-standard techniques. There is an easier-to-use possibility for an estimate on the bounce approximating the potential barrier with a triangle [316].

The decay probability per unit volume was given by $\Gamma/V = Ae^{-B/\hbar}$ (in the following we work again with $\hbar = 1$), where the coefficient A can be either estimated by $(100 \text{ GeV})^4$ or the barrier height, $\Delta V_+ = V_M - V_+$. In [316] a pocket calculator formula is given for the bounce action

$$B = \frac{2\pi^2}{3} \frac{[(\Delta\phi_+)^2 - (\Delta\phi_-)^2]^2}{\Delta V_+}. \quad (4.72)$$

We determine B using the triangle method for the potential in Fig. 22 with $\mu = 3910 \text{ GeV}$:

X	ϕ_X	$\text{Re } V_X(\phi_X)$
+	174 GeV	$-5.1 \times 10^7 \text{ GeV}^4$
M	373 GeV	$2.1 \times 10^8 \text{ GeV}^4$
-	484 GeV	$-3.6 \times 10^8 \text{ GeV}^4$

and obtain $S_E[\phi_{\text{bounce}}] \approx 18.8$ which is a ridiculously small number compared to (meta)stable vacua with $S_E \geq 400$. The decay time follows from Γ/V after multiplication with the volume of the past light-cone which is basically the age of our universe to the fourth power, T_U^4 . We have

$$\tau_{\text{vac}} = \frac{\Delta V_+}{T_U^4} e^B T_U \approx 2 \times 10^{-111} T_U.$$

If we were in such a configuration, our vacuum would immediately decay. Neighboring regions in parameter space behave the same. Especially

Note the scaling factor of $\sqrt{2}$ according to the definition in Eq. (4.67).

We define $\Delta\phi_+ = \phi_M - \phi_+$ and $\Delta\phi_- = \phi_- - \phi_M$.

Ridiculously, because we have to compare the exponents, $e^{18.8}/e^{400} \approx 3 \times 10^{-166}$.

the difference $(\Delta\phi_+)^2 - (\Delta\phi_-)^2$ is roughly the same because the second minimum is driven by the one-loop vev . For deeper second minima, B gets even more reduced because ΔV_+ increases. The transition from metastable to unstable in cosmological terms happens very rapidly as a function of μ .

CHARGE AND COLOR BREAKING GLOBAL MINIMUM Do we know what the global minimum is? In general, it is arbitrarily difficult to find the global minimum of a multivariate polynomial—in our case the function contains also logarithms. Numerical algorithms may hang up in a local minimum or overshoot the global one. However, in our special case depicted in Fig. 22, we can find out whether the deeper minimum is an impostor or not.

We have argued that the tunneling to the deeper minimum happens immediately, so the theory has to be expanded around the new vacuum. A vev of about 600 GeV influences the masses. The fermion masses are directly $\sim \langle h_u^0 \rangle$, so the top quark is just heavier. But the squark masses have a non-linear dependency on the $vevs$: while the stop mass matrix scales in the diagonal as well as the off-diagonal elements with h_u^0 , the sbottom mixing gets significantly enhanced via the $\mu Y_b h_u^0$ -term in the off-diagonal—which drives one eigenvalue negative and therewith one eigenstate tachyonic.

A negative sbottom mass squared means that the potential (its second derivative with respect to the fields, in this case the sbottom fields, gives the mass matrix) has a non-convex direction aligned with the corresponding mass eigenstate. Non-convex potentials, however, are a sign that we are expanding around a wrong point and the more global minimum is expected to lie in direction of the non-convexity. In this case, the global minimum is charge and color breaking and related to a sbottom vev $\langle \tilde{b}_1 \rangle$.

This observation is clear in regions excluded by the deeper second minimum shown in Fig. 22 and gets unclear if the smaller vev is related to the deeper minimum. To figure out whether the CCB minimum in the tachyonic sbottom direction really is deeper, so if $V(\langle \tilde{b}_1 \rangle) < V(v_u)$, needs investigation of the full scalar potential and goes beyond the scope of this thesis. One point to check remains, which are the tree-level (and “empirical” or improved) CCB constraints of [241, 242, 297]. It is easy to check that for the parameter point in use ($M_{\text{SUSY}} = 1 \text{ TeV}$, $\mu = 3910 \text{ GeV}$, $A_t = -1468 \text{ GeV}$) the CCB bounds of [242, 297] are fulfilled where the “empirical” one of [241] is violated. This conclusion about tree-level CCB minima stays unchanged compared with [287] despite of the updated numerics. We therefore assume to be safe from CCB minima of the tree-level potential without further investigation. Nevertheless, we want to stress that we get a *loop-induced* CCB minimum depending on the larger $\langle h_u^0 \rangle > v_u$ which cannot be accessed using standard tools [317, 318]. A more careful and quantitative analysis of this property and potential stronger bounds on CCB minima has to be done as a follow-up of [287].

In Chapter 3 we have discussed neutrino flavor physics in the context of supersymmetric theories, where Chapter 4 was devoted to the question of the electroweak vacuum being stable under supersymmetric quantum corrections. We have restricted ourselves in Chapter 4 to the contributions from the third generation (s)quarks because their coupling to the Higgs fields is governed by large Yukawa couplings. The instability which we found appears close to the electroweak scale and can therefore be discussed and analyzed without reference to any high scale physics.

It is well-known that the SM effective potential reveals a metastable vacuum state in the light of present data [274] where the principle scale of instability is determined by the point where the Higgs quartic coupling turns negative [283, 319, 320]. Also it is well-known that the presence of seesaw neutrinos alter the statement about stability, instability or metastability [274, 285].

In this Chapter, we shall examine the influence of heavy Majorana neutrinos to the stability discussion we deduced for the SUSY corrections. Working with neutrinos, it is an important and necessary task to confirm the stability of the low-energy theory. Furthermore, it is an interesting proof to see whether some high-scale dynamics may render the low-energy vacuum unstable. Going this way, we get information from a very high scale which will never be directly accessible by experiment.

There is, however, an issue to be treated with care. For the quark–squark one-loop contribution to the Higgs effective potential, we have identified a new vacuum arising just behind the corner at a scale where the logarithms of the one-loop potential are small anyway. This naïve estimate fails as soon as particle masses in the loop differ very much from the (fixed) renormalization scale. Already for the stability discussion of the SM effective potential evaluated for classical field values around the Planck scale, one has to resum the large logarithms by means of the renormalization group. In this approach, the renormalization scale is not taken at a fixed value (as was e. g. done in Chapter 4 where we chose $Q = M_{\text{SUSY}}$) but $Q \sim \bar{\phi}$ to improve perturbation theory and reduce the size of the logarithm $\ln(\bar{\phi}/Q)$ [267]. The several-scale approach was addressed in the literature and solved very elegantly and easy to implement with the decoupling method [284, 322] which is briefly reviewed in the following and then applied to our problem of SUSY with type I seesaw. The decoupling of heavier degrees of freedom allows us to consider at low scales only contributions from below the threshold. The scale dependence of the effective potential part stemming from those heavy fields is mild in a way,

In general, in a one-field problem one chooses $Q = M^2(\bar{\phi})$ [321], which in massive ϕ^4 -theory turns to $Q \sim \bar{\phi}$ at large values of the classical field $\bar{\phi}$.

that it only enters through the parameters in the 1-loop part and therefore is of higher order.

The issue of instability is related to large field values since the effective potential at low field values is determined basically by the SM and new physics appearing at some higher scale alters the behavior of that potential. Heavy neutrinos (and sneutrinos) start to play an important role above their masses—below, the heavy states are integrated out and the light neutrino masses are suppressed by the scale in the spirit of the see-saw mechanism. If right-handed neutrinos are well separated in mass and show a strong hierarchy as well as when we want to incorporate standard SUSY contributions from the (s)top-(s)bottom sector, the choice of M_R (or say the heaviest ν_R) as the overall scale seems unreliable because now we would introduce exactly large logarithms as $\log(M_{\text{SUSY}}/M_R)$. The choice $Q = M_R$ as universal scale choice for all renormalization scale dependent quantities is in such a case a bad choice.

A proper and efficient way to cope with different scales and deal with the decoupling of heavy particles was suggested in Ref. [284]. The effective potential contribution of fields with independent masses M_1 and M_2 can be given by

$$V_1 = \frac{1}{64\pi^2} \left[N_1 M_1^4 \log \frac{M_1^2}{Q^2} \theta_1 + N_2 M_2^4 \log \frac{M_2^2}{Q^2} \theta_2 \right], \quad (5.1)$$

where $\theta_i = \theta(Q - M_i(\bar{\phi}))$ is the step function taking care of the decoupling below M_i and the prefactors N_i account for degrees of freedom. The influence of those fields to the β -functions comes in the same way:

$$\beta_\lambda = Q \frac{d\lambda}{dQ} = \sum_i {}_i\beta_\lambda \theta_i, \quad (5.2)$$

where ${}_i\beta_\lambda$ denotes the contribution from field i to the β -function for some coupling λ .

In general, this can be generalized to an arbitrary number of heavy fields. For our purpose, however, two are enough, where one will be identified with the scale of heavy neutrinos and the other one with the SUSY scale.

The advantage of Eq. (5.1) compared to multi-scale approaches where for each heavy mass an *individual* renormalization scale is chosen [323] is the occurrence of only *one* global renormalization scale (which has to be properly adjusted) and a simple inclusion of β -functions according to Eq. (5.2). The authors of [284] argue that two arguments lead to the preferred scale $Q^* = Q = \min_i \{M_i(\bar{\phi})\}$. First, the complete potential $V = V_0 + V_1$ has to be scale independent, so $dV/dQ = 0$ (which is the reasoning behind the RG improvement). Second, they want to choose Q in such a way that the loop expansion behaves best, especially $\Delta V = V - V_1$ is small (or $V_1 = 0$). At the scale Q^* , tree-level and one-loop potential are identical and only the RG improved tree-level potential has to be evaluated with running couplings at the scale Q^* . Note that the β -functions look differently in each regime.

However, already the light neutrino mass drastically destabilizes the potential introducing a UFB-direction as pointed out in Sec. 5.1.

Decoupling is meant in a very simple sense: the corresponding part is just set to zero. Also, at the scale $Q^2 = M_i^2(\bar{\phi})$, the logarithm itself is zero, so no discontinuity is introduced in the one-loop potential at the threshold.

The improvement of the one-loop potential $V = V_0 + V_1$ needs the use of two-loop RGE, which are available for the MSSM extended with right-handed neutrinos [164, 165]. To get a basic feeling of the neutrino-neutrino influence on the Higgs effective potential, we constrain ourselves in the following to one generation of leptons.

5.1 NEUTRINOS DESTABILIZING THE EFFECTIVE POTENTIAL

Neutrinos are fermions and therefore destabilize the effective potential anyway by the negative prefactor. It is very obvious and easy to see, that already light seesaw neutrinos significantly destabilize the Higgs potential. A clear observation is that light neutrinos enter dramatically, once the classical Higgs field value is not restricted to be at the SM vacuum. If we develop the potential for large $\langle h_u^0 \rangle$, the neutrino contribution grows quadratically with the field as can be seen from the seesaw formula. Let us consider a simple type I seesaw with a Majorana mass for the right-handed neutrino, see Eq. (2.38):

$$\begin{aligned} -\mathcal{L}_m^\nu &= \frac{1}{2} (\nu_L, \nu_L^c) \mathcal{M}_\nu(h_u^0) \begin{pmatrix} \nu_L \\ \nu_L^c \end{pmatrix} + \text{h. c.} \\ &= \frac{1}{2} (\nu_L, \nu_L^c) \begin{pmatrix} 0 & Y_\nu h_u^0 \\ Y_\nu^T h_u^0 & M_R \end{pmatrix} \begin{pmatrix} \nu_L \\ \nu_L^c \end{pmatrix} + \text{h. c.} , \end{aligned} \quad (5.3)$$

using left-handed Weyl spinors, and the eigenvalues of $\mathcal{M}_\nu(h^0)$ are

$$m_{\nu_{1,2}}(h_u^0) = \frac{1}{2} \left(M_R \pm \sqrt{4(Y_\nu h_u^0)^2 + M_R^2} \right). \quad (5.4)$$

We expand in the large right-handed mass M_R and obtain the well-known seesaw formula for the light neutrino, while the other one stays heavy

$$m_{\nu_\ell}(h_u^0) \approx -\frac{(Y_\nu h_u^0)^2}{M_R}, \quad m_{\nu_h} \approx M_R. \quad (5.5)$$

Below the scale M_R , only the light fields are active and only those contribute to the effective potential. The heavy contribution is kept away with a theta function in the spirit of Eq. (5.1). We want to have a light neutrino below 1 eV, so let us take for the moment $M_R = 10^{14}$ GeV and $Y_\nu = 1$ in order to have $m_{\nu_\ell}(174 \text{ GeV}) \approx 0.3$ eV. The light neutrino Higgs effective potential is then given by

$$\begin{aligned} V_1^\nu(h_u^0) &= -\frac{1}{32\pi^2} m_{\nu_\ell}^4(h_u^0) \left(\ln \frac{m_{\nu_\ell}^2(h_u^0)}{Q^2} - \frac{3}{2} \right) \\ &= -\frac{1}{32\pi^2} \frac{(Y_\nu h_u^0)^8}{M_R^4} \left(\ln \frac{(Y_\nu h_u^0)^4}{M_R^2 Q^2} - \frac{3}{2} \right). \end{aligned} \quad (5.6)$$

There are some issues to be clarified: which renormalization scale we shall take and what to do with the RG scaling of the involved parameters. Moreover, the effective theory is not the correct description at scales

We keep the notation of the 2HDM, where one Higgs doublet couples to up-type fermions and therefore also to neutrinos, which we called H_u . Its neutral component is h_u^0 . For the discussion in this section where only one direction in scalar field space is of interest, it does not matter whether there are more fields. We also only take a look at the pure one-loop effective potential and its behavior at large field values. The tree potential can be estimated as $\lambda \langle h_u^0 \rangle^2$ in the large field regime. The question of (in)stability reduces then to the question whether $|V_1^\nu| > V_0$ at some point.

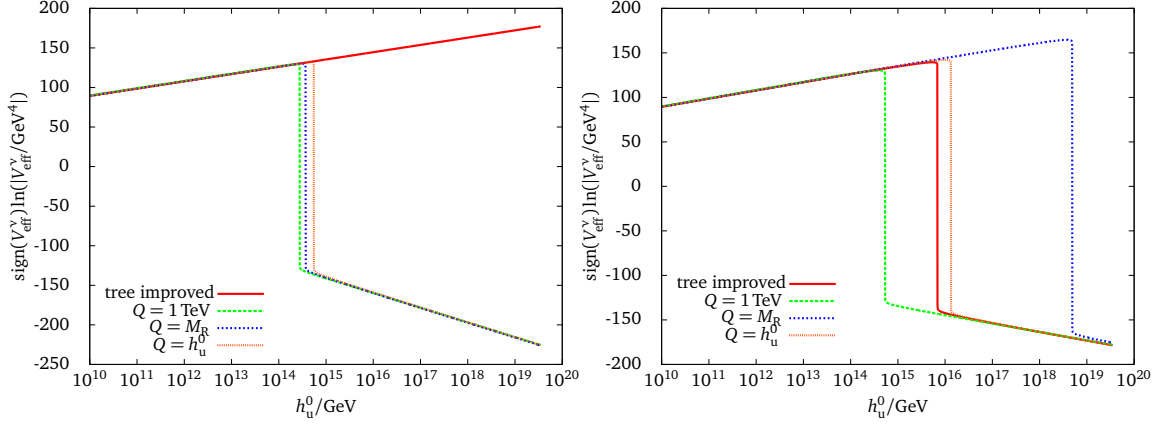


FIGURE 24: We plot the effective potential in a smart way inspired by [280], where $V_{\text{eff}}^\nu = V_0 + V_1^\nu$ and $V_0 = \lambda(h_u^0)^4$. On the left side, we only add the effective neutrino mass operator. The plot on the right side has the correct UV completion. In both plots, the red line shows the RGI tree-level potential, which on the left side is unaffected by the heavy scale because its β -function does not feel the presence of the heavy scale. On the right side, the tree-improved potential drops negative beyond the scale of right-handed neutrinos. In both cases, the one-loop potential is unbounded from below as long as no new physics at the Planck scale (or below) rescues it. The other lines show specific choices of the renormalization scale: the fixed values $Q = 1 \text{ TeV}$ (green) and $Q = M_R = 10^{14} \text{ GeV}$ (blue). In the case where the RG evolution of λ is not influenced by heavy fields, the scale choice in V_1^ν basically makes no difference and the instability scale is always at the same point with an uncertainty about one quarter order of magnitude. This changes once the running is altered: Obviously, the fixed scale choices either underestimate or overestimate the instability scale. If we take $Q = h_u^0$ (orange) as the value of the classical field, the RGI tree potential and the one-loop potential drop negative at roughly the same scale.

larger than M_R , so in any case the UV completion has to be properly considered in the stability discussion. For the latter point, we restrict ourselves to the simple type I seesaw of Eq. (5.3) where only one additional fermionic state appears at the high scale. To address the RG behavior of the one-loop effective potential (5.6), we have to take into account the self-coupling of the tree-level part. The neutrino mass operator can be written as $m_{\nu_\ell}(h_u^0) = (h_u^0)^2 \kappa$, where κ has mass dimension -1 and a certain running in the SM and MSSM [181]. Below the scale M_R we just have the β -function for κ in addition. Above, the other β -functions get altered. The relevant RGE are given in App. B.

Note that the fermionic contribution to the Higgs effective potential is always negative. So the light neutrinos as well as the heavy ones turn the potential negative at some point and the potential will be unbounded from below. We show the effective potential in some variations in Fig. 24.

We compare in Fig 24 several choices for the renormalization scale at which running parameters are evaluated—and find agreement to what was generically proposed in the literature (namely $Q \sim \bar{\phi}$). For that purpose, we discuss the tree and the one-loop potential (unfortunately only one-loop RGE are available for the Higgs self-coupling under presence of right-handed neutrinos) with running couplings evaluated at certain

The one-loop RGI potential actually has to be evaluated using two-loop RGE.

scales. The high-energy (or high field value) behavior of the effective potential is governed by the quartic coupling, so we only have $\lambda(h_u^0)^4$ as tree-level potential and therewith

$$V_{\text{eff}}(h_u^0) = V_0 + V_1^\nu \\ = \lambda(h_u^0)^4 - \frac{1}{32\pi^2} \sum_{i=1,2} m_{\nu_i}^4(h_u^0) \left(\ln \frac{m_{\nu_i}^2(h_u^0)}{Q^2} - \frac{3}{2} \right),$$

with $m_{\nu_{1,2}}(h_u^0)$ given in Eq. (5.4). First of all, we cannot take $Q = m(\bar{\phi})$ to make the logarithm vanish as usually suggested because there are two different field dependent masses in the logarithm. The closest suggestion would be to set $Q = M_R$ which, however, also produces large logarithms in the regime $h_u^0 \sim M_R$ (which grow for $h_u^0 > M_R$) and is rather a fragile choice. Similar considerations hold for a fixed but low scale, $Q = 1 \text{ TeV}$. The proper renormalization scale at which the effective potential has to be evaluated is indeed $Q \sim h_u^0$, for which the logarithms get smaller beyond M_R . In Fig. 24, we show these three choices of the renormalization scale Q in the one-loop potential with running couplings evaluated at the same scale. Additionally, we display the pure tree-level potential with a running self-coupling. When we include only the effective light neutrino mass given in Eq. (5.5) (which is obviously wrong), the RGI tree potential is unaffected by any heavy scale. If we include the effect of right-handed neutrinos in the running of λ , we already reproduce the same UFB behavior as the one-loop potential shows—and the difference from the full inclusion of V_1^ν is rather mild in the shift of the instability.

The alternative would be to take the multi-scale approach by [323] and choose different scales for both logarithms. Although the renormalization scale is an unphysical scale it gets a more physical meaning via the relation to the field strength of the classical “external” field, $Q = \bar{\phi}$.

5.2 SNEUTRINOS STABILIZING THE EFFECTIVE POTENTIAL

The one-loop effective Higgs potential in the presence of neutrinos is UFB below the Planck scale. For this main statement there is no difference if only an effective “light” neutrino Majorana mass is taken into account or a UV complete theory including heavy Majorana neutrinos. The statement may get altered if a different UV completion is considered like a type II seesaw inspired model with heavy scalars: scalars contribute to the effective potential with a positive sign where fermions always give a negative contribution.

How does the situation change when the theory is supersymmetrized? In a SUSY theory, bosonic and fermionic degrees of freedom are equal, so for exact SUSY one would expect the loop contribution of neutrino superfield components to be exactly canceled. As pointed out already before in Chapters 2 and 3, the seesaw mechanism is transferred to the sneutrino sector as well and we expect heavy sneutrinos at the scale M_R . We only consider one generation of neutrinos. A supersymmetrized version with heavy right-handed neutrinos at say $M_R = 10^{12} \text{ GeV}$ is completely stable concerning the influence of neutrinos. However, at this stage we can say nothing about stability against sneutrino vevs.

Our purpose, however, is not to survey all popular neutrino extensions of the SM but rather to check whether the simple SUSY seesaw type I discussed and exploited in Chapter 3 leads to a potentially unstable electroweak scale vacuum.

In the following, we show the neutrino-sneutrino effective potential, where the analytic calculation can be very easily done and deduce its stability below the scale of right-handed neutrinos. The results are eventually not surprising: what we shall see is that the large separation of scales (M_{SUSY} vs. M_{R}) makes any negative fermionic contribution to the effective potential vanish, because SUSY is more or less unbroken at the high scale and the splitting in the mass spectrum of $\mathcal{O}(M_{\text{SUSY}})$ is a small perturbation which actually plays no role compared to the large amplitude of the Higgs field, we are interested in.

We set the stage with the following superpotential (we omit flavor indices and explicitly work with only one generation)

$$\mathcal{W} \supset \mu H_{\text{d}} \cdot H_{\text{u}} + Y^{\nu} H_{\text{u}} \cdot L_{\text{L}} N_{\text{R}} - Y^{\ell} H_{\text{d}} \cdot L_{\text{L}} E_{\text{R}} + \frac{1}{2} M^{\text{R}} N_{\text{R}} N_{\text{R}}, \quad (5.7)$$

from which the sneutrino mass terms can be calculated as the bilinears in the F -terms (see Sec. 2.2):

$$V_{\text{F}}(\phi, \phi^*) = \frac{\partial \mathcal{W}^{\dagger}}{\partial \phi^*} \left| \frac{\partial \mathcal{W}}{\partial \phi} \right|, \quad (5.8)$$

where ϕ is the scalar component of a chiral supermultiplet. The Higgs and lepton superfields were already introduced in Sec. 2.4.

In the exact SUSY limit, the mass terms of the scalar neutrinos are determined by Eq. (5.8). However, since SUSY is broken, we introduce the common soft SUSY breaking Lagrangian for one generation of sneutrinos:

$$V_{\text{soft}}^{\tilde{\nu}} = (\tilde{m}_{\text{L}}^2) \tilde{\nu}_{\text{L}}^* \tilde{\nu}_{\text{L}} + (\tilde{m}_{\text{R}}^2) \tilde{\nu}_{\text{R}}^* \tilde{\nu}_{\text{R}} + (A^{\nu} h_{\text{u}}^0 \tilde{\nu}_{\text{L}} \tilde{\nu}_{\text{R}}^* + B_{\nu}^2 \tilde{\nu}_{\text{R}}^* \tilde{\nu}_{\text{R}}^* + \text{h. c.}). \quad (5.9)$$

The mass matrix can then be written in a four-dimensional basis:

$$-\mathcal{L}_{\text{m}}^{\tilde{\nu}} = \frac{1}{2} (\tilde{\nu}_{\text{L}}^*, \tilde{\nu}_{\text{L}}, \tilde{\nu}_{\text{R}}, \tilde{\nu}_{\text{R}}^*) \begin{pmatrix} \mathcal{M}_{\text{LL}}^2 & \mathcal{M}_{\text{LR}}^2 \\ (\mathcal{M}_{\text{LR}}^2)^* & \mathcal{M}_{\text{RR}}^2 \end{pmatrix} \begin{pmatrix} \tilde{\nu}_{\text{L}} \\ \tilde{\nu}_{\text{L}}^* \\ \tilde{\nu}_{\text{R}} \\ \tilde{\nu}_{\text{R}}^* \end{pmatrix},$$

where the 2×2 Higgs field dependent sub-matrices are given by

$$\mathcal{M}_{\text{LL}}^2 = \begin{pmatrix} \tilde{m}_{\text{L}}^2 + |Y_{\nu} h_{\text{u}}^0|^2 & 0 \\ 0 & (\tilde{m}_{\text{L}}^2)^* + |Y_{\nu} h_{\text{u}}^0|^2 \end{pmatrix}, \quad (5.10\text{a})$$

$$\mathcal{M}_{\text{LR}}^2 = \begin{pmatrix} h_{\text{u}}^{0*} Y_{\nu}^* M_{\text{R}} & h_{\text{u}}^{0*} A_{\nu}^* - \mu^* h_{\text{d}}^{0*} \\ h_{\text{u}}^0 A_{\nu} - \mu h_{\text{d}}^0 & h_{\text{u}}^0 Y_{\nu} M_{\text{R}}^* \end{pmatrix}, \quad (5.10\text{b})$$

$$\mathcal{M}_{\text{RR}}^2 = \begin{pmatrix} \tilde{m}_{\text{R}}^2 + |Y_{\nu} h_{\text{u}}^0|^2 + |M_{\text{R}}|^2 & 2(B^2)^* \\ 2B^2 & (\tilde{m}_{\text{R}}^2)^* + |Y_{\nu} h_{\text{u}}^0|^2 + |M_{\text{R}}|^2 \end{pmatrix}. \quad (5.10\text{c})$$

Note that we neglected D -term contributions $\sim M_{\text{Z}}^2$ proportional to gauge couplings. In the following we will restrict ourselves to the one-family

case and also keep the B_ν^2 parameter out of the discussion for convenience. Nevertheless, its presence does neither change the RGE for M_R nor does it directly contribute to the Higgs potential. It may be of interest once we are interested in sneutrino ν evs at a high scale which is not our purpose at the moment.

For a real mass matrix in the limit $h_d^0 = 0$, the four mass eigenvalues can be directly calculated

$$m_{\tilde{\nu}_{1,\dots,4}}^2(h_2^0) = \frac{1}{2} \left[M_R^2 + 2M_\xi^2 + 2Y_\nu^2|h_2^0|^2 \pm \sqrt{M_R^4 + 4|h_2^0|^2 (A_\nu \pm M_R Y_\nu)^2} \right], \quad (5.11)$$

assuming left and right soft masses being equal: $M_\xi^2 = m_L^2 = m_R^2$.

In the following discussion, we also ignore the trilinear coupling A_ν which is relatively suppressed by $1/M_R^2$ as can be seen from Eq. (5.11). Assuming all SUSY-breaking parameters being $\mathcal{O}(M_\xi)$, A_ν would only become important if it was $\mathcal{O}(M_R)$.

The field dependent masses can be nicely written down in a way to estimate their importance compared to M_R using $\varepsilon = 4Y_\nu^2|h_2^0|^2/M_R^2$ as

$$m_{\nu_{1,2}} = \frac{M_R}{2} \left(1 \pm \sqrt{1 + \varepsilon} \right), \quad (5.12a)$$

$$m_{\tilde{\nu}_{1,\dots,4}}^2 = \frac{M_R^2}{2} \left(1 + \frac{2M_\xi^2}{M_R^2} + \frac{\varepsilon}{2} \pm \sqrt{1 + \varepsilon} \right). \quad (5.12b)$$

We interpret M_R and Y_ν as running parameters evaluated at some scale Q , where we take $Q = h_u^0$. The fermionic contribution to the effective potential gets a factor two due to the spin degrees of freedom. In our approximation, however, also $m_{\tilde{\nu}_1} = m_{\tilde{\nu}_2}$ and $m_{\tilde{\nu}_3} = m_{\tilde{\nu}_4}$ and therefore the individual sneutrino contributions can be seen as one light and one heavy—garnished with a factor of two. So in the SUSY limit ($M_\xi \rightarrow 0$) both contributions indeed exactly cancel. With our knowledge of the multi-scale treatment of the effective potential, we state

$$V_1^{\nu,\tilde{\nu}} = \frac{1}{32\pi^2} \left[-m_{\nu_1}^4 \left(\log(m_{\nu_1}^2 / (h_u^0)^2) - 3/2 \right) - m_{\nu_2}^4 \left(\log(m_{\nu_2}^2 / (h_u^0)^2) - 3/2 \right) \theta(h_u^0 - M_R) + m_{\tilde{\nu}_1}^4 \left(\log(m_{\tilde{\nu}_1}^2 / (h_u^0)^2) - 3/2 \right) \theta(h_u^0 - M_\xi) + m_{\tilde{\nu}_3}^4 \left(\log(m_{\tilde{\nu}_3}^2 / (h_u^0)^2) - 3/2 \right) \theta(h_u^0 - M_R) \right]. \quad (5.13)$$

Approximately, $m_{\nu_2} \approx m_{\tilde{\nu}_3} \approx M_R$ and an extension to three degenerate (s)neutrinos can be made via multiplication with three. Eq. (5.13) does not contain a cosmological constant term because $m_{\nu_1}(h_u^0)$ vanishes for $h_u^0 \rightarrow 0$ and the other contributions are cut away from zero with the θ -

The $h_d^0 = 0$ scenario leaves the μ -term out of the discussion.

We are counting from light (1) to heavy (2 or 4).

For simplicity, we use a fixed step in the θ -functions with either M_ξ or M_R . And ignore the discontinuities by thresholds in the following discussion anyway, where we are only interested in the behavior of the full one-loop effective potential above the heavy neutrino threshold.

function. The analytic expression for the one-loop effective potential follows from Eqs. (5.12a):

$$\begin{aligned}
V_1^{y,\bar{y}} = & \frac{M_R^4}{128\pi^2} \left\{ \theta(h_u^0 - M_R) \left(1 + \frac{2M_S^2}{M_R^2} + \frac{\varepsilon}{2} + \sqrt{1+\varepsilon} \right)^2 \times \right. \\
& \left[\ln \left(1 + \frac{2M_S^2}{M_R^2} + \frac{\varepsilon}{2} + \sqrt{1+\varepsilon} \right) + \ln \left(\frac{M_R^2}{2(h_u^0)^2} \right) - \frac{3}{2} \right] \\
& + \theta(h_u^0 - M_S) \left(1 + \frac{2M_S^2}{M_R^2} + \frac{\varepsilon}{2} - \sqrt{1+\varepsilon} \right)^2 \times \\
& \left[\ln \left(1 + \frac{2M_S^2}{M_R^2} + \frac{\varepsilon}{2} - \sqrt{1+\varepsilon} \right) + \ln \left(\frac{M_R^2}{2(h_u^0)^2} \right) - \frac{3}{2} \right] \\
& - \frac{1}{4} \theta(h_u^0 - M_R) \left(1 + \sqrt{1+\varepsilon} \right)^4 \times \\
& \left[\ln \left[\left(1 + \sqrt{1+\varepsilon} \right)^2 \right] + \ln \left(\frac{M_R^2}{4(h_u^0)^2} \right) - \frac{3}{2} \right] \\
& \left. - \frac{1}{4} \left(1 - \sqrt{1+\varepsilon} \right)^4 \left[\ln \left[\left(1 - \sqrt{1+\varepsilon} \right)^2 \right] + \ln \left(\frac{M_R^2}{4(h_u^0)^2} \right) - \frac{3}{2} \right] \right\}. \tag{5.14}
\end{aligned}$$

For the discussion around the scale of right-handed neutrinos, we take $Q^2 = M_R^2$: Eq. (5.14) suggests this scale choice since the only large logarithms like $\ln(M_S^2/M_R^2)$ appear in the ‘‘cosmological constant’’ piece which is not present anyway because cut away by the θ -functions. We expand in $\varepsilon = 4Y_\nu^2|h_u^0|^2/M_R^2$ to figure out the dominant behavior below the scale M_R —and find positive coefficients:

Also the potentially large logarithm $\ln(M_S^2/M_R^2)$ in the ε^2 part is suppressed by the small prefactor M_S^2/M_R^2 .

$$\begin{aligned}
\frac{32\pi^2}{M_R^4} V_1^{y,\bar{y}} = & \varepsilon \left[\left(1 + \frac{M_S^2}{M_R^2} \right) \ln \left(1 + \frac{M_S^2}{M_R^2} \right) - \frac{M_S^2}{M_R^2} \right] + \\
& \frac{\varepsilon^2}{8} \left[\left(1 - \frac{M_S^2}{M_R^2} \right) \ln \left(1 + \frac{M_S^2}{M_R^2} \right) + \frac{M_S^2}{M_R^2} \ln \left(\frac{M_S^2}{M_R^2} \right) \right] \tag{5.15} \\
& + \mathcal{O}(\varepsilon^3).
\end{aligned}$$

Beyond $h_u^0 = M_R$ or $\varepsilon = 1$, the expansion in ε breaks down and only the complete sum gives the appropriate result. Anyhow we do not need the expansion beyond: the potential is not driven into an instability before the heavy states enter the game and it shall not beyond. As stated before, we add and subtract basically the same and the one-loop potential is indeed given by the RGI tree-level potential. The running of the gauge couplings is not altered by the heavy Majorana neutrinos as was the running of the Higgs self-coupling in the non-SUSY theory of Sec. 5.1. We even cannot show any propaganda plot, because there is no propaganda to show.

5.3 ABSOLUTE STABILITY?

The outcome of the preceding section is not overwhelming and even not surprising. However, we can state that a supersymmetrized version of a UV extension with SUSY broken at the TeV scale or any scale well below the scale of new physics is stable against further vacua in the SM v_{ev} direction. As we stated above, we cannot say anything about sneutrino v_{ev} s at the moment, especially when all the soft breaking A - and B -terms are taken into account. We dare to generalize our findings from type I seesaw with Majorana neutrinos to any not yet thought of theory. As long as SUSY is broken at a much smaller scale, the contributions to the effective potential at higher scales are canceled.

Without knowledge of high-scale physics, especially without knowledge of any quantum-gravitational interaction around the Planck scale, there is no statement about absolute stability of the effective potential and the electroweak vacuum possible as was pointed out in [282]. However, an exact supersymmetric theory does not introduce *further* instabilities. Moreover, the running of the Higgs quartic is determined by the running of the gauge couplings (squared) which never run negative. We therefore conclude that any SUSY theory is expected to be stable beyond the Planck scale with respect to SM-like minima. Even softly broken SUSY is approximately exact up there and therefore no such second minimum at a high scale as in the SM [274] shows up. The dynamics of the electroweak vacuum at the electroweak scale is then only determined by SUSY scale physics.

The inclusion of the full scalar potential in the (ν) MSSM respecting all possible sfermion v_{ev} s is beyond the scope of the present discussion.

The authors of [282] state that any higher-dimensional operator (of dimension six, eight) suppressed with the Planck mass changes the behavior below the Planck scale.

SUMMARY OF CHAPTERS 4 AND 5 We have explicitly recalculated the one-loop effective Higgs potential in the presence of third-generation squarks and have found the formation of a minimum at one-loop order in Chapter 4. In the combination of tree-level and one-loop potentials, the loop induced minimum may appear deeper than the standard minimum in the direction of one neutral Higgs component (we showed results in the h_u^0 -direction). The new minimum, however, gives tachyonic sbottom masses which indicate a global charge and color breaking minimum with $\langle \bar{b} \rangle \neq 0$. From the requirement of both minima being degenerate, we can formulate an exclusion limit on the parameters of the theory and we have explicitly shown such limits in the μ - $\tan\beta$ plane. Heavier SUSY masses shift the limit to larger values of both μ and $\tan\beta$. The influence of $\tan\beta$ resummation on the bottom Yukawa coupling leads to the requirement $\text{sign}A_t = -\text{sign}\mu$ on the relative signs of A_t and μ to produce this observation. We are therefore quite complementary to existing bounds on these parameters from vacuum stability.

The same calculation of the effective potential in presence of (heavy) neutrinos and sneutrinos has shown that no further instability is introduced in the SUSY theory. The non-SUSY description of neutrino masses (the effective theory as well as the UV completion with right-handed Majorana neutrinos) instead results in an effective potential which is unbounded from below up to the Planck scale. The SUSY version in contrast is well bounded from below.

Be content with what you have; rejoice in the way things are. When you realize there is nothing lacking, the whole world belongs to you.

—Laozi

An amazing amount of work was put into a deeper understanding of our three matter families, their mixing and why their masses are so different [324–367, we for sure only refer to a small fraction of papers dealing with that topic]. In this concluding chapter, we shall address a minimalistic approach slightly orthogonal to what was discussed in Chapter 3: how much do we need to know about mass matrices and how many assumptions do we need to impose in order to get a viable description of flavor mixing. The results of this chapter have been published in [205].

The gauge structure of the SM defines the largest global flavor symmetry which is allowed reflecting the remaining symmetry if Yukawa couplings are switched off: $[U(3)]^5$. There is one $U(3)$ -factor for each gauge representation; taking right-handed (singlet) neutrinos into account, we have

$$[U(3)]^6 = U(3)_Q \times U(3)_u \times U(3)_d \times U(3)_L \times U(3)_e \times U(3)_\nu.$$

The Yukawa couplings, which break this maximal flavor symmetry group, are strongly hierarchical and differ over several orders of magnitude

$$\begin{aligned} \hat{Y}_u : \hat{Y}_c : \hat{Y}_t &\approx 10^{-6} : 10^{-3} : 1, & \hat{Y}_d : \hat{Y}_s : \hat{Y}_b &\approx 10^{-4} : 10^{-2} : 1, \\ \hat{Y}_e : \hat{Y}_\mu : \hat{Y}_\tau &\approx 10^{-4} : 10^{-2} : 1. \end{aligned}$$

The smallness of the first and second generation Yukawa couplings allows to impose a smaller symmetry group, $[U(2)]^6$, whereas only first generation vanishing Yukawas lead to $[U(1)]^6$. We propose a *minimal breaking of maximal flavor symmetry* by the following symmetry breaking chain:

$$U(3) \xrightarrow{\Lambda_3} U(2) \xrightarrow{\Lambda_2} U(1) \xrightarrow{\Lambda_1} \text{nothing}. \quad (6.1)$$

The scales Λ_i at which the symmetry breaking occurs may be largely separated: $\Lambda_3 \gg \Lambda_2 \gg \Lambda_1$ similar to the hierarchy of Yukawa couplings $\hat{Y}_3 \gg \hat{Y}_2 \gg \hat{Y}_1$ for third, second and first generation.

We remark the similarity to radiative mass and flavor models briefly discussed in Sec. 2.2.3. On our approach, however, we try to be as model-independent as possible and only require Eq. (6.1) happening simultaneously in the up and the down sector (i. e. $\Lambda_i^u = \Lambda_i^d = \Lambda_i^Q$).

The principle of minimal flavor violation relying on $U(3)$ and $U(2)$ symmetries and discrete subgroups was applied in many aspects of flavor phenomenology e. g. in [89, 104, 346, 366, 368–383]

The application e. g. of RFV techniques may be even simplified with the procedure presented here.

In the gaugeless limit, we observe $U(45)$ or $U(48)$, see Sec. 2.1.1.

Fermion masses are directly proportional to Yukawa couplings, $m_x = vY_x / \sqrt{2}$.

We omit obvious trivial $U(1)$ factors that are left: also in the SM with all Yukawa couplings non-vanishing, there are still accidental symmetries known as baryon and lepton number.

6.1 HIERARCHICAL MASS MATRICES

The hierarchy of fermion masses following from the minimal breaking of maximal flavor symmetry allows us to reversely approximate fermion mass matrices by matrices of lower rank [384–387]. The matrix rank gives the number of linearly independent columns or rows of a matrix. A generic three-generation mass matrix has rank = 3, a U(2)-symmetric mass matrix only rank = 1. We decompose the generic mass matrix \mathbf{m}^f by its *singular value decomposition* as of Eq. (2.7) with left- and right-singular matrices \mathbf{S}_L^f and \mathbf{S}_R^f , respectively, that are build up of their singular vectors

$$\mathbf{S}_L^f = \left[\vec{s}_{L,1}^f, \vec{s}_{L,2}^f, \vec{s}_{L,3}^f \right], \quad \left(\mathbf{S}_R^f \right)^\dagger = \left[\vec{s}_{R,1}^{f\dagger}, \vec{s}_{R,2}^{f\dagger}, \vec{s}_{R,3}^{f\dagger} \right],$$

and find the diagonal matrix $\hat{\mathbf{m}}^f$

$$\hat{\mathbf{m}}^f = \left[\left(\vec{s}_{L,1}^f \frac{m_1^f}{m_2^f} \vec{s}_{R,1}^{f\dagger} + \vec{s}_{L,2}^f \vec{s}_{R,2}^{f\dagger} \right) \frac{m_2^f}{m_3^f} + \vec{s}_{L,3}^f \vec{s}_{R,3}^{f\dagger} \right] m_3^f, \quad (6.2)$$

with the singular values m_i^f that obey $m_3^f > m_2^f > m_1^f \geq 0$.

We now see that with a realistic fermion mass spectrum, $m_3^f \gg m_2^f \gg m_1^f$, the mass ratios in Eq. (6.2) are small, and we get a rank-one approximation by neglecting both m_2^f/m_3^f and m_1^f/m_2^f

$$\check{\mathbf{m}}_{r=1}^f = \vec{s}_{L,3}^f \vec{s}_{R,3}^{f\dagger} = \begin{pmatrix} 0 & 0 & 0 \\ 0 & 0 & 0 \\ 0 & 0 & 1 \end{pmatrix}, \quad (6.3)$$

where we divided by the largest mass m_3^f . We keep the notation $\check{}$ for normalization with respect to m_3^f . Correspondingly, neglecting only \check{m}_1^f , we find the rank-two approximation which has a potentially arbitrary 2×2 sub-matrix left reverting the singular value decomposition:

$$\check{\mathbf{m}}_{r=2}^f = \vec{s}_{L,2}^f \check{m}_2^f \vec{s}_{R,3}^{f\dagger} + \vec{s}_{L,3}^f \vec{s}_{R,3}^{f\dagger} = \begin{pmatrix} 0 & 0 & 0 \\ 0 & \check{m}_{22}^f & \check{m}_{23}^f \\ 0 & \check{m}_{32}^f & \check{m}_{33}^f \end{pmatrix}. \quad (6.4)$$

A closer look at the 2-3 block of Eq. (6.4) shows a hierarchy in its elements

$$|\check{m}_{33}^f|^2 \gg |\check{m}_{23}^f|^2, |\check{m}_{32}^f|^2 \gg |\check{m}_{22}^f|^2.$$

Confining ourselves only to an order-of-magnitude discussion, we neglect all contributions $\mathcal{O}(\check{m}_{22}^f) = \mathcal{O}(|\check{m}_{23}^f|^2)$ and work with the approximation $\check{m}_{22}^f = 0$ which does not alter the result for the mixing angle to leading order, see Appendix C of [205]. Moreover, the off-diagonals can be constrained as $|\check{m}_{23}^f| = |\check{m}_{32}^f|$, leading to the requirement for the mass matrix

The lower-rank approximation theorem is known as Eckart–Young–Mirsky or simply Eckart–Young theorem, though it is better to call it Schmidt–Mirsky theorem [388].

Singular values of mass matrices correspond to the physical fermion masses. Each vector of left- and right-handed fermions is rotated with the left- and right-singular matrix into the mass eigenbasis.

Eq. (6.3) is a rank-one matrix, labeled with $r=1$.

Inversion of Eq. (2.7), $\hat{\mathbf{m}} = \mathbf{S}_L \mathbf{m} \mathbf{S}_R^\dagger$, gives $\mathbf{m} = \mathbf{S}_R^\dagger \hat{\mathbf{m}} \mathbf{S}_R$.

to be normal. Only the phases are unconstrained, so we impose for the 2×2 submatrix

$$\check{m}^f = \begin{pmatrix} 0 & |\check{m}_{23}^f| e^{i\delta_{23}^f} \\ |\check{m}_{32}^f| e^{i\delta_{32}^f} & \check{m}_{33}^f \end{pmatrix}. \quad (6.5)$$

We then reparametrize the mixing matrix (i. e. the left-singular matrix—right-singular matrices are unobservable in weak charged current interactions) via the two invariants of the Hermitian product $\mathbf{n}^f = \mathbf{m}^f \mathbf{m}^{f\dagger}$,

$$\begin{aligned} \text{Tr } \mathbf{n}^f &= m_2^{f2} + m_3^{f2} = 2|m_{23}^f|^2 + |m_{33}^f|^2, \\ \det \mathbf{n}^f &= m_2^{f2} m_3^{f2} = |m_{23}^f|^4, \end{aligned}$$

and find

$$|\check{m}_{23}^f| = \sqrt{\check{m}_2^f}, \quad \text{and} \quad |\check{m}_{33}^f| = 1 - \check{m}_2^f. \quad (6.6)$$

The mixing angle is found to be $\tan \theta_{23}^f = \sqrt{\check{m}_{23}^f} = \sqrt{m_2^f/m_3^f}$, and the rotation matrix can be expressed in terms of this angle and one complex phase (other phases are unphysical and can be rotated away)

$$\mathbf{s}_{23}^{L,f}(\check{m}_2^f, \delta_{23}^f) = \frac{1}{\sqrt{1 + \check{m}_2^f}} \begin{pmatrix} 1 & e^{-i\delta_{23}^f} \sqrt{\check{m}_2^f} \\ -e^{i\delta_{23}^f} \sqrt{\check{m}_2^f} & 1 \end{pmatrix}. \quad (6.7)$$

With Eq. (6.7), we have the left-singular matrix for an f -type fermion. The weak mixing matrix is composed out of up- and down-type mixing, $\mathbf{V}_{23} = \mathbf{s}_{23}^{L,u} (\mathbf{s}_{23}^{L,d})^\dagger$. For the two-generation case we have

$$\mathbf{V}_{23} = \text{diag} \left(1, e^{-i\delta_{23}^u} \right) \begin{pmatrix} \sqrt{1 - \zeta^2} e^{-i\delta_0} & \zeta e^{-i\delta} \\ -\zeta e^{i\delta} & \sqrt{1 - \zeta^2} e^{i\delta_0} \end{pmatrix} \text{diag} \left(1, e^{i\delta_{23}^d} \right). \quad (6.8)$$

The phase δ_{23}^u factored out can be absorbed in a global rephasing of third generation quarks. We keep the phases δ and δ_0 to analyze their origin and to keep track of the phases of the individual rotations, so δ_{23}^u and δ_{23}^d for later purpose. The parameters of Eq. (6.8) are found to be

$$\zeta = \sin \theta_{23} = \sqrt{\frac{\check{m}_2^u + \check{m}_2^d - 2\sqrt{\check{m}_2^u \check{m}_2^d} \cos(\delta_{23}^u - \delta_{23}^d)}{(1 + \check{m}_2^u)(1 + \check{m}_2^d)}}, \quad (6.9a)$$

$$\tan \delta = \frac{\check{m}_2^d \sin(\delta_{23}^u - \delta_{23}^d)}{\check{m}_2^u - \check{m}_2^d \cos(\delta_{23}^u - \delta_{23}^d)}, \quad (6.9b)$$

$$\tan \delta_0 = \frac{\check{m}_2^u \check{m}_2^d \sin(\delta_{23}^u - \delta_{23}^d)}{1 + \check{m}_2^u \check{m}_2^d \cos(\delta_{23}^u - \delta_{23}^d)}. \quad (6.9c)$$

Expanding in the small mass ratios \check{m}_2^f we may obtain $\tan \delta_0 \approx 0$ and $\tan \delta \approx -\tan(\delta_{23}^u - \delta_{23}^d)$.

A normal matrix obeys $\mathbf{m} \mathbf{m}^\dagger = \mathbf{m}^\dagger \mathbf{m}$.

See [333, 335, 345, 357].

This can be seen from Eq. (2.9) with $\mathbf{S}_L^u = \mathbf{S}_L^Q$ and $\mathbf{S}_L^d = (\mathbf{S}_L^Q)^\dagger \mathbf{v}^\dagger$.

It is important to note, that two unitary mixing matrices do not commute as real orthogonal 2×2 matrices do, and the new mixing angle is not just $\theta_{23} = \theta_{23}^u \pm \theta_{23}^d$ as well as the phase $\delta \neq \delta_{23}^u \pm \delta_{23}^d$.

6.2 FULL HIERARCHY AND THE NEED FOR CORRECTIONS

We construct the full hierarchy and full-rank picture following the consecutive breakdown of $U(3)$ symmetries. The two-generation description from Sec. 6.1 can be easily generalized to two-flavor mixings within three generations by filling up 3×3 matrices with zeros where appropriate. In view of minimal flavor symmetry breaking, the 2-3 mixing acts “first” on the mass matrix. Therefore,

Each individual rotation is given by

$$\mathbf{S}(\theta, \delta) = \begin{pmatrix} c_\theta & s_\theta e^{-i\delta} \\ -s_\theta e^{i\delta} & c_\theta \end{pmatrix}. \quad \mathbf{S}_L^f = \mathbf{S}_{12}^{L,f}(\theta_{12}^f, \delta_{12}^f) \mathbf{S}_{13}^{L,f}(\theta_{13}^f, \delta_{13}^f) \mathbf{S}_{23}^{L,f}(\theta_{23}^f, \delta_{23}^f). \quad (6.10)$$

The weak mixing matrices are then combined as

$$\mathbf{V}_{\text{CKM}} = \mathbf{S}_{12}^{L,u} \mathbf{S}_{13}^{L,u} \mathbf{S}_{23}^{L,u} (\mathbf{S}_{23}^{L,d})^\dagger (\mathbf{S}_{13}^{L,d})^\dagger (\mathbf{S}_{12}^{L,d})^\dagger, \quad \text{and}$$

$$\mathbf{U}_{\text{CKM}} = \mathbf{S}_{12}^{L,e} \mathbf{S}_{13}^{L,e} \mathbf{S}_{23}^{L,e} (\mathbf{S}_{23}^{L,\nu})^\dagger (\mathbf{S}_{13}^{L,\nu})^\dagger (\mathbf{S}_{12}^{L,\nu})^\dagger.$$

Building up the mixing matrices from lower-rank approximated mass matrices, we have to take care of all equally large contributions. The leading order 2-3 rotation $\mathbf{S}_{23}^{(0)}$ diagonalizes the Hermitian product of a hierarchical mass matrix of type (6.4)

We have to keep in mind, that the object of interest is $\mathbf{m}\mathbf{m}^\dagger$.

$$\begin{pmatrix} 0 & 0 & 0 \\ 0 & X^2 & X \\ 0 & X & 1-X^2 \end{pmatrix} \xrightarrow{\mathbf{S}_{23}^{(0)}} \begin{pmatrix} 0 & 0 & 0 \\ 0 & 0 & 0 \\ 0 & 0 & 1 \end{pmatrix} + \mathcal{O}(X^3),$$

Comparing the masses, we conclude that $\mathcal{O}(\sqrt{\check{m}_1^f}) = X^2$.

where X is $\mathcal{O}(\sqrt{\check{m}_2^f})$. Now, the transition to the full-rank matrix comes along with new contributions $\mathcal{O}(\sqrt{\check{m}_1^f})$ everywhere: in general, the lower-rank approximated matrix differs in all elements from the higher-rank one,

$$\begin{pmatrix} * & * & * \\ * & * & * \\ * & * & 1 \end{pmatrix} \quad \text{with} \quad * = \mathcal{O}(\sqrt{\check{m}_1^f}).$$

The inclusion of the smallest mass leads also to nonzero matrix elements where previously neglected $\sim X^3$ terms were present. For a reasonable description of the mixing matrices including all missing pieces already in the 2-3 rotation, $\mathcal{O}(\sqrt{\check{m}_1^f}) \sim X^2$ as well as $\mathcal{O}(\check{m}_1^f \check{m}_2^f) \sim X^3$. We include those “corrections” by correcting rotations like the composition

The description can also be applied to the 1-3 mixing with $\check{m}_2^f \rightarrow \check{m}_1^f$ and $\check{\varepsilon} = (\check{m}_2^f)^2$.

$$\mathbf{S}_{23}^{L,f(1)} = \mathbf{S}_{23}^{L,f}(\pm\check{\varepsilon}) \mathbf{S}_{23}^{L,f}(\check{m}_2^f) = \begin{pmatrix} \cos \theta_{23}^{f,(1)} & \sin \theta_{23}^{f,(1)} \\ -\sin \theta_{23}^{f,(1)} & \cos \theta_{23}^{f,(1)} \end{pmatrix},$$

where the composed rotation angle is with $\check{\varepsilon} = \check{m}_1^f, \check{m}_1^f \check{m}_2^f$

$$\sin \theta_{23}^{f,(1)} = \frac{\sqrt{\check{m}_2^f} \pm \sqrt{\check{\varepsilon}}}{(1 + \check{m}_2^f)(1 + \check{\varepsilon})}.$$

For small ε the mixing angle only changes slightly, as expected for a perturbation. This procedure appears to be equivalent to the adding of a much more complicated term in the leading order mass matrix:

$$-\sqrt{\varepsilon} \left[1 + \left(\check{m}_2^f \right)^2 - 2\check{m}_2^f + \sqrt{\varepsilon \check{m}_2^f} \left(\check{m}_2^f - 1 \right) \right] (1 - \varepsilon).$$

Collecting all corrections, we then find

$$\mathbf{S}_{23}^{\text{L},f(2)} = \mathbf{S}_{23}^{\text{L},f} \left(\check{m}_1^f \check{m}_2^f \right) \mathbf{S}_{23}^{\text{L},f} \left(\check{m}_1^f \right) \mathbf{S}_{23}^{\text{L},f} \left(\check{m}_2^f \right). \quad (6.11a)$$

A similar discussion now holds for the succeeding 1-3 rotation, where $\mathcal{O} \left(\check{m}_1^f \right) = \mathcal{O} \left((\check{m}_2^f)^2 \right)$ and the $\mathcal{O} \left(\check{m}_1^f \check{m}_2^f \right)$ rotation has also to be included:

$$\mathbf{S}_{13}^{\text{L},f(2)} = \mathbf{S}_{13}^{\text{L},f} \left(\check{m}_1^f \check{m}_2^f \right) \mathbf{S}_{13}^{\text{L},f} \left((\check{m}_2^f)^2 \right) \mathbf{S}_{13}^{\text{L},f} \left(\check{m}_1^f \right). \quad (6.11b)$$

Finally, the 1-2 rotation can be exactly solved and we have

$$\mathbf{S}_{12}^{\text{L},f} = \mathbf{S}_{12}^{\text{L},f} \left(\check{m}_1^f / \check{m}_2^f, \delta_{12}^f \right). \quad (6.11c)$$

The only physical relevant phase can sit in the 1-2 rotation: following the rank evolution of mass matrices, where the rank-one mass matrix has a U(2) symmetry left in the 1-2 block. The other phases (which were omitted in Eqs. (6.11)) are either zero or maximal (π) corresponding to a rotation either in the same or the opposite direction than the leading order rotation so that there is no CP violation connected to them.

6.3 MIXING ANGLES FROM MASS RATIOS

We motivated a description of individual rotations parametrized by mass ratios as physical parameters only. Fermion masses are the singular values of mass matrices and eigenvalues of the Hermitian product. We cannot set the overall scale (say the largest mass value) since a scale factor can always be multiplied out. The CP-phase in the weak mixing matrix has to be constructed in a similar manner out of the mass ratios. However, the origin of CP violation stays unclear. In principle, there occurs at each fundamental rotation one complex phase which we take either zero or π except for the 1-2 rotation. In any case, the phases always appear in pairs as in Eqs. (6.9) and therefore we only keep track of one of them.

The existence of CP violation in quark flavor physics enforces at least one complex parameter. As we argued above, only δ_{12} can carry any information about CP nonconservation, so we take it maximally CP violating: $\delta_{12} = \frac{\pi}{2}$. This somewhat arbitrary choice gets obvious looking into the “data”, see Fig. 25. In any case, we do not want to take δ_{12} or even δ_{CP} as free parameter. We can show that it is not only possible to reproduce the mixing angles (or CKM elements) but also the CP-phase (or Jarlskog invariant) with fermion masses only. A similar line of arguments is followed in [389, 390].

We keep in mind that we actually describe rotations in three dimensions, so all matrices shall be 3×3 matrices where the nontrivial (i. e. nonzero and $\neq 1$) entries are distributed to the right positions.

It is interesting to note that we want to describe four mixing parameters in the CKM and PMNS matrix (three angles and one phase) by four mass ratios, $\check{m}_1^{u,v}$, $\check{m}_2^{u,v}$, $\check{m}_1^{d,e}$ and $\check{m}_2^{d,e}$.

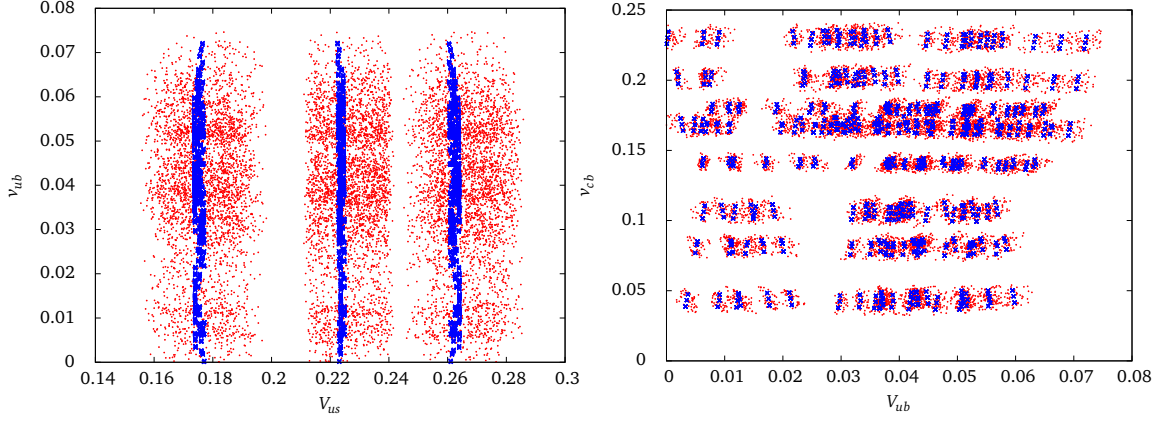


FIGURE 25: We show the upper right corner of the CKM matrix (V_{ub} over V_{us} left and V_{cb} over V_{ub} right) as it results from Eqs. (6.12a) and (6.12b) with values for the masses plugged in. The small red dots scatter over the 1σ regimes for the measured quark masses, where the blue crosses show the results from the central values. All phases in Eq. (6.12b) were allowed to take one of the values $\{0, \frac{\pi}{2}, \pi\}$.

We deconstruct the CKM and PMNS matrices as $\mathbf{V}_{\text{CKM}} = \mathbf{S}_L^u (\mathbf{S}_L^d)^\dagger$ and $\mathbf{U}_{\text{PMNS}} = \mathbf{S}_L^e (\mathbf{S}_L^v)^\dagger$ with

$$\begin{aligned} \mathbf{S}_L^u &= \mathbf{S}_{12}^{L,u} \left(\frac{m_u}{m_c} \right) \mathbf{S}_{13}^{L,u} \left(\frac{m_u m_c}{m_t^2} \right) \mathbf{S}_{13}^{L,u} \left(\frac{m_c^2}{m_t^2} \right) \mathbf{S}_{13}^{L,u} \left(\frac{m_u}{m_t} \right) \\ &\quad \times \mathbf{S}_{23}^{L,u} \left(\frac{m_u m_c}{m_t^2} \right) \mathbf{S}_{23}^{L,u} \left(\frac{m_u}{m_t} \right) \mathbf{S}_{23}^{L,u} \left(\frac{m_c}{m_t} \right), \end{aligned} \quad (6.12a)$$

$$\begin{aligned} \mathbf{S}_L^{d\dagger} &= \mathbf{S}_{23}^{L,d\dagger} \left(\frac{m_s}{m_b}, \delta_{23}^{(0)} \right) \mathbf{S}_{23}^{L,d\dagger} \left(\frac{m_d}{m_b}, \delta_{23}^{(1)} \right) \mathbf{S}_{23}^{L,d\dagger} \left(\frac{m_d m_s}{m_b^2}, \delta_{23}^{(2)} \right) \\ &\quad \times \mathbf{S}_{13}^{L,d\dagger} \left(\frac{m_d}{m_b}, \delta_{13}^{(0)} \right) \mathbf{S}_{13}^{L,d\dagger} \left(\frac{m_s^2}{m_b^2}, \delta_{13}^{(1)} \right) \mathbf{S}_{13}^{L,d\dagger} \left(\frac{m_d m_s}{m_b^2}, \delta_{13}^{(2)} \right) \\ &\quad \times \mathbf{S}_{12}^{L,d\dagger} \left(\frac{m_d}{m_s}, \delta_{12} \right), \end{aligned} \quad (6.12b)$$

$$\begin{aligned} \mathbf{S}_L^e &= \mathbf{S}_{12}^{L,e} \left(\frac{m_e}{m_\mu} \right) \mathbf{S}_{13}^{L,e} \left(\frac{m_\mu^2}{m_\tau^2} \right) \mathbf{S}_{13}^{L,e} \left(\frac{m_e m_\mu}{m_\tau^2} \right) \mathbf{S}_{13}^{L,e} \left(\frac{m_e}{m_\tau} \right) \\ &\quad \times \mathbf{S}_{23}^{L,e} \left(\frac{m_e m_\mu}{m_\tau^2} \right) \mathbf{S}_{23}^{L,e} \left(\frac{m_e}{m_\tau} \right) \mathbf{S}_{23}^{L,e} \left(\frac{m_\mu}{m_\tau} \right), \end{aligned} \quad (6.12c)$$

$$\begin{aligned} \mathbf{S}_L^{v\dagger} &= \mathbf{S}_{23}^{L,v\dagger} \left(\frac{m_{\nu_2}}{m_{\nu_3}}, \delta_{23}^{(0)} \right) \mathbf{S}_{23}^{L,v\dagger} \left(\frac{m_{\nu_1}}{m_{\nu_3}}, \delta_{23}^{(1)} \right) \mathbf{S}_{23}^{L,v\dagger} \left(\frac{m_{\nu_1} m_{\nu_2}}{m_{\nu_3}^2}, \delta_{23}^{(2)} \right) \\ &\quad \times \mathbf{S}_{13}^{L,v\dagger} \left(\frac{m_{\nu_1}}{m_{\nu_3}}, \delta_{13}^{(0)} \right) \mathbf{S}_{13}^{L,v\dagger} \left(\frac{m_{\nu_2}^2}{m_{\nu_3}^2}, \delta_{13}^{(1)} \right) \mathbf{S}_{13}^{L,v\dagger} \left(\frac{m_{\nu_1} m_{\nu_2}}{m_{\nu_3}^2}, \delta_{13}^{(2)} \right) \\ &\quad \times \mathbf{S}_{12}^{L,v\dagger} \left(\frac{m_{\nu_1}}{m_{\nu_2}}, \delta_{12} \right). \end{aligned} \quad (6.12d)$$

TABLE 2: We show the input values of quark masses and their values at the Z scale $Q = M_Z$ by virtue of the RunDec package [391]. The mass inputs correspond to the experimentally measured values while the outputs, evaluated at the Z pole, include the resummation of higher order corrections from QCD by the RG running. RunDec takes properly into account the decoupling of heavy quarks below their scale. Charm and bottom quark can also be simultaneously decoupled [392]. All masses are given in GeV.

Input [23, PDG 2012]	Output
$m_u(2 \text{ GeV}) = 0.0023^{+0.0007}_{-0.0005}$	$m_u(M_Z) = 0.0013^{+0.0004}_{-0.0003}$
$m_d(2 \text{ GeV}) = 0.0048^{+0.0005}_{-0.0003}$	$m_d(M_Z) = 0.0028^{+0.0003}_{-0.0002}$
$m_s(2 \text{ GeV}) = 0.095 \pm 0.005$	$m_s(M_Z) = 0.055 \pm 0.003$
$m_c(m_c) = 1.275 \pm 0.025$	$m_c(M_Z) = 0.622 \pm 0.012$
$m_b(m_b) = 4.18 \pm 0.03$	$m_b(M_Z) = 2.85 \pm 0.02$
$m_t(\text{OS}) = 173.07 \pm 1.24$	$m_t(M_Z) = 172.16^{+1.47}_{-1.46}$

6.3.1 Quark mixing

With the previous work, we can plug in the numbers for the quark masses as given in Tab. 2 and propagate the errors (the errors given in Eq. (6.13) are seen to be purely parametrical). The results have to be compared with the global fit values for CKM elements as shown in Eq. (2.11) and are found to be in an astonishingly good agreement within the errors:

$$|\mathbf{V}_{\text{CKM}}^{\text{prop}}| = \begin{pmatrix} 0.974^{+0.004}_{-0.003} & 0.225^{+0.016}_{-0.011} & 0.0031^{+0.0018}_{-0.0015} \\ 0.225^{+0.016}_{-0.011} & 0.974^{+0.004}_{-0.003} & 0.039^{+0.005}_{-0.004} \\ 0.0087^{+0.0010}_{-0.0008} & 0.038^{+0.004}_{-0.004} & 0.9992^{+0.0002}_{-0.0001} \end{pmatrix}. \quad (6.13)$$

6.3.2 Lepton mixing

The lepton case is a bit more involved because we only know the masses partially. However, we can revert the procedure and predict the neutrino mass spectrum out of the measured mixing matrix. For the 1-2 mixing we have

$$|U_{e2}| \approx \sqrt{\frac{\check{m}_{e\mu} + \check{m}_{\nu 12} - 2\sqrt{\check{m}_{e\mu}\check{m}_{\nu 12}} \cos(\delta_{12}^e - \delta_{12}^\nu)}{(1 + \check{m}_{e\mu})(1 + \check{m}_{\nu 12})}}, \quad (6.14)$$

Our choice of phases in Eq. (6.12b):
 $\delta_{12} = \frac{\pi}{2}$,
 $\delta_{13}^{(0)} = 0$,
 $\delta_{13}^{(1)} = \pi$,
 $\delta_{13}^{(2)} = \pi$,
 $\delta_{23}^{(0)} = 0$,
 $\delta_{23}^{(1)} = \pi$,
 $\delta_{23}^{(2)} = \pi$.

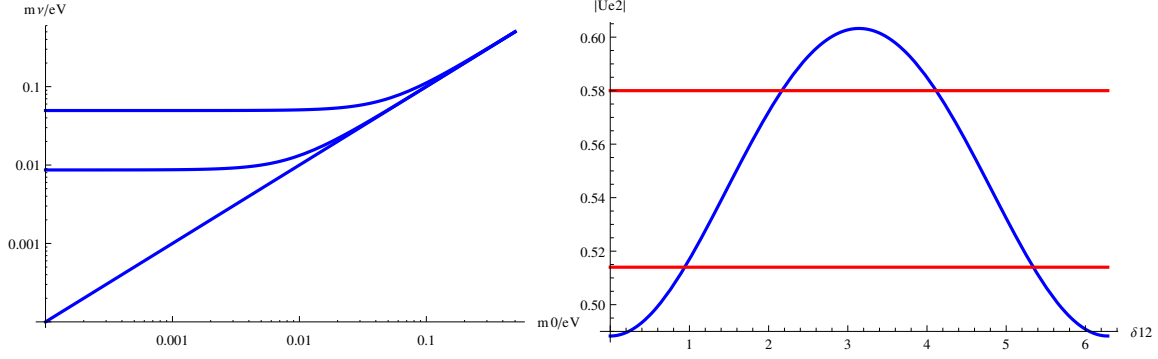


FIGURE 26: For low values of $m_{\nu}^{(0)}$, the neutrino mass spectrum is hierarchical in contrast to quasi-degenerate as shown on the left. The right plot shows the dependence of $|U_{e2}|$ on the phase δ_{12}^{ν} . The experimentally allowed 3σ ranges are indicated by the horizontal red lines. The best fit point lies surprisingly close to $\delta_{12}^{\nu} = \frac{\pi}{2}$. Figure taken from [205].

with $\check{m}_{e\mu} = m_e/m_{\mu}$ and $\check{m}_{\nu 12} = m_{\nu_1}/m_{\nu_2}$. The neutrino spectrum can be obtained inverting Eq. (6.14) to get a solution $\check{m}_{\nu 12}(U_{e2})$ and therewith

$$\begin{aligned} m_{\nu_2} &= \sqrt{\Delta m_{21}^2 / (1 - \check{m}_{\nu 12}^2)}, \\ m_{\nu_1} &= \sqrt{m_{\nu_2}^2 - \Delta m_{21}^2}, \\ m_{\nu_3} &= \sqrt{\Delta m_{31}^2 - \Delta m_{21}^2 + m_{\nu_2}^2}. \end{aligned} \quad (6.15)$$

With the analogous choice (motivated by the observation of Fig. 26) of the 1-2 phase as in the CKM case, $\delta_{12}^e - \delta_{12}^{\nu} = \frac{\pi}{2}$, we get

We use $\check{m}_e = m_e/m_{\mu} = 0.00474$
and
 $|U_{e2}| = \sin \theta_{12} = 0.54 \dots 0.56$.

$$\check{m}_{\nu_1} = \frac{|U_{e2}|^2(1 + \check{m}_e) - \check{m}_e}{1 - |U_{e2}|^2(1 + \check{m}_e)} = 0.41 \dots 0.45 \quad (6.16)$$

Errors are added linearly to be conservative. However, this neutrino mass spectrum is clearly non-degenerate. In this way, the results of this chapter might be of importance if there is no neutrino mass measurement in the near future as desired for the corrections of Sec. 3.2.

and estimate the neutrino mass spectrum to be

$$\begin{aligned} m_{\nu_1} &= (0.0041 \pm 0.0015) \text{ eV}, \\ m_{\nu_2} &= (0.0096 \pm 0.0005) \text{ eV}, \\ m_{\nu_3} &= (0.050 \pm 0.001) \text{ eV}. \end{aligned}$$

It is interesting to note that the sum of all light neutrino masses is $\sum m_{\nu} = 0.0637 \pm 0.003$ and thereby perfectly fine with cosmology, see [199].

The mass hierarchy in neutrinos, though existent, is not as strong as in the charged fermion case. However, the result of our description relying only on the minimal breaking of a maximal flavor symmetry shows also for the PMNS matrix an astonishingly good agreement with the global fit data shown in Eq. (2.44)

$$|U_{\text{PMNS}}^{\text{PROP}}| = \begin{pmatrix} 0.83_{-0.05}^{+0.04} & 0.54_{-0.09}^{+0.06} & 0.14 \pm 0.03 \\ 0.38_{-0.06}^{+0.04} & 0.57_{-0.04}^{+0.03} & 0.73 \pm 0.02 \\ 0.41_{-0.06}^{+0.04} & 0.61_{-0.04}^{+0.03} & 0.67 \pm 0.02 \end{pmatrix}, \quad (6.17)$$

where we assigned the phases of Eq. (6.12d) to be $\delta_{12} = \frac{\pi}{2}$, $\delta_{13}^{(0)} = 0$, $\delta_{13}^{(1)} = \pi$, $\delta_{13}^{(2)} = \pi$, $\delta_{23}^{(0)} = \pi$, $\delta_{23}^{(1)} = \pi$ and $\delta_{23}^{(2)} = 0$. We remark an exchange of $\delta_{23}^{(0)} \leftrightarrow \delta_{23}^{(2)}$ compared to the CKM case.

Similar results for the neutrino masses were found by [200, 201, 360] for hierarchical charged lepton masses. However, the third mixing angle θ_{13} was predicted too low with 3° .

The deeper reason behind this replacement has still to be found out.

6.3.3 CP violation

A measure of CP violation in fermion mixing is given by the Jarlskog invariant [393]

$$J = \text{Im} \left(V_{ij} V_{kl} V_{il}^* V_{kj}^* \right). \quad (6.18)$$

A vanishing J indicates CP conservation. With the decomposition of mixing matrix elements in terms of mass ratios, we can give an approximate analytic formula for J for both quark ($f = q$ and $a = u, b = d$) and lepton ($f = \ell$ and $a = e, b = \nu$) mixing [205]

$$J_f \approx \cos \theta_{12}^b \sin \theta_{12}^b \sin \theta_{23}^f \left(\sin \theta_{12}^a \sin \theta_{23}^f + \sin \theta_{13}^a - \sin \theta_{12}^b \right), \quad (6.19)$$

where

with $\check{m}_{ij}^x = m_i^x / m_j^x$

$$\begin{aligned} \sin \theta_{23}^f &= \frac{|V_{23}^f|}{\sqrt{1 - |V_{13}^f|^2}}, & \sin \theta^{a(b)} &= \sqrt{\frac{\check{m}_{12}^{a(b)}}{1 + \check{m}_{12}^{a(b)}}} \quad \text{and} \\ \sin \theta_{13}^{a(b)} &\approx \frac{\pm \sqrt{\check{m}_{12}^{a(b)} + \sqrt{\check{m}_{13}^{a(b)} \check{m}_{23}^{a(b)}} + \check{m}_{23}^{a(b)}}}{(1 + \check{m}_{13}^{a(b)}) (1 + \check{m}_{13}^{a(b)} \check{m}_{23}^{a(b)}) (1 + (\check{m}_{23}^{a(b)})^2)}. \end{aligned}$$

For the quark case, we have

$$J_q = \text{Im} \left(V_{us} V_{cb} V_{ub}^* V_{cs}^* \right) = \left(2.6_{-1.0}^{+1.3} \right) \times 10^{-5},$$

which has to be compared with $J_q = \left(3.06_{-0.20}^{+0.21} \right) \times 10^{-5}$ [23] and due to our large error is found to be in agreement. In the lepton sector there has no CP violation yet been observed, so only an upper bound on the Jarlskog invariant can be set, $J_\ell^{\text{max}} = 0.033 \pm 0.010$ [132]. We find a result close to this maximal value,

$$J_\ell = \text{Im} \left(U_{e2} U_{\mu 2} U_{e3}^* U_{\mu 2}^* \right) = 0.031_{-0.007}^{+0.006}.$$

This corresponds to a ‘‘prediction’’ of $\delta_{\text{CP}} \approx 70^\circ$ from the central values via $J_\ell = J_\ell^{\text{max}} \sin \delta_{\text{CP}}$. In any case, we are compatible with maximal CP violation ($\delta_{\text{CP}} = 90^\circ$) as well as $\delta_{\text{CP}} = 45^\circ$ taking the lower error limit.

SUMMARY OF CHAPTER 6 We presented a formulation of fermion mixing based on the observation that in absence of Yukawa couplings, the SM fermion content intrinsically has an enhanced symmetry group, $[U(3)]^6$. Breaking this *maximal flavor symmetry* in a minimal way by only introducing the masses (diagonal Yukawa couplings), we could demonstrate that with hierarchical fermion masses as they are observed in nature, we are able to reproduce the mixing patterns for both quark and lepton mixing without further assumptions. Especially no specific patterns for the fermion mass matrices (“texture zeros”) are needed. The rather mild hierarchy for neutrinos, whose mass spectrum has been predicted by this minimal breaking of maximal flavor symmetry, gives a handle on large neutrino mixing. Moreover, the strong connection of fermion masses and mixing allows to predict the neutrino mass spectrum, taking neutrino mixing and the charged lepton masses as input. We have found a lightest neutrino mass $m_\nu^{(0)} = 4.1 \text{ meV}$ which is well below any direct detection possibility.

The neutrino mass ratios, which govern the results for the mixing angles, are large!

The derived mixing matrices are in surprisingly good agreement with the experimentally measured flavor mixing. By imposing only one non-trivial CP-phase in the fundamental rotations, we are also in agreement with the effective CP-phase as determined via the Jarlskog invariant. It is a crucial point for further investigations, that $\delta_{12} = \frac{\pi}{2}$ and all other phases are either zero or π . This is also interesting in a model building perspective: we do not have to predict an arbitrary, continuous CP-phase but can choose phases of the individual rotations out of discrete values $\{0, \frac{\pi}{2}, \pi\}$.

There can be a lot of work done with the results of this chapter in mind: what is the origin of CP violation? Is there maybe a discrete symmetry behind yielding discrete δ_{ij} ? How can we model the successive symmetry breakdown? Is there a SUSY description inspired by RFV possible? Each symmetry breaking step occurs with the introduction of one Yukawa coupling for the corresponding fermion generation. Can we combine flavor breaking, electroweak breaking and SUSY breaking?

*Ich kann's bis heute nicht verwinden,
deshalb erzähl' ich's auch nicht gern:
den Stein der Weisen wollt' ich finden
und fand nicht mal des Pudels Kern.*

—Heinz Erhardt

*I have not yet
overcome, that's
why I don't like to
tell it gladly: I
wanted to find the
philosopher's stone,
and I haven't even
found the core of
the poodle.*

We have addressed the influence of quantum corrections to neutrino masses and mixings and found enhanced corrections in case of a quasi-degenerate mass spectrum that have the power to completely generate the flavor mixing irrespective of any tree-level flavor model. Especially the case with trivial mixing at tree-level connected to exact degenerate neutrino masses was shown to give the observed deviations from the degenerate spectrum and simultaneously generate large mixing angles. We have calculated threshold corrections in an extension of the Minimal Supersymmetric Standard Model including right-handed Majorana neutrinos in Chapter 3. The existence of right-handed neutrinos and Majorana masses at a very high scale can be motivated from grand unified theories. We have analyzed the impact of flavor non-universal SUSY breaking terms and proposed a description of neutrino mixing in terms of SUSY breaking parameters in the context of the MSSM, extending previous ideas on RFV in the literature. The driving force is given by contributions $\sim A_{ij}^{\nu}/M_{\text{SUSY}}$ that do not decouple with the SUSY scale. Even with very heavy SUSY spectra, this non-decoupling contribution to rather low-energy flavor physics persists. Additionally, we have shown that the presence of hierarchical right-handed (s)neutrinos alone can substantially alter mixing patterns—a result which is also in line with what was found for the Standard Model with right-handed neutrinos before. We have performed a Dyson resummation of the enhanced contributions to neutrino mixing and found a stabilization of the description with respect to the neutrino mass. The same combination $A_{ij}^{\nu}/M_{\text{SUSY}}$ was found to give an equally good description of neutrino mixing for the full neutrino mass range: This is a kind of “non-decoupling” contribution with respect to the neutrino mass. Without resummation, smaller corrections are needed to give the same mixing. Once resummation is switched on, the same parameters give an equally well generation of neutrino mixing irrespective of the neutrino mass.

SUSY threshold corrections also affect the effective Higgs potential and alter conclusions about electroweak symmetry breaking. We have found and described a new class of vacua in Chapter 4, where the term *vacuum* describes the ground state of the theory or a minimum of the effective potential. Finding the global minimum is a challenging task. However, we discovered regions in the SUSY parameter space that treat the electroweak

minimum with $v = 246 \text{ GeV}$ as *false* vacuum. These findings are essential to constrain parameter regions. Transitions to the deeper minimum were found to happen nearly instantaneously, so those constraints can be seen as strict without referring to metastability and the life-time of our universe. Moreover, the results hint towards a charge and color breaking global minimum and therefore extend existing bounds at tree-level. The full analysis including colored directions in field space has not yet been performed and is left for future work.

We have combined the discussion of vacuum stability in the MSSM with the right-handed neutrino extension in chapter 5. Without Supersymmetry, the existence of the effective neutrino mass operator as well as the extension with singlet neutrinos at a high scale render the Higgs potential unbounded from below—a behavior that better shall be avoided. The supersymmetric version, however, rescues the potential and also does not induce further instabilities neither at the SUSY scale nor at the scale of heavy neutrinos. At the high scale, SUSY appears to be effectively exact and SUSY masses are only a small perturbation; so the contributions to the effective potential exactly cancel summing up fermionic (neutrino) and bosonic (sneutrino) contributions.

Finally, we have elaborated on a different view of fermion mixing and how to parametrize the mixing angles in terms of mass ratios only. We found a minimal breaking of the maximal flavor symmetry group $[\text{U}(3)]^6$ together with hierarchical masses sufficient to reproduce the observed mixing patterns for quarks as well as leptons. Moreover, by inverting the procedure, we predict the lightest neutrino mass to be $m_\nu^{(0)} = (4.1 \pm 1.5) \text{ meV}$. The large error is result of the still large uncertainties in neutrino physics (Δm^2 as well as the PMNS matrix itself). By the same description, we also predict the CP violating phase in lepton physics to be rather large (close to maximal, $\frac{\pi}{2}$).

The main results of this thesis are a description of neutrino mixing at quantum level with the restriction to a quasi-degenerate physical mass spectrum—and genuine one-loop bounds from vacuum stability on SUSY parameters. Also the description of fermion mixing angles in terms of mass ratios may be lined with a radiative origin of the minimal flavor breaking chain, which is kept for future work.

A.1 SPINOR NOTATION AND CHARGE CONJUGATION

We collect the necessary notations and rules to deal with left-handed Weyl spinors and charge conjugation. The Weyl spinor notation turns out to be more convenient. A four-component Dirac spinor Ψ is written in the chiral basis with left- and right-handed Weyl spinors ψ_L and ψ_R as

$$\Psi = \begin{pmatrix} \psi_L \\ \psi_R^\dagger \end{pmatrix}. \quad (\text{A.1})$$

We use an index free notation (there is no need to introduce dotted indices for our purpose and write a bit sloppy ψ_R^\dagger as a column). The left- and right-handed fields can be projected out with $P_L = \frac{1}{2}(1 - \gamma_5)$ and $P_R = \frac{1}{2}(1 + \gamma_5)$,

$$\psi_L = P_L \Psi = \begin{pmatrix} \psi_L \\ 0 \end{pmatrix}, \quad \psi_R = P_R \Psi = \begin{pmatrix} 0 \\ \psi_R^\dagger \end{pmatrix}.$$

Charge conjugation is defined as

$$C : \Psi \rightarrow \Psi^c = C \bar{\Psi}^T, \quad (\text{A.2})$$

where $C = i\gamma^2\gamma^0$ with $C^\dagger = C^T = C^{-1} = -C$ and $\bar{\Psi} = \Psi^\dagger\gamma^0$. The charge conjugation of a left-handed field gives a right-handed one and vice versa:

$$C : \psi_L \rightarrow (\psi_L)^c = (\Psi^c)_R \equiv \psi_R^c, \quad \psi_R \rightarrow (\psi_R)^c = (\Psi^c)_L \equiv \psi_L^c. \quad (\text{A.3})$$

It follows clearly that

$$\Psi^c = C \bar{\Psi}^T = \begin{pmatrix} \psi_R^c \\ \psi_L^c \end{pmatrix},$$

and therewith $(\psi_R)^c = \psi_L^c$ which is the left-handed component of the charge conjugated Dirac spinor.

Dirac mass terms are $\bar{\Psi}\Psi = \psi_L^\dagger\psi_R^\dagger + \psi_L\psi_R$, Majorana mass terms $\Psi^T C \Psi = \psi_L\psi_L + \psi_L^c\psi_L^c$ (with $\psi_R = \psi_L^c$).

A.2 NEUTRALINO AND CHARGINO MASS AND MIXING MATRICES

The chargino and neutralino mass matrices follow basically from the soft breaking Lagrangian Eq. (2.28), the superpotential Eq. (2.26) which contributes the μ -term $\mu H_d \cdot H_u$, and the gauge interaction (after spontaneous symmetry breaking, so with $h_{u,d}^0 \rightarrow \nu_{u,d}$).

A good compilation of two- and four-spinor notation and its applications can be found in [394].

We have $\gamma_5 = i\gamma^0\gamma^1\gamma^2\gamma^3$ with the Dirac γ -matrices γ^μ that satisfy $\{\gamma^\mu, \gamma^\nu\} = 2g^{\mu\nu}$.

By abuse of notation we write $(\Psi)_X = P_X\Psi$ with $X = L, R$.

We decided to write $(\psi_R)^c = \psi_R^c$ in the definition of the MSSM superfields in Chapter 2 and label with $_R$ the gauge representation there and wherever applied.

The Lagrangian part defining the mass basis for charginos is given by

$$\begin{aligned}\mathcal{L}_{\text{mass}}^{\text{C}} &= -\frac{g_2}{\sqrt{2}} \left(\nu_{\text{d}} \tilde{\lambda}^+ \tilde{h}_{\text{d}}^- + \nu_{\text{u}} \tilde{\lambda}^- \tilde{h}_{\text{u}}^+ + \text{h. c.} \right) \\ &\quad - \left(M_2 \tilde{\lambda}^+ \tilde{\lambda}^- + \mu \tilde{h}_{\text{d}}^+ \tilde{h}_{\text{u}}^- + \text{h. c.} \right) \\ &\equiv - \left(\psi^- \right)^{\text{T}} \mathcal{M}_{\text{C}} \psi^+ + \text{h. c.},\end{aligned}\tag{A.4}$$

where $\psi^+ = (\tilde{\lambda}^+, \tilde{h}_{\text{u}}^+)^{\text{T}}$ and $\psi^- = (\tilde{\lambda}^-, \tilde{h}_{\text{d}}^-)^{\text{T}}$. The mass matrix

$$\mathcal{M}_{\text{C}} = \begin{pmatrix} M_2 & \sqrt{2} M_W \sin \beta \\ \sqrt{2} M_W \cos \beta & \mu \end{pmatrix}\tag{A.5}$$

can be diagonalized with a bi-unitary transformation

$$Z_-^{\text{T}} \mathcal{M}_{\text{C}} Z_+ = \hat{\mathcal{M}}_{\text{C}} = \text{diagonal}.\tag{A.6}$$

The charged mass eigenstates (“charginos”) are defined as

$$\tilde{\chi}_+ = Z_+^* \left(\tilde{\lambda}^+, \tilde{h}_{\text{u}}^+ \right)^{\text{T}} \quad \text{and} \quad \tilde{\chi}_- = Z_-^* \left(\tilde{\lambda}^-, \tilde{h}_{\text{d}}^- \right)^{\text{T}}.$$

Analogously, we have for the neutral electroweakinos and higgsinos

$$\begin{aligned}\mathcal{L}_{\text{mass}}^{\text{N}} &= -\frac{g_2}{2} \tilde{\lambda}_3 \left(\nu_{\text{d}} \tilde{h}_{\text{d}}^0 - \nu_{\text{u}} \tilde{h}_{\text{u}}^0 \right) + \frac{g_1}{2} \tilde{\lambda}_0 \left(\nu_{\text{d}} \tilde{h}_{\text{d}}^0 - \nu_{\text{u}} \tilde{h}_{\text{u}}^0 \right) \\ &\quad + \mu \tilde{h}_{\text{d}}^0 \tilde{h}_{\text{u}}^0 - \frac{1}{2} M_2 \tilde{\lambda}_3 \tilde{\lambda}_3 - \frac{1}{2} M_1 \tilde{\lambda}_0 \tilde{\lambda}_0 + \text{h. c.} \\ &\equiv -\frac{1}{2} \left(\psi^0 \right)^{\text{T}} \mathcal{M}_{\text{N}} \psi^0 + \text{h. c.},\end{aligned}\tag{A.7}$$

where $\psi^0 = (\tilde{\lambda}_0, \tilde{\lambda}_3, \tilde{h}_{\text{d}}^0, \tilde{h}_{\text{u}}^0)$. The mass matrix

$$\mathcal{M}_{\text{N}} = \begin{pmatrix} M_1 & 0 & -c_{\beta} s_W M_Z & c_{\beta} s_W M_Z \\ 0 & M_2 & c_{\beta} c_W M_Z & -s_{\beta} c_W \\ -c_{\beta} s_W M_Z & c_{\beta} c_W M_Z & 0 & \mu \\ s_{\beta} s_W M_Z & -s_{\beta} c_W M_Z & \mu & 0 \end{pmatrix}\tag{A.8}$$

is Takagi-diagonalized with a unitary matrix Z_{N}

$$\mathcal{M}_{\text{N}}^{\text{diag}} = Z_{\text{N}}^{\text{T}} \mathcal{M}_{\text{N}} Z_{\text{N}},\tag{A.9}$$

such that

$$\tilde{\chi}_0 = Z_{\text{N}}^* \left(\tilde{\lambda}_0, \tilde{\lambda}_3, \tilde{h}_{\text{d}}^0, \tilde{h}_{\text{u}}^0 \right)$$

are the neutral mass eigenstates (“neutralinos”).

A.3 SFERMION MASS AND MIXING MATRICES

UP AND DOWN SFERMION MASS MATRICES IN THE MSSM We restrict ourselves to the derivation of selectron and sneutrino mass matrices in the MSSM, where the squark sector follows analogously. The more involved situation with Majorana neutrinos is given below. We include right-handed neutrinos already without Majorana masses.

The scalar mass Lagrangian is contained in the soft breaking Lagrangian and the F - and D -term potential,

$$V^{\tilde{f}} = V_{\text{soft}}^{\tilde{f}} + V_F^{\tilde{f}} + V_D^{\tilde{f}}.$$

We collect the individual contributions from Eqs. (2.28), (2.21) and (2.23),

$$-\mathcal{L}_{\text{soft}}^{\tilde{\ell}} = \tilde{\ell}_{L,i}^* (\tilde{\mathbf{m}}_\ell^2)_{ij} \tilde{\ell}_{L,j} + \tilde{e}_{R,i}^* (\tilde{\mathbf{m}}_e^2)_{ij} \tilde{e}_{R,j} + \tilde{\nu}_{R,i}^* (\tilde{\mathbf{m}}_\nu^2)_{ij} \tilde{\nu}_{R,j} \\ + \left[h_d \cdot \tilde{\ell}_{L,i} A_{ij}^e \tilde{e}_{R,j}^* + \tilde{\ell}_{L,i} \cdot h_u A_{ij}^\nu \tilde{\nu}_{R,j}^* + \text{h. c.} \right], \quad (\text{A.10})$$

$$V_F^{\tilde{f}} = [F_i^* F_i]_{\tilde{f}^* \tilde{f}} = \left[\frac{\partial \mathcal{W}^\dagger}{\partial \phi_i^\dagger} \left| \frac{\partial \mathcal{W}}{\partial \phi_i} \right| \right]_{\tilde{f}^* \tilde{f}}, \quad (\text{A.11})$$

$$V_D^{\tilde{f}} = \left[\frac{1}{2} D_\alpha^a D_\alpha^a \right]_{\tilde{f}^* \tilde{f}} = \left[\frac{1}{2} g_\alpha^2 \left(\phi_i^\dagger T_{ij}^{a,\alpha} \phi_j \right) \left(\phi_{i'}^\dagger T_{i'j'}^{a,\alpha} \phi_{j'} \right) \right]_{\tilde{f}^* \tilde{f}}. \quad (\text{A.12})$$

The exhausting part are the F -terms as derivatives of the superpotential. Sfermion mass terms are obtained after electroweak breaking, so each occurrence of $h_{u,d}^0$ has to be replaced by its vev.

Mass terms are the bilinear terms in the Lagrangian, so only $\sim \tilde{f}^ \tilde{f}$ are needed.*

$$V_F^{\tilde{f}} \Big|_{\text{vev}} = \left| \mu^* v_d - \tilde{\nu}_{L,i}^* Y_{ij}^{\nu*} \tilde{\nu}_{R,j} \right|^2 + \left| \mu^* v_u - \tilde{e}_{L,i}^* Y_{ij}^{e*} \tilde{e}_{R,j} \right|^2 \\ + \sum_i \left| Y_{ij}^e \langle h_d \rangle \cdot \tilde{\ell}_{L,j} \right|^2 + \sum_i \left| Y_{ij}^\nu \langle h_u \rangle \cdot \tilde{\ell}_{L,i} \right|^2 \\ + \sum_i \left| v_d Y_{ij}^{e*} \tilde{e}_{R,j} \right|^2 + \sum_i \left| v_u Y_{ij}^{\nu*} \tilde{\nu}_{R,j} \right|^2 \\ \stackrel{\text{mass}}{=} - \underbrace{\mu v_d Y_{ij}^\nu \tilde{\nu}_{L,i}^* \tilde{\nu}_{R,j}}_{\mu \cot \beta \tilde{v}_L^D m_\nu^D \tilde{\nu}_R} - \underbrace{\mu v_u Y_{ij}^e \tilde{e}_{L,i}^* \tilde{e}_{R,j}}_{\mu \tan \beta \tilde{e}_L^D m_e \tilde{e}_R} + \text{h. c.} \quad (\text{A.13}) \\ + \underbrace{v_d^2 \tilde{e}_{L,j'}^* Y_{j'i}^e Y_{ji}^{e*} \tilde{e}_{L,j}}_{\tilde{e}_L^\dagger m_e m_e^\dagger \tilde{e}_L} + \underbrace{v_u^2 \tilde{\nu}_{L,j'}^* Y_{j'i}^\nu Y_{ji}^{\nu*} \tilde{\nu}_{L,j}}_{\tilde{\nu}_L^\dagger m_\nu^D m_\nu^{D\dagger} \tilde{\nu}_L} \\ + \underbrace{v_d^2 \tilde{e}_{R,j'}^* Y_{ij'}^{e*} Y_{ij}^e \tilde{e}_{R,j}}_{\tilde{e}_R^\dagger m_e^\dagger m_e \tilde{e}_R} + \underbrace{v_u^2 \tilde{\nu}_{R,j'}^* Y_{ij'}^{\nu*} Y_{ij}^\nu \tilde{\nu}_{R,j}}_{\tilde{\nu}_R^\dagger m_\nu^{D\dagger} m_\nu^D \tilde{\nu}_R}.$$

The D -terms can be easily read off and are contributions $\sim g_{1,2}^2$

$$V_D^{\tilde{\ell}} = \frac{1}{4} g_1^2 (|h_d|^2 - |h_u|^2) \sum_i (|\tilde{\ell}_{L,i}|^2 - 2|\tilde{e}_{R,i}|^2) \\ + \frac{1}{4} g_2^2 (h_d^\dagger \vec{\tau} h_d + h_u^\dagger \vec{\tau} h_u) \tilde{\ell}_{L,i}^\dagger \vec{\tau} \tilde{\ell}_{L,i},$$

The objects $T_{3L}^{\tilde{f}}$ are the third components of weak isospin, so the $SU(2)_L$ charge of sfermions \tilde{f} .

where $\tau_i/2$, $i = 1, 2, 3$ are the generators of $SU(2)_L$.

Combining to mass matrices, we get

$$\mathcal{M}_{\tilde{\nu}}^2 = \begin{pmatrix} \tilde{m}_{\tilde{\ell}}^2 + M_Z^2 T_{3L}^{\tilde{\nu}} \cos 2\beta \mathbf{1} + \mathbf{m}_{\tilde{\nu}}^D \mathbf{m}_{\tilde{\nu}}^{D\dagger} & -\mathbf{m}_{\tilde{\nu}}^D \mu \cot \beta + \nu_u \mathbf{A}_{\tilde{\nu}}^* \\ -\mathbf{m}_{\tilde{\nu}}^{D\dagger} \mu^* \cot \beta + \nu_u \mathbf{A}_{\tilde{\nu}}^T & \tilde{m}_{\tilde{\nu}}^2 + \mathbf{m}_{\tilde{\nu}}^{D\dagger} \mathbf{m}_{\tilde{\nu}}^D \end{pmatrix}, \quad (\text{A.14a})$$

$$\mathcal{M}_{\tilde{e}}^2 = \begin{pmatrix} \tilde{m}_{\tilde{\ell}}^2 + M_Z^2 (T_{3L}^{\tilde{e}} - Q_e \sin^2 \theta_w) \cos 2\beta \mathbf{1} + \mathbf{m}_e \mathbf{m}_e^\dagger & -\mathbf{m}_e \mu \tan \beta + \nu_d \mathbf{A}_e^* \\ -\mathbf{m}_e^\dagger \mu^* \tan \beta + \nu_d \mathbf{A}_e^T & \tilde{m}_{\tilde{e}}^2 + M_Z^2 Q_e \cos 2\beta \sin^2 \theta_w \mathbf{1} + \mathbf{m}_e^\dagger \mathbf{m}_e \end{pmatrix}, \quad (\text{A.14b})$$

in a basis $\vec{f} = (\tilde{f}_L, \tilde{f}_R)^T$, such that $-\mathcal{L}_{\vec{f}}^{\text{mass}} = \sum_{\vec{f}} \vec{f}^\dagger \mathcal{M}_{\vec{f}}^2 \vec{f}$.

SNEUTRINO SQUARED MASS MATRIX AND MIXING MATRIX Extending the MSSM by right-handed neutrinos and giving them a Majorana mass leads to a seesaw-like mechanism in the sneutrino sector. Similar to the seesaw-extended Standard Model, where the neutrino spectrum gets doubled, the sneutrino spectrum gets quadrupled. Why that? The MSSM contains only three sneutrino states. Including right-handed fields, the number of states get doubled, although half of them are singlets under the SM gauge group. Moreover, due to Dirac and Majorana masses, the physical spectrum gets even more enlarged. Effectively, we are left with six light, more or less active states, and six heavy singlet-like states. A priori, the sneutrino squared mass matrix is therefore a 12×12 matrix, which can be perturbatively block-diagonalized similar to the neutrino mass matrix. The complete procedure is described in great detail by [140].

We choose the following basis: $\vec{N} = (\tilde{\nu}_L, \tilde{\nu}_L^*, \tilde{\nu}_R^*, \tilde{\nu}_R)^T$ (such that $-\mathcal{L}_{\text{mass}}^{\tilde{\nu}} = \vec{N}^\dagger (\mathcal{M}_{\tilde{\nu}})^2 \vec{N}$) and classify chirality conserving (LL, RR) and chirality changing blocks:

$$\mathcal{M}_{\tilde{\nu}}^2 = \frac{1}{2} \begin{pmatrix} \mathcal{M}_{LL}^2 & \mathcal{M}_{LR}^2 \\ (\mathcal{M}_{LR}^2)^\dagger & \mathcal{M}_{RR}^2 \end{pmatrix},$$

with

$$\mathcal{M}_{LL}^2 = \begin{pmatrix} \tilde{m}_{\tilde{\ell}}^2 + \frac{1}{2} M_Z^2 \cos 2\beta \mathbf{1} + \mathbf{m}_{\tilde{\nu}}^D \mathbf{m}_{\tilde{\nu}}^{D\dagger} & \mathbf{0} \\ \mathbf{0} & (\tilde{m}_{\tilde{\ell}}^2)^\dagger + \frac{1}{2} M_Z^2 \cos 2\beta \mathbf{1} + \mathbf{m}_{\tilde{\nu}}^{D*} \mathbf{m}_{\tilde{\nu}}^{D\dagger} \end{pmatrix}, \quad (\text{A.15a})$$

$$\mathcal{M}_{RL}^2 = \begin{pmatrix} \mathbf{m}_{\tilde{\nu}}^D \mathbf{M}_R & -\mu \cot \beta \mathbf{m}_{\tilde{\nu}}^D + \nu_u \mathbf{A}_{\tilde{\nu}}^* \\ -\mu^* \cot \beta \mathbf{m}_{\tilde{\nu}}^{D*} + \nu_u \mathbf{A}_{\tilde{\nu}} & \mathbf{m}_{\tilde{\nu}}^{D*} \mathbf{M}_R^* \end{pmatrix}, \quad (\text{A.15b})$$

$$\mathcal{M}_{RR}^2 = \begin{pmatrix} (\tilde{m}_{\tilde{\nu}}^2)^\dagger + \mathbf{m}_{\tilde{\nu}}^{D\dagger} \mathbf{m}_{\tilde{\nu}}^D + \mathbf{M}_R^* \mathbf{M}_R & 2(\mathbf{B}^2)^* \\ 2\mathbf{B}^2 & \tilde{m}_{\tilde{\nu}}^2 + \mathbf{m}_{\tilde{\nu}}^{D\dagger} \mathbf{m}_{\tilde{\nu}}^D + \mathbf{M}_R \mathbf{M}_R^* \end{pmatrix}. \quad (\text{A.15c})$$

A.4 FEYNMAN RULES FOR THE TYPE I SEESAW-EXTENDED MSSM

The relevant vertices for the lepton flavor changing self energies are triple vertices for the lepton-slepton-gaugino and -higgsino interactions:

$$i\Gamma_{\nu_f}^{\tilde{\nu}_s \tilde{\chi}_k^0} = -\frac{i}{\sqrt{2}} \left\{ \left[(g_2 Z_{2k}^N - g_1 Z_{1k}^N) \mathcal{Z}_{is}^{\tilde{\nu}*} (\mathbf{U}_{\text{PMNS}})_{if} \right] P_L \quad (\text{A.16a}) \right. \\ \left. + \left[(g_2 Z_{2k}^{N*} - g_1 Z_{1k}^{N*}) \mathcal{Z}_{is}^{\tilde{\nu}} (\mathbf{U}_{\text{PMNS}}^*)_{if} \right] P_R \right\},$$

$$i\Gamma_{e_i}^{\tilde{e}_s \tilde{\chi}_k^0} = \frac{i}{\sqrt{2}} \left\{ \left((g_2 Z_{2k}^N + g_1 Z_{1k}^N) W_{is}^{\tilde{e}} - y_{ij}^e Z_{3k}^N W_{j+3,s}^{\tilde{e}} \right) P_L \quad (\text{A.16b}) \right. \\ \left. - \left(\sqrt{2} g_1 Z_{1k}^N W_{i+3,s}^{\tilde{e}} + y_{ji}^{e*} Z_{3k}^N W_{js}^{\tilde{e}} \right) P_R \right\},$$

$$i\Gamma_{\nu_f}^{\tilde{e}_s \tilde{\chi}_k^+} = -i \left[g_2 Z_{1k}^- W_{is}^{\tilde{e}*} - y_{ij}^{e*} Z_{2k}^- W_{j+3,s}^{\tilde{e}*} \right] (\mathbf{U}_{\text{PMNS}})_{if} P_L, \quad (\text{A.16c})$$

$$i\Gamma_{e_i}^{\tilde{\nu}_s (\tilde{\chi}_k^+)^c} = -i \left[g_2 Z_{1k}^+ \mathcal{Z}_{i,s}^{\tilde{\nu}*} P_L - y_{ij}^e Z_{2k}^- \mathcal{Z}_{js}^{\tilde{\nu}} P_R \right], \quad (\text{A.16d})$$

where summation over double indices is understood.

The vertices of Eqs. (A.16) are given for an incoming standard model fermion, outgoing chargino or neutralino as well as sfermion. They generically follow from an interaction Lagrangian like

$$\mathcal{L}_{\text{int}} = \bar{f}_i \Gamma_{ff}^{\tilde{f}_s \tilde{\chi}_k} \tilde{\chi}_k \tilde{f}_f + \text{h. c.}$$

Each vertex comes along with the corresponding chirality projector:

$$\Gamma_{ff}^{\tilde{f}_s \tilde{\chi}_k} = \Gamma_{L,ff}^{\tilde{f}_s \tilde{\chi}_k} P_L + \Gamma_{R,ff}^{\tilde{f}_s \tilde{\chi}_k} P_R.$$

The mixing matrices diagonalize the mass matrices in the following manner:

- Chargino mixing: $\mathbf{Z}_-^T \mathcal{M}_C \mathbf{Z}_+ = (\mathcal{M}_C)^{\text{diag}}$,
- Neutralino mixing: $\mathbf{Z}_N^T \mathcal{M}_N \mathbf{Z}_N = (\mathcal{M}_N)^{\text{diag}}$,
- Slepton mixing: $\mathbf{W}_{\tilde{e}}^\dagger \mathcal{M}_{\tilde{e}}^2 \mathbf{W}_{\tilde{e}} = (\mathcal{M}_{\tilde{e}}^2)^{\text{diag}}$,
- Sneutrino mixing:

$$\mathcal{W}_{\tilde{\nu}}^\dagger \mathcal{M}_{\tilde{\nu}}^2 \mathcal{W}_{\tilde{\nu}} = \mathcal{W}_{\tilde{\nu}}^\dagger \mathcal{P}^\dagger \mathcal{M}_{\tilde{\nu}}^2 \mathcal{P} \mathcal{W}_{\tilde{\nu}} = (\mathcal{M}_{\tilde{\nu}}^2)^{\text{diag}},$$

such that $\mathcal{Z}_{\tilde{\nu}} = \mathcal{P} \mathcal{W}_{\tilde{\nu}}$ diagonalizes the original mass matrix $\mathcal{M}_{\tilde{\nu}}^2$ and therefore:

$$\mathcal{Z}_{is}^{\tilde{\nu}} = \frac{1}{\sqrt{2}} \left(\mathcal{W}_{is}^{\tilde{\nu}} + i \mathcal{W}_{i+3,s}^{\tilde{\nu}} \right) \quad \text{and} \\ \mathcal{Z}_{i+3,s}^{\tilde{\nu}} = \frac{1}{\sqrt{2}} \left(\mathcal{W}_{is}^{\tilde{\nu}} - i \mathcal{W}_{i+3,s}^{\tilde{\nu}} \right)$$

appear in the vertices of Eqs. (A.16).

- Neutrino mixing: The PMNS mixing matrix can be determined from the neutrino mass matrix $\hat{\mathbf{m}}_\nu = \mathbf{U}_{\text{PMNS}}^* \mathbf{m}_\nu \mathbf{U}_{\text{PMNS}}^\dagger$, where m_ν is the effective light neutrino mass matrix and the charged lepton masses can be taken diagonal (otherwise there would be a contribution to the PMNS mixing similar to the CKM mixing from both up and down sector: $\mathbf{U}_{\text{PMNS}} = \mathbf{V}_{e,L}^\dagger \mathbf{U}_{\nu,L}$, where $\mathbf{V}_{e,L}$ rotates the left-handed electron fields).

A.5 LOOP FUNCTIONS

The evaluation of the one-loop potential as well as the supersymmetric threshold corrections to neutrino masses and mixing needs standard scalar loop integrals. In all cases, only solutions with either $p_{\text{ext}}^2 = 0$ (approximation for neutrino self-energies with heavy SUSY loops) or no external momenta at all (effective potential) are needed. The n -point integrals in the sea-urchin derivation of the effective potential can be reduced to derivatives of tadpole integrals. We follow the notation of [216].

In dimensional regularization [395] the tadpole integral is given by

$$A_0(m) = \frac{1}{i\pi^2} \int d^4k \frac{1}{k^2 - m^2 + i0} \quad (\text{A.17})$$

$$\rightarrow \frac{Q^{2\varepsilon}}{i\pi^2} \int \frac{d^D k}{(2\pi)^{-2\varepsilon}} \frac{1}{k^2 - m^2 + i0},$$

with the arbitrary renormalization scale Q . The $i0$ prescription evades the singularities on the real axis and is omitted in the following propagators. Evaluation of the D -dimensional integral then yields

$$A_0(m) = m^2 \left(\Delta_\varepsilon - \ln \frac{m^2}{Q^2} + 1 \right) + \mathcal{O}(\varepsilon), \quad (\text{A.18})$$

with $\Delta_\varepsilon = \frac{1}{\varepsilon} - \gamma_E + \log 4\pi$. Where necessary, we work in the modified minimal subtraction ($\overline{\text{MS}}$) scheme and subtract Δ_ε (not only the pole $\frac{1}{\varepsilon}$) with the counterterms.

Similarly, the two-point integral is given by

$$B_0(p^2; m_1, m_2) = \frac{(2\pi Q)^{2\varepsilon}}{i\pi^2} \int \frac{d^D k}{(k^2 - m_1^2) ((k+p)^2 - m_2^2)}. \quad (\text{A.19})$$

The momentum independent three- and four-point functions are consequently

$$C_0(m_1, m_2, m_3) = \frac{(2\pi Q)^{2\varepsilon}}{i\pi^2} \int \frac{d^D k}{\mathcal{D}_1 \mathcal{D}_2 \mathcal{D}_3}, \quad (\text{A.20})$$

$$D_0(m_1, m_2, m_3, m_4) = \frac{(2\pi Q)^{2\varepsilon}}{i\pi^2} \int \frac{d^D k}{\mathcal{D}_1 \mathcal{D}_2 \mathcal{D}_3 \mathcal{D}_4}, \quad (\text{A.21})$$

with $\mathcal{D}_i = k^2 - m_i^2$.

The dimensionality of space-time is “reduced” to $D = 4 - 2\varepsilon$. Physical results are then obtained in the limit $\varepsilon \rightarrow 0$.

γ_E is the Euler constant, $\gamma_E \approx 0.577$.

We finally list the $\overline{\text{MS}}$ -subtracted expressions for the loop functions:

Results partially transferred from [89] and [85].

$$A_0(m) = m^2 - m^2 \ln \frac{m^2}{Q^2}, \quad (\text{A.22a})$$

$$B_0(m_1, m_2) = 1 - \frac{m_1^2 + m_2^2}{m_1^2 - m_2^2} \ln \frac{m_1}{m_2} - \ln \frac{m_1 m_2}{Q^2}, \quad (\text{A.22b})$$

$$B_1(m_1, m_2) = \frac{1}{2} \ln \frac{m_1 m_2}{Q^2} - \frac{3}{4} - \frac{m_2^2}{2(m_1^2 - m_2^2)} + \left(\frac{m_1^4}{(m_1^2 - m_2^2)^2} - \frac{1}{2} \right) \frac{m_1}{m_2}, \quad (\text{A.22c})$$

$$C_0(m_1, m_2, m_3) = \frac{m_1^2 m_2^2 \ln \frac{m_2^2}{m_1^2} + m_2^2 m_3^2 \ln \frac{m_3^2}{m_2^2} + m_1^2 m_3^2 \ln \frac{m_1^2}{m_3^2}}{(m_1^2 - m_2^2)(m_1^2 - m_3^2)(m_2^2 - m_3^2)} \quad (\text{A.22d})$$

$$D_0(m_1, m_2, m_3, m_4) = \frac{C_0(m_1, m_2, m_3) - C_0(m_1, m_2, m_4)}{m_3^2 - m_4^2}. \quad (\text{A.22e})$$

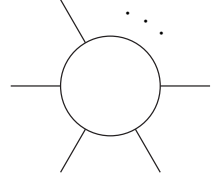
In Sec. 4.1.3, we calculate explicitly the 4-point function (and later n -point functions) for *equal* masses, $D_0(m, m, m, m)$. Obviously, there is a relation with $A_0(m) = \Xi \int \frac{d^D k}{k^2 - m^2}$

$$\Xi = \frac{(2\pi Q)^{2\epsilon}}{i\pi^2}$$

$$D_0(m, m, m, m) = \Xi \int \frac{d^D k}{(k^2 - m^2)^4} = \frac{1}{3!} \left(\frac{d}{dm^2} \right)^3 A_0(m).$$

This easily can be generalized to an n -point scalar integral:

$$I_n(m) = \Xi \int \frac{d^D k}{(k^2 - m^2)^n} = \frac{1}{(n-1)!} \left(\frac{d}{dm^2} \right)^{n-1} A_0(m).$$



On the other side, with $A_0(m) = m^2 - \ln(m^2/Q^2)$, we have

$$\begin{aligned} \frac{d}{dm^2} A_0(m) &= 1 - \frac{1}{m^2}, & \left(\frac{d}{dm^2} \right)^2 A_0(m) &= \frac{1}{(m^2)^2}, \\ \left(\frac{d}{dm^2} \right)^3 A_0(m) &= -\frac{2}{(m^2)^3}, & \left(\frac{d}{dm^2} \right)^4 A_0(m) &= \frac{6}{(m^2)^4} \\ \hookrightarrow \left(\frac{d}{dm^2} \right)^n A_0(m) &= (-1)^n \frac{(n-1)!}{(m^2)^n}. \end{aligned}$$

In combination, we can write

$$\begin{aligned} I_n(m) &= \frac{1}{(n-1)!} \left(\frac{d}{dm^2} \right)^{n-1} A_0(m) = \frac{(n-2)! (-1)^{n-1}}{(n-1)! (m^2)^{n-1}} \\ &= (-1)^{n-1} (n-1) / (m^2)^{n-1}. \end{aligned}$$

RELEVANT RENORMALIZATION GROUP EQUATIONS IN THE SM AND BEYOND

B.1 SM WITH HEAVY SINGLET NEUTRINOS

Unfortunately, all RG including heavy Majorana singlets without SUSY are only available to one-loop order. In the MSSM, two-loop results exist. We nevertheless exploit the two-loop RGE for the SM (without heavy singlets) and add the neutrino part above the threshold to one-loop order. The RGE used for the study of the RGI potential are given by the following equations with $t = \ln(Q/Q_0)$ with some arbitrary but fixed scale Q_0 .

$$\begin{aligned}
\frac{d\lambda}{dt} = & \frac{1}{16\pi^2} \left(-Y_\tau^4 - d_R Y_b^4 + \frac{9}{16} g_2^4 + \frac{3}{8} g_1^2 g_2^2 + \frac{3}{16} g_1^4 \right. & \text{(B.1a)} \\
& + 2\lambda Y_\tau^2 + 2d_R \lambda Y_b^2 - \frac{9}{2} \lambda g_2^2 - \frac{3}{2} \lambda g_1^2 + 12\lambda^2 - 2d_R Y_t^2 \lambda + Y_t^4 \Big) \\
& + \frac{1}{(16\pi^2)^2} \left(5Y_\tau^6 + 5d_R Y_b^6 - \frac{3}{8} g_2^4 Y_\tau^2 - \frac{3}{8} d_R g_2^4 Y_b^2 \right. \\
& + g_2^6 \left(\frac{497}{32} - \frac{1}{2} N_G - \frac{1}{2} N_G d_R \right) - 2g_1^2 Y_\tau^4 + \frac{2}{9} d_R g_1^2 Y_b^4 \\
& + \frac{11}{4} g_1^2 g_2^2 Y_\tau^2 + \frac{3}{4} d_R g_1^2 g_2^2 Y_b^2 - g_1^2 g_2^4 \left(\frac{97}{96} + \frac{1}{6} N_G + \frac{1}{6} N_G d_R \right) \\
& - \frac{25}{8} g_1^4 Y_\tau^2 + \frac{5}{24} d_R g_1^4 Y_b^2 - g_1^4 g_2^2 \left(\frac{239}{96} + \frac{1}{2} N_G + \frac{11}{54} N_G d_R \right) \\
& - g_1^6 \left(\frac{59}{96} + \frac{1}{2} N_G + \frac{11}{54} N_G d_R \right) - \frac{1}{2} \lambda Y_\tau^4 - \frac{1}{2} d_R \lambda Y_b^4 \\
& + \frac{15}{4} \lambda g_2^2 Y_\tau^2 + \frac{15}{4} d_R \lambda g_2^2 Y_b^2 - \lambda g_2^4 \left(\frac{313}{16} - \frac{5}{4} N_G - \frac{5}{4} N_G d_R \right) \\
& + \frac{25}{4} \lambda g_1^2 Y_\tau^2 + \frac{25}{36} d_R \lambda g_1^2 Y_b^2 + \frac{39}{8} \lambda g_1^2 g_2^2 \\
& + \lambda g_1^4 \left(\frac{229}{48} + \frac{5}{4} N_G + \frac{55}{108} N_G d_R \right) - 24\lambda^2 Y_\tau^2 - 24d_R \lambda^2 Y_b^2 \\
& + 54\lambda^2 g_2^2 + 18\lambda^2 g_1^2 - 156\lambda^3 - d_R Y_t^2 Y_b^4 - \frac{3}{8} d_R Y_t^2 g_2^4 + \frac{7}{4} d_R Y_t^2 g_1^2 g_2^2 \\
& - \frac{19}{24} d_R Y_t^2 g_1^4 - 7d_R Y_t^2 \lambda Y_b^2 + \frac{15}{4} d_R Y_t^2 \lambda g_2^2 + \frac{85}{36} d_R Y_t^2 \lambda g_1^2 \\
& - 24d_R Y_t^2 \lambda^2 - d_R Y_t^4 Y_b^2 - \frac{4}{9} d_R Y_t^4 g_1^2 - \frac{1}{2} d_R Y_t^4 \lambda + 5d_R Y_t^6 \\
& - 4C_f d_r g_3^2 Y_b^4 + 10C_f d_R g_3^2 \lambda Y_b^2 + 10C_f d_R g_3^2 Y_t^2 \lambda - 4C_f d_R g_3^2 Y_t^4 \Big) \\
& + \frac{\theta(Q - M_R)}{16\pi^2} \left(\lambda Y_\nu^2 - 2Y_\nu^4 \right),
\end{aligned}$$

We are using the β function for the Higgs self-coupling as provided by [396] with $h = 1/16\pi^2$, $d_R = 3$, $N_G = 3$, $C_f = 4/3$.

$$\frac{d\kappa}{dt} = \frac{1}{16\pi^2} \left(-Y_e^2 + 6Y_t^2 + 6Y_b^2 - 3g_2^2 + \lambda + \theta(Q - M_R)3Y_\nu^2 \right) \kappa, \quad (\text{B.1b})$$

$$\frac{dM_R}{dt} = \frac{1}{16\pi^2} \left(2Y_\nu^2 M_R \theta(Q - M_R), \right) \quad (\text{B.1c})$$

$$\frac{dY_\nu}{dt} = \frac{1}{16\pi^2} \theta(Q - M_R) \left(\frac{5}{2}Y_\nu^2 - \frac{1}{2}Y_e^2 + 3Y_t^2 + 3Y_b^2 - \frac{9}{20}g_1^2 - \frac{9}{4}g_2^2 \right) Y_\nu, \quad (\text{B.1d})$$

$$\frac{dY_e}{dt} = \frac{1}{16\pi^2} Y_e \left(\frac{5}{2}Y_e^2 + 3Y_b^2 + 3Y_t^2 - \theta(Q - M_R) \frac{1}{2}Y_\nu^2 - \frac{9}{4}g_1^2 - \frac{9}{4}g_2^2 \right), \quad (\text{B.1e})$$

$$\frac{dY_b}{dt} = \frac{1}{16\pi^2} Y_b \left(\frac{9}{2}Y_b^2 + \frac{3}{2}Y_t^2 + Y_e^2 + \theta(Q - M_R)Y_\nu^2 - \frac{1}{4}g_1^2 - \frac{9}{4}g_2^2 - 8g_3^2 \right), \quad (\text{B.1f})$$

$$\frac{dY_t}{dt} = \frac{1}{16\pi^2} Y_t \left(\frac{9}{2}Y_t^2 + \frac{3}{2}Y_b^2 + Y_e^2 + \theta(Q - M_R)Y_\nu^2 - \frac{17}{20}g_1^2 - \frac{9}{4}g_2^2 - 8g_3^2 \right), \quad (\text{B.1g})$$

$$\frac{dg_1}{dt} = \frac{1}{16\pi^2} \frac{41}{10} g_1^3, \quad (\text{B.1h})$$

$$\frac{dg_2}{dt} = -\frac{1}{16\pi^2} \frac{19}{16} g_2^3, \quad (\text{B.1i})$$

$$\frac{dg_3}{dt} = -\frac{1}{16\pi^2} 7g_3^3. \quad (\text{B.1j})$$

B.2 MSSM WITH HEAVY SINGLET NEUTRINOS

Singlet neutrinos do not influence the gauge couplings at one loop. However, there is a significant impact for the two-loop RGE [397]:

$$\begin{aligned} \frac{d g_1}{d t} = & \frac{1}{16\pi^2} \frac{33}{5} g_1^3 + \frac{1}{(16\pi^2)^2} \left(\frac{199}{25} g_1^5 + \frac{27}{5} g_1^3 g_2^2 + \frac{88}{5} g_1^3 g_3^2 \right. \\ & \left. - \frac{26}{5} Y_t^2 g_1^3 - \frac{6}{5} \theta(Q - M_R) Y_\nu^2 g_1^3 \right), \end{aligned} \quad (\text{B.2a})$$

$$\begin{aligned} \frac{d g_2}{d t} = & \frac{1}{16\pi^2} g_2^3 + \frac{1}{(16\pi^2)^2} \left(\frac{9}{5} g_1^2 g_2^3 + 25 g_2^5 + 24 g_2^3 g_3^2 - 6 Y_t^2 g_2^3 \right. \\ & \left. - 2 \theta(Q - M_R) Y_\nu^2 g_2^3 \right), \end{aligned} \quad (\text{B.2b})$$

$$\begin{aligned} \frac{d g_3}{d t} = & \frac{1}{16\pi^2} (-3 g_3^3) + \\ & \frac{1}{(16\pi^2)^2} \left(\frac{11}{5} g_1^2 g_3^3 + 9 g_3^3 g_2^2 + 14 g_3^5 - 4 Y_t^2 g_3^3 \right). \end{aligned} \quad (\text{B.2c})$$

Two-loop RGE for neutrino parameters in various seesaw models can be found in [165], especially the equations for the MSSM extended by singlet neutrinos:

$$\begin{aligned} \frac{d Y_t}{d t} = & \frac{1}{16\pi^2} \left(\left(-\frac{13}{15} g_1^2 - 3 g_2^2 - \frac{16}{3} g_3^2 \right) Y_t + 6 Y_t^3 + Y_b^2 Y_t \right. \\ & \left. + \theta(Q - M_R) Y_\nu^2 Y_t \right) + \frac{1}{(16\pi^2)^2} \left(Y_t \left(-2 Y_b^4 - 2 Y_b^2 Y_t^2 - 4 Y_t^4 \right. \right. \\ & \left. \left. - 3 Y_b^4 - Y_b^2 Y_e^2 - 9 Y_t^4 - \theta(Q - M_R) (Y_\nu^2 Y_e^2 - 3 Y_\nu^4) + \frac{2}{5} g_1^2 Y_b^2 \right. \right. \\ & \left. \left. + \frac{2}{5} g_1^2 Y_t^2 + 6 g_2^2 Y_t^2 + \frac{4}{5} g_1^2 Y_t^2 + 16 g_3^2 Y_t^2 + \frac{2743}{450} g_1^4 \right. \right. \\ & \left. \left. + g_1^2 g_2^2 + \frac{15}{2} g_2^4 + \frac{136}{45} g_1^2 g_3^2 + 8 g_2^2 g_3^2 - \frac{16}{9} g_3^4 \right) \right), \end{aligned} \quad (\text{B.2d})$$

$$\begin{aligned} \frac{d Y_b}{d t} = & \frac{1}{16\pi^2} \left(\left(-\frac{7}{15} g_1^2 - 3 g_2^2 - \frac{16}{3} g_3^2 \right) Y_b + 6 Y_b^3 + Y_t^2 Y_b + Y_e^2 Y_b \right) \\ & + \frac{1}{(16\pi^2)^2} \left(Y_b \left(-4 Y_b^4 - 2 Y_t^2 Y_b^2 - 2 Y_t^4 - 9 Y_b^4 - 3 Y_t^2 Y_b^2 \right. \right. \\ & \left. \left. - 3 Y_e^4 - \theta(Q - M_R) (Y_e^2 Y_\nu^2 + Y_t^2 Y_\nu^2) - 9 Y_b^4 - 3 Y_b^2 Y_e^2 - 3 Y_t^4 \right. \right. \\ & \left. \left. + g_2^2 Y_b^2 + \frac{4}{5} g_1^2 Y_b^2 + \frac{4}{5} g_1^2 Y_t^2 - \frac{2}{5} g_1^2 Y_b^2 + \frac{6}{5} g_1^2 Y_e^2 + 16 g_3^2 Y_b^2 \right. \right. \\ & \left. \left. + \frac{587}{90} g_1^4 + g_1^2 g_2^2 + \frac{15}{2} g_2^4 + \frac{8}{9} g_1^2 g_3^2 + 8 g_2^2 g_3^2 - \frac{16}{9} g_3^4 \right) \right), \end{aligned} \quad (\text{B.2e})$$

$$\begin{aligned}
\frac{dY_e}{dt} = & \frac{1}{16\pi^2} \left(\left(-\frac{9}{5}g_1^2 - 3g_2^2 \right) Y_e + 3Y_b^2 Y_e + 4Y_e^3 \right. \\
& \left. + \theta(Q - M_R) Y_\nu^2 Y_e \right) + \frac{1}{(16\pi^2)^2} \left(Y_e \left(-4Y_e^4 - 9Y_e^2 Y_b^2 \right. \right. \\
& - 3Y_e^4 - 9Y_b^4 - 3Y_b^2 Y_t^2 - 3Y_e^4 - \theta(Q - M_R) (3Y_\nu^2 Y_e^2 + 2Y_\nu^4 \\
& + Y_\nu^4 + 3Y_\nu^2 Y_t^2) + \frac{6}{5}g_1^2 Y_e^2 + 6g_2^2 Y_e^2 \\
& \left. \left. - \frac{2}{5}g_1^2 Y_b^2 + 16g_3^2 Y_b^2 + \frac{27}{2}g_1^4 + \frac{9}{5}g_1^2 g_2^2 + \frac{15}{2}g_2^4 \right) \right), \quad (\text{B.2f})
\end{aligned}$$

$$\begin{aligned}
\frac{dY_\nu}{dt} = & \theta(Q - M_R) \frac{1}{16\pi^2} \left(\left(-\frac{3}{5}g_1^2 - 3g_2^2 \right) Y_\nu + 4Y_\nu^3 + Y_e^2 Y_\nu \right. \\
& \left. + 3Y_t^2 Y_\nu \right) + \frac{1}{(16\pi^2)^2} \left(Y_\nu \left(-2Y_e^4 - 2Y_e^2 Y_\nu^2 - 4Y_\nu^4 \right. \right. \\
& - 3Y_e^2 Y_b^2 - Y_e^4 - 3Y_\nu^4 - 9Y_\nu^2 Y_t^2 - Y_\nu^2 Y_e^2 - 3Y_\nu^4 - 3Y_b^2 Y_t^2 \\
& - 9Y_t^4 + \frac{6}{5}g_1^2 Y_e^2 + \frac{6}{5}g_1^2 Y_\nu^2 + 6g_2^2 Y_\nu^2 + \frac{4}{5}g_1^2 Y_t^2 + 16g_3^2 Y_t^2 \\
& \left. \left. + \frac{207}{50}g_1^4 + \frac{9}{5}g_1^2 g_2^2 + \frac{15}{2}g_2^4 \right) \right), \quad (\text{B.2g})
\end{aligned}$$

$$\begin{aligned}
\frac{dM_R}{dt} = & \theta(Q - M_R) \left(\frac{1}{16\pi^2} 4M_R Y_\nu^2 + \frac{1}{(16\pi^2)^2} 2M_R (2Y_\nu^2 Y_e^2 - 2Y_\nu^4 \right. \\
& \left. - 6Y_\nu^2 Y_t^2 - 2Y_\nu^4 + \frac{6}{5}g_1^2 Y_\nu^2 + 6g_2^2 Y_\nu^2) \right), \quad (\text{B.2h})
\end{aligned}$$

$$\begin{aligned}
\frac{d\kappa}{dt} = & \frac{1}{16\pi^2} \left(2Y_e^2 \kappa + 6Y_t \kappa - \left(\frac{6}{5}g_1^2 + 6g_2^2 \right) \kappa \right) + \frac{1}{(16\pi^2)^2} \times \\
& \left(\left(-6Y_t^2 Y_b^2 - 18Y_t^4 - (2Y_e^2 Y_\nu^2 + 6Y_\nu^4) \theta(Q - M_R) + \frac{8}{5}g_1^2 Y_t^2 \right. \right. \\
& + 32g_2^2 Y_t^2 + \frac{207}{25}g_1^4 + \frac{18}{5}g_1^2 g_2^2 + 15g_2^4) \kappa - \kappa (4Y_e^4 + \\
& \left. \left. 2(-\frac{6}{5}g_1^2 + Y_e^2 + 3Y_b^2) Y_e^2 + 2\theta(Q - M_R) (4Y_\nu^4 + 3Y_t^2 Y_\nu^2) \right) \right). \quad (\text{B.2i})
\end{aligned}$$

BIBLIOGRAPHY

- [1] **PLANCK Collaboration**, P. Ade *et al.*, “Planck 2015 results. XIII. Cosmological parameters”, [arXiv:1502.01589 \[astro-ph.CO\]](#).
- [2] B. W. Lee and S. Weinberg, “Cosmological Lower Bound on Heavy Neutrino Masses”, *Phys.Rev.Lett.* **39** (1977) 165–168.
- [3] G. Jungman, M. Kamionkowski, and K. Griest, “Supersymmetric dark matter”, *Phys.Rept.* **267** (1996) 195–373, [arXiv:hep-ph/9506380 \[hep-ph\]](#).
- [4] S. Glashow, “Partial Symmetries of Weak Interactions”, *Nucl.Phys.* **22** (1961) 579–588.
- [5] S. Weinberg, “A Model of Leptons”, *Phys.Rev.Lett.* **19** (1967) 1264–1266.
- [6] A. Salam, “Weak and Electromagnetic Interactions”, in *8th Nobel Symposium: Elementary Particle Theory*, M. Svartholm, ed. 1968.
- [7] H. Fritzsch and M. Gell-Mann, “Current algebra: Quarks and what else?”, in *Proceedings of the 16th International Conference on High-Energy Physics*, J. Jackson and A. Roberts, eds. 1972. [hep-ph/0208010](#).
- [8] H. Fritzsch, M. Gell-Mann, and H. Leutwyler, “Advantages of the Color Octet Gluon Picture”, *Phys.Lett.* **B47** (1973) 365–368.
- [9] J. Goldstone, “Field Theories with Superconductor Solutions”, *Nuovo Cim.* **19** (1961) 154–164.
- [10] J. Goldstone, A. Salam, and S. Weinberg, “Broken Symmetries”, *Phys.Rev.* **127** (1962) 965–970.
- [11] P. W. Higgs, “Broken symmetries, massless particles and gauge fields”, *Phys.Lett.* **12** (1964) 132–133.
- [12] P. W. Higgs, “Broken Symmetries and the Masses of Gauge Bosons”, *Phys.Rev.Lett.* **13** (1964) 508–509.
- [13] F. Englert and R. Brout, “Broken Symmetry and the Mass of Gauge Vector Mesons”, *Phys.Rev.Lett.* **13** (1964) 321–323.
- [14] G. Guralnik, C. Hagen, and T. Kibble, “Global Conservation Laws and Massless Particles”, *Phys.Rev.Lett.* **13** (1964) 585–587.
- [15] **ATLAS Collaboration**, G. Aad *et al.*, “Observation of a new particle in the search for the Standard Model Higgs boson with the ATLAS detector at the LHC”, *Phys.Lett.* **B716** (2012) 1–29, [arXiv:1207.7214 \[hep-ex\]](#).
- [16] **CMS Collaboration**, S. Chatrchyan *et al.*, “Observation of a new boson at a mass of 125 GeV with the CMS experiment at the LHC”, *Phys.Lett.* **B716** (2012) 30–61, [arXiv:1207.7235 \[hep-ex\]](#).
- [17] L. Ryder, *Quantum Field Theory*. Cambridge University Press, 1985.
- [18] M. E. Peskin and D. V. Schroeder, *An Introduction to quantum field theory*. Westview Press, 1995.
- [19] O. Eberhardt, G. Herbert, H. Lacker, A. Lenz, A. Menzel, *et al.*, “Impact of a Higgs boson at a mass of 126 GeV on the standard model with three and four fermion generations”, *Phys.Rev.Lett.* **109** (2012) 241802, [arXiv:1209.1101 \[hep-ph\]](#).
- [20] N. Cabibbo, “Unitary Symmetry and Leptonic Decays”, *Phys.Rev.Lett.* **10** (1963) 531–533.
- [21] M. Kobayashi and T. Maskawa, “CP Violation in the Renormalizable Theory of Weak Interaction”, *Prog.Theor.Phys.* **49** (1973) 652–657.

- [22] L.-L. Chau and W.-Y. Keung, “Comments on the Parametrization of the Kobayashi-Maskawa Matrix”, *Phys.Rev.Lett.* **53** (1984) 1802.
- [23] **Particle Data Group**, K. Olive *et al.*, “Review of Particle Physics”, *Chin.Phys.* **C38** (2014) 090001.
- [24] R. Mohapatra, S. Antusch, K. Babu, G. Barenboim, M.-C. Chen, *et al.*, “Theory of neutrinos: A White paper”, *Rept.Prog.Phys.* **70** (2007) 1757–1867, [arXiv:hep-ph/0510213 \[hep-ph\]](#).
- [25] H. Kalka and G. Soff, *Supersymmetrie*. Teubner, 1997.
- [26] S. R. Coleman and J. Mandula, “All Possible Symmetries of the S Matrix”, *Phys.Rev.* **159** (1967) 1251–1256.
- [27] R. Haag, J. T. Lopuszanski, and M. Sohnius, “All Possible Generators of Supersymmetries of the S Matrix”, *Nucl.Phys.* **B88** (1975) 257.
- [28] J. Wess, “From symmetry to supersymmetry”, *The European Physical Journal C* **59** no. 2, (2009) 177–183.
- [29] V. Gates, E. Kangaroo, M. Roachcock, and W. Gall, “Stuperspace”, *Physica* **15D** (1985) 289–293.
- [30] J. Wess and J. Bagger, *Supersymmetry and supergravity*. Princeton University Press, 1992.
- [31] J. Wess and B. Zumino, “Supergauge Transformations in Four-Dimensions”, *Nucl.Phys.* **B70** (1974) 39–50.
- [32] M. Drees, R. Godbole, and P. Roy, *Theory and phenomenology of sparticles: An account of four-dimensional N=1 supersymmetry in high energy physics*. World Scientific Publishing, 2004.
- [33] E. Witten, “Dynamical Breaking of Supersymmetry”, *Nucl.Phys.* **B188** (1981) 513.
- [34] I. Affleck, M. Dine, and N. Seiberg, “Dynamical Supersymmetry Breaking in Supersymmetric QCD”, *Nucl.Phys.* **B241** (1984) 493–534.
- [35] I. Affleck, M. Dine, and N. Seiberg, “Dynamical Supersymmetry Breaking in Four-Dimensions and Its Phenomenological Implications”, *Nucl.Phys.* **B256** (1985) 557.
- [36] M. Dine and A. E. Nelson, “Dynamical supersymmetry breaking at low-energies”, *Phys.Rev.* **D48** (1993) 1277–1287, [arXiv:hep-ph/9303230 \[hep-ph\]](#).
- [37] K. A. Intriligator, N. Seiberg, and D. Shih, “Dynamical SUSY breaking in meta-stable vacua”, *JHEP* **0604** (2006) 021, [arXiv:hep-th/0602239 \[hep-th\]](#).
- [38] L. O’Raifeartaigh, “Spontaneous Symmetry Breaking for Chiral Scalar Superfields”, *Nucl.Phys.* **B96** (1975) 331.
- [39] P. Fayet and J. Iliopoulos, “Spontaneously Broken Supergauge Symmetries and Goldstone Spinors”, *Phys.Lett.* **B51** (1974) 461–464.
- [40] G. Giudice and R. Rattazzi, “Theories with gauge mediated supersymmetry breaking”, *Phys.Rept.* **322** (1999) 419–499, [arXiv:hep-ph/9801271 \[hep-ph\]](#).
- [41] M. Dine, W. Fischler, and M. Srednicki, “Supersymmetric Technicolor”, *Nucl.Phys.* **B189** (1981) 575–593.
- [42] S. Dimopoulos and S. Raby, “Supercolor”, *Nucl.Phys.* **B192** (1981) 353.
- [43] S. Weinberg, “Implications of Dynamical Symmetry Breaking”, *Phys.Rev.* **D13** (1976) 974–996.
- [44] L. Susskind, “Dynamics of Spontaneous Symmetry Breaking in the Weinberg-Salam Theory”, *Phys.Rev.* **D20** (1979) 2619–2625.
- [45] S. Dimopoulos and L. Susskind, “Mass Without Scalars”, *Nucl.Phys.* **B155** (1979) 237–252.
- [46] G. F. Giudice, M. A. Luty, H. Murayama, and R. Rattazzi, “Gaugino mass without singlets”, *JHEP* **9812** (1998) 027, [arXiv:hep-ph/9810442 \[hep-ph\]](#).
- [47] L. Randall and R. Sundrum, “Out of this world supersymmetry breaking”, *Nucl.Phys.* **B557** (1999) 79–118, [arXiv:hep-th/9810155 \[hep-th\]](#).

- [48] A. H. Chamseddine, R. L. Arnowitt, and P. Nath, “Locally Supersymmetric Grand Unification”, *Phys.Rev.Lett.* **49** (1982) 970.
- [49] A. Arbey, M. Battaglia, A. Djouadi, F. Mahmoudi, and J. Quevillon, “Implications of a 125 GeV Higgs for supersymmetric models”, *Phys.Lett.* **B708** (2012) 162–169, [arXiv:1112.3028 \[hep-ph\]](#).
- [50] L. Girardello and M. T. Grisaru, “Soft Breaking of Supersymmetry”, *Nucl.Phys.* **B194** (1982) 65.
- [51] L. Hall and L. Randall, “Weak scale effective supersymmetry”, *Phys.Rev.Lett.* **65** (1990) 2939–2942.
- [52] P. Fayet, “Supergauge Invariant Extension of the Higgs Mechanism and a Model for the electron and Its Neutrino”, *Nucl.Phys.* **B90** (1975) 104–124.
- [53] H. E. Haber and G. L. Kane, “The Search for Supersymmetry: Probing Physics Beyond the Standard Model”, *Phys.Rept.* **117** (1985) 75–263.
- [54] H. P. Nilles, “Supersymmetry, Supergravity and Particle Physics”, *Phys.Rept.* **110** (1984) 1–162.
- [55] G. Giudice and A. Masiero, “A Natural Solution to the mu Problem in Supergravity Theories”, *Phys.Lett.* **B206** (1988) 480–484.
- [56] J. R. Ellis, J. Gunion, H. E. Haber, L. Roszkowski, and F. Zwirner, “Higgs Bosons in a Nonminimal Supersymmetric Model”, *Phys.Rev.* **D39** (1989) 844.
- [57] H. E. Haber, “Higgs boson masses and couplings in the minimal supersymmetric model”, in *Perspectives on Higgs Physics II*, G. Kane, ed. World Scientific, Singapore, 1997. and references therein.
- [58] J. F. Gunion and H. E. Haber, “The CP conserving two Higgs doublet model: The Approach to the decoupling limit”, *Phys.Rev.* **D67** (2003) 075019, [arXiv:hep-ph/0207010 \[hep-ph\]](#).
- [59] H. E. Haber and R. Hempfling, “Can the mass of the lightest Higgs boson of the minimal supersymmetric model be larger than m_Z ?”, *Phys.Rev.Lett.* **66** (1991) 1815–1818.
- [60] J. R. Ellis, G. Ridolfi, and F. Zwirner, “Radiative corrections to the masses of supersymmetric Higgs bosons”, *Phys.Lett.* **B257** (1991) 83–91.
- [61] Y. Okada, M. Yamaguchi, and T. Yanagida, “Upper bound of the lightest Higgs boson mass in the minimal supersymmetric standard model”, *Prog.Theor.Phys.* **85(1)** (1991) 1–6.
- [62] J. R. Ellis, G. Ridolfi, and F. Zwirner, “On radiative corrections to supersymmetric Higgs boson masses and their implications for LEP searches”, *Phys.Lett.* **B262** (1991) 477–484.
- [63] R. Hempfling and A. H. Hoang, “Two loop radiative corrections to the upper limit of the lightest Higgs boson mass in the minimal supersymmetric model”, *Phys.Lett.* **B331** (1994) 99–106, [arXiv:hep-ph/9401219 \[hep-ph\]](#).
- [64] S. Heinemeyer, W. Hollik, and G. Weiglein, “QCD corrections to the masses of the neutral CP - even Higgs bosons in the MSSM”, *Phys.Rev.* **D58** (1998) 091701, [arXiv:hep-ph/9803277 \[hep-ph\]](#).
- [65] S. Heinemeyer, W. Hollik, and G. Weiglein, “Precise prediction for the mass of the lightest Higgs boson in the MSSM”, *Phys.Lett.* **B440** (1998) 296–304, [arXiv:hep-ph/9807423 \[hep-ph\]](#).
- [66] S. Heinemeyer, W. Hollik, and G. Weiglein, “The Masses of the neutral CP - even Higgs bosons in the MSSM: Accurate analysis at the two loop level”, *Eur.Phys.J.* **C9** (1999) 343–366, [arXiv:hep-ph/9812472 \[hep-ph\]](#).
- [67] J. Espinosa and M. Quiros, “Two loop radiative corrections to the mass of the lightest Higgs boson in supersymmetric standard models”, *Phys.Lett.* **B266** (1991) 389–396.
- [68] H. E. Haber and R. Hempfling, “The Renormalization group improved Higgs sector of the minimal supersymmetric model”, *Phys.Rev.* **D48** (1993) 4280–4309, [arXiv:hep-ph/9307201 \[hep-ph\]](#).

- [69] J. Casas, J. Espinosa, M. Quiros, and A. Riotto, “The Lightest Higgs boson mass in the minimal supersymmetric standard model”, *Nucl.Phys.* **B436** (1995) 3–29, [arXiv:hep-ph/9407389 \[hep-ph\]](#).
- [70] M. S. Carena, J. Espinosa, M. Quiros, and C. Wagner, “Analytical expressions for radiatively corrected Higgs masses and couplings in the MSSM”, *Phys.Lett.* **B355** (1995) 209–221, [arXiv:hep-ph/9504316 \[hep-ph\]](#).
- [71] M. S. Carena, M. Quiros, and C. Wagner, “Effective potential methods and the Higgs mass spectrum in the MSSM”, *Nucl.Phys.* **B461** (1996) 407–436, [arXiv:hep-ph/9508343 \[hep-ph\]](#).
- [72] H. E. Haber, R. Hempfling, and A. H. Hoang, “Approximating the radiatively corrected Higgs mass in the minimal supersymmetric model”, *Z.Phys.* **C75** (1997) 539–554, [arXiv:hep-ph/9609331 \[hep-ph\]](#).
- [73] M. S. Carena, H. Haber, S. Heinemeyer, W. Hollik, C. Wagner, *et al.*, “Reconciling the two loop diagrammatic and effective field theory computations of the mass of the lightest CP - even Higgs boson in the MSSM”, *Nucl.Phys.* **B580** (2000) 29–57, [arXiv:hep-ph/0001002 \[hep-ph\]](#).
- [74] S. Heinemeyer, W. Hollik, and G. Weiglein, “FeynHiggs: A Program for the calculation of the masses of the neutral CP even Higgs bosons in the MSSM”, *Comput.Phys.Commun.* **124** (2000) 76–89, [arXiv:hep-ph/9812320 \[hep-ph\]](#).
- [75] G. Degrandi, S. Heinemeyer, W. Hollik, P. Slavich, and G. Weiglein, “Towards high precision predictions for the MSSM Higgs sector”, *Eur.Phys.J.* **C28** (2003) 133–143, [arXiv:hep-ph/0212020 \[hep-ph\]](#).
- [76] M. Frank, T. Hahn, S. Heinemeyer, W. Hollik, H. Rzehak, *et al.*, “The Higgs Boson Masses and Mixings of the Complex MSSM in the Feynman-Diagrammatic Approach”, *JHEP* **0702** (2007) 047, [arXiv:hep-ph/0611326 \[hep-ph\]](#).
- [77] T. Hahn, S. Heinemeyer, W. Hollik, H. Rzehak, and G. Weiglein, “High-precision predictions for the light CP-even Higgs Boson Mass of the MSSM”, [arXiv:1312.4937 \[hep-ph\]](#).
- [78] B. Allanach, “SOFTSUSY: a program for calculating supersymmetric spectra”, *Comput.Phys.Commun.* **143** (2002) 305–331, [arXiv:hep-ph/0104145 \[hep-ph\]](#).
- [79] A. Djouadi, J.-L. Kneur, and G. Moultaka, “SuSpect: A Fortran code for the supersymmetric and Higgs particle spectrum in the MSSM”, *Comput.Phys.Commun.* **176** (2007) 426–455, [arXiv:hep-ph/0211331 \[hep-ph\]](#).
- [80] W. Porod, “SPheno, a program for calculating supersymmetric spectra, SUSY particle decays and SUSY particle production at e^+e^- colliders”, *Comput.Phys.Commun.* **153** (2003) 275–315, [arXiv:hep-ph/0301101 \[hep-ph\]](#).
- [81] R. Harlander, P. Kant, L. Mihaila, and M. Steinhauser, “Higgs boson mass in supersymmetry to three loops”, *Phys.Rev.Lett.* **100** (2008) 191602, [arXiv:0803.0672 \[hep-ph\]](#).
- [82] P. Kant, R. Harlander, L. Mihaila, and M. Steinhauser, “Light MSSM Higgs boson mass to three-loop accuracy”, *JHEP* **1008** (2010) 104, [arXiv:1005.5709 \[hep-ph\]](#).
- [83] J. L. Feng, P. Kant, S. Profumo, and D. Sanford, “Three-Loop Corrections to the Higgs Boson Mass and Implications for Supersymmetry at the LHC”, *Phys.Rev.Lett.* **111** (2013) 131802, [arXiv:1306.2318 \[hep-ph\]](#).
- [84] P. Marquard and N. Zerf, “SLAM, a Mathematica interface for SUSY spectrum generators”, *Comput.Phys.Commun.* **185** (2014) 1153–1171, [arXiv:1309.1731 \[hep-ph\]](#).
- [85] M. Gorbahn, S. Jager, U. Nierste, and S. Trine, “The supersymmetric Higgs sector and $B - \bar{B}$ mixing for large $\tan \beta$ ”, *Phys.Rev.* **D84** (2011) 034030, [arXiv:0901.2065 \[hep-ph\]](#).
- [86] S. M. Barr and A. Zee, “A New Approach to the electron-Muon Mass Ratio”, *Phys.Rev.* **D15** (1977) 2652.

- [87] J. Ferrandis, “Radiative mass generation and suppression of supersymmetric contributions to flavor changing processes”, *Phys.Rev.* **D70** (2004) 055002, [arXiv:hep-ph/0404068 \[hep-ph\]](#).
- [88] J. Ferrandis and N. Haba, “Supersymmetry breaking as the origin of flavor”, *Phys.Rev.* **D70** (2004) 055003, [arXiv:hep-ph/0404077 \[hep-ph\]](#).
- [89] A. Crivellin and U. Nierste, “Supersymmetric renormalisation of the CKM matrix and new constraints on the squark mass matrices”, *Phys.Rev.* **D79** (2009) 035018, [arXiv:0810.1613 \[hep-ph\]](#).
- [90] A. Crivellin, “CKM Elements from Squark Gluino Loops”, [arXiv:0905.3130 \[hep-ph\]](#).
- [91] A. Crivellin, L. Hofer, and U. Nierste, “The MSSM with a Softly Broken $U(2)^3$ Flavor Symmetry”, vol. EPS-HEP2011, p. 145. PoS, 2011. [arXiv:1111.0246 \[hep-ph\]](#).
- [92] W. Altmannshofer, C. Frugiuele, and R. Harnik, “Fermion Hierarchy from Sfermion Anarchy”, *JHEP* **1412** (2014) 180, [arXiv:1409.2522 \[hep-ph\]](#).
- [93] S. Weinberg, “Electromagnetic and weak masses”, *Phys.Rev.Lett.* **29** (1972) 388–392.
- [94] G. Segre, “Mass Generation by Radiative Corrections in Minimal $SO(10)$ ”, *Phys.Lett.* **B103** (1981) 355–358.
- [95] L. E. Ibanez, “Hierarchical Suppression of Radiative Quark and Lepton Masses in Supersymmetric GUTs”, *Phys.Lett.* **B117** (1982) 403.
- [96] L. E. Ibanez, “Radiative Fermion Masses in Grand Unified Theories”, *Nucl.Phys.* **B193** (1981) 317.
- [97] T. Banks, “Supersymmetry and the Quark Mass Matrix”, *Nucl.Phys.* **B303** (1988) 172.
- [98] E. Ma, “Radiative Quark and Lepton Masses Through Soft Supersymmetry Breaking”, *Phys.Rev.* **D39** (1989) 1922.
- [99] F. Borzumati, G. R. Farrar, N. Polonsky, and S. D. Thomas, “Soft Yukawa couplings in supersymmetric theories”, *Nucl.Phys.* **B555** (1999) 53–115, [arXiv:hep-ph/9902443 \[hep-ph\]](#).
- [100] R. Hempfling, “Yukawa coupling unification with supersymmetric threshold corrections”, *Phys.Rev.* **D49** (1994) 6168–6172.
- [101] L. J. Hall, V. A. Kostelecky, and S. Raby, “New Flavor Violations in Supergravity Models”, *Nucl.Phys.* **B267** (1986) 415.
- [102] A. Crivellin and U. Nierste, “Chirally enhanced corrections to FCNC processes in the generic MSSM”, *Phys.Rev.* **D81** (2010) 095007, [arXiv:0908.4404 \[hep-ph\]](#).
- [103] A. Crivellin and J. Girrbach, “Constraining the MSSM sfermion mass matrices with light fermion masses”, *Phys.Rev.* **D81** (2010) 076001, [arXiv:1002.0227 \[hep-ph\]](#).
- [104] A. Crivellin, L. Hofer, U. Nierste, and D. Scherer, “Phenomenological consequences of radiative flavor violation in the MSSM”, *Phys.Rev.* **D84** (2011) 035030, [arXiv:1105.2818 \[hep-ph\]](#).
- [105] A. Crivellin, *Non-minimal Flavor Violation in the Minimal Supersymmetric Standard Model*. PhD thesis, Karlsruhe Institut für Technologie, 2010.
- [106] J. Girrbach, *Flavourverletzung in supersymmetrischen vereinheitlichten Theorien*. PhD thesis, Karlsruhe Institut für Technologie, 2011.
- [107] G. D’Ambrosio, G. Giudice, G. Isidori, and A. Strumia, “Minimal flavor violation: An Effective field theory approach”, *Nucl.Phys.* **B645** (2002) 155–187, [arXiv:hep-ph/0207036 \[hep-ph\]](#).
- [108] A. J. Buras, “Minimal flavor violation”, *Acta Phys.Polon.* **B34** (2003) 5615–5668, [arXiv:hep-ph/0310208 \[hep-ph\]](#).
- [109] S. AbdusSalam, C. Burgess, and F. Quevedo, “MFV Reductions of MSSM Parameter Space”, *JHEP* **1502** (2015) 073, [arXiv:1411.1663 \[hep-ph\]](#).
- [110] A. Denner and T. Sack, “Renormalization of the Quark Mixing Matrix”, *Nucl.Phys.* **B347** (1990) 203–216.

- [111] B. A. Kniehl and A. Pilaftsis, “Mixing renormalization in Majorana neutrino theories”, *Nucl.Phys.* **B474** (1996) 286–308, [arXiv:hep-ph/9601390 \[hep-ph\]](#).
- [112] J. Girrbach, S. Mertens, U. Nierste, and S. Wiesenfeldt, “Lepton flavour violation in the MSSM”, *JHEP* **1005** (2010) 026, [arXiv:0910.2663 \[hep-ph\]](#).
- [113] H. Georgi, “Unified Gauge Theories”, in *Theories and Experiments in High-Energy Physics*, A. Perlmutter and S. Widmayer, eds. 1975.
- [114] H. Fritzsch and P. Minkowski, “Unified Interactions of Leptons and Hadrons”, *Annals Phys.* **93** (1975) 193–266.
- [115] H. Georgi and S. Glashow, “Unity of All Elementary Particle Forces”, *Phys.Rev.Lett.* **32** (1974) 438–441.
- [116] T. Kibble, G. Lazarides, and Q. Shafi, “Walls Bounded by Strings”, *Phys.Rev.* **D26** (1982) 435.
- [117] R. N. Mohapatra and B. Sakita, “SO(2N) Grand Unification in an SU(N) Basis”, *Phys.Rev.* **D21** (1980) 1062.
- [118] F. Wilczek and A. Zee, “Families from Spinors”, *Phys.Rev.* **D25** (1982) 553.
- [119] H. Georgi and D. V. Nanopoulos, “Masses and Mixing in Unified Theories”, *Nucl.Phys.* **B159** (1979) 16.
- [120] G. Lazarides, Q. Shafi, and C. Wetterich, “Proton Lifetime and Fermion Masses in an SO(10) Model”, *Nucl.Phys.* **B181** (1981) 287–300.
- [121] C. S. Aulakh, B. Bajc, A. Melfo, G. Senjanovic, and F. Vissani, “The Minimal supersymmetric grand unified theory”, *Phys.Lett.* **B588** (2004) 196–202, [arXiv:hep-ph/0306242 \[hep-ph\]](#).
- [122] K. Huitu, J. Maalampi, and M. Raidal, “Supersymmetric left-right model and its tests in linear colliders”, *Nucl.Phys.* **B420** (1994) 449–467, [arXiv:hep-ph/9312235 \[hep-ph\]](#).
- [123] T. Clark, T.-K. Kuo, and N. Nakagawa, “A SO(10) Supersymmetric Grand Unified Theory”, *Phys.Lett.* **B115** (1982) 26.
- [124] D.-G. Lee, “Symmetry breaking and mass spectra in the minimal supersymmetric SO(10) grand unified theory”, *Phys.Rev.* **D49** (1994) 1417–1426.
- [125] A. Dueck and W. Rodejohann, “Fits to SO(10) Grand Unified Models”, *JHEP* **1309** (2013) 024, [arXiv:1306.4468 \[hep-ph\]](#).
- [126] S. Bertolini, T. Schwetz, and M. Malinsky, “Fermion masses and mixings in SO(10) models and the neutrino challenge to SUSY GUTs”, *Phys.Rev.* **D73** (2006) 115012, [arXiv:hep-ph/0605006 \[hep-ph\]](#).
- [127] M. Parida and B. Cajej, “High scale perturbative gauge coupling in R-parity conserving SUSY SO(10) with larger proton lifetime”, *Eur.Phys.J.* **C44** (2005) 447–457, [arXiv:hep-ph/0507030 \[hep-ph\]](#).
- [128] W. G. Hollik, “Leptonflavourverletzung in einer supersymmetrischen Theorie mit Links-Rechts-Symmetrie”, Karlsruhe Institut für Technologie, 2012. Diplomarbeit.
- [129] R. N. Mohapatra and G. Senjanovic, “Neutrino Mass and Spontaneous Parity Violation”, *Phys.Rev.Lett.* **44** (1980) 912.
- [130] C. Aulakh and R. N. Mohapatra, “Implications of Supersymmetric SO(10) Grand Unification”, *Phys.Rev.* **D28** (1983) 217.
- [131] J. C. Pati and A. Salam, “Lepton Number as the Fourth Color”, *Phys.Rev.* **D10** (1974) 275–289.
- [132] M. Gonzalez-Garcia, M. Maltoni, and T. Schwetz, “Updated fit to three neutrino mixing: status of leptonic CP violation”, *JHEP* **1411** (2014) 052, [arXiv:1409.5439 \[hep-ph\]](#).
- [133] E. K. Akhmedov, “Neutrino physics”, [arXiv:hep-ph/0001264 \[hep-ph\]](#).
- [134] R. Mohapatra and P. Pal, *Massive neutrinos in physics and astrophysics*, vol. 72. 2nd ed., 2004.

- [135] B. Pontecorvo, “Inverse beta processes and nonconservation of lepton charge”, *Sov.Phys.JETP* **7** (1958) 172–173.
- [136] Z. Maki, M. Nakagawa, and S. Sakata, “Remarks on the unified model of elementary particles”, *Prog.Theor.Phys.* **28** (1962) 870–880.
- [137] T. Takagi, “On an algebraic problem related to an analytic theorem of Carathéodory and Fejér and on an allied theorem of Landau”, *Japan J. Math.* **1** (1924) 83–93.
- [138] Y. Farzan, “Effects of the neutrino B term on slepton mixing and electric dipole moments”, *Phys.Rev.* **D69** (2004) 073009, [arXiv:hep-ph/0310055 \[hep-ph\]](#).
- [139] Y. Farzan, “Effects of the neutrino B-term on the Higgs mass parameters and electroweak symmetry breaking”, *JHEP* **0502** (2005) 025, [arXiv:hep-ph/0411358 \[hep-ph\]](#).
- [140] A. Dedes, H. E. Haber, and J. Rosiek, “Seesaw mechanism in the sneutrino sector and its consequences”, *JHEP* **0711** (2007) 059, [arXiv:0707.3718 \[hep-ph\]](#).
- [141] S. Heinemeyer, J. Hernandez-Garcia, M. Herrero, X. Marcano, and A. Rodriguez-Sanchez, “Radiative corrections to M_h from three generations of Majorana neutrinos and sneutrinos”, [arXiv:1407.1083 \[hep-ph\]](#).
- [142] Y. Grossman and H. E. Haber, “Sneutrino mixing phenomena”, *Phys.Rev.Lett.* **78** (1997) 3438–3441, [arXiv:hep-ph/9702421 \[hep-ph\]](#).
- [143] R. Davis, “Solar neutrinos. II: Experimental”, *Phys.Rev.Lett.* **12** (1964) 303–305.
- [144] J. N. Bahcall, “Solar neutrinos. I: Theoretical”, *Phys.Rev.Lett.* **12** (1964) 300–302.
- [145] J. N. Bahcall, “Solar neutrinos”, *Phys.Rev.Lett.* **17** (1966) 398–401.
- [146] J. Davis, Raymond, D. S. Harmer, and K. C. Hoffman, “Search for neutrinos from the sun”, *Phys.Rev.Lett.* **20** (1968) 1205–1209.
- [147] J. N. Bahcall, N. A. Bahcall, and G. Shaviv, “Present status of the theoretical predictions for the Cl-36 solar neutrino experiment”, *Phys.Rev.Lett.* **20** (1968) 1209–1212.
- [148] V. Gribov and B. Pontecorvo, “Neutrino astronomy and lepton charge”, *Phys.Lett.* **B28** (1969) 493.
- [149] S. Weinberg, “Baryon and Lepton Nonconserving Processes”, *Phys.Rev.Lett.* **43** (1979) 1566–1570.
- [150] M. Doi, T. Kotani, H. Nishiura, K. Okuda, and E. Takasugi, “Neutrino Masses and the Double Beta Decay”, *Phys.Lett.* **B103** (1981) 219.
- [151] T. Cheng and L.-F. Li, “Neutrino Masses, Mixings and Oscillations in SU(2) x U(1) Models of Electroweak Interactions”, *Phys.Rev.* **D22** (1980) 2860.
- [152] J. Schechter and J. Valle, “Neutrinoless Double beta Decay in SU(2) x U(1) Theories”, *Phys.Rev.* **D25** (1982) 2951.
- [153] F. Klinkhamer, “Neutrino mass and the Standard Model”, *Mod.Phys.Lett.* **A28** (2013) 1350010, [arXiv:1112.2669 \[hep-ph\]](#).
- [154] P. Minkowski, “ $\mu \rightarrow e\gamma$ at a Rate of One Out of 1-Billion Muon Decays?”, *Phys.Lett.* **B67** (1977) 421.
- [155] T. Yanagida, “Horizontal Symmetry and Masses of Neutrinos”, in *Workshop on the Baryon Number of the Universe and Unified theories*, pp. 95–99. 1979.
- [156] M. Gell-Mann, P. Ramond, and R. Slansky, “Complex Spinors and Unified Theories”, in *Supergravity*. 1979. [arXiv:1306.4669 \[hep-th\]](#).
- [157] M. Magg and C. Wetterich, “Neutrino Mass Problem and Gauge Hierarchy”, *Phys.Lett.* **B94** (1980) 61.
- [158] J. Schechter and J. Valle, “Neutrino Masses in SU(2) x U(1) Theories”, *Phys.Rev.* **D22** (1980) 2227.

- [159] M. Doi, T. Kotani, H. Nishiura, K. Okuda, and E. Takasugi, “CP Violation in Majorana Neutrinos”, *Phys.Lett.* **B102** (1981) 323.
- [160] S. M. Bilenky, J. Hosek, and S. Petcov, “On Oscillations of Neutrinos with Dirac and Majorana Masses”, *Phys.Lett.* **B94** (1980) 495.
- [161] D. Aristizabal Sierra, A. Degee, L. Dorame, and M. Hirsch, “Systematic classification of two-loop realizations of the Weinberg operator”, [arXiv:1411.7038](https://arxiv.org/abs/1411.7038) [hep-ph].
- [162] E. Ma, “Pathways to naturally small neutrino masses”, *Phys.Rev.Lett.* **81** (1998) 1171–1174, [arXiv:hep-ph/9805219](https://arxiv.org/abs/hep-ph/9805219) [hep-ph].
- [163] T. Yanagida, “Horizontal Symmetry and Masses of Neutrinos”, *Prog.Theor.Phys.* **64** (1980) 1103.
- [164] S. Antusch, J. Kersten, M. Lindner, and M. Ratz, “Neutrino mass matrix running for nondegenerate seesaw scales”, *Phys.Lett.* **B538** (2002) 87–95, [arXiv:hep-ph/0203233](https://arxiv.org/abs/hep-ph/0203233) [hep-ph].
- [165] S. Antusch, J. Kersten, M. Lindner, M. Ratz, and M. A. Schmidt, “Running neutrino mass parameters in see-saw scenarios”, *JHEP* **0503** (2005) 024, [arXiv:hep-ph/0501272](https://arxiv.org/abs/hep-ph/0501272) [hep-ph].
- [166] H. Fritzsch and P. Minkowski, “Parity Conserving Neutral Currents and Righthanded Neutrinos”, *Nucl.Phys.* **B103** (1976) 61.
- [167] D. Ross and M. Veltman, “Neutral Currents and the Higgs Mechanism”, *Nucl.Phys.* **B95** (1975) 135.
- [168] M. Veltman, “Limit on Mass Differences in the Weinberg Model”, *Nucl.Phys.* **B123** (1977) 89.
- [169] K. Chetyrkin, M. Faisst, J. H. Kuhn, P. Maierhofer, and C. Sturm, “Four-Loop QCD Corrections to the ρ Parameter”, *Phys.Rev.Lett.* **97** (2006) 102003, [arXiv:hep-ph/0605201](https://arxiv.org/abs/hep-ph/0605201) [hep-ph].
- [170] D. Asner, T. Barklow, C. Calancha, K. Fujii, N. Graf, *et al.*, “ILC Higgs White Paper”, [arXiv:1310.0763](https://arxiv.org/abs/1310.0763) [hep-ph].
- [171] J. F. Gunion, H. E. Haber, G. L. Kane, and S. Dawson, “The Higgs Hunter’s Guide”, *Front.Phys.* **80** (2000) 1–448.
- [172] R. Foot, H. Lew, X. He, and G. C. Joshi, “Seesaw Neutrino Masses Induced by a Triplet of Leptons”, *Z.Phys.* **C44** (1989) 441.
- [173] M. S. Chanowitz, J. R. Ellis, and M. K. Gaillard, “The Price of Natural Flavor Conservation in Neutral Weak Interactions”, *Nucl.Phys.* **B128** (1977) 506.
- [174] H. Georgi and D. V. Nanopoulos, “Ordinary Predictions from Grand Principles: T Quark Mass in $O(10)$ ”, *Nucl.Phys.* **B155** (1979) 52.
- [175] J. Casas and A. Ibarra, “Oscillating neutrinos and $\mu \rightarrow e, \gamma$ ”, *Nucl.Phys.* **B618** (2001) 171–204, [arXiv:hep-ph/0103065](https://arxiv.org/abs/hep-ph/0103065) [hep-ph].
- [176] E. J. Chun and S. Pokorski, “Slepton flavor mixing and neutrino masses”, *Phys.Rev.* **D62** (2000) 053001, [arXiv:hep-ph/9912210](https://arxiv.org/abs/hep-ph/9912210) [hep-ph].
- [177] P. H. Chankowski, A. Ioannisian, S. Pokorski, and J. Valle, “Neutrino unification”, *Phys.Rev.Lett.* **86** (2001) 3488–3491, [arXiv:hep-ph/0011150](https://arxiv.org/abs/hep-ph/0011150) [hep-ph].
- [178] E. J. Chun, “Lepton flavor violation and radiative neutrino masses”, *Phys.Lett.* **B505** (2001) 155–160, [arXiv:hep-ph/0101170](https://arxiv.org/abs/hep-ph/0101170) [hep-ph].
- [179] P. H. Chankowski and S. Pokorski, “Quantum corrections to neutrino masses and mixing angles”, *Int.J.Mod.Phys.* **A17** (2002) 575–614, [arXiv:hep-ph/0110249](https://arxiv.org/abs/hep-ph/0110249) [hep-ph].
- [180] P. H. Chankowski and Z. Pluciennik, “Renormalization group equations for seesaw neutrino masses”, *Phys.Lett.* **B316** (1993) 312–317, [arXiv:hep-ph/9306333](https://arxiv.org/abs/hep-ph/9306333) [hep-ph].
- [181] K. Babu, C. N. Leung, and J. T. Pantaleone, “Renormalization of the neutrino mass operator”, *Phys.Lett.* **B319** (1993) 191–198, [arXiv:hep-ph/9309223](https://arxiv.org/abs/hep-ph/9309223) [hep-ph].

- [182] S. Antusch, M. Drees, J. Kersten, M. Lindner, and M. Ratz, “Neutrino mass operator renormalization revisited”, *Phys.Lett.* **B519** (2001) 238–242, [arXiv:hep-ph/0108005 \[hep-ph\]](#).
- [183] S. Antusch, M. Drees, J. Kersten, M. Lindner, and M. Ratz, “Neutrino mass operator renormalization in two Higgs doublet models and the MSSM”, *Phys.Lett.* **B525** (2002) 130–134, [arXiv:hep-ph/0110366 \[hep-ph\]](#).
- [184] N. Haba, N. Okamura, and M. Sugiura, “The Renormalization group analysis of the large lepton flavor mixing and the neutrino mass”, *Prog.Theor.Phys.* **103** (2000) 367–377, [arXiv:hep-ph/9810471 \[hep-ph\]](#).
- [185] J. R. Ellis and S. Lola, “Can neutrinos be degenerate in mass?”, *Phys.Lett.* **B458** (1999) 310–321, [arXiv:hep-ph/9904279 \[hep-ph\]](#).
- [186] J. Casas, J. Espinosa, A. Ibarra, and I. Navarro, “Naturalness of nearly degenerate neutrinos”, *Nucl.Phys.* **B556** (1999) 3–22, [arXiv:hep-ph/9904395 \[hep-ph\]](#).
- [187] J. Casas, J. Espinosa, A. Ibarra, and I. Navarro, “Nearly degenerate neutrinos, supersymmetry and radiative corrections”, *Nucl.Phys.* **B569** (2000) 82–106, [arXiv:hep-ph/9905381 \[hep-ph\]](#).
- [188] J. Casas, J. Espinosa, A. Ibarra, and I. Navarro, “General RG equations for physical neutrino parameters and their phenomenological implications”, *Nucl.Phys.* **B573** (2000) 652–684, [arXiv:hep-ph/9910420 \[hep-ph\]](#).
- [189] P. H. Chankowski, W. Krolikowski, and S. Pokorski, “Fixed points in the evolution of neutrino mixings”, *Phys.Lett.* **B473** (2000) 109–117, [arXiv:hep-ph/9910231 \[hep-ph\]](#).
- [190] K. Balaji, A. S. Dighe, R. Mohapatra, and M. Parida, “Generation of large flavor mixing from radiative corrections”, *Phys.Rev.Lett.* **84** (2000) 5034–5037, [arXiv:hep-ph/0001310 \[hep-ph\]](#).
- [191] K. Balaji, R. Mohapatra, M. Parida, and E. Paschos, “Large neutrino mixing from renormalization group evolution”, *Phys.Rev.* **D63** (2001) 113002, [arXiv:hep-ph/0011263 \[hep-ph\]](#).
- [192] N. Haba, Y. Matsui, N. Okamura, and M. Sugiura, “The Effect of Majorana phase in degenerate neutrinos”, *Prog.Theor.Phys.* **103** (2000) 145–150, [arXiv:hep-ph/9908429 \[hep-ph\]](#).
- [193] N. Haba, Y. Matsui, and N. Okamura, “The Effects of Majorana phases in three generation neutrinos”, *Eur.Phys.J.* **C17** (2000) 513–520, [arXiv:hep-ph/0005075 \[hep-ph\]](#).
- [194] W. G. Hollik, “Radiative generation of neutrino mixing: degenerate masses and threshold corrections”, *Phys.Rev.* **D91** (2015) 033001, [arXiv:1412.4585 \[hep-ph\]](#).
- [195] **Troitsk Collaboration**, V. Aseev *et al.*, “An upper limit on electron antineutrino mass from Troitsk experiment”, *Phys.Rev.* **D84** (2011) 112003, [arXiv:1108.5034 \[hep-ex\]](#).
- [196] C. Kraus, B. Bornschein, L. Bornschein, J. Bonn, B. Flatt, *et al.*, “Final results from phase II of the Mainz neutrino mass search in tritium beta decay”, *Eur.Phys.J.* **C40** (2005) 447–468, [arXiv:hep-ex/0412056 \[hep-ex\]](#).
- [197] **KATRIN Collaboration**, A. Osipowicz *et al.*, “KATRIN: A Next generation tritium beta decay experiment with sub-eV sensitivity for the electron neutrino mass. Letter of intent”, [arXiv:hep-ex/0109033 \[hep-ex\]](#).
- [198] **GERDA Collaboration**, M. Agostini *et al.*, “Results on Neutrinoless Double- β Decay of ^{76}Ge from Phase I of the GERDA Experiment”, *Phys.Rev.Lett.* **111** no. 12, (2013) 122503, [arXiv:1307.4720 \[nucl-ex\]](#).
- [199] **PLANCK Collaboration**, P. Ade *et al.*, “Planck 2013 results. XVI. Cosmological parameters”, *Astron.Astrophys.* (2014), [arXiv:1303.5076 \[astro-ph.CO\]](#).
- [200] H. Fritzsch and Z.-Z. Xing, “Lepton mass hierarchy and neutrino oscillations”, *Phys.Lett.* **B372** (1996) 265–270, [arXiv:hep-ph/9509389 \[hep-ph\]](#).

- [201] H. Fritzsch and Z.-z. Xing, “Large leptonic flavor mixing and the mass spectrum of leptons”, *Phys.Lett.* **B440** (1998) 313–318, [arXiv:hep-ph/9808272 \[hep-ph\]](#).
- [202] K. Babu, E. Ma, and J. Valle, “Underlying A(4) symmetry for the neutrino mass matrix and the quark mixing matrix”, *Phys.Lett.* **B552** (2003) 207–213, [arXiv:hep-ph/0206292 \[hep-ph\]](#).
- [203] S. Morisi, D. Forero, J. Romão, and J. Valle, “Neutrino mixing with revamped A_4 flavor symmetry”, *Phys.Rev.* **D88** no. 1, (2013) 016003, [arXiv:1305.6774 \[hep-ph\]](#).
- [204] **Daya Bay Collaboration**, F. An *et al.*, “Improved Measurement of Electron Antineutrino Disappearance at Daya Bay”, *Chin.Phys.* **C37** (2013) 011001, [arXiv:1210.6327 \[hep-ex\]](#).
- [205] W. G. Hollik and U. J. S. Salazar, “The double mass hierarchy pattern: simultaneously understanding quark and lepton mixing”, *Nucl.Phys.* **B892** (2015) 364–389, [arXiv:1411.3549 \[hep-ph\]](#).
- [206] W. G. Hollik, “Neutrino Mixing from SUSY breaking”, [arXiv:1504.03270 \[hep-ph\]](#).
- [207] W. Grimus and L. Lavoura, “One loop corrections to the seesaw mechanism in the multiHiggs doublet standard model”, *Phys.Lett.* **B546** (2002) 86–95, [arXiv:hep-ph/0207229 \[hep-ph\]](#).
- [208] D. Aristizabal Sierra and C. E. Yaguna, “On the importance of the 1-loop finite corrections to seesaw neutrino masses”, *JHEP* **1108** (2011) 013, [arXiv:1106.3587 \[hep-ph\]](#).
- [209] W. Hollik, “(Quasi-)Degeneration, Quantum Corrections and Neutrino Mixing”, 2014. [arXiv:1411.2946 \[hep-ph\]](#). Proceedings of the 17th International Moscow School of Physics and 42nd ITEP Winter School of Physics.
- [210] P. Harrison, D. Perkins, and W. Scott, “Tri-bimaximal mixing and the neutrino oscillation data”, *Phys.Lett.* **B530** (2002) 167, [arXiv:hep-ph/0202074 \[hep-ph\]](#).
- [211] B. A. Kniehl and A. Sirlin, “Renormalization in general theories with inter-generation mixing”, *Phys.Rev.* **D85** (2012) 036007, [arXiv:1201.4333 \[hep-ph\]](#).
- [212] B. A. Kniehl, “All-Order Renormalization of the Propagator Matrix for Fermionic Systems with Flavor Mixing”, *Phys.Rev.Lett.* **112** no. 7, (2014) 071603, [arXiv:1308.3140 \[hep-ph\]](#).
- [213] B. A. Kniehl and A. Sirlin, “Considerations concerning the generalization of the Dirac equations to unstable fermions”, *Phys.Rev.* **D90** no. 7, (2014) 077901, [arXiv:1409.5869 \[hep-ph\]](#).
- [214] B. A. Kniehl, “Propagator mixing renormalization for Majorana fermions”, *Phys.Rev.* **D89** no. 11, (2014) 116010, [arXiv:1404.5908 \[hep-th\]](#).
- [215] B. A. Kniehl, “All-order renormalization of propagator matrix for unstable Dirac fermions”, *Phys.Rev.* **D89** no. 9, (2014) 096005.
- [216] M. Bohm, A. Denner, and H. Joos, *Gauge theories of the strong and electroweak interaction*. B.G. Teubner, 3rd ed., 2001.
- [217] K. Aoki, Z. Hioki, M. Konuma, R. Kawabe, and T. Muta, “Electroweak Theory. Framework of On-Shell Renormalization and Study of Higher Order Effects”, *Prog.Theor.Phys.Suppl.* **73** (1982) 1–225.
- [218] S. Pokorski, *Gauge Field Theories*. Cambridge University Press, 2nd ed., 2000.
- [219] S. R. Coleman and E. J. Weinberg, “Radiative Corrections as the Origin of Spontaneous Symmetry Breaking”, *Phys.Rev.* **D7** (1973) 1888–1910.
- [220] R. Jackiw, “Functional evaluation of the effective potential”, *Phys.Rev.* **D9** (1974) 1686.
- [221] S. Lee and A. M. Sciaccaluga, “Evaluation of Higher Order Effective Potentials with Dimensional Regularization”, *Nucl.Phys.* **B96** (1975) 435.
- [222] A. Dannenberg, “Dysfunctional Methods and the Effective Potential”, *Phys.Lett.* **B202** (1988) 110.
- [223] D. J. Callaway, “Nonperturbative Analysis of the Effective Potential in the $O(N)$ Model”, *Phys.Rev.* **D27** (1983) 2974.

- [224] Y. Nambu, “S Matrix in semiclassical approximation”, *Phys.Lett.* **B26** (1968) 626–629.
- [225] R. Jackiw and K. Johnson, “Dynamical Model of Spontaneously Broken Gauge Symmetries”, *Phys.Rev.* **D8** (1973) 2386–2398.
- [226] J. Cornwall and R. Norton, “Spontaneous Symmetry Breaking Without Scalar Mesons”, *Phys.Rev.* **D8** (1973) 3338–3346.
- [227] M. Sher, “Electroweak Higgs Potentials and Vacuum Stability”, *Phys.Rept.* **179** (1989) 273–418.
- [228] E. J. Weinberg and A.-q. Wu, “Understanding complex perturbative effective potentials”, *Phys.Rev.* **D36** (1987) 2474.
- [229] K. Symanzik, “Renormalizable models with simple symmetry breaking. 1. Symmetry breaking by a source term”, *Commun.Math.Phys.* **16** (1970) 48–80.
- [230] J. Iliopoulos, C. Itzykson, and A. Martin, “Functional Methods and Perturbation Theory”, *Rev.Mod.Phys.* **47** (1975) 165.
- [231] L. O’Raifeartaigh and G. Parravicini, “Effective Fields and Discontinuities in the Effective Potential”, *Nucl.Phys.* **B111** (1976) 501.
- [232] F. Cooper and B. Freedman, “Renormalizing the Effective Potential for Spontaneously Broken $g\phi^4$ Field Theory”, *Nucl.Phys.* **B239** (1984) 459.
- [233] J. Langer, “Theory of the condensation point”, *Annals Phys.* **41** (1967) 108–157.
- [234] J. Langer, “Statistical theory of the decay of metastable states”, *Annals Phys.* **54** (1969) 258–275.
- [235] R. W. Haymaker and J. Perez-Mercader, “Convexity of the Effective Potential”, *Phys.Rev.* **D27** (1983) 1948.
- [236] S. R. Coleman, R. Jackiw, and H. D. Politzer, “Spontaneous Symmetry Breaking in the O(N) Model for Large N”, *Phys.Rev.* **D10** (1974) 2491.
- [237] S. R. Coleman, “The Fate of the False Vacuum. 1. Semiclassical Theory”, *Phys.Rev.* **D15** (1977) 2929–2936.
- [238] J. Callan, Curtis G. and S. R. Coleman, “The Fate of the False Vacuum. 2. First Quantum Corrections”, *Phys.Rev.* **D16** (1977) 1762–1768.
- [239] T. Banks, C. M. Bender, and T. T. Wu, “Coupled anharmonic oscillators. 1. Equal mass case”, *Phys.Rev.* **D8** (1973) 3346–3378.
- [240] E. J. Weinberg, “Vacuum decay in theories with symmetry breaking by radiative corrections”, *Phys.Rev.* **D47** (1993) 4614–4627, [arXiv:hep-ph/9211314](https://arxiv.org/abs/hep-ph/9211314) [hep-ph].
- [241] A. Kusenko, P. Langacker, and G. Segre, “Phase transitions and vacuum tunneling into charge and color breaking minima in the MSSM”, *Phys.Rev.* **D54** (1996) 5824–5834, [arXiv:hep-ph/9602414](https://arxiv.org/abs/hep-ph/9602414) [hep-ph].
- [242] N. Blinov and D. E. Morrissey, “Vacuum Stability and the MSSM Higgs Mass”, *JHEP* **1403** (2014) 106, [arXiv:1310.4174](https://arxiv.org/abs/1310.4174) [hep-ph].
- [243] S. R. Coleman and F. De Luccia, “Gravitational Effects on and of Vacuum Decay”, *Phys.Rev.* **D21** (1980) 3305.
- [244] C. Froggatt and H. B. Nielsen, “Standard model criticality prediction: Top mass 173 ± 5 GeV and Higgs mass 135 ± 9 GeV”, *Phys.Lett.* **B368** (1996) 96–102, [arXiv:hep-ph/9511371](https://arxiv.org/abs/hep-ph/9511371) [hep-ph].
- [245] C. D. Froggatt and H. Nielsen, “Cryptobaryonic dark matter”, *Phys.Rev.Lett.* **95** (2005) 231301, [arXiv:astro-ph/0508513](https://arxiv.org/abs/astro-ph/0508513) [astro-ph].
- [246] C. Froggatt and H. Nielsen, “Tunguska Dark Matter Ball”, [arXiv:1403.7177](https://arxiv.org/abs/1403.7177) [hep-ph].
- [247] D. Bennett, H. B. Nielsen, and I. Picek, “Understanding Fine Structure Constants and Three Generations”, *Phys.Lett.* **B208** (1988) 275.

- [248] D. Bennett and H. B. Nielsen, “Predictions for nonAbelian fine structure constants from multicriticality”, *Int.J.Mod.Phys.* **A9** (1994) 5155–5200, [arXiv:hep-ph/9311321 \[hep-ph\]](#).
- [249] S. Weinberg, “Mass of the Higgs Boson”, *Phys.Rev.Lett.* **36** (1976) 294–296.
- [250] A. D. Linde, “Dynamical Symmetry Restoration and Constraints on Masses and Coupling Constants in Gauge Theories”, *JETP Lett.* **23** (1976) 64–67.
- [251] P. Frampton, “Vacuum Instability and Higgs Scalar Mass”, *Phys.Rev.Lett.* **37** (1976) 1378.
- [252] A. D. Linde, “Vacuum Instability, Cosmology and Constraints on Particle Masses in the Weinberg-Salam Model”, *Phys.Lett.* **B92** (1980) 119.
- [253] M. Lindner, “Implications of Triviality for the Standard Model”, *Z.Phys.* **C31** (1986) 295.
- [254] B. Grzadkowski and M. Lindner, “Stability of Triviality Mass Bounds in the Standard Model”, *Phys.Lett.* **B178** (1986) 81.
- [255] M. Lindner, M. Sher, and H. W. Zaglauer, “Probing Vacuum Stability Bounds at the Fermilab Collider”, *Phys.Lett.* **B228** (1989) 139.
- [256] P. B. Arnold, “Can the Electroweak Vacuum Be Unstable?”, *Phys.Rev.* **D40** (1989) 613.
- [257] M. Sher, “Precise vacuum stability bound in the standard model”, *Phys.Lett.* **B317** (1993) 159–163, [arXiv:hep-ph/9307342 \[hep-ph\]](#).
- [258] G. Altarelli and G. Isidori, “Lower limit on the Higgs mass in the standard model: An Update”, *Phys.Lett.* **B337** (1994) 141–144.
- [259] J. Casas, J. Espinosa, and M. Quiros, “Improved Higgs mass stability bound in the standard model and implications for supersymmetry”, *Phys.Lett.* **B342** (1995) 171–179, [arXiv:hep-ph/9409458 \[hep-ph\]](#).
- [260] J. Espinosa and M. Quiros, “Improved metastability bounds on the standard model Higgs mass”, *Phys.Lett.* **B353** (1995) 257–266, [arXiv:hep-ph/9504241 \[hep-ph\]](#).
- [261] J. Casas, J. Espinosa, and M. Quiros, “Standard model stability bounds for new physics within LHC reach”, *Phys.Lett.* **B382** (1996) 374–382, [arXiv:hep-ph/9603227 \[hep-ph\]](#).
- [262] V. Branchina and H. Faivre, “Effective potential (in)stability and lower bounds on the scalar (Higgs) mass”, *Phys.Rev.* **D72** (2005) 065017, [arXiv:hep-th/0503188 \[hep-th\]](#).
- [263] F. Bezrukov, M. Y. Kalmykov, B. A. Kniehl, and M. Shaposhnikov, “Higgs Boson Mass and New Physics”, *JHEP* **1210** (2012) 140, [arXiv:1205.2893 \[hep-ph\]](#).
- [264] L. Di Luzio and L. Mihaila, “On the gauge dependence of the Standard Model vacuum instability scale”, *JHEP* **1406** (2014) 079, [arXiv:1404.7450 \[hep-ph\]](#).
- [265] A. Andreassen, W. Frost, and M. D. Schwartz, “Consistent Use of Effective Potentials”, [arXiv:1408.0287 \[hep-ph\]](#).
- [266] A. Andreassen, W. Frost, and M. D. Schwartz, “Consistent Use of the Standard Model Effective Potential”, *Phys.Rev.Lett.* **113** no. 24, (2014) 241801, [arXiv:1408.0292 \[hep-ph\]](#).
- [267] C. Ford, D. Jones, P. Stephenson, and M. Einhorn, “The Effective potential and the renormalization group”, *Nucl.Phys.* **B395** (1993) 17–34, [arXiv:hep-lat/9210033 \[hep-lat\]](#).
- [268] I. Drummond and R. Fidler, “The Effective Potential for the Yang-Mills Field”, *Nucl.Phys.* **B90** (1975) 77.
- [269] C. Burgess, V. Di Clemente, and J. Espinosa, “Effective operators and vacuum instability as heralds of new physics”, *JHEP* **0201** (2002) 041, [arXiv:hep-ph/0201160 \[hep-ph\]](#).
- [270] G. Isidori, G. Ridolfi, and A. Strumia, “On the metastability of the standard model vacuum”, *Nucl.Phys.* **B609** (2001) 387–409, [arXiv:hep-ph/0104016 \[hep-ph\]](#).
- [271] G. Isidori, V. S. Rychkov, A. Strumia, and N. Tetradis, “Gravitational corrections to standard model vacuum decay”, *Phys.Rev.* **D77** (2008) 025034, [arXiv:0712.0242 \[hep-ph\]](#).

- [272] J. Espinosa, G. Giudice, and A. Riotto, “Cosmological implications of the Higgs mass measurement”, *JCAP* **0805** (2008) 002, [arXiv:0710.2484 \[hep-ph\]](#).
- [273] J. Ellis, J. Espinosa, G. Giudice, A. Hoecker, and A. Riotto, “The Probable Fate of the Standard Model”, *Phys.Lett.* **B679** (2009) 369–375, [arXiv:0906.0954 \[hep-ph\]](#).
- [274] J. Elias-Miro, J. R. Espinosa, G. F. Giudice, G. Isidori, A. Riotto, *et al.*, “Higgs mass implications on the stability of the electroweak vacuum”, *Phys.Lett.* **B709** (2012) 222–228, [arXiv:1112.3022 \[hep-ph\]](#).
- [275] M. Holthausen, K. S. Lim, and M. Lindner, “Planck scale Boundary Conditions and the Higgs Mass”, *JHEP* **1202** (2012) 037, [arXiv:1112.2415 \[hep-ph\]](#).
- [276] K. Chetyrkin and M. Zoller, “Three-loop β -functions for top-Yukawa and the Higgs self-interaction in the Standard Model”, *JHEP* **1206** (2012) 033, [arXiv:1205.2892 \[hep-ph\]](#).
- [277] G. Degrandi, S. Di Vita, J. Elias-Miro, J. R. Espinosa, G. F. Giudice, *et al.*, “Higgs mass and vacuum stability in the Standard Model at NNLO”, *JHEP* **1208** (2012) 098, [arXiv:1205.6497 \[hep-ph\]](#).
- [278] I. Masina, “Higgs boson and top quark masses as tests of electroweak vacuum stability”, *Phys.Rev.* **D87** no. 5, (2013) 053001, [arXiv:1209.0393 \[hep-ph\]](#).
- [279] D. Buttazzo, G. Degrandi, P. P. Giardino, G. F. Giudice, F. Sala, *et al.*, “Investigating the near-criticality of the Higgs boson”, *JHEP* **1312** (2013) 089, [arXiv:1307.3536 \[hep-ph\]](#).
- [280] V. Branchina and E. Messina, “Stability, Higgs Boson Mass and New Physics”, *Phys.Rev.Lett.* **111** (2013) 241801, [arXiv:1307.5193 \[hep-ph\]](#).
- [281] V. Branchina, E. Messina, and A. Platania, “Top mass determination, Higgs inflation, and vacuum stability”, *JHEP* **1409** (2014) 182, [arXiv:1407.4112 \[hep-ph\]](#).
- [282] V. Branchina, E. Messina, and M. Sher, “Lifetime of the electroweak vacuum and sensitivity to Planck scale physics”, *Phys.Rev.* **D91** no. 1, (2015) 013003, [arXiv:1408.5302 \[hep-ph\]](#).
- [283] M. F. Zoller, *Dreischleifen-Betafunktionen und die Stabilität des Vakuums im Standardmodell*. PhD thesis, Karlsruher Institut für Technologie, 2014.
- [284] J. Casas, V. Di Clemente, and M. Quiros, “The Effective potential in the presence of several mass scales”, *Nucl.Phys.* **B553** (1999) 511–530, [arXiv:hep-ph/9809275 \[hep-ph\]](#).
- [285] J. Casas, V. Di Clemente, A. Ibarra, and M. Quiros, “Massive neutrinos and the Higgs mass window”, *Phys.Rev.* **D62** (2000) 053005, [arXiv:hep-ph/9904295 \[hep-ph\]](#).
- [286] J. Casas, V. Di Clemente, and M. Quiros, “The Standard model instability and the scale of new physics”, *Nucl.Phys.* **B581** (2000) 61–72, [arXiv:hep-ph/0002205 \[hep-ph\]](#).
- [287] M. Bobrowski, G. Chalons, W. G. Hollik, and U. Nierste, “Vacuum stability of the effective Higgs potential in the Minimal Supersymmetric Standard Model”, *Phys.Rev.* **D90** no. 3, (2014) 035025, [arXiv:1407.2814 \[hep-ph\]](#).
- [288] B. M. Kastening, “Renormalization group improvement of the effective potential in massive ϕ^4 theory”, *Phys.Lett.* **B283** (1992) 287–292.
- [289] S. P. Martin, “Two loop effective potential for the minimal supersymmetric standard model”, *Phys.Rev.* **D66** (2002) 096001, [arXiv:hep-ph/0206136 \[hep-ph\]](#).
- [290] J. Casas, A. Lleyda, and C. Munoz, “Strong constraints on the parameter space of the MSSM from charge and color breaking minima”, *Nucl.Phys.* **B471** (1996) 3–58, [arXiv:hep-ph/9507294 \[hep-ph\]](#).
- [291] J. Frere, D. Jones, and S. Raby, “Fermion Masses and Induction of the Weak Scale by Supergravity”, *Nucl.Phys.* **B222** (1983) 11.
- [292] L. Alvarez-Gaume, J. Polchinski, and M. B. Wise, “Minimal Low-Energy Supergravity”, *Nucl.Phys.* **B221** (1983) 495.

- [293] C. Kounnas, A. Lahanas, D. V. Nanopoulos, and M. Quiros, “Low-Energy Behavior of Realistic Locally Supersymmetric Grand Unified Theories”, *Nucl.Phys.* **B236** (1984) 438.
- [294] L. E. Ibanez and C. Lopez, “N=1 Supergravity, the Weak Scale and the Low-Energy Particle Spectrum”, *Nucl.Phys.* **B233** (1984) 511.
- [295] M. Claudson, L. J. Hall, and I. Hinchliffe, “Low-Energy Supergravity: False Vacua and Vacuous Predictions”, *Nucl.Phys.* **B228** (1983) 501.
- [296] M. Drees, M. Gluck, and K. Grassie, “A New Class of False Vacua in Low-energy $N = 1$ Supergravity Theories”, *Phys.Lett.* **B157** (1985) 164.
- [297] J. Gunion, H. Haber, and M. Sher, “Charge / Color Breaking Minima and a-Parameter Bounds in Supersymmetric Models”, *Nucl.Phys.* **B306** (1988) 1.
- [298] C. Le Mouel and G. Moulhaka, “Novel electroweak symmetry breaking conditions from quantum effects in the MSSM”, *Nucl.Phys.* **B518** (1998) 3–36, [arXiv:hep-ph/9711356 \[hep-ph\]](#).
- [299] J. Casas and S. Dimopoulos, “Stability bounds on flavor violating trilinear soft terms in the MSSM”, *Phys.Lett.* **B387** (1996) 107–112, [arXiv:hep-ph/9606237 \[hep-ph\]](#).
- [300] G. Gamberini, G. Ridolfi, and F. Zwirner, “On Radiative Gauge Symmetry Breaking in the Minimal Supersymmetric Model”, *Nucl.Phys.* **B331** (1990) 331–349.
- [301] H. Komatsu, “New Constraints on Parameters in the Minimal Supersymmetric Model”, *Phys.Lett.* **B215** (1988) 323.
- [302] C. Le Mouel, “Optimal charge and color breaking conditions in the MSSM”, *Nucl.Phys.* **B607** (2001) 38–76, [arXiv:hep-ph/0101351 \[hep-ph\]](#).
- [303] B. de Carlos and J. Casas, “One loop analysis of the electroweak breaking in supersymmetric models and the fine tuning problem”, *Phys.Lett.* **B309** (1993) 320–328, [arXiv:hep-ph/9303291 \[hep-ph\]](#).
- [304] D. Chowdhury, R. M. Godbole, K. A. Mohan, and S. K. Vempati, “Charge and Color Breaking Constraints in MSSM after the Higgs Discovery at LHC”, *JHEP* **1402** (2014) 110, [arXiv:1310.1932 \[hep-ph\]](#).
- [305] M. Endo, T. Moroi, and M. M. Nojiri, “Footprints of Supersymmetry on Higgs Decay”, [arXiv:1502.03959 \[hep-ph\]](#).
- [306] J.-h. Park, “Metastability bounds on flavour-violating trilinear soft terms in the MSSM”, *Phys.Rev.* **D83** (2011) 055015, [arXiv:1011.4939 \[hep-ph\]](#).
- [307] P. Ferreira, “A Full one loop charge and color breaking effective potential”, *Phys.Lett.* **B509** (2001) 120–130, [arXiv:hep-ph/0008115 \[hep-ph\]](#).
- [308] P. Ferreira, “Minimization of a one loop charge breaking effective potential”, *Phys.Lett.* **B512** (2001) 379–391, [arXiv:hep-ph/0102141 \[hep-ph\]](#).
- [309] Y. Fujimoto, L. O’Raifeartaigh, and G. Parravicini, “Effective Potential for Nonconvex Potentials”, *Nucl.Phys.* **B212** (1983) 268.
- [310] P. Ferreira, “One-loop charge and colour breaking associated with the top Yukawa coupling”, [arXiv:hep-ph/0406234 \[hep-ph\]](#).
- [311] L. O’Raifeartaigh and G. Parravicini, “Effective Potential for Chiral Scalar Superfields”, *Nucl.Phys.* **B111** (1976) 516.
- [312] M. S. Carena, D. Garcia, U. Nierste, and C. E. Wagner, “Effective Lagrangian for the $\bar{t}bH^+$ interaction in the MSSM and charged Higgs phenomenology”, *Nucl.Phys.* **B577** (2000) 88–120, [arXiv:hep-ph/9912516 \[hep-ph\]](#).
- [313] L. J. Hall, R. Rattazzi, and U. Sarid, “The Top quark mass in supersymmetric SO(10) unification”, *Phys.Rev.* **D50** (1994) 7048–7065, [arXiv:hep-ph/9306309 \[hep-ph\]](#).

- [314] M. S. Carena, M. Olechowski, S. Pokorski, and C. Wagner, “Electroweak symmetry breaking and bottom - top Yukawa unification”, *Nucl.Phys.* **B426** (1994) 269–300, [arXiv:hep-ph/9402253 \[hep-ph\]](#).
- [315] D. M. Pierce, J. A. Bagger, K. T. Matchev, and R.-j. Zhang, “Precision corrections in the minimal supersymmetric standard model”, *Nucl.Phys.* **B491** (1997) 3–67, [arXiv:hep-ph/9606211 \[hep-ph\]](#).
- [316] M. J. Duncan and L. G. Jensen, “Exact tunneling solutions in scalar field theory”, *Phys.Lett.* **B291** (1992) 109–114.
- [317] J. Camargo-Molina, B. O’Leary, W. Porod, and F. Staub, “Stability of the CMSSM against sfermion VEVs”, *JHEP* **1312** (2013) 103, [arXiv:1309.7212 \[hep-ph\]](#).
- [318] J. Camargo-Molina, B. O’Leary, W. Porod, and F. Staub, “Vevacious: A Tool For Finding The Global Minima Of One-Loop Effective Potentials With Many Scalars”, *Eur.Phys.J.* **C73** no. 10, (2013) 2588, [arXiv:1307.1477 \[hep-ph\]](#).
- [319] M. Zoller, “Vacuum stability in the SM and the three-loop β -function for the Higgs self-interaction”, in *What We Would Like LHC to Give Us*, A. Zichichi, ed., pp. 557–566. World Scientific, 2014. Proceedings of the International School of Subnuclear Physics, Erice.
- [320] M. F. Zoller, “Standard Model beta-functions to three-loop order and vacuum stability”, 2014. Proceedings of the 17th International Moscow School of Physics and 42nd ITEP Winter School of Physics.
- [321] M. Bando, T. Kugo, N. Maekawa, and H. Nakano, “Improving the effective potential”, *Phys.Lett.* **B301** (1993) 83–89, [arXiv:hep-ph/9210228 \[hep-ph\]](#).
- [322] M. Bando, T. Kugo, N. Maekawa, and H. Nakano, “Improving the effective potential: Multimass scale case”, *Prog.Theor.Phys.* **90** (1993) 405–418, [arXiv:hep-ph/9210229 \[hep-ph\]](#).
- [323] M. B. Einhorn and D. T. Jones, “A new renormalization group approach to multiscale problems”, *Nucl.Phys.* **B230** (1984) 261.
- [324] R. Gatto, G. Sartori, and M. Tonin, “Weak Selfmasses, Cabibbo Angle, and Broken SU(2) x SU(2)”, *Phys.Lett.* **B28** (1968) 128–130.
- [325] N. Cabibbo and L. Maiani, “Dynamical interrelation of weak, electromagnetic and strong interactions and the value of theta”, *Phys.Lett.* **B28** (1968) 131–135.
- [326] R. Oakes, “SU(2) x SU(2) breaking and the Cabibbo angle”, *Phys.Lett.* **B29** (1969) 683–685.
- [327] K. Tanaka and P. Tarjanne, “Cabibbo angle and selfconsistency condition”, *Phys.Rev.Lett.* **23** (1969) 1137–1139.
- [328] H. Genz, J. Katz, L. Ram Mohan, and S. Tatur, “Chiral symmetry breaking and the cabibbo angle”, *Phys.Rev.* **D6** (1972) 3259–3265.
- [329] H. Pagels, “Vacuum Stability and the Cabibbo Angle”, *Phys.Rev.* **D11** (1975) 1213.
- [330] A. De Rujula, H. Georgi, and S. Glashow, “A Theory of Flavor Mixing”, *Annals Phys.* **109** (1977) 258.
- [331] A. Ebrahim, “Chiral SU(4) x SU(4) Symmetry Breaking and the Cabibbo Angle”, *Phys.Lett.* **B69** (1977) 229–230.
- [332] H. Fritzsch, “Weak Interaction Mixing in the Six - Quark Theory”, *Phys.Lett.* **B73** (1978) 317–322.
- [333] H. Fritzsch, “Calculating the Cabibbo Angle”, *Phys.Lett.* **B70** (1977) 436.
- [334] R. N. Mohapatra and G. Senjanovic, “Cabibbo Angle, CP Violation and Quark Masses”, *Phys.Lett.* **B73** (1978) 176.
- [335] S. Weinberg, “The Problem of Mass”, *Trans.New York Acad.Sci.* **38** (1977) 185–201.

- [336] F. Wilczek and A. Zee, “Discrete Flavor Symmetries and a Formula for the Cabibbo Angle”, *Phys.Lett.* **B70** (1977) 418.
- [337] F. Wilczek and A. Zee, “Horizontal Interaction and Weak Mixing Angles”, *Phys.Rev.Lett.* **42** (1979) 421.
- [338] D. Wyler, “The Cabibbo Angle in the $SU(2)_L \times U(1)$ Gauge Theories”, *Phys.Rev.* **D19** (1979) 330.
- [339] H. Fritzsch, “Quark Masses and Flavor Mixing”, *Nucl.Phys.* **B155** (1979) 189.
- [340] H. Fritzsch, “Hierarchical Chiral Symmetries and the Quark Mass Matrix”, *Phys.Lett.* **B184** (1987) 391.
- [341] P. H. Frampton and Y. Okada, “Simplified symmetric quark mass matrices and flavor mixing”, *Mod.Phys.Lett.* **A6** (1991) 2169–2172.
- [342] J. L. Rosner and M. P. Worah, “Models of the quark mixing matrix”, *Phys.Rev.* **D46** (1992) 1131–1140.
- [343] L. J. Hall and A. Rasin, “On the generality of certain predictions for quark mixing”, *Phys.Lett.* **B315** (1993) 164–169, [arXiv:hep-ph/9303303 \[hep-ph\]](#).
- [344] P. Ramond, R. Roberts, and G. G. Ross, “Stitching the Yukawa quilt”, *Nucl.Phys.* **B406** (1993) 19–42, [arXiv:hep-ph/9303320 \[hep-ph\]](#).
- [345] S. Raby, “Introduction to theories of fermion masses”, [arXiv:hep-ph/9501349 \[hep-ph\]](#).
- [346] R. Barbieri, L. J. Hall, S. Raby, and A. Romanino, “Unified theories with $U(2)$ flavor symmetry”, *Nucl.Phys.* **B493** (1997) 3–26, [arXiv:hep-ph/9610449 \[hep-ph\]](#).
- [347] T. Ito and M. Tanimoto, “The Unitarity triangle and quark mass matrices on the NNI basis”, *Phys.Rev.* **D55** (1997) 1509–1514, [arXiv:hep-ph/9603393 \[hep-ph\]](#).
- [348] Z.-z. Xing, “Implications of the quark mass hierarchy on flavor mixings”, *J.Phys.* **G23** (1997) 1563–1578, [arXiv:hep-ph/9609204 \[hep-ph\]](#).
- [349] S.-S. Xue, “Quark masses and mixing angles”, *Phys.Lett.* **B398** (1997) 177–186, [arXiv:hep-ph/9610508 \[hep-ph\]](#).
- [350] A. Rasin, “Diagonalization of quark mass matrices and the Cabibbo-Kobayashi-Maskawa matrix”, [arXiv:hep-ph/9708216 \[hep-ph\]](#).
- [351] A. Rasin, “Hierarchical quark mass matrices”, *Phys.Rev.* **D58** (1998) 096012, [arXiv:hep-ph/9802356 \[hep-ph\]](#).
- [352] D. Falcone and F. Tramontano, “Relation between quark masses and weak mixings”, *Phys.Rev.* **D59** (1999) 017302, [arXiv:hep-ph/9806496 \[hep-ph\]](#).
- [353] A. Mondragon and E. Rodriguez-Jauregui, “The Breaking of the flavor permutational symmetry: Mass textures and the CKM matrix”, *Phys.Rev.* **D59** (1999) 093009, [arXiv:hep-ph/9807214 \[hep-ph\]](#).
- [354] A. Mondragon and E. Rodriguez-Jauregui, “The CP violating phase δ_{13} and the quark mixing angles θ_{13} , θ_{23} and θ_{12} from flavor permutational symmetry breaking”, *Phys.Rev.* **D61** (2000) 113002, [arXiv:hep-ph/9906429 \[hep-ph\]](#).
- [355] G. Branco, D. Emmanuel-Costa, and R. Gonzalez Felipe, “Texture zeros and weak basis transformations”, *Phys.Lett.* **B477** (2000) 147–155, [arXiv:hep-ph/9911418 \[hep-ph\]](#).
- [356] H. Fritzsch and Z.-z. Xing, “The Light quark sector, CP violation, and the unitarity triangle”, *Nucl.Phys.* **B556** (1999) 49–75, [arXiv:hep-ph/9904286 \[hep-ph\]](#).
- [357] H. Fritzsch and Z.-z. Xing, “Mass and flavor mixing schemes of quarks and leptons”, *Prog.Part.Nucl.Phys.* **45** (2000) 1–81, [arXiv:hep-ph/9912358 \[hep-ph\]](#).
- [358] R. Roberts, A. Romanino, G. G. Ross, and L. Velasco-Sevilla, “Precision test of a fermion mass texture”, *Nucl.Phys.* **B615** (2001) 358–384, [arXiv:hep-ph/0104088 \[hep-ph\]](#).

- [359] H. Fritzsch and Z.-z. Xing, “Four zero texture of Hermitian quark mass matrices and current experimental tests”, *Phys.Lett.* **B555** (2003) 63–70, [arXiv:hep-ph/0212195](#) [hep-ph].
- [360] H. Fritzsch and Z.-z. Xing, “Lepton mass hierarchy and neutrino mixing”, *Phys.Lett.* **B634** (2006) 514–519, [arXiv:hep-ph/0601104](#) [hep-ph].
- [361] H. Fritzsch and Z.-z. Xing, “Relating the neutrino mixing angles to a lepton mass hierarchy”, *Phys.Lett.* **B682** (2009) 220–224, [arXiv:0911.1857](#) [hep-ph].
- [362] G. Branco, D. Emmanuel-Costa, and C. Simoes, “Nearest-Neighbour Interaction from an Abelian Symmetry and Deviations from Hermiticity”, *Phys.Lett.* **B690** (2010) 62–67, [arXiv:1001.5065](#) [hep-ph].
- [363] H. Ishimori, T. Kobayashi, H. Ohki, Y. Shimizu, H. Okada, *et al.*, “Non-Abelian Discrete Symmetries in Particle Physics”, *Prog.Theor.Phys.Suppl.* **183** (2010) 1–163, [arXiv:1003.3552](#) [hep-th].
- [364] M. Gupta and G. Ahuja, “Flavor mixings and textures of the fermion mass matrices”, *Int. Jour. Mod. Phys. A*, **27** (2012) 1230033, [arXiv:1302.4823](#) [hep-ph].
- [365] Z.-z. Xing, “Model-independent access to the structure of quark flavor mixing”, *Phys.Rev.* **D86** (2012) 113006, [arXiv:1211.3890](#) [hep-ph].
- [366] F. González Canales, A. Mondragón, M. Mondragón, U. J. Saldaña Salazar, and L. Velasco-Sevilla, “Quark sector of S3 models: classification and comparison with experimental data”, *Phys.Rev.* **D88** (2013) 096004, [arXiv:1304.6644](#) [hep-ph].
- [367] S. F. King and C. Luhn, “Neutrino Mass and Mixing with Discrete Symmetry”, *Rept.Prog.Phys.* **76** (2013) 056201, [arXiv:1301.1340](#) [hep-ph].
- [368] L. J. Hall and H. Murayama, “A Geometry of the generations”, *Phys.Rev.Lett.* **75** (1995) 3985–3988, [arXiv:hep-ph/9508296](#) [hep-ph].
- [369] R. Barbieri, G. Dvali, and L. J. Hall, “Predictions from a U(2) flavor symmetry in supersymmetric theories”, *Phys.Lett.* **B377** (1996) 76–82, [arXiv:hep-ph/9512388](#) [hep-ph].
- [370] R. Barbieri, L. J. Hall, and A. Romanino, “Consequences of a U(2) flavor symmetry”, *Phys.Lett.* **B401** (1997) 47–53, [arXiv:hep-ph/9702315](#) [hep-ph].
- [371] C. D. Carone and L. J. Hall, “Neutrino physics from a U(2) flavor symmetry”, *Phys.Rev.* **D56** (1997) 4198–4206, [arXiv:hep-ph/9702430](#) [hep-ph].
- [372] M. Tanimoto, “Neutrino mass matrix with U(2) flavor symmetry and its test in neutrino oscillation experiments”, *Phys.Rev.* **D57** (1998) 1983–1986, [arXiv:hep-ph/9706497](#) [hep-ph].
- [373] L. J. Hall and N. Weiner, “U(2) and maximal mixing of muon-neutrino”, *Phys.Rev.* **D60** (1999) 033005, [arXiv:hep-ph/9811299](#) [hep-ph].
- [374] R. Barbieri, P. Creminelli, and A. Romanino, “Neutrino mixings from a U(2) flavor symmetry”, *Nucl.Phys.* **B559** (1999) 17–26, [arXiv:hep-ph/9903460](#) [hep-ph].
- [375] A. Aranda, C. D. Carone, and R. F. Lebed, “U(2) flavor physics without U(2) symmetry”, *Phys.Lett.* **B474** (2000) 170–176, [arXiv:hep-ph/9910392](#) [hep-ph].
- [376] J. Kubo, A. Mondragon, M. Mondragon, and E. Rodriguez-Jauregui, “The Flavor symmetry”, *Prog.Theor.Phys.* **109** (2003) 795–807, [arXiv:hep-ph/0302196](#) [hep-ph].
- [377] S. Morisi, “S(3) family permutation symmetry and quark masses: A Model independent approach”, [arXiv:hep-ph/0604106](#) [hep-ph].
- [378] F. Feruglio and Y. Lin, “Fermion Mass Hierarchies and Flavour Mixing from a Minimal Discrete Symmetry”, *Nucl.Phys.* **B800** (2008) 77–93, [arXiv:0712.1528](#) [hep-ph].
- [379] R. Jora, J. Schechter, and M. Naem Shahid, “Perturbed S(3) neutrinos”, *Phys.Rev.* **D80** (2009) 093007, [arXiv:0909.4414](#) [hep-ph].

- [380] T. Teshima and Y. Okumura, “Quark/lepton mass and mixing in S_3 invariant model and CP-violation of neutrino”, *Phys.Rev.* **D84** (2011) 016003, [arXiv:1103.6127 \[hep-ph\]](#).
- [381] R. Barbieri, D. Buttazzo, F. Sala, and D. M. Straub, “Flavour physics from an approximate $U(2)^3$ symmetry”, *JHEP* **1207** (2012) 181, [arXiv:1203.4218 \[hep-ph\]](#).
- [382] G. Blankenburg, G. Isidori, and J. Jones-Perez, “Neutrino Masses and LFV from Minimal Breaking of $U(3)^5$ and $U(2)^5$ flavor Symmetries”, *Eur.Phys.J.* **C72** (2012) 2126, [arXiv:1204.0688 \[hep-ph\]](#).
- [383] A. J. Buras and J. Girrbach, “On the Correlations between Flavour Observables in Minimal $U(2)^3$ Models”, *JHEP* **1301** (2013) 007, [arXiv:1206.3878 \[hep-ph\]](#).
- [384] E. Schmidt, “Zur Theorie der linearen und nichtlinearen Integralgleichungen - I. Teil: Entwicklung willkürlicher Funktionen nach Systemen vorgeschriebener”, *Mathematische Annalen* **63** no. 4, (1907) 433–476.
- [385] G. Eckart and G. Young, “The approximation of one matrix by another of lower rank”, *Psychometrika* **1** (1936) 211–218.
- [386] L. Mirsky, “Symmetric gauge functions and unitarily invariant norms”, *Quart. J. Math.* **11** (1960) 50–59.
- [387] G. Golub, A. Hoffman, and G. Stewart, “A generalization of the Eckart-Young-Mirsky matrix approximation theorem”, *Linear Algebra and Its Applications* **88-89** no. C, (1987) 317–327.
- [388] G. Stewart, “On the early history of the singular value decomposition”, *SIAM Review* **35** no. 4, (1993) 551–566.
- [389] I. Masina, “A Maximal atmospheric mixing from a maximal CP violating phase”, *Phys.Lett.* **B633** (2006) 134–140, [arXiv:hep-ph/0508031 \[hep-ph\]](#).
- [390] I. Masina and C. A. Savoy, “Real and imaginary elements of fermion mass matrices”, *Nucl.Phys.* **B755** (2006) 1–20, [arXiv:hep-ph/0603101 \[hep-ph\]](#).
- [391] K. Chetyrkin, J. H. Kuhn, and M. Steinhauser, “RunDec: A Mathematica package for running and decoupling of the strong coupling and quark masses”, *Comput.Phys.Commun.* **133** (2000) 43–65, [arXiv:hep-ph/0004189 \[hep-ph\]](#).
- [392] A. G. Grozin, M. Hoeschele, J. Hoff, M. Steinhauser, M. Hoschele, *et al.*, “Simultaneous decoupling of bottom and charm quarks”, *JHEP* **1109** (2011) 066, [arXiv:1107.5970 \[hep-ph\]](#).
- [393] C. Jarlskog, “Commutator of the Quark Mass Matrices in the Standard Electroweak Model and a Measure of Maximal CP Violation”, *Phys.Rev.Lett.* **55** (1985) 1039.
- [394] H. K. Dreiner, H. E. Haber, and S. P. Martin, “Two-component spinor techniques and Feynman rules for quantum field theory and supersymmetry”, *Phys.Rept.* **494** (2010) 1–196, [arXiv:0812.1594 \[hep-ph\]](#).
- [395] G. 't Hooft and M. Veltman, “Regularization and Renormalization of Gauge Fields”, *Nucl.Phys.* **B44** (1972) 189–213.
- [396] K. Chetyrkin and M. Zoller, “ β -function for the Higgs self-interaction in the Standard Model at three-loop level”, *JHEP* **1304** (2013) 091, [arXiv:1303.2890 \[hep-ph\]](#).
- [397] J. Casas, J. Espinosa, A. Ibarra, and I. Navarro, “Neutrinos and gauge unification”, *Phys.Rev.* **D63** (2001) 097302, [arXiv:hep-ph/0004166 \[hep-ph\]](#).

ACKNOWLEDGMENTS

Δεν ελπίζω τίποτα, δεν φοβούμαι τίποτα,
λυτρώθηκα από το νου κι από την καρδιά,
ανέβηκα πιο πάνω, είμαι λεύτερος.

—Nikos Kazantzakis

*I do not hope for
anything. I do not
fear anything, I
have freed myself
from both the mind
and the heart, I
have mounted
much higher, I am
free.*

First of all, I do not want to thank my supervisor of this thesis, but my father—and also my mother for bearing and supporting me the last three years. Especially I want to thank my father, who did not prevent me introducing a degeneracy in namespace—and causing some confusion in the world of (theoretical) particle physics.

Secondly, I am very glad to thank Uli Nierste for supervising my PhD thesis and keeping me in his group after the diploma. During the evolution of the project even though the main focus changed, he always encouraged me to go further.

Next, I want to thank Maggie Mühlleitner that she agreed unhesitatingly to be my second examiner and read and comment on this thesis. Thanks also to her, Uli as well as Max Zoller, Martin Spinrath and Ulises Jesús Saldaña Salazar who have read and commented on parts of this thesis.

This thesis, my PhD project and the life as researcher was supported during the last years by the Graduiertenkolleg GRK 1694 (Elementarteilchenphysik bei höchster Energie und höchster Präzision), a research training group funded by the Deutsche Forschungsgemeinschaft. During six months in the first year of my PhD, I got a KIT internal grant named “Feasibility Studies of Young Scientists” (FYS) to investigate quantum corrections to neutrino physics. I thank the Council for Research and Promotion of Young Scientists (CRYs) for giving me this opportunity. The Karlsruhe House of Young Scientists (KHYS) supported me and my scientific work several times: there was the participation at the International School Cargèse 2012 funded by them. Furthermore, we got grant to organize a Young Scientists workshop in Fall 2014 about “Flavorful Ways to New Physics”. Finally, they facilitated the stay of Ulises Jesús Saldaña Salazar at the KIT from June to October 2014.

The work which was performed in context of this thesis would never have been possible without the infrastructural support by the institute, especially all the SysAdmins who themselves are and have been mostly

PhD students and partly postdocs: thanks to Peter Marquard, Thomas Hermann, Jens Hoff, Otto Eberhardt, David Kunz, Christoph Wiegand and Alexander Hasselhuhn from the TTP—and Johannes Bell, Bastian Feigl, Christian Röhr and Robin Roth from “the other institute” ITP. Moreover, I want to thank our secretaries for the administrative support: Martina Schorn, the good mind of the TTP; Isabelle Junge for the GRK and Barbara Lepold for the graduate school KSETA.

Physicswise, I have to thank the following people for collaboration in essential parts of this thesis: I am very thankful for innumerable valuable discussions with Markus Bobrowski about Radiative Flavor Violation in extensions of the MSSM and effective potentials and vacuum instabilities. Moreover, I am indebted to Stefan Pokorski to hinting me towards the degenerate neutrinos and threshold corrections. A project which started during his visit in Karlsruhe in fall 2013 found its way into this thesis and the bibliography [194]. Very many thanks also to Ulises Jesús Saldaña Salazar for his collaboration in [205] and his visit in Karlsruhe’s summer of 2014.

I cannot list every helpful discussion but want to emphasize such with Luca Di Luzio, Luminita Mihaila and Max Zoller especially about effective potentials; many enlightening conversations in the dawn of my PhD existence with Peter Marquard and Nikolai Zerf; discussions about physics and life in the institute and on sailing trips have been enjoyed together with Jens Hoff, Maik Höschele and Max Zoller (also with Ulises during a cold summer in Sweden). Special thanks also for the friendly atmosphere, company and coffee breaks to (in addition to names already mentioned in this paragraph) Nastya Bierweiler, Tobias Kasprzik, Thomas Hermann, Jonathan Grigo, David Kunz, Philipp Frings and Yasmin Anstruther—and Uli Nierste to let me in on the secret of the queen of clubs.

Finally, I want to thank all those who were being in charge of one of the most important subject namely coffee (and especially those who endeavored to keep up the continued supply chain): Sebastian Merkt, Mario Prausa, Peter Wichers and Thomas Deppisch.

COLOPHON

This document has been typeset with \LaTeX using the typographical look-and-feel `classicthesis` developed by André Miede. Postcard will be sent.

All Feynman diagrams have been drawn with Jos Vermaseren's `Axodraw`; data plots have been plotted using `Gnuplot` and \LaTeX performed via a bash script provided by Tobias Kaszprzik. The layout of mathematical formulae is shaped with the `mathdesign` package.

All numerical and symbolical calculations and evaluations have been performed with the computer algebra system `Mathematica` of versions 8 and 9.